Disease Markers

Find the Essence through the Phenomena: Cardiovascular Diseases and Biomarkers 2019

Lead Guest Editor: Shipeng Wei
Guest Editors: Agata M. Bielecka-Dabrowa and Zhongjie Shi

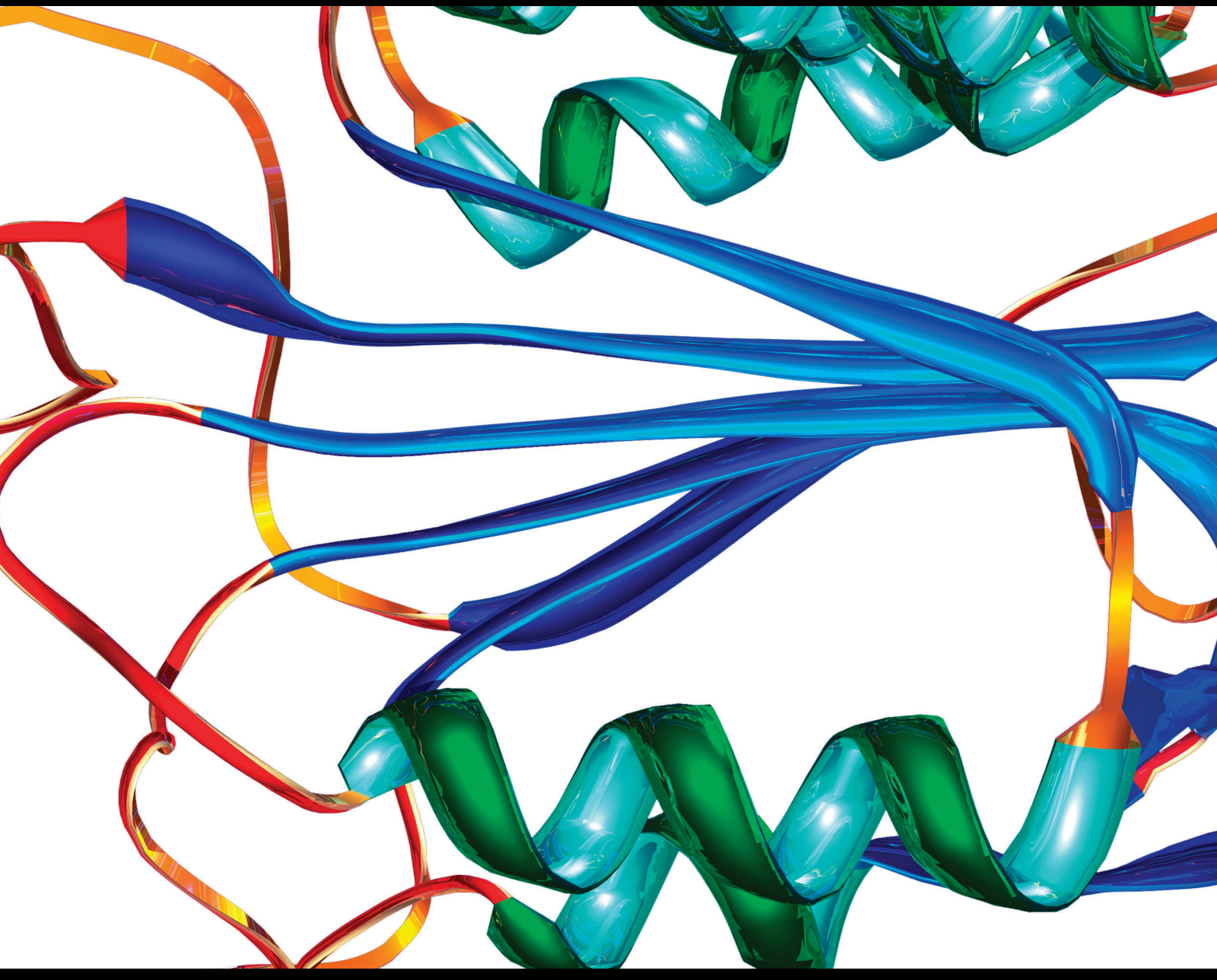

Find the Essence through the Phenomena: Cardiovascular Diseases and Biomarkers 2019

Disease Markers

Find the Essence through the Phenomena: Cardiovascular Diseases and Biomarkers 2019

Lead Guest Editor: Shipeng Wei
Guest Editors: Agata M. Bielecka-Dabrowa and Zhongjie Shi

Contents

Hindawi
Disease Markers
Volume 2020, Article ID 1959364, 2 pages
https://doi.org/10.1155/2020/1959364

Editorial

Find the Essence through the Phenomena: Cardiovascular Diseases and Biomarkers 2019

Shipeng Wei,[1] **Agata M. Bielecka-Dabrowa**,[2] **and Zhongjie Shi**[3]

[1]*MercyOne Des Moines Medical Center, Des Moines, USA*
[2]*Medical University of Lodz, Lodz, Poland*
[3]*Wayne State University, Detroit, MI, USA*

Correspondence should be addressed to Shipeng Wei; swei@mercydesmoines.org

Received 13 December 2019; Accepted 23 December 2019; Published 28 September 2020

This special issue is a continuous effort of our successful 2018 special issue to discover novel biomarkers in the risk prediction, screening, diagnosis, progression, and prognosis cardiovascular diseases. We are happy to see real-time advances in the field with different study methods in different stages of diseases.

1. Biomarkers in Myocardial Ischemia or Infarction

C. Fu et al. reported that low expression of bradykinin B2 receptor on circulating progenitor cells indicated the poor outcomes of myocardial infarction, based on data from 174 myocardial infarction patients. V. A. M. Goulart et al. were able to identify alterations in the glycerophospholipids, alpha-linolenic acid, and sphingolipid metabolisms in ST-segment elevation myocardial infarction patients, using ultra-high-performance liquid chromatography-tandem mass spectrometry and MS-based flow injection analysis. J. Zhao et al. reported by meta-analysis that circulating microRNA-499 can be used as a diagnostic biomarker for acute myocardial infarction. Q. Ouyang et al. studied the effects of apelin on left ventricular-arterial coupling and mechanical efficiency in rats with ischemic heart failure and found that rats with ischemic HF were characterized by deteriorated left ventricular mechanoenergetics. Apelin improves mechanical efficiency by the inhibiting cardiac fibrosis and apoptosis in left ventricular myocardium, reducing collagen deposition in the aorta and dilating the resistant artery. K. Pieszko et al. employed machine learning techniques and hematological markers in a robust enrollment of 5053 patients and found that neutrophil count and red cell distribution width have a strong association with all-cause mortality after acute coronary syndrome. R. Rajtar-Salwa et al. showed the time-synchronized relationship between ischemia and left ventricular dysfunction assessed by high-sensitive troponin I and N-terminal pro B-type NT-pro natriuretic peptide. M. Mocan et al. reviewed biomarkers of inflammation in left ventricular diastolic dysfunction, which had been previously associated with a heart failure mechanism.

2. Biomarkers in Heart Failure

P. Perge et al. found that vitamin D deficiency predicts poor clinical outcomes in heart failure patients undergoing cardiac resynchronization therapy. C.-H. Wang et al. showed the feasibility of amino acid-based metabolic profile in functional and prognostic assessment for heart failure outpatients. D. Simeunovic et al. showed the role of glutathione transferase P1 polymorphism in individual susceptibility to oxidative stress, inflammation, and endothelial dysfunction in coronary artery disease and idiopathic dilated cardiomyopathy. T.-L. Chuang et al. investigated the role of bone mineral density in the prediction of cardiovascular disease through atherogenic indexes in nonobese adults.

3. Biomarkers at a Specific Stage of Diseases

T. Fang et al. found that the preoperative serum CEA, CA125, and CA19-9 levels can help predict the resectability of cholangiocarcinoma. X. Liu et al. showed the preoperative

abnormal changes in respiratory rate, TPTEF/TE, VPEF/VE, and lung compliance are indicative of the risk of postoperative pulmonary complications in infants with congenital heart diseases. W. Su et al. reported the use of integrated microfluidic device for enrichment and identification of circulating tumor cells from the blood of patients with colorectal cancer. M. Walentowicz-Sadlecka et al. found that placental soluble fms-like tyrosine kinase-1 (sFlt-1) and sFlt-1/25(OH)D ratio can be used as a diagnostic tool in gestational hypertension, preeclampsia, and gestational diabetes mellitus. I. Mozos et al. presented the links between high-sensitivity C-reactive protein (hsCRP) and pulse wave analysis in middle-aged patients with hypertension and high normal blood pressure (HNBP). Furthermore, vitamin D level, hsCRP, and low-density lipoprotein cholesterol provide valuable information in middle-aged hypertensive and HNBP patients, related to arterial stiffness and early arterial aging.

With so many novel and valuable biomarkers found and are being continuously found, we are closer to the essence of the phenomena and are more confident in the battle against cardiovascular diseases in the future.

Conflicts of Interest

The authors declare no conflict of interest.

Shipeng Wei
Agata M. Bielecka-Dabrowa
Zhongjie Shi

Hindawi
Disease Markers
Volume 2019, Article ID 4145821, 7 pages
https://doi.org/10.1155/2019/4145821

Research Article

Vitamin D Deficiency Predicts Poor Clinical Outcomes in Heart Failure Patients Undergoing Cardiac Resynchronization Therapy

P. Perge, A. M. Boros, L. Gellér, I. Osztheimer, Sz Szilágyi, T. Tahin, A. Apor, K. V. Nagy, E. Zima, L. Molnár, B. Merkely, and G. Széplaki

Heart and Vascular Center, Semmelweis University, Városmajor utca 68, Budapest 1122, Hungary

Correspondence should be addressed to B. Merkely; merkely.bela@kardio.sote.hu

Received 1 February 2019; Accepted 6 May 2019; Published 13 October 2019

Guest Editor: Agata Bielecka-Dabrowa

Background and Aims. Resynchronization therapy (CRT) improves mortality and induces reverse remodeling in heart failure (HF) patients with reduced ejection fraction and wide QRS. Nonetheless, some patients do not improve despite the optimal medical therapy and right indications for device implantation. Therefore, finding biomarkers suitable for identification of those patients is crucial. Vitamin D plays a classic hormonal role in the regulation of bone metabolism and also has physiological functions in wide range of nonskeletal tissues. Based on recent studies, low levels of vitamin D seem to directly contribute to pathogenesis and worsening of HF. We planned to assess the role of vitamin D levels on clinical outcomes of HF patients undergoing CRT. *Methods and Results*. We enrolled 136 HF patients undergoing CRT. Total plasma vitamin D levels were measured at baseline and 6 months later. Primary endpoint was 5-year all-cause mortality; secondary endpoint was lack of good clinical response, defined as less than 15% increase of left ventricular ejection fraction after six months. During follow-up, 58 patients reached the primary, and 45 patients reached the secondary endpoint. Vitamin D levels less than 24.13 ng/mL predicted 5-year mortality ($p = 0.045$) and poor clinical response ($p = 0.03$) after adjusting to all significant baseline predictors. *Conclusion*. Our study showed that vitamin D deficiency has a significant impact in heart failure patients; it is an independent predictor of lack of midterm clinical response and long-term mortality in patients undergoing CRT. Therefore, monitoring vitamin D status of heart failure patients could be of clinical significance.

1. Introduction

Heart failure (HF) bears a major public health impact with constantly growing incidence, despite continuous improvements in prevention, diagnosis, and therapy [1]. Cardiac resynchronization therapy (CRT) is an effective therapeutic option for symptomatic HF patients with severely reduced left ventricular ejection fraction (LVEF) and wide QRS. In most patients, mortality and morbidity are reduced, while functional capacity and HF symptoms are improved [2, 3]. Despite the repeated refinements in the guidelines for optimal patient selection, poor clinical response to CRT is still prevalent [4], thus recognizing further predictors of outcome is crucial.

Vitamin D, initially known as a key hormone of bone metabolism, has several extraskeletal physiologic functions. Based upon recent studies, vitamin D is an important regulator of the renin-angiotensin-aldosterone system (RAAS), inflammatory cytokines, and extracellular matrix (ECM) turnover. Moreover, vitamin D deficiency directly contributes to pathogenesis of HF by the loss of above modulating mechanisms, causing remodeling of the heart [5]. Numerous cross-sectional and longitudinal studies showed that vitamin D deficiency is associated with increased risk of HF; in addition, worse prognosis of already diagnosed HF was also demonstrated [6]. Interestingly, vitamin D supplementation in primary or secondary prevention of HF is controversial; there is no definitive evidence supporting a favorable role of vitamin D supplementation [7].

There is limited data in the literature assessing the role of vitamin D deficiency in predicting clinical response to CRT. The results of previous small-scale studies suggest that patients with low levels of vitamin D show inadequate six-month clinical response to CRT [8, 9]; however, no

data exists regarding hard endpoints. The aim of our study was to determine the predictive value of vitamin D deficiency on the long-term mortality after CRT and confirm the association with poor midterm clinical response.

2. Methods

2.1. Study Population. 141 consecutive HF patients were enrolled to our prospective, single-center, observational study. The purpose of the study was to evaluate the prognostic value of various biomarkers in a cohort of HF patients previously described in details, including routine laboratory markers, uric acid, complement components, and novel HF biomarkers [10–14]. This present study focused on the role of vitamin D levels in the prognosis after CRT implantation.

We enrolled chronic heart failure patients with optimal medical therapy, symptomatic HF (New York Heart Association functional class II-IVa), left ventricular ejection fraction (LVEF) below 35%, and wide QRS complex (>120 msec) in the baseline electrocardiogram (ECG). Vitamin D supplementation was not included in the medical therapy before enrolment and during the follow-up. The patients underwent CRT implantation according to the current guidelines [15] in the Heart and Vascular Center of Semmelweis University, Budapest, between September 2009 and December 2010. Severe systemic inflammatory and hematologic diseases and active malignancies were considered as exclusion criteria; we excluded 4 patients based on these conditions; furthermore, we did not have complete dataset of one patient.

2.2. Clinical Endpoints and Follow-Up. The primary endpoint of the study was five-year all-cause mortality. Good clinical response, defined as an at least 15% increase of LVEF after six months of CRT, was considered as the secondary endpoint. All patients gave written informed consent before enrolment to the study. The investigation conformed to the Declaration of Helsinki; the study protocol was approved by the local Ethics Committee.

The follow-up period lasted five years; we conducted visits at six months, two years, and five years after CRT implantation. Detailed physical examinations, laboratory tests, ECG, and echocardiography were performed in a total of 136 patients at baseline. At follow-up visits, functional status of the patients was evaluated by assessing the NYHA classification; their medical therapy and relevant adverse medical events were documented. Laboratory blood analyses, echocardiography, and ECG were repeated at six months.

2.3. Laboratory Measurements, Exposure to Sunlight, and Echocardiography. We obtained venous blood samples from the patients, afterwards processed the serum and ethylenediaminetetraacetic acid plasma aliquots within two hours after sampling. Samples were stored at -80°C for later laboratory measurements. Total serum 25(OH)-vitamin D levels were measured with Roche Elecsys vitamin D total assay kits (Cat. No.: 05894913190, Roche Diagnostics, Mannheim, Germany. Reference value is >30 ng/mL in the Central Laboratory of Semmelweis University, respectively). N-terminal of the prohormone brain natriuretic peptide (NT-proBNP) levels was measured using Roche Elecsys NT-proBNP II kits (Cat. No.: 04842464190, Roche Diagnostics, Mannheim, Germany) with a Cobas e 411 analyzer (Roche Diagnostics, Mannheim, Germany). Serum calcium levels were measured CA2 kits (Cat. No.: 05061482190, Roche Diagnostics, Mannheim, Germany) with a Cobas Integra 400 Plus analyzer (Roche Diagnostics, Mannheim, Germany).

Exposure to sunlight was assessed by the cumulative hours of sunshine in the 30-day preceding enrolment, based upon the public databases of the National Meteorological Service [16].

Echocardiography and offline measurements were carried out by licensed echocardiographic experts using a Phillips iE 33 system, Philips Xcelera R3.1.L1, and Philips Qlab 9.0 software. LVEF was calculated using Simpson's biplane method. The reproducibility of echocardiographic measurements was determined; interobserver and intraobserver variability was assessed with Lin's concordance correlation coefficient using 12-12 pair of sample data; substantial correlation was proven, as described previously in this cohort (interobserver variability: $\rho_c = 0.956$ (0.89-0.98); intraobserver variability: $\rho_c = 0.96$ (0.89-0.97)).

2.4. Statistical Analysis. As the majority of the variables showed nonparametric distributions, the data were expressed as the medians with interquartile ranges or as percentages with the event numbers. Continuous variables were compared with the Wilcoxon matched pair test and the Mann-Whitney test, as appropriate. A chi-squared test was applied for categorical data comparisons. The Cox and univariate logistic regression analyses were applied to determine the baseline predictors of 5-year mortality and the lack of good clinical response; the continuous variables were standardized by one standard deviation increase for the regression analyses. We used receiver operating characteristic (ROC) analysis, and the continuous variables were dichotomized and then the Kaplan-Meier curves were compared using the log-rank tests. In the multivariable Cox regression and logistic regression models, the baseline model included variables with $p < 0.1$ value from the univariate analysis, and further adjusted models were built in a forward stepwise manner.

In the present study, a two-tailed p value of <0.05 was considered statistically significant. Statistical analyses were performed using IBM SPSS 22 (Apache Software Foundation, USA) and GraphPad Prism 6.03 (GraphPad Software, Inc., USA) software products.

3. Results

3.1. Baseline Characteristics and Effects of CRT on the Study Population. The baseline characteristics of the 136 patients are detailed in Table 1; the comparison of surviving patients and nonsurvivors is showed. Deceased patients had higher LVEF and NT-proBNP levels at baseline, while the proportion of patients with left bundle branch block (LBBB) and beta blocker therapy was significantly lower. Baseline plasma vitamin D level of the patients were 20.9 ng/mL (15.2-31.7), and

Table 1: Baseline characteristics.

Clinical variables	All patients ($n = 136$)	Surviving patients ($n = 78$)	Deceased patients ($n = 58$)	p value
Age (years)	67 (60-73)	67 (60-71)	70 (62-74)	0.067
Gender (male)	81 (110)	76 (59)	88 (51)	0.078
BMI (kg/m^2)	27 (24-30)	27 (25-30)	27 (23-29)	0.196
Ischemic HF	57 (78)	53 (41)	64 (37)	0.201
LBBB	82 (112)	91 (71)	71 (41)	0.003
CRT-D	16 (22)	18 (14)	14 (8)	0.533
Opt. lead position	74 (100)	73 (57)	74 (43)	0.896
QRS (msec)	163 (141-184)	164 (141-184)	163 (144-185)	0.691
LVEF (%)	28 (23-33)	28 (23-32)	34 (25-40)	<0.001
LVESV (mL)	211 (154-276)	218 (160-276)	207 (141-268)	0.353
LVEDV (mL)	303 (251-361)	313 (251-382)	299 (242-343)	0.448
NYHA III- IV	86 (117)	86 (117)	91 (53)	0.138
Hypertension	56 (76)	55 (43)	57 (33)	0.054
Hyperlipidemia	24 (33)	22 (17)	28 (16)	0.423
Diabetes mellitus	37 (50)	33 (26)	41 (24)	0.339
ACEi/ARB	96 (130)	97 (76)	93 (54)	0.277
BB	90 (122)	95 (74)	83 (48)	0.022
MRI	71 (96)	74 (58)	65 (33)	0.258
Calcium (mmol/L)	2.43 (2.34-2.49)	2.43 (2.36-2.49)	2.41 (2.32-2.50)	0.922
NT-proBNP (pg/mL)	2612 (1377-5124)	2101 (1000-3555)	4035 (2125-6479)	<0.001
Sunlight (hours)	156 (67-241)	157 (102-241)	148 (66.7-221)	0.748

Data is expressed as median with interquartile range for continuous variables and as percentage with event numbers for categorical variables. BMI: body mass index; ischemic HF: ischemic etiology of the heart failure; LBBB: left bundle branch block; CRT-D: cardiac resynchronization therapy with implantable cardioverter defibrillator; Opt. lead position: lateral or posterolateral left ventricular lead position; LVEF: left ventricular ejection fraction; LVESV: left ventricular end systolic volume; LVEDV: left ventricular end diastolic volume; NYHA III-IV: New York Heart Association classification 3-4; ACEi/ARB: angiotensin convertase inhibitor/angiotensin receptor blocker therapy; BB: beta blocker therapy; MRI: mineralocorticoid receptor inhibitor therapy; NT-proBNP: N-terminal of the prohormone brain natriuretic peptide, sunlight: cumulative duration of sunlight in the 30 days prior enrolment.

we observed no significant change after six months of CRT (6 months: 21.5 (16.2-28.3), $p = 0.43$). The study population was described in detail previously; LVEF and left ventricular end-systolic and end-diastolic volumes (LVESV and LVEDV) decreased significantly [14].

3.2. Association of Baseline Vitamin D Concentrations with Clinical Outcomes. 58 patients (43%) died during the 5-year follow-up; those who survived had significantly higher baseline vitamin D levels at baseline (23.07 (16.58-31.73) vs. 18.3 (13.81-23.75) ng/mL, $p = 0.018$). In 45 patients (33%), we observed the lack of good clinical response six months after CRT implantation; similarly, we measured increased baseline vitamin D levels in patients with good clinical response (22.56 (15.6-31.87) vs. 18.12 (13.95-23.43) ng/mL, $p = 0.027$).

To establish an optimal cut-point for the further assessment of the clinical outcomes, we used receiver operating characteristic analysis. Plasma vitamin D below 24.13 ng/mL seemed to be an optimal cut-point for 5-year mortality (AUC = 0.62 (0.52-0.71), $p = 0.018$; sensitivity: 78% (65-87); specificity: 45% (34-58)) and lack of 6-month clinical response (AUC = 0.62 (0.52-0.71), $p = 0.027$; sensitivity: 80% (65-90); specificity: 42% (32-53)), respectively (Figure 1).

Next, we created groups of patients with baseline vitamin D below and over 24.13 ng/mL. The use of beta blockers was the only parameter that differed significantly between the subgroups; almost all patients in the group with higher vitamin D levels were on beta blockers (98% vs. 85%, $p = 0.015$). Sunlight exposure before enrolment did not differ significantly between groups ($p = 0.56$). When analyzing the severity of heart failure, there was no difference between groups at baseline reflected by the NT-proBNP levels (2626 (1683-5214) vs. 2518 (988-4791), $p = 0.18$) or the NYHA class (2.97 ± 0.48 vs. 2.91 ± 0.57, $p = 0.61$). NT-proBNP levels remained significantly elevated only in the subgroup of patients with low vitamin D levels (1216 (337-2214) vs. 2116 (927-3865) $p = 0.019$) (Figure 2). Moreover, their functional status (NYHA class) also did not improve (1.9 ± 0.42 vs. 2.21 ± 0.5, $p = 0.001$) (Figure 3).

3.3. Predictors of 5-Year Mortality and Lack of Good Clinical Response. We analyzed the 5-year all-cause mortality by univariate Cox regression and the six-month clinical response using univariate logistic regression analysis. Vitamin D level lower than 24.13 ng/mL was significantly associated with increased risk of long-term mortality (HR 2.25 (1.21-4.17),

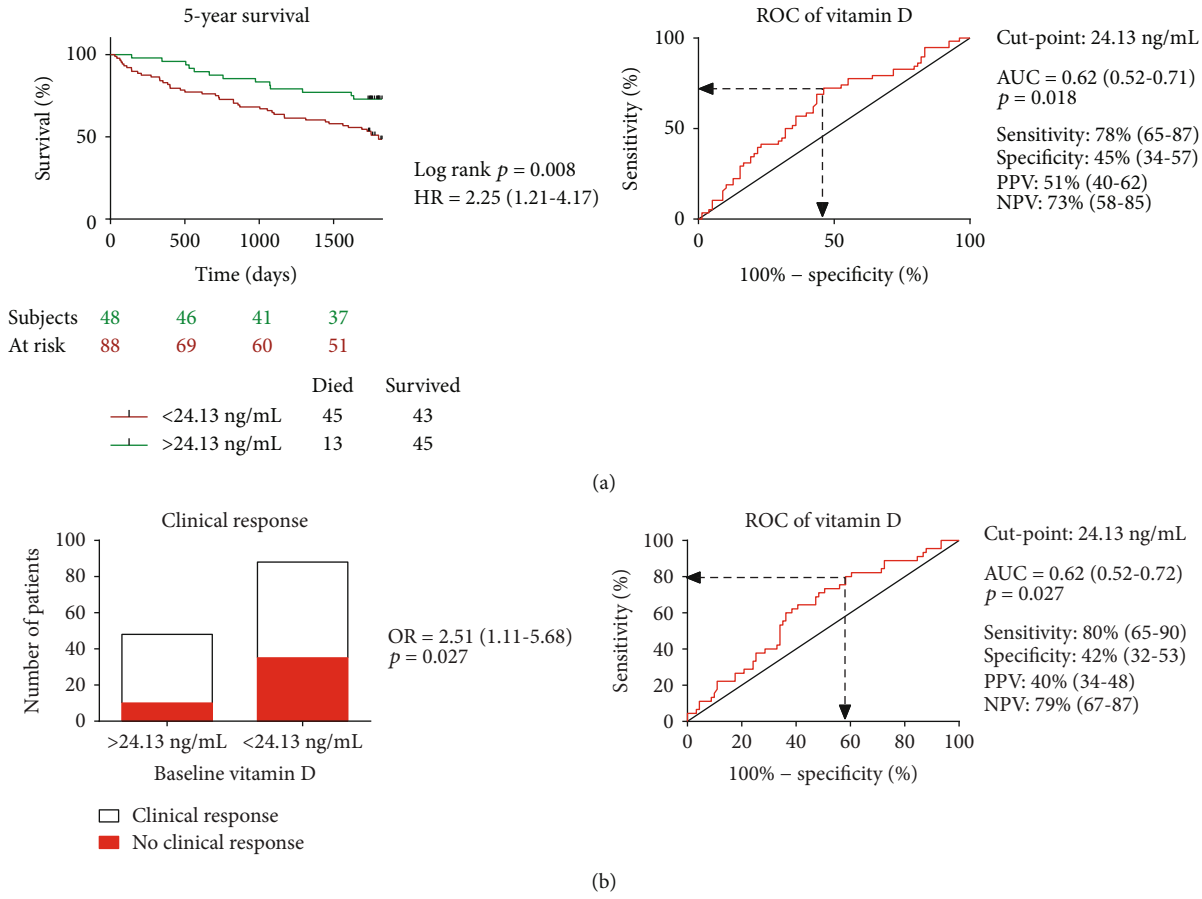

Figure 1: Impact of baseline vitamin D on five-year mortality and clinical response. Receiver operating characteristic analysis was performed for determining the optimal cutoff point for baseline plasma vitamin D levels. The odds and hazard ratios refer to the presence versus the absence of a baseline plasma vitamin D level < 24.13 ng/mL. (a) We compared the Kaplan-Meier survival curves by the log-rank test in patient groups of baseline plasma vitamin D levels below and over 24.13 ng/mL. We tested the 5-year mortality by using Cox regression analysis. (b) Clinical response, defined as a relative increase of at least 15% in the LVEF 6 months after implantation, was visualized by the contingency bar plot. We tested the lack of clinical response by using logistic regression analysis. HR: hazard ratio; OR: odds ratio; AUC: area under the curve; NPV: negative predictive value; PPV: positive predictive value.

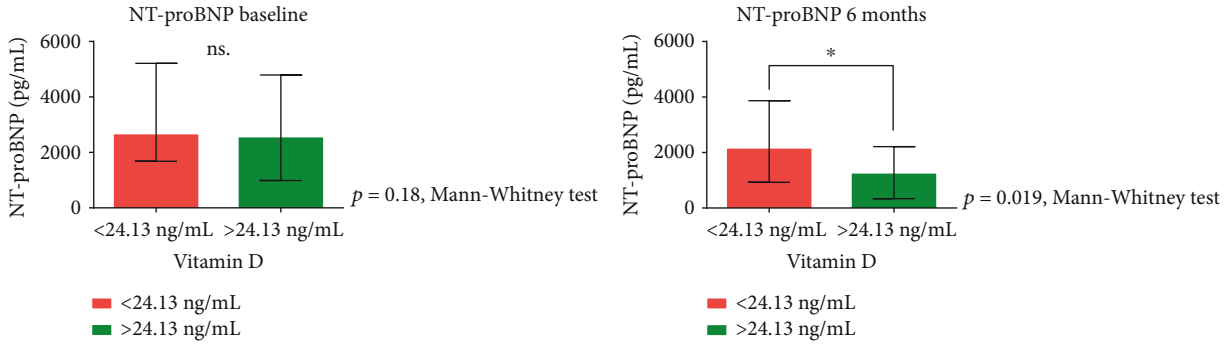

Figure 2: Plasma NT-proBNP levels at baseline and after six months of CRT. We compared the baseline and six-month plasma NT-proBNP levels in patients groups of baseline plasma vitamin D levels below and above 24.13 ng/mL using the Mann-Whitney test. CRT: cardiac resynchronization therapy; NT-proBNP: N-terminal of the prohormone brain natriuretic peptide.

$p = 0.008$) and lack of good clinical response (OR 2.51 (1.11-5.68), $p = 0.027$) (Figure 1).

As described in detail previously, LBBB ($p < 0.0001$), use of beta blocker therapy ($p = 0.003$), and increasing NT-proBNP levels ($p < 0.0001$) predicted all-cause mortality; increasing age proved to bear a marginally significant predictive capacity ($p = 0.07$). Relevant baseline clinical variables related to lack of good clinical response were hypertension ($p = 0.08$), hyperlipidaemia ($p = 0.09$), mineralocorticoid receptor inhibitor therapy ($p = 0.06$), and increasing levels

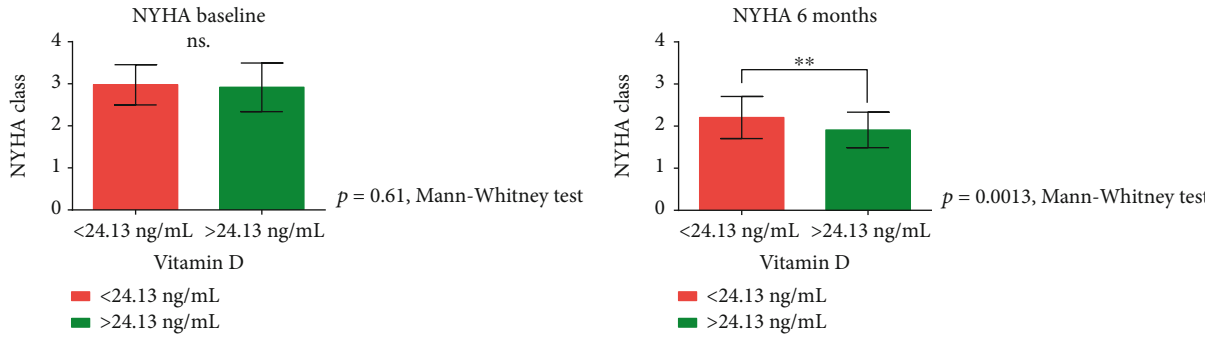

Figure 3: Severity of heart failure at baseline and after six months of CRT. We compared the baseline and six-month severity of heart failure using NYHA classification in patient groups of baseline plasma vitamin D levels below and above 24.13 ng/mL using the Mann-Whitney test. CRT: cardiac resynchronization therapy; NYHA class: classification of heart failure according to the New York Heart Association.

of NT-proBNP ($p = 0.22$). The detailed results of univariate logistic and Cox regression statistical analyses are showed in Supplementary Table 1.

To determine the independent influence of decreased vitamin D levels on mortality, we set up a basic multivariable Cox regression model with the baseline clinical variables shown to be relevant by the univariate analysis ($p < 0.10$). Thus, the baseline multivariable model included age, LBBB, use of beta blocker therapy, and baseline NT-proBNP. In the following step, we entered vitamin D levels into the baseline model in a forward stepwise way. Vitamin D levels under 24.13 ng/mL predicted mortality in the multivariable model as well (HR = 1.92 (1.02-1.45), $p = 0.045$).

We use the same method to investigate the clinical response. We included the relevant factors to the basic multivariable model: hypertension, hyperlipidemia, mineralocorticoid receptor inhibitor therapy, and increasing levels of NT-proBNP. We entered vitamin D levels into the baseline model in a forward stepwise way. Similar to mortality prediction, vitamin D was an independent predictor of lack of good clinical response (OR = 2.62 (1.01-6.25), $p = 0.03$). The detailed results of multivariate logistic and Cox regression statistical analyses are showed in Supplementary Table 2.

4. Discussion

4.1. Synopsis of Key Findings. Vitamin D levels under 24.13 ng/mL predicted long-term mortality and poor clinical response in HF patients undergoing CRT independently of all relevant baseline predictors including NT-proBNP. Furthermore, patients with vitamin D insufficiency had significantly higher NT-proBNP levels and suffered from more severe HF six months after CRT.

4.2. Possible Mechanisms and Explanation. Chronic HF is an emerging disease in the high- and middle-income countries, affecting millions of people and requiring considerable amount of healthcare expenditure. HF development is considered a compound pathophysiological process, involving the activation of neurohormonal and inflammatory pathways, tissue remodeling. Wide range of pharmaceutical and device-based treatment is available, yet the overall outcome of HF is still poor [17].

Vitamin D has been considered the key regulator of calcium and phosphorus homeostasis and bone mineralization. Besides the regulation of bone metabolism, recent studies showed that vitamin D has numerous extraskeletal functions. It plays various regulatory roles in several mechanisms considered fundamental in development of HF [18]. Vitamin D suppresses the expression of renin and RAAS activity [19] and modulates the turnover of the ECM by enhancing the production of matrix metalloproteinase inhibitors [20], and experimental studies showed that it promotes myocyte contraction and relaxation by modulating the calcium influx [21]. In case of vitamin D deficiency, with the loss of the previous regulating effects, hypertrophy, ECM deposition, and myocardial fibrosis may arise.

Clinical studies also confirmed that vitamin D has a strong impact in HF. The risk of developing HF was increased in longitudinal studies in case of low levels of vitamin D, while prevalent vitamin D deficiency was found among HF patients [6]. Furthermore, it was associated with significantly worse prognosis [22, 23].

Although vitamin D deficiency contributes to the development of HF by several described regulatory mechanisms, the clear beneficial effect of vitamin D supplementation in HF patients is still under debate, based upon recent randomized studies [24, 25]. Further randomized studies with consistent enrolment criteria are needed to validate the benefit.

Previous small studies also suggested that low levels of vitamin D predict poor 6-month response after CRT implantation [8, 9], yet there was no data available regarding long-term mortality. In our study, we also confirmed the role of vitamin D in the prediction of the lack of good clinical response after CRT. Baseline vitamin D levels under 24.13 ng/mL were significantly associated with poor clinical response, independently of all relevant baseline predictors. Patients with lower baseline vitamin D levels had 2.5-fold risk of lack of good clinical response after CRT.

Furthermore, we demonstrated that reduced baseline vitamin D levels were significant predictors of 5-year mortality after CRT; the mortality risk was independent of all relevant baseline predictors. Patients with vitamin D levels under 24.13 ng/mL had more than 2-fold mortality risk during the follow-up.

We used the NYHA classification of HF and NT-proBNP levels as surrogate markers to further assess the clinical response of patients. Interestingly, at baseline there were no significant differences between groups of patients with vitamin D levels below and above 24.13 ng/mL. After six months of CRT, patients with reduced vitamin D levels had significantly higher NT-proBNP levels and NYHA classes, indicating a more severe stage of HF, enhanced progression, and poor clinical response.

According to the 2011 classification by the Institute of Medicine, 25(OH)-vitamin D levels below 20 ng/mL are considered inadequacy, while levels between 20 and 50 ng/mL are considered adequacy [26]. Our statistically verified cut-point reaching almost the limit of vitamin D inadequacy also supports the previous findings regarding the close association of low vitamin D levels and poor clinical outcomes in HF.

4.3. Limitations. Remarkable limitations of our study are the relatively small sample size and the single-center design. All-cause mortality was considered as the primary endpoint; cause of death was not investigated separately in this analysis due to the relatively low event numbers. The assessment of the sunlight exposure of patients can only credited as an approximate, since the average cumulative hours of sunshine in Hungary were calculated. Our results can be represented as hypothesis-generating findings; this observation does not prove direct causality between vitamin D levels and prognosis in HF patients undergoing CRT. Validation with prospective, multicenter studies is necessary.

5. Conclusion

Our results further verify the previous findings concerning the association of reduced vitamin D levels with the poor prognosis in various HF populations. Decreased baseline vitamin D levels predicted poor outcomes after CRT, functional status, and clinical response. Long-term survival of the patients was significantly worse compared with patients with adequate baseline vitamin D levels. Therefore, assessing the vitamin D homeostasis of HF patients before CRT implantation might be helpful in identifying the high-risk patients, among whom nonresponse should be anticipated.

Data Availability

The data used to support the findings of this study are available from the corresponding author upon request.

Disclosure

A previous version of the manuscript has been published as an abstract in the EP Europace Supplements following the Cardiostim EHRA Europace 2016 Congress (poster presentation no. 001986).

Conflicts of Interest

The authors declare that there is no conflict of interest regarding the publication of this article.

Authors' Contributions

Merkely B. and Széplaki G. contributed equally to the work and both should be regarded as last authors of the article.

Acknowledgments

Our observational study was supported in the form of unrestricted research grants by the Hungarian Foundation Programs "Semmelweis Egyetem Híd Projekt" (Grant: TÁMOP-4.2.2-08/1/KMR-2008-0004), "Semmelweis Egyetem Magiszter Program" (Grant: TÁMOP-4.2.2./B10/1.-210-0013), Hungarian Scientific Research Fund (Grant: OTKA K 105555), "Az orvos-, egészségtudományi- és gyógyszerészképzés tudományos műhelyeinek fejlesztése" (Grant: EFOP-3.6.3-VEKOP-16-2017-00009), and János Bolyai Research Scholarships of the Hungarian Academy of Sciences.

Supplementary Materials

Supplementary Tables 1 and 2: the detailed results of logistic and Cox regression statistical analyses are presented, including both univariate and multivariate models. *(Supplementary Materials)*

References

[1] E. Braunwald, "Heart failure," *JACC: Heart Failure*, vol. 1, no. 1, pp. 1–20, 2013.

[2] J. G. Cleland, J. C. Daubert, E. Erdmann et al., "The effect of cardiac resynchronization on morbidity and mortality in heart failure," *New England Journal of Medicine*, vol. 352, no. 15, pp. 1539–1549, 2005.

[3] A. S. Tang, G. A. Wells, M. Talajic et al., "Cardiac-resynchronization therapy for mild-to-moderate heart failure," *New England Journal of Medicine*, vol. 363, no. 25, pp. 2385–2395, 2010.

[4] Q. Zhang, Y. Zhou, and C. M. Yu, "Incidence, definition, diagnosis, and management of the cardiac resynchronization therapy nonresponder," *Current Opinion in Cardiology*, vol. 30, no. 1, pp. 40–49, 2015.

[5] V. Rai and D. K. Agrawal, "Role of vitamin D in cardiovascular diseases," *Endocrinology and Metabolism Clinics of North America*, vol. 46, no. 4, pp. 1039–1059, 2017.

[6] C. D'Amore, F. Marsico, A. Parente et al., "Vitamin D deficiency and clinical outcome in patients with chronic heart failure: a review," *Nutrition, Metabolism and Cardiovascular Diseases*, vol. 27, no. 10, pp. 837–849, 2017.

[7] W. L. Jiang, H. B. Gu, Y. F. Zhang, Q. Q. Xia, J. Qi, and J. C. Chen, "Vitamin D supplementation in the treatment of chronic heart failure: a meta-analysis of randomized controlled trials," *Clinical Cardiology*, vol. 39, no. 1, pp. 56–61, 2016.

[8] H. Sunman, A. Özkan, H. Yorgun et al., "Vitamin D levels predict the response to cardiac resynchronization therapy in patients with systolic heart failure," *Turk Kardiyoloji Dernegi Arsivi-Archives of the Turkish Society of Cardiology*, vol. 44, no. 8, pp. 670–676, 2016.

[9] A. Separham, L. Pourafkari, B. Kazemi et al., "Vitamin D deficiency and functional response to CRT in heart failure patients," *Herz*, vol. 44, no. 2, pp. 147–154, 2019.

[10] A. M. Boros, P. Perge, Z. Jenei et al., "Measurement of the red blood cell distribution width improves the risk prediction in cardiac resynchronization therapy," *Disease Markers*, vol. 2016, Article ID 7304538, 13 pages, 2016.

[11] A. M. Boros, G. Széplaki, P. Perge et al., "The ratio of the neutrophil leucocytes to the lymphocytes predicts the outcome after cardiac resynchronization therapy," *Europace*, vol. 18, no. 5, pp. 747–754, 2016.

[12] G. Széplaki, A. M. Boros, S. Szilágyi et al., "Complement C3a predicts outcome in cardiac resynchronization therapy of heart failure," *Inflammation Research*, vol. 65, no. 12, pp. 933–940, 2016.

[13] A. M. Boros, P. Perge, K. V. Nagy et al., "The impact of cardiac resynchronization therapy on routine laboratory parameters," *Interventional Medicine and Applied Science*, vol. 9, no. 1, pp. 1–8, 2017.

[14] P. Perge, A. M. Boros, S. Szilágyi et al., "Novel biomarkers in cardiac resynchronization therapy: hepatocyte growth factor is an independent predictor of clinical outcome," *Revista Española de Cardiología (English Edition)*, vol. 72, no. 1, pp. 48–55, 2019.

[15] P. E. Vardas, A. Auricchio, J. J. Blanc et al., "Guidelines for cardiac pacing and cardiac resynchronization therapy: the task force for cardiac pacing and cardiac resynchronization therapy of the European Society of Cardiology. Developed in collaboration with the European Heart Rhythm Association," *European Heart Journal*, vol. 28, no. 18, pp. 2256–2295, 2007.

[16] https://www.met.hu/eghajlat/magyarorszag_eghajlata/eghajlati_adatsorok/Budapest/adatok/napi_adatok/.

[17] E. Tanai and S. Frantz, "Pathophysiology of heart failure," *Comprehensive Physiology*, vol. 6, no. 1, pp. 187–214, 2015.

[18] A. Pourdjabbar, G. Dwivedi, and H. Haddad, "The role of vitamin D in chronic heart failure," *Current Opinion in Cardiology*, vol. 28, no. 2, pp. 216–222, 2013.

[19] Y. C. Li, J. Kong, M. Wei, Z. F. Chen, S. Q. Liu, and L. P. Cao, "1,25-Dihydroxyvitamin D_3 is a negative endocrine regulator of the renin-angiotensin system," *The Journal of Clinical Investigation*, vol. 110, no. 2, pp. 229–238, 2002.

[20] K. T. Weber, W. B. Weglicki, and R. U. Simpson, "Macro- and micronutrient dyshomeostasis in the adverse structural remodelling of myocardium," *Cardiovascular Research*, vol. 81, no. 3, pp. 500–508, 2009.

[21] R. U. Simpson, S. H. Hershey, and K. A. Nibbelink, "Characterization of heart size and blood pressure in the vitamin D receptor knockout mouse," *The Journal of Steroid Biochemistry and Molecular Biology*, vol. 103, no. 3-5, pp. 521–524, 2007.

[22] I. Gotsman, A. Shauer, D. R. Zwas et al., "Vitamin D deficiency is a predictor of reduced survival in patients with heart failure; vitamin D supplementation improves outcome," *European Journal of Heart Failure*, vol. 14, no. 4, pp. 357–366, 2012.

[23] D. Gruson, B. Ferracin, S. A. Ahn et al., "1,25-Dihydroxyvitamin D to PTH(1-84) ratios strongly predict cardiovascular death in heart failure," *PLoS One*, vol. 10, no. 8, article e0135427, 2015.

[24] K. K. Witte, R. Byrom, J. Gierula et al., "Effects of vitamin D on cardiac function in patients with chronic HF: the VINDICATE study," *Journal of the American College of Cardiology*, vol. 67, no. 22, pp. 2593–2603, 2016.

[25] A. Zittermann, J. B. Ernst, S. Prokop et al., "Vitamin D supplementation and bone turnover in advanced heart failure: the EVITA trial," *Osteoporosis International*, vol. 29, no. 3, pp. 579–586, 2018.

[26] A. C. Ross, J. A. E. Manson, S. A. Abrams et al., "The 2011 report on dietary reference intakes for calcium and vitamin D from the Institute of Medicine: what clinicians need to know," *The Journal of Clinical Endocrinology & Metabolism*, vol. 96, no. 1, pp. 53–58, 2011.

Hindawi
Disease Markers
Volume 2019, Article ID 1045098, 9 pages
https://doi.org/10.1155/2019/1045098

Research Article

Bone Mineral Density as a Predictor of Atherogenic Indexes of Cardiovascular Disease, Especially in Nonobese Adults

Tzyy-Ling Chuang,[1,2] **Jiunn-Wen Lin**,[3] **and Yuh-Feng Wang**[1,2]

[1]*Department of Nuclear Medicine, Dalin Tzu Chi Hospital, Buddhist Tzu Chi Medical Foundation, Chiayi, Taiwan*
[2]*School of Medicine, Tzu Chi University, Hualien, Taiwan*
[3]*Department of Cardiology, Dalin Tzu Chi Hospital, Buddhist Tzu Chi Medical Foundation, Chiayi, Taiwan*

Correspondence should be addressed to Yuh-Feng Wang; yuhfeng@gmail.com

Received 13 February 2019; Revised 10 May 2019; Accepted 27 June 2019; Published 4 September 2019

Guest Editor: Agata Bielecka-Dabrowa

Purpose. This study is aimed at determining whether bone mineral density (BMD) values are related to atherogenic indexes (AIs) and could predict the risk of cardiovascular disease (CVD) in southern Taiwanese adults. *Methods*. Medical records of 3249 adults who underwent health examinations between June 2014 and February 2018 at a regional hospital in southern Taiwan were reviewed. Data collected included health history, anthropomorphic characteristics, exercise habits, diets (vegetarian or nonvegetarian), clinical laboratory results (lipid profile, systemic blood pressure (SBP), glucose level, creatinine (Cre) level, and hemoglobin (Hb) level), and bone mineral density (BMD), which were used to identify the associations of these parameters, especially BMD, with lipid profile and calculated AIs through simple and multiple linear regressions. *Results*. The mean age of the patients was 58.0 years, and 71.4% were male. Body mass index (BMI), SBP, glucose level, Cre level, Hb level, and all BMD values were positively correlated with triglyceride (TG) level and AIs and were negatively correlated with high-density lipoprotein cholesterol (HDL-C) level. The significant positive correlations of BMD at all the measured sites with AIs remained after adjusting for age, sex, SBP, glucose level, Cre level, Hb level, smoking, exercise habits, and vegetarian state. The expanded adjusting model for TG/HDL-C remained significant at all the BMD measured sites in nonobese men, at bilateral femoral neck and total hips in nonobese women, and at the bilateral total hips in obese women. *Conclusions*. AIs are predictive markers for CVD, and BMD values are predictors of AIs, especially the novel AI, i.e., TG/HDL-C ratio, in nonobese adult men and women after dividing the patients into subgroups to eliminate the effect of BMI as a confounding factor. Thus, BMD values could predict AIs of CVD, especially in nonobese adults.

1. Introduction

Family history, age, smoking, hypertension, diabetes mellitus, low physical activity, and obesity are risk factors for coronary artery disease (CAD) [1]. Traditional lipid profile includes triglyceride (TG), total cholesterol (TCH), and low-density lipoprotein cholesterol (LDL-C), which are all atherogenic, and high-density lipoprotein cholesterol (HDL-C), which is cardioprotective [2–4]. Atherogenic indexes (AIs) are ratios that have atherogenic particles in the numerator and HDL-C in the denominator [5]. The ratios of TCH/HDL-C, LDL-C/HDL-C, and TG/HDL-C (a recent most novel index) could be predictors of CAD risk and extent [1, 5, 6]. Moreover, TCH/HDL-C and LDL-C/HDL-C ratios are useful and simple indexes of ischemic heart disease and cardiovascular disease (CVD) [1, 7, 8]. TG/HDL-C value is found to be a good marker for cardiometabolic risk ratio, and Log(TG/HDL-C) may be a strong marker for predicting the risk of CAD [8, 9].

Previous studies suggested that atherosclerosis and osteoporosis are linked by common risk factors and pathomechanisms [10–12]. Atherosclerosis could include calcified, noncalcified, or mixed lesions. Our previous study suggested that bone microarchitecture remodeling becomes more active when early coronary artery calcification (CAC) occurs [13]. A prediction model based on hypertension,

hyperlipidemia, TG, and L-spine T-score explained 73.2% of the variance of CAC [14]. Evaluating the correlation between CVD and bone mineral density (BMD) should take their respective factors into consideration. For example, age and menopause act on both in the same direction, whereas body mass index (BMI) acts on them in different directions [15].

The relationship of BMD and lipid profile, especially AIs, remains to be clearly established. HDL-C is reported to be inversely related to BMD [15–17]; however, some studies reported no [18] or positive [19] correlation between HDL-C and BMD. Results of other lipids showed inconsistency [18–23]. A previous study reported that TCH/HDL-C was positively correlated with both femoral neck BMD and total hip BMD [24]. This finding motivated us to conduct this study. Hence, our study is aimed at clarifying the relationship of BMD with AIs and at identifying whether BMD could be an indirect or direct predictor of CVD.

2. Materials and Methods

2.1. Subjects. This retrospective study included adults who underwent health examinations between June 2014 and February 2018 at the preventive medical center of a regional teaching hospital in southern Taiwan. Subjects who previously underwent internal fixation or total hip replacement at sites where BMD was measured were excluded. This study was approved by the ethics committee of our institution, who waived the requirement for informed consent from each patient. Questionnaire records included (1) history of hypertension, diabetes mellitus, and hyperlipidemia; (2) history of smoking and drinking; (3) anthropomorphic characteristics (age, sex, and BMI); (4) exercise habit of greater or equal to 3 times a week; and (5) diet habit of vegetarian or nonvegetarian.

BMI was defined as a person's weight in kilograms divided by the square of the person's height in meters (kg/m^2). We also divided the population into four subgroups according to sex and obesity status. Classification of nonobese (BMI ≤ 24.9) and obese (BMI ≥ 25.0) subjects was based on the values indicated by the World Health Organization.

2.2. Laboratory Data. The clinical laboratory findings obtained during health examinations included the following: TG, TCH, LDL-C, HDL-C, systolic blood pressure (SBP), glucose level before meal, creatinine (Cre) level, and hemoglobin (Hb) level. The three AIs in this study were TG/HDL-C, TCH/HDL-C, and LDL-C/HDL-C (atherogenic particles in the numerator and HDL-C in the denominator).

2.3. Bone Mineral Density. BMD was assessed by dual-energy X-ray absorptiometry (DXA) using a Discovery Wi DXA system (Hologic Inc.). The areas where BMD was measured included the lumbar spine, the bilateral femoral neck, and the total hip regions. The same densitometer was used for all the patients to ensure accurate comparisons.

2.4. Statistical Analysis. Results were expressed as mean ± standard deviation or number (percentage), as appropriate. Differences in means or frequencies were tested using the chi-square test or t-test, as appropriate. Simple linear regression analysis between the parameters and lipid profile and AIs was performed. Simple linear regression between the possible confounding parameters and BMD values was also analyzed. Multiple linear regression analysis was conducted using BMD values of each measured site as the independent variable and AIs as the dependent variables for three models adjusted for the following: (1) age and sex, (2) BMI, and (3) age, sex, SBP, glucose, Cre, Hb, smoking, exercise, and vegetarian. Further, multiple linear regression analysis of the novel AI (i.e., TG/HDL-C) and BMD values was performed for the subgroups after adjusting for age, SBP, glucose level, Cre level, Hb level, smoking, exercise, and vegetarian. All statistical analyses were performed using PASW Statistics 18 suite (SPSS Inc., Chicago, IL).

3. Results

3.1. Subject Characteristics. Medical records of 3249 adults were included. The demographic and clinical characteristics of the subjects are presented in Table 1. The study population was predominantly male (71.4%), with a mean age of 58.0 ± 11.2 years. Analysis of clinical characteristics indicated that 26.9% of the patients had hypertension, 9.6% had diabetes, and 6.9% had hyperlipidemia; moreover, 5.2% were smokers, 42.8% had the habit of exercise, and 42.8% were vegetarians. Significant differences between male and female subjects in smoking, exercise, or diet habits, BMI, SBP, Cre, Hb, TG, TCH, HDL-C, and three calculated AIs were found.

3.2. Simple Linear Regression. The lipid profile and AIs were the dependent variables. Age showed significant negative associations with all the lipid profile parameters, except HDL-C level, which showed no correlation. BMI, glucose level, and Hb level showed significant positive correlations with all the lipid profile parameters, except HDL-C level, which showed a negative association. SBP and Cre level were positively correlated with TG level and the three AIs and were inversely correlated with HDL-C level. Male gender and smoking habit were positively correlated with all lipid profile and AIs. Exercise showed negative correlation with atherogenic lipid profile and AIs. Vegetarian diet had negative relationship with TCH, LDL-C, HDL-C, TCH/HDL-C, and LDL-C/HDL-C (Table 2).

3.3. Bone Mineral Density. Mean lumbar spine BMD values on DXA were 0.988 ± 0.148 g/cm^2 for men, 0.878 ± 0.146 g/cm^2 for women, and 0.957 ± 0.156 g/cm^2 for all patients. Significant differences in BMD values of the lumbar spine, bilateral femoral neck, and total hip regions between males and females were observed (Table 1).

Moreover, BMD of all the measured sites was significantly positively correlated with TG level and the three AIs and was negatively associated with HDL-C level. All BMD values, except the left femoral neck BMD value, were negatively correlated with TCH level. BMD values at all the sites had no statistically significant relationship with LDL-C levels (Table 2).

For all measured sites, elder age and vegetarian had lower BMDs; moreover, male gender, BMI, Cre, Hb, and smoking

Table 1: Demographic and clinical characteristics of study participants.

N	All 3249	Male 2320	Female 929	p value
Age (range) (years)	58.0 ± 11.2 (16–90)	57.9 ± 11.4 (16–90)	58.4 ± 10.6 (20–88)	0.300
Smoking (%)	169 (5.2)	165 (7.1)	4 (0.4)	**<0.001**
Hypertension (%)	875 (26.9)	633 (27.3)	242 (26.0)	0.473
Diabetes mellitus (%)	311 (9.6)	229 (9.9)	82 (8.8)	0.361
Hyperlipidemia (%)	225 (6.9)	160 (6.9)	65 (7.0)	0.919
Exercise	1389 (42.8%)	1048 (45.2%)	341 (36.7%)	**<0.001**
Vegetarian	1392 (42.8%)	863 (37.2%)	529 (56.9%)	**<0.001**
BMI (kg/m^2)	24.4 ± 3.4	24.7 ± 3.3	23.5 ± 3.5	**<0.001**
SBP (mmHg)	130.0 ± 20.0	131.6 ± 19.1	124.3 ± 20.4	**<0.001**
Glucose (mg/dL)	107.0 ± 22.4	107.4 ± 22.8	105.9 ± 21.3	0.096
Cre (mg/dL)	1.00 ± 0.31	1.07 ± 0.29	0.82 ± 0.29	**<0.001**
Hb (g/dL)	14.7 ± 1.6	15.3 ± 1.3	13.4 ± 1.3	**<0.001**
TG (mg/dL)	125.1 ± 75.1	130.1 ± 79.1	112.6 ± 62.5	**<0.001**
TCH (mg/dL)	180.9 ± 37.0	178.1 ± 36.8	187.8 ± 36.7	**<0.001**
LDL-C (mg/dL)	117.3 ± 31.8	116.6 ± 31.6	119.0 ± 32.2	0.052
HDL-C (mg/dL)	46.0 ± 13.8	43.4 ± 12.4	52.3 ± 14.9	**<0.001**
TG/HDL-C	3.2 ± 2.6	3.4 ± 2.8	2.5 ± 2.0	**<0.001**
TCH/HDL-C	4.2 ± 1.3	4.4 ± 1.3	3.8 ± 1.2	**<0.001**
LDL-C/HDL-C	2.8 ± 1.0	2.9 ± 1.0	2.5 ± 0.9	**<0.001**
L-spine BMD (g/cm^2)	0.957 ± 0.156	0.988 ± 0.148	0.878 ± 0.146	**<0.001**
Right hip neck BMD (g/cm^2)	0.710 ± 0.126	0.736 ± 0.122	0.647 ± 0.112	**<0.001**
Right hip total BMD (g/cm^2)	0.820 ± 0.147	0.861 ± 0.133	0.720 ± 0.134	**<0.001**
Left hip neck BMD (g/cm^2)	0.710 ± 0.126	0.735 ± 0.122	0.646 ± 0.112	**<0.001**
Left hip total BMD (g/cm^2)	0.824 ± 0.149	0.865 ± 0.134	0.724 ± 0.136	**<0.001**

Values in bold represent significant values ($p < 0.05$). BMI: body mass index; SBP: systolic blood pressure; Cre: creatinine; Hb: hemoglobin; TG: triglyceride; TCH: total cholesterol; LDL-C: low-density lipoprotein cholesterol; HDL-C: high-density lipoprotein cholesterol.

had positive effect with BMDs. SBP and glucose showed positive correlation with BMD values of lumbar spine and bilateral total hips. Exercise only had significant positive relationship with the left total hip BMD (Table 3).

3.4. Multiple Linear Regression. In the analysis of the association of BMD and AIs, multivariate linear regression showed that BMD values at all the regions were positively correlated with AIs in model 1 and model 3 (Table 4). However, in model 2 (adjusted for BMI), all BMD values had a positive correlation with TG/HDL-C ratio but had no relationship with LDL-C/HDL-C ratio. In addition, only the total hip BMD values were positively correlated with TCH/HDL-C ratio (Table 4).

3.5. Subgroup Characteristics. Of the 3249 subjects, 1998 were nonobese (women 656 and men 1342) and 1251 were obese (women 273 and men 978). Multiple regression analysis at sites of BMD and AI of TG/HDL-C ratio in subgroups dividing by sex and obesity after adjustment of age, SBP, glucose, Cre, Hb, smoking, habits of exercise, and vegetarian diet showed major significant positive correlations in all regions at male nonobese subgroup, in bilateral femoral neck and total hip regions at female nonobese subgroup, and in bilateral total hip regions of obese females (Table 5).

4. Discussion

Lipid abnormalities, such as elevated TCH and LDL-C levels or low HDL-C level, are related to atherosclerosis [5], and TCH/HDL-C and LDL-C/HDL-C ratios have been shown to be good predictors of CAD than lipid alone [1, 4, 6]. High TG-low HDL-C dyslipidemia, which is the consequence of abdominal obesity and insulin resistance, is commonly associated with an increased concentration of small, dense LDL particles, which are atherogenic [1]. Although some lipid variables are associated with CAD extent, the TG/HDL-C ratio showed the strongest association with CAD extent [5]. Moreover, a previous study of Chinese patients with type II diabetes with stable CAD demonstrated that elevated TG/HDL-C ratio could also be a useful predictor of future cardiovascular events [25].

Yamaguchi et al. and Poli et al. found an inverse association between BMD and serum LDL-C levels in postmenopausal women, but somewhat different in the BMD

Table 2: Simple linear regression for the data analysis: correlation between parameters and lipid profiles and atherogenic indexes by simple regression analysis.

	TG		TCH		LDL-C		HDL-C		TG/HDL-C		TCH/HDL-C		LDL-C/HDL-C	
	r	*p*	*r*	*p*	*r*	*p*	*r*	*p*	*r*	*p*	*r*	*p*	*r*	*p*
Age	*-0.066*	**<0.001**	*-0.048*	**0.006**	*-0.069*	**<0.001**	0.010	0.562	*-0.57*	**0.001**	*-0.045*	**0.010**	*-0.060*	**0.001**
Sex (male = 1, female = 0)	0.321	**<0.001**	0.318	**<0.001**	0.431	**<0.001**	0.323	**<0.001**	0.427	**<0.001**	0.321	**<0.001**	0.318	**<0.001**
BMI	0.270	**<0.001**	0.046	**0.008**	0.103	**<0.001**	*-0.353*	**<0.001**	0.293	**<0.001**	0.346	**<0.001**	0.322	**<0.001**
SBP	0.088	**<0.001**	0.026	0.139	0.031	0.077	*-0.102*	**<0.001**	0.092	**<0.001**	0.110	**<0.001**	0.096	**<0.001**
Glucose	0.177	**<0.001**	0.045	**0.010**	0.036	**0.042**	*-0.135*	**<0.001**	0.171	**<0.001**	0.150	**<0.001**	0.116	**<0.001**
Cre	0.104	**<0.001**	*-0.030*	0.082	*-0.011*	0.540	*-0.151*	**<0.001**	0.129	**<0.001**	0.129	**<0.001**	0.110	**<0.001**
Hb	0.182	**<0.001**	0.122	**<0.001**	0.171	**<0.001**	*-0.180*	**<0.001**	0.183	**<0.001**	0.245	**<0.001**	0.252	**<0.001**
Smoking	0.076	**<0.001**	0.115	**<0.001**	0.081	**<0.001**	0.110	**<0.001**	0.073	**<0.001**	0.076	**<0.001**	0.115	**<0.001**
Exercise	*-0.070*	**<0.001**	*-0.075*	**<0.001**	*-0.076*	**<0.001**	0.021	0.222	*-0.056*	**0.001**	*-0.074*	**<0.001**	*-0.076*	**<0.001**
Vegetarian	-0.024	0.167	*-0.190*	**<0.001**	*-0.169*	**<0.001**	*-0.075*	**<0.001**	0.001	0.935	*-0.067*	**<0.001**	*-0.074*	**<0.001**
L-spine BMD	0.100	**<0.001**	*-0.049*	**0.005**	*-0.009*	0.623	*-0.188*	**<0.001**	0.130	**<0.001**	0.136	**<0.001**	0.125	**<0.001**
Right neck BMD	0.121	**<0.001**	*-0.039*	**0.026**	0.003	0.882	*-0.185*	**<0.001**	0.149	**<0.001**	0.143	**<0.001**	0.132	**<0.001**
Right total BMD	0.145	**<0.001**	*-0.037*	**0.034**	*-0.003*	0.848	*-0.215*	**<0.001**	0.164	**<0.001**	0.163	**<0.001**	0.142	**<0.001**
Left neck BMD	0.112	**<0.001**	*-0.029*	0.101	0.015	0.407	*-0.178*	**<0.001**	0.138	**<0.001**	0.144	**<0.001**	0.137	**<0.001**
Left total BMD	0.144	**<0.001**	*-0.036*	**0.038**	*-0.002*	0.914	*-0.232*	**<0.001**	0.168	**<0.001**	0.178	**<0.001**	0.154	**<0.001**

Values in bold represent significant values ($p < 0.05$), and values in *italic* represent negative correlation. BMI: body mass index; SBP: systolic blood pressure; Cre: creatinine; Hb: hemoglobin, TG: triglyceride; TCH: total cholesterol; LDL-C: low-density lipoprotein cholesterol; HDL-C: high-density lipoprotein cholesterol.

Table 3: Simple linear regression for the data analysis: correlation between possible confounding parameters and BMDs by simple regression analysis.

	L-spine BMD		Right neck BMD		Right total BMD		Left neck BMD		Left total BMD	
	r	*p*	*r*	*p*	*r*	*p*	*r*	*p*	*r*	*p*
Age	*-0.118*	**<0.001**	*-0.335*	**<0.001**	*-0.151*	**<0.001**	*-0.328*	**<0.001**	*-0.131*	**<0.001**
Sex (male = 1, female = 0)	0.321	**<0.001**	0.318	**<0.001**	0.431	**<0.001**	0.323	**<0.001**	0.427	**<0.001**
BMI	0.327	**<0.001**	0.336	**<0.001**	0.380	**<0.001**	0.343	**<0.001**	0.395	**<0.001**
SBP	0.076	**<0.001**	0.024	0.166	0.134	**<0.001**	0.026	0.133	0.130	**<0.001**
Glucose	0.059	**0.001**	*-0.017*	0.342	0.037	**0.034**	*-0.004*	0.801	0.052	**0.003**
Cre	0.161	**<0.001**	0.105	**<0.001**	0.179	**<0.001**	0.117	**<0.001**	0.180	**<0.001**
Hb	0.183	**<0.001**	0.248	**<0.001**	0.303	**<0.001**	0.252	**<0.001**	0.291	**<0.001**
Smoking	0.076	**<0.001**	0.115	**<0.001**	0.081	**<0.001**	0.110	**<0.001**	0.073	**<0.001**
Exercise	0.022	0.214	*-0.013*	0.460	0.021	0.228	*-0.013*	0.462	0.035	**0.043**
Vegetarian	*-0.164*	**<0.001**	*-0.156*	**<0.001**	*-0.123*	**<0.001**	*-0.170*	**<0.001**	*-0.117*	**<0.001**

Values in bold represent significant values ($p < 0.05$), and values in italic represent negative correlation. BMI: body mass index; SBP: systolic blood pressure; Cre: creatinine; Hb: hemoglobin.

measured sites [18, 19]. However, Adami et al. reported a significant positive association of serum LDL-C levels with BMD in elderly female subjects [20]. Inconsistent findings of the relationship of TCH level with BMD were also reported; moreover, some studies showed no significant correlation [21, 22]. In a South Korean population-based study of subjects aged 19–80 years, TCH and LDL-C levels were inversely associated with BMD in both premenopausal ($N = 375$) and postmenopausal ($N = 355$) women [23]. In a 2018 meta-analysis of postmenopausal women, TCH and LDL-C levels were higher in the osteoporosis group than in the normal bone density group [26]. In our study, we showed inverse relationships of TCH level with BMD at some sites (L-spine, right femoral neck, and bilateral total hips); however, no relationship between LDL-C level and BMD was observed.

In a prospective cohort of adults with type 1 diabetes and low-to-normal TG levels, TG at baseline independently predicted CAC progression over 6 years [27]. A previous study also showed that TG levels have a significant positive correlation with BMD values at the trochanter site among postmenopausal Korean women and a negative correlation with lumbar BMD values in the premenopausal Korean women [23]. A study in Saudi Arabia showed that glucose and TG are positively associated with total hip BMD [24], which is consistent with the findings

Table 4: Multiple linear regression for the data analysis: correlation between parameters of bone mineral density and atherogenic indexes by multiple regression analysis after adjustment.

	TG/HDL-C		TCH/HDL-C		LDL-C/HDL-C	
	r	*p*	*r*	*p*	*r*	*p*
Adjusted for age and sex						
L-spine BMD	0.080	**<0.001**	0.082	**<0.001**	0.068	**<0.001**
Right neck BMD	0.100	**<0.001**	0.089	**<0.001**	0.070	**<0.001**
Right total BMD	0.107	**<0.001**	0.087	**<0.001**	0.070	**<0.001**
Left neck BMD	0.085	**<0.001**	0.089	**<0.001**	0.076	**<0.001**
Left total BMD	0.114	**<0.001**	0.117	**<0.001**	0.086	**<0.001**
Adjusted for BMI						
L-spine BMD	0.038	**0.033**	0.026	0.137	0.022	0.219
Right neck BMD	0.057	**0.001**	0.030	0.083	0.027	0.123
Right total BMD	0.061	**0.001**	0.036	**0.040**	0.023	0.203
Left neck BMD	0.042	**0.018**	0.029	0.103	0.030	0.088
Left total BMD	0.063	**0.001**	0.049	**0.007**	0.032	0.079
Adjusted for age, sex, SBP, glucose, Cre, Hb, smoking, exercise, and vegetarian						
L-spine BMD	0.071	**<0.001**	0.070	**<0.001**	0.058	**0.001**
Right neck BMD	0.092	**<0.001**	0.077	**<0.001**	0.059	**0.002**
Right total BMD	0.088	**<0.001**	0.073	**<0.001**	0.047	**0.012**
Left neck BMD	0.076	**<0.001**	0.074	**<0.001**	0.062	**0.001**
Left total BMD	0.095	**<0.001**	0.095	**<0.001**	0.067	**<0.001**

Values in bold represent significant values ($p < 0.05$), and values in italic represent negative correlation. BMI: body mass index; SBP: systolic blood pressure; Cre: creatinine; Hb: hemoglobin; TG: triglyceride; TCH: total cholesterol; LDL-C: low-density lipoprotein cholesterol; HDL-C: high-density lipoprotein cholesterol.

Table 5: Multiple linear regression for the data analysis: correlation between parameters of bone mineral density and atherogenic index of TG/HDL-C in subgroups dividing by sex (female/male) and obesity (nonobese/obese) with multiple regression analysis after adjustment of age, SBP, glucose, Cre, Hb, smoking, exercise, and vegetarian.

Adjusted for age, SBP, glucose, Cre, Hb, smoking, exercise, and vegetarian	Female nonobese (656)		Female obese (273)		Male nonobese (1342)		Male obese (978)	
	r	*p*	*r*	*p*	*r*	*p*	*r*	*p*
L-spine BMD	0.076	0.076	0.029	0.663	0.061	**0.024**	0.004	0.907
Right neck BMD	0.134	**0.002**	0.113	0.087	0.060	**0.032**	*-0.012*	0.718
Right total BMD	0.089	**0.023**	0.166	**0.006**	0.070	**0.010**	*-0.049*	0.125
Left neck BMD	0.108	**0.011**	0.112	0.087	0.058	**0.039**	*-0.050*	0.134
Left total BMD	0.104	**0.008**	0.178	**0.003**	0.065	**0.016**	*-0.049*	0.118

Values in bold represent significant values ($p < 0.05$), and values in italic represent negative correlation. SBP: systolic blood pressure; Cre: creatinine; Hb: hemoglobin.

of a related study in Italy [20]. In our study, which involved Taiwanese adults, TG levels were shown to have a consistent significant positive correlation with BMD values at all the measured sites.

Furthermore, our study showed an inverse relationship between HDL-C level and BMD values at all the sites. In contrast, previous studies showed no [18], positive [19], or negative [15, 17] relationship in postmenopausal women. Moreover, a negative relationship was noted in healthy women and men after adjusting for weight, height, and fat mass in an Italian study [20]. HDL-C levels were not associated with BMD values at any of the sites in pre- and postmenopausal subjects in a study in Korea [23]. These differences could be attributed to different study populations, age distribution, race, statistical methods, and/or adjustments.

Alissa et al. reported that TCH/HDL-C ratio was positively correlated with both femoral neck BMD and total hip BMD in 180 postmenopausal women recruited from a catheterization laboratory [24]. Adami et al. also reported that LDL-C/HDL-C ratio in women showed significantly positive relationship with BMD values after adjusting for body weight, height, and fat mass [20]. A significant negative relationship was found between whole-body bone mineral content and HDL-C/LDL-C ratio in Chinese men and women [28]. In our study, we expanded the sample size to 3249 Taiwanese adults undergoing health exam, and BMD values at all the measured sites showed significant positive associations with all three AIs (TG/HDL-C, TCH/HDL-C, and LDL-C/HDL-C ratios) in nonadjusted and some adjusted conditions.

Log(TG/HDL-C) is a strong marker for the prediction of the risk of atherosclerosis, CAD, and CVD [7]; reflects the true relationship between protective and atherogenic lipoprotein; and is associated with the size of a pre- and anti-atherogenic lipoprotein particles [29]. And it is significantly positively correlated with BMI [7], so as our AI markers by naive linear regression without log. Similar to another study of HDL-C and BMD [15], the significant correlation of the novel AI, i.e., TG/HDL-C, with BMD disappeared when the correlative variables of sex and BMI were introduced. Hence, we divided our population into subgroups according to sex and BMI (obesity or nonobesity). After adjusting for age, SBP, glucose level, Cre level, Hb level, smoking, exercise, and vegetarian state, BMD at nonobese adults, except lumbar spines of nonobese women, still showed a significant positive relationship with TG/HDL-C ratio and can predict it. This is the most concrete evidence to support the purpose of our study. Moreover, total hip BMD values also could predict TG/HDL-C in the female obese subgroups. The lack of significance of lumbar spine BMD of nonobese women could be explained by the difficulty in lumbar spine BMD measurement in elderly subjects and the possibility of obtaining higher values owing to degenerative changes, such as aortic calcifications or osteophytes, which could in turn result in a "no association" finding [23]. To determine the true current status and a possible altered physiological condition after treatment, models were adjusted for clinical laboratory data instead of comorbidities.

Factors influencing BMD include age, sex, BMI, smoking, race, glucocorticoids, hyperlipidemia, and diabetes [30, 31]. A strong positive correlation between Cre clearance or Cre and bone mass or BMD values exists [32]. Our study also showed significant linear associations between Cre and TG levels and between Cre and AIs and an inverse correlation between Cre and HDL-C levels. A previous study found partial positive associations between Hb level and BMD in men but negative associations in women [33], whereas another study showed no relationship [34]. Interestingly, our data showed a significant positive association of Hb level with lipid profile, except HDL-C level, which showed a significant negative relationship, and AIs. Despite inconsistent results in the literature on smoking and BMD [35], they often showed inverse relationship [36]. Our opposite result (positive relationship) is probably due to the small percentage of smoking and older age of the nonsmoking population (58.4 ± 0.2 vs. 50.8 ± 0.9 years, $p < 0.001$). Significant high atherogenic indices and proatherogenic lipids (TG, TCH, LDL-C, very LDL-C, and non-HDL-C) were observed in smokers compared to controls [37, 38]. Exercise benefits BMD in premenopausal women [39] and maintains BMD in postmenopausal women [40]. Regular exercise improves HDL-C and decreases TG, TCH, LDL-C, and VLDL [41]. Physical exercise improves not only lipid profile but also AIs [42, 43]. Long-term practitioners of vegan vegetarian were found to being classified as having osteopenia of the femoral neck [44]. Another study showed that the proportion of subjects with osteopenia or osteoporosis also appeared comparable between vegetarians and nonvegetarians of both sex [45]. Vegetarian diets effectively lower blood concentrations of TCH, LDL-C, HDL-C, and non-HDL-C, but vegetarian diets did not significantly affect blood TG concentrations [46]. After adjustment for age, sex, SBP, glucose level, Cre level, Hb level, smoking, exercise, and vegetarian state, BMD values at all the measured sites showed a significant positive correlation with the three AIs.

Bone turnover is not simply regulated by osteoblasts and osteoclasts that produce and resorb bone, respectively. Bone formation involves other more complex elements at the molecular level. Atherosclerosis and vascular calcification are complicated dynamic processes related to the regulation of oxidized lipids, leptin, bone matrix proteins (osteopontin, osteocalcin, and bone morphogenetic protein), calcification inhibitors (osteoprotegerin, matrix Gla protein, and fetuin-A), osteogene expression, and inflammatory cytokines (TNF-α, CRP, and CD40-CD154) [11, 13, 47–50]. Moreover, exogenous lipids have been implicated in the regulation of osteoblastic differentiation [51, 52], and the products of cholesterol biosynthetic pathway are important for the proper development of marrow stromal cells. Studies have found that hypercholesterolemia and the resulting deposition and oxidation of lipids in tissues result in atherosclerosis [53] and are related to osteoporotic bone loss [54]. Thus, atherosclerosis is related not only to lipids but also to bone biosynthetic factors.

The conflicting findings between our study and those in some previous studies on the association of low BMD with cardiovascular risk or events [24, 55, 56] could be due to the difference in the interaction of calcified and noncalcified atherosclerosis with lipid pathway and could be because our study sample was composed of mostly normal and asymptomatic adults undergoing a health examination. Trabecular bone score value positively predicted moderate CAC but showed no association with the high CAC group in a previous study [13]. Non-HDL-C, which is a marker of subclinical atherosclerosis, was more strongly associated with CAC than with all other conventional lipid values [57]. Noninvasive methods could determine the presence and extent of CAD, especially by CAC, HDL-C, and TG/HDL-C ratio assays [58]. The use of BMD as a predictor of AIs of CVD is a novel concept.

However, this is a retrospective study and has some limitation. First, we had no information of body fat percent or fat mass, which may be confounding factors on the association between the BMD and AIs. Second, we did not have the medication data either. Lipid-lowering medications, such as statins and fibrates, have some effects on lipid profiles. Especially, statins are thought to have significant effects on both lipid profiles and BMD. However, since the percentage of hyperlipidemia is 6.9% and the population size is 3249 subjects, the possible interference to our result could be eliminated.

5. Conclusions

AIs are significant predictors of CVD, and BMD values are predictors of AIs. Observation showed significant positive relationships of BMD with the three AIs and especially with the AI of TG/HDL-C in nonobese men (at all the sites),

nonobese women (at the femoral neck and total hip), and obese women (at the total hip) after dividing the study subjects into subgroups and after further adjustments to eliminate the effect of BMI as a confounding factor. Thus, BMD values could predict the AIs of CVD, especially in nonobese adults.

Data Availability

The data used to support the findings of this study are available from the corresponding author upon request.

Conflicts of Interest

Tzyy-Ling Chuang, Jiunn-Wen Lin, and Yuh-Feng Wang declare that they have no conflict of interest regarding the publication of this article.

References

[1] I. Lemieux, B. Lamarche, C. Couillard et al., "Total cholesterol/HDL cholesterol ratio vs LDL cholesterol/HDL cholesterol ratio as indices of ischemic heart disease risk in men: the Quebec cardiovascular study," *Archives of Internal Medicine*, vol. 161, no. 22, pp. 2685–2692, 2001.

[2] W. P. Castelli, R. J. Garrison, P. W. Wilson, R. D. Abbott, S. Kalousdian, and W. B. Kannel, "Incidence of coronary heart disease and lipoprotein cholesterol levels: the Framingham study," *JAMA*, vol. 256, no. 20, pp. 2835–2838, 1986.

[3] T. Gordon, W. P. Castelli, M. C. Hjortland, W. B. Kannel, and T. R. Dawber, "High density lipoprotein as a protective factor against coronary heart disease. The Framingham study," *The American Journal of Medicine*, vol. 62, no. 5, pp. 707–714, 1977.

[4] W. P. Castelli, K. Anderson, P. W. F. Wilson, and D. Levy, "Lipids and risk of coronary heart disease The Framingham study," *Annals of Epidemiology*, vol. 2, no. 1-2, pp. 23–28, 1992.

[5] P. L. da Luz, D. Favarato, J. R. Faria-Neto Junior, P. Lemos, and A. C. P. Chagas, "High ratio of triglycerides to HDL-cholesterol predicts extensive coronary disease," *Clinics*, vol. 63, no. 4, pp. 427–432, 2008.

[6] M. K. Hong, P. A. Romm, K. Reagan, C. E. Green, and C. E. Rackley, "Usefulness of the total cholesterol to high-density lipoprotein cholesterol ratio in predicting angiographic coronary artery disease in women," *The American Journal of Cardiology*, vol. 68, no. 17, pp. 1646–1650, 1991.

[7] S. Niroumand, M. Khajedaluee, M. Khadem-Rezaiyan et al., "Atherogenic index of plasma (AIP): a marker of cardiovascular disease," *Medical Journal of the Islamic Republic of Iran*, vol. 29, p. 240, 2015.

[8] T. T. Wu, Y. Gao, Y. Y. Zheng, Y. T. Ma, and X. Xie, "Atherogenic index of plasma (AIP): a novel predictive indicator for the coronary artery disease in postmenopausal women," *Lipids in Health and Disease*, vol. 17, no. 1, p. 197, 2018.

[9] C. S. Weiler Miralles, L. M. Wollinger, D. Marin, J. P. Genro, V. Contini, and S. Morelo Dal Bosco, "Waist-to-height ratio (WHtR) and triglyceride to HDL-C ratio (TG/HDL-c) as predictors of cardiometabolic risk," *Nutrición Hospitalaria*, vol. 31, no. 5, pp. 2115–2121, 2015.

[10] D. P. Kiel, L. I. Kauppila, L. A. Cupples, M. T. Hannan, C. J. O'Donnell, and P. W. F. Wilson, "Bone loss and the progression of abdominal aortic calcification over a 25 year period: the Framingham heart study," *Calcified Tissue International*, vol. 68, no. 5, pp. 271–276, 2001.

[11] C. M. Giachelli, L. Liaw, C. E. Murry, S. M. Schwartz, and M. Almeida, "Osteopontin expression in cardiovascular diseases," *Annals of the New York Academy of Sciences*, vol. 760, 1 Osteopontin, pp. 109–126, 1995.

[12] L. B. Tanko, Y. Z. Bagger, and C. Christiansen, "Low bone mineral density in the hip as a marker of advanced atherosclerosis in elderly women," *Calcified Tissue International*, vol. 73, no. 1, pp. 15–20, 2003.

[13] T. L. Chuang, F. T. Hsiao, Y. D. Li, and Y. F. Wang, "TBS predict coronary artery calcification in adults," *BioMed Research International*, vol. 2016, Article ID 8391589, 6 pages, 2016.

[14] T.-L. Chuang, F.-T. Hsiao, Y.-D. Li, and Y.-F. Wang, "Bone mineral density in evaluation of the severity of coronary artery calcification," *Annals of Nuclear Medicine and Molecular Imaging*, vol. 30, no. 2, pp. 55–61, 2017.

[15] P. D'Amelio, S. Di Bella, C. Tamone et al., "HDL cholesterol and bone mineral density in normal-weight postmenopausal women: is there any possible association?," *Panminerva Medica*, vol. 50, no. 2, pp. 89–96, 2008.

[16] F. Orio, S. Palomba, T. Cascella, S. Savastano, G. Lombardi, and A. Colao, "Cardiovascular complications of obesity in adolescents," *Journal of Endocrinological Investigation*, vol. 30, no. 1, pp. 70–80, 2007.

[17] P. D'Amelio, G. P. Pescarmona, A. Gariboldi, and G. C. Isaia, "High density lipoproteins (HDL) in women with postmenopausal osteoporosis: a preliminary study," *Menopause*, vol. 8, no. 6, pp. 429–432, 2001.

[18] A. Poli, F. Bruschi, B. Cesana, M. Rossi, R. Paoletti, and P. G. Crosignani, "Plasma low-density lipoprotein cholesterol and bone mass densitometry in postmenopausal women," *Obstetrics and Gynecology*, vol. 102, no. 5, Part 1, pp. 922–926, 2003.

[19] T. Yamaguchi, T. Sugimoto, S. Yano et al., "Plasma lipids and osteoporosis in postmenopausal women," *Endocrine Journal*, vol. 49, no. 2, pp. 211–217, 2002.

[20] S. Adami, V. Braga, M. Zamboni et al., "Relationship between lipids and bone mass in 2 cohorts of healthy women and men," *Calcified Tissue International*, vol. 74, no. 2, pp. 136–142, 2004.

[21] E. J. Samelson, L. A. Cupples, M. T. Hannan et al., "Long-term effects of serum cholesterol on bone mineral density in women and men: the Framingham osteoporosis study," *Bone*, vol. 34, no. 3, pp. 557–561, 2004.

[22] L.-. Y. Wu, T.-. C. Yang, S.-. W. Kuo et al., "Correlation between bone mineral density and plasma lipids in Taiwan," *Endocrine Research*, vol. 29, no. 3, pp. 317–325, 2003.

[23] L. H. Cui, M. H. Shin, E. K. Chung et al., "Association between bone mineral densities and serum lipid profiles of pre- and post-menopausal rural women in South Korea," *Osteoporosis International*, vol. 16, no. 12, pp. 1975–1981, 2005.

[24] E. M. Alissa, W. A. Alnahdi, N. Alama, and G. A. Ferns, "Bone mineral density and cardiovascular risk factors in postmenopausal women with coronary artery disease," *BoneKEy Reports*, vol. 4, p. 758, 2015.

[25] S. H. Yang, Y. du, X. L. Li et al., "Triglyceride to high-density lipoprotein cholesterol ratio and cardiovascular events in diabetics with coronary artery disease," *The American Journal of the Medical Sciences*, vol. 354, no. 2, pp. 117–124, 2017.

[26] Y. Y. Chen, W. W. Wang, L. Yang, W. W. Chen, and H. X. Zhang, "Association between lipid profiles and osteoporosis in postmenopausal women: a meta-analysis," *European Review for Medical and Pharmacological Sciences*, vol. 22, no. 1, pp. 1–9, 2018.

[27] P. Bjornstad, D. M. Maahs, R. P. Wadwa et al., "Plasma triglycerides predict incident albuminuria and progression of coronary artery calcification in adults with type 1 diabetes: the coronary artery calcification in type 1 diabetes study," *Journal of Clinical Lipidology*, vol. 8, no. 6, pp. 576–583, 2014.

[28] Y. H. Hsu, S. A. Venners, H. A. Terwedow et al., "Relation of body composition, fat mass, and serum lipids to osteoporotic fractures and bone mineral density in Chinese men and women," *The American Journal of Clinical Nutrition*, vol. 83, no. 1, pp. 146–154, 2006.

[29] M. Dobiasova, J. Frohlich, M. Sedova, M. C. Cheung, and B. G. Brown, "Cholesterol esterification and atherogenic index of plasma correlate with lipoprotein size and findings on coronary angiography," *Journal of Lipid Research*, vol. 52, no. 3, pp. 566–571, 2011.

[30] M. Walker, A. C. Janot, M. Yu, H. K. Grewal, M. R. Lammi, and L. A. Saketkoo, "Assessment of protective factors of bone mineral density in a New Orleans sarcoidosis population," *American Journal of Respiratory and Critical Care Medicine*, vol. 191, article A3759, 2015.

[31] H.-S. Lee, "The factors influencing the bone mineral density in Korean adult men: based on Korea national health and nutrition examination survey 2010~2011 data," *Korean Journal of Community Nutrition*, vol. 22, no. 2, pp. 136–144, 2017.

[32] J. H. Huh, S. I. Choi, J. S. Lim, C. H. Chung, J. Y. Shin, and M. Y. Lee, "Lower serum creatinine is associated with low bone mineral density in subjects without overt nephropathy," *PLoS One*, vol. 10, no. 7, article e0133062, 2015.

[33] Y. H. Oh, J. H. Moon, and B. Cho, "Association between hemoglobin level and bone mineral density in Korean adults," *Journal of Bone Metabolism*, vol. 24, no. 3, pp. 161–173, 2017.

[34] R. J. Valderrábano, P. Buzkova, P. Y. Chang et al., "Association of bone mineral density with hemoglobin and change in hemoglobin among older men and women: the cardiovascular health study," *Bone*, vol. 120, pp. 321–326, 2019.

[35] D. Strozyk, T. M. Gress, and L. P. Breitling, "Smoking and bone mineral density: comprehensive analyses of the third National Health and Nutrition Examination Survey (NHANES III)," *Archives of Osteoporosis*, vol. 13, no. 1, p. 16, 2018.

[36] R. Ghadimi, S. R. Hosseini, S. Asefi, A. Bijani, B. Heidari, and M. Babaei, "Influence of smoking on bone mineral density in elderly men," *International Journal of Preventive Medicine*, vol. 9, no. 1, p. 111, 2018.

[37] N. S. Neki, "Lipid profile in chronic smokers – a clinical study," *JIACM*, vol. 3, no. 1, pp. 51–54, 2002.

[38] A. Agbecha and A. E. Ameh, "Atherogenic indices and smoking habits in cigarette smokers," *Environmental Disease*, vol. 3, no. 2, p. 38, 2018.

[39] G. A. Kelley, K. S. Kelley, and W. M. Kohrt, "Exercise and bone mineral density in premenopausal women: a meta-analysis of randomized controlled trials," *International Journal of Endocrinology*, vol. 2013, Article ID 741639, 16 pages, 2013.

[40] N. A. de Almeida Carvalho, S. Bittar, B. E. Matsuda Marangoni, and C. Santili, "The impact of exercising on bone mineral density in women exercising on bone mineral density," *Journal of Exercise, Sports & Orthopedics*, vol. 1, pp. 1–7, 2014.

[41] J. C. Oranwa, I. S. Ogbu, J. E. Ikekpeazu, K. C. Onyekwelu, E. A. Esom, and M. C. Ugonabo, "Lipid profile of people engaged in regular exercise," *Annals of Medical and Health Sciences Research*, vol. 7, pp. 36–39, 2017.

[42] Z. Stranska, M. Matoulek, Z. Vilikus, S. Svacina, and P. Stransky, "Aerobic exercise has beneficial impact on atherogenic index of plasma in sedentary overweigh and obese women," *Neuro Endocrinology Letters*, vol. 32, no. 1, pp. 102–108, 2011.

[43] S. Shen, Y. Lu, Y. Dang et al., "Effect of aerobic exercise on the atherogenic index of plasma in middle-aged Chinese men with various body weights," *International Journal of Cardiology*, vol. 230, pp. 1–5, 2017.

[44] J. F. Chiu, S. J. Lan, C. Y. Yang et al., "Long-term vegetarian diet and bone mineral density in postmenopausal Taiwanese women," *Calcified Tissue International*, vol. 60, no. 3, pp. 245–249, 1997.

[45] Y. F. Wang, J. S. Chiu, M. H. Chuang, J. E. Chiu, and C. L. Lin, "Bone mineral density of vegetarian and non-vegetarian adults in Taiwan," *Asia Pacific Journal of Clinical Nutrition*, vol. 17, no. 1, pp. 101–106, 2008.

[46] F. Wang, J. Zheng, B. Yang, J. Jiang, Y. Fu, and D. Li, "Effects of vegetarian diets on blood lipids: a systematic review and meta-analysis of randomized controlled trials," *Journal of the American Heart Association*, vol. 4, no. 10, article e002408, 2015.

[47] P. Lanzer, M. Boehm, V. Sorribas et al., "Medial vascular calcification revisited: review and perspectives," *European Heart Journal*, vol. 35, no. 23, pp. 1515–1525, 2014.

[48] K. Amann, "Media calcification and intima calcification are distinct entities in chronic kidney disease," *Clinical Journal of the American Society of Nephrology*, vol. 3, no. 6, pp. 1599–1605, 2008.

[49] J. C. Fleet and J. M. Hock, "Identification of osteocalcin mRNA in nonosteoid tissue of rats and humans by reverse transcription-polymerase chain reaction," *Journal of Bone and Mineral Research*, vol. 9, no. 10, pp. 1565–1573, 1994.

[50] Y. Tintut and L. L. Demer, "Recent advances in multifactorial regulation of vascular calcification," *Current Opinion in Lipidology*, vol. 12, no. 5, pp. 555–560, 2001.

[51] M. C. Kruger and D. F. Horrobin, "Calcium metabolism, osteoporsis and essential fatty acids: a review," *Progress in Lipid Research*, vol. 36, no. 2-3, pp. 131–151, 1997.

[52] B. A. Watkins, C. L. Shen, J. P. McMurtry et al., "Dietary lipids modulate bone prostaglandin E_2 production, insulin-like growth factor-I concentration and formation rate in chicks," *The Journal of Nutrition*, vol. 127, no. 6, pp. 1084–1091, 1997.

[53] R. Ross, "Atherosclerosis–an inflammatory disease," *The New England Journal of Medicine*, vol. 340, no. 2, pp. 115–126, 1999.

[54] F. Parhami, A. Garfinkel, and L. L. Demer, "Role of lipids in osteoporosis," *Arteriosclerosis, Thrombosis, and Vascular Biology*, vol. 20, no. 11, pp. 2346–2348, 2000.

[55] L. B. Tanko, C. Christiansen, D. A. Cox, M. J. Geiger, M. A. McNabb, and S. R. Cummings, "Relationship between osteoporosis and cardiovascular disease in postmenopausal women," *Journal of Bone and Mineral Research*, vol. 20, no. 11, pp. 1912–1920, 2005.

[56] E. J. Samelson, D. P. Kiel, K. E. Broe et al., "Metacarpal cortical area and risk of coronary heart disease: the Framingham study," *American Journal of Epidemiology*, vol. 159, no. 6, pp. 589–595, 2004.

[57] S. H. Orakzai, K. Nasir, M. Blaha, R. S. Blumenthal, and P. Raggi, "Non-HDL cholesterol is strongly associated with coronary artery calcification in asymptomatic individuals," *Atherosclerosis*, vol. 202, no. 1, pp. 289–295, 2009.

[58] A. B. A. Bampi, C. E. Rochitte, D. Favarato, P. A. Lemos, and P. L. da Luz, "Comparison of non-invasive methods for the detection of coronary atherosclerosis," *Clinics*, vol. 64, no. 7, pp. 675–682, 2009.

Hindawi
Disease Markers
Volume 2019, Article ID 5870239, 10 pages
https://doi.org/10.1155/2019/5870239

Research Article

Assessment of the SFlt-1 and sFlt-1/25(OH)D Ratio as a Diagnostic Tool in Gestational Hypertension (GH), Preeclampsia (PE), and Gestational Diabetes Mellitus (GDM)

Malgorzata Walentowicz-Sadlecka[1], **Piotr Domaracki**[1], **Pawel Sadlecki**[1], **Joanna Siodmiak**[2], **Marek Grabiec**[1], **Pawel Walentowicz**[1], **Maria Teresa Arias Moliz**[3] and **Grazyna Odrowaz-Sypniewska**[1]

[1]*Department of Obstetrics and Gynecology, L. Rydygier Collegium Medicum in Bydgoszcz, Nicolaus Copernicus University, ul. Ujejskiego 75, Bydgoszcz 85-168, Poland*
[2]*Department of Laboratory Medicine, L. Rydygier Collegium Medicum in Bydgoszcz, Nicolaus Copernicus University, M. Curie Skłodowskiej 9, Bydgoszcz 85-094, Poland*
[3]*Department of Microbiology, University of Granada, Avda. del Hospicio, 18071 Granada, Spain*

Correspondence should be addressed to Malgorzata Walentowicz-Sadlecka; walentowiczm@cm.umk.pl

Received 23 January 2019; Revised 3 May 2019; Accepted 17 June 2019; Published 6 August 2019

Guest Editor: Zhongjie Shi

Background. Placental soluble fms-like tyrosine kinase-1 (sFlt-1), an antagonist of vascular endothelial growth factor, is considered an etiological factor of endothelial damage in pregnancy pathologies. An increase in the sFlt-1 level is associated with alterations of endothelial integrity. In contrast, vitamin D exerts a protective effect and low concentrations of 25(OH)D may have an adverse effect on common complications of pregnancy, such as gestational hypertension (GH), preeclampsia (PE), and gestational diabetes mellitus (GDM). The aim of this study was to analyze the levels of sFlt-1 in Polish women with physiological pregnancies and pregnancies complicated by GH, PE, and GDM. Moreover, we analyzed relationships between the maternal serum sFlt-1 level and the sFlt-1 to 25(OH)D ratio and the risk of GH and PE. *Material and Methods*. The study included 171 women with complicated pregnancies; among them are 45 with GH, 23 with PE, and 103 with GDM. The control group was comprised of 36 women with physiological pregnancies. Concentrations of sFl-1 and 25(OH)D were measured before delivery, with commercially available immunoassays. *Results*. Women with GH differed significantly from the controls in terms of their serum sFlt-1 levels (5797 pg/ml vs. 3531 pg/ml, $p = 0.0014$). Moreover, a significant difference in sFlt-1 concentrations was found between women with PE and those with physiological pregnancies (6074 pg/ml vs. 3531 pg/ml, $p < 0.0001$). GDM did not exert a statistically significant effect on serum sFlt-1 levels. Both logistic regression and ROC analysis demonstrated that elevated concentration of sFlt-1 was associated with greater risk of GH (AUC = 0.70, $p = 0.0001$) and PE (AUC = 0.82, $p < 0.0001$). Also, the sFlt-1 to 25(OH)D ratio, with the cutoff values of 652 (AUC = 0.74, $p < 0.0001$) and 653 (AUC = 0.88, $p < 0.0001$), respectively, was identified as a significant predictor of GH and PE. *Conclusions*. Determination of the sFlt-1/25(OH)D ratio might provide additional important information and, thus, be helpful in the identification of patients with PE and GH, facilitating their qualification for intensive treatment and improving the neonatal outcomes.

1. Introduction

Preeclampsia (PE) and gestational diabetes mellitus (GDM) are two of the most important causes of pregnancy complications. The incidence of both these conditions has been gradually increasing worldwide, up to 5% for PE and up to 13% for GDM [1, 2]. Gestational hypertension (GH) is a leading cause of morbidity and mortality in pregnant women, fetuses, and newborns [3]. PE manifests after 20 weeks of gestation and constitutes a life-threatening condition for

both fetuses and pregnant women. The prevalence of GH increases with age and is higher in overweight and obese women [4].

The term "diabetes" refers to a group of metabolic diseases associated with hyperglycemia resulting from impaired secretion or function of insulin [5]. To be classified as gestational, diabetes needs to be detected for the first time during pregnancy [6]; the proportion of pregnancies complicated by GDM is estimated at 3-12% [7]. Aside from patient's age, the risk of GDM increases with body weight and is particularly high in obese women. A British population-based study demonstrated that the proportion of obese pregnant women has nearly doubled, from 9-10% in early 1990's to 16-19% in the first years of the 21st century [8]. Pregnant women with GDM are at increased risk of GH and PE; insulin resistance and hyperglycemia are associated with greater oxidative stress which contributes to endothelial dysfunction in blood vessels and predisposes to hypertension [9].

An antiangiogenic factor, soluble fms-like tyrosine kinase 1 (sFlt-1), was shown to play an important role in the pathogenesis of many conditions related to vascular endothelium. sFlt-1 is an endogenous inhibitor of vascular endothelial growth factor (VEGF). Binding to VEGF proteins, sFlt-1 reduces their pool that can interact with transmembrane receptors and, hence, attenuates the VEGF-mediated signaling [10]. This contributes to impairment of angiogenesis and greater vascular permeability leading to the loss of serum proteins [11]. Available evidence suggests that elevated levels of sFlt-1 might be associated with the occurrence of PE and other pregnancy complications, such as intrauterine growth restriction, preterm labor, and miscarriage [12]. Importantly, an increase in the sFlt-1 level can be observed well before the first clinical manifestations of gestational complications, which implies that this parameter could be used to distinguish between physiological and high-risk pregnancies [13].

Vitamin D deficiency is associated with endothelial dysfunction. Epidemiological studies demonstrated a link between the low maternal level of vitamin D and higher incidence of GH and showed that deficiency of this vitamin may be an independent risk factor of PE [14]. Activation of vitamin D receptors is known to promote VEGF expression; further, an adequate level of vitamin D and appropriate expression of vitamin D receptors (VDRs) were shown to be fundamental for angiogenic function of endothelial cells and their protection against oxidative damage [15]. In our previous study, we found a significant association between the low serum level of vitamin D and the risk of preeclampsia; the area under ROC curve (AUC) for serum vitamin D as a predictor of PE was 70.3% [16].

The aim of this study was to analyze serum levels of sFlt-1 and the values of the sFlt-1 to 25(OH)D ratio in Polish women with physiological pregnancies and pregnancies complicated by GH, PE, and GDM. Identification of a link between the sFlt-1 level and the risk of pregnancy complications could play an important role in the prediction of their occurrence, thus, contributing to better outcomes in pregnant women and their offspring.

2. Materials and Methods

The study, conducted in 2013-2015 at the Department of Obstetrics and Gynecology, Ludwik Rydygier Collegium Medicum in Bydgoszcz, Nicolaus Copernicus University of Torun, included 207 women with singleton pregnancies (all Caucasians of Polish nationality, residents of Kuyavian-Pomeranian Province). The age of the study participants ranged between 19 and 40 years.

The study group included 171 women—45 patients with GH, 23 with PE, and 103 with GDM. Women who presented with concomitant GH and GDM were excluded from the study. GH was defined as a systolic blood pressure > 140 mmHg or diastolic blood pressure > 90 mmHg on two or more measurements at least six hours apart, occurring after 20 weeks of gestation, without concomitant proteinuria. PE was defined as the onset of hypertension (systolic blood pressure ≥ 140 mmHg or diastolic blood pressure ≥ 90 mmHg) in a previously normotensive woman, coexisting with proteinuria (at least 0.3 g of protein in a 24-hour urine sample) without a concomitant urinary tract infection. GDM was detected based on the result of a 75 g oral glucose tolerance test (OGTT) conducted between 24 and 28 weeks of gestation. Women with GDM were stratified according to the type of this condition, G1 or G2, in line with the White classification [6]. Type A1 (corresponding to GDM G1) was defined as an abnormal result of OGTT, normal blood glucose levels during fasting and one/two hours after a meal, and the ability to control glycemia solely with a dietary modification. Type A2 (corresponding to GDM G2) was defined as an abnormal result of OGTT, abnormal glucose levels during fasting and/or after a meal, and the inability to control glycemia without additional therapy with insulin or other agents. All study patients presented with appropriate-for-gestational-age (AGA) pregnancies. Women after in vitro fertilization, as well as those with comorbidities, were excluded from the study. Serum concentrations of sFlt-1 and 25(OH)D were determined during hospital stay shortly before delivery. Women who presented with abnormal blood pressure were additionally examined for the severity of GH and the presence of PE. Other clinicodemographic variables included in the analysis were maternal age, parity, body mass index (BMI), gestational age at delivery, route of delivery, birth weight, and pH of the umbilical cord blood. The control group included 36 women with uncomplicated pregnancies, normal arterial blood pressure, and glucose concentrations. All blood samples were obtained in the third trimester, 1-7 days before delivery. All controls were matched for the gestational age.

2.1. Methods. 10 ml blood samples were obtained from the cubital vein and immediately separated by centrifugation. The sera were stored at -80°C until the analysis. Serum concentrations of sFlt-1 were determined with the fully automated Elecsys® electrochemiluminescence assay (Roche Diagnostics, Manheim, Germany). The assay was performed using Roche immunoanalyzer Elecsys® 2010/cobas e411, in line with the manufacturer's instruction. The detection range

of the assay was 10-85 000 pg/ml, and the limit of quantification amounted to 15 pg/ml. Interassay coefficient of variation (CV) for the sFlt-1 assay was 4.3% at a mean concentration of 98 pg/ml (PreciControl Multimarker 1, Roche Diagnostics, Manheim, Germany) and 3.8% at 1 020 pg/ml (PreciControl Multimarker 2, Roche Diagnostics, Manheim, Germany). The limit of detection for the test was 10 pg/ml. Serum 25(OH)D concentration was determined by ELISA (25-hydroxy vitamin D EIA), Immunodiagnostic Systems Ltd., in the Department of Laboratory Diagnostics, Ludwik Rydygier Collegium Medicum, Nicolaus Copernicus University in Torun; the sensitivity was 2.0 ng/ml (5 nmol/l) and the assay measured range was 2.7–152 ng/ml (6.8–380 nmol/l). A certified reference material (NIST Standard Reference Material (SRM) 972) was used for vitamin D measurement. The method remained under RIQAS control, and the results of the assay are within the reference range for this control. The inter- and intraassay variabilities were 5.3% and 4.6%. A concentration of 25(OH)D < 10 ng/ml (<25 nmol/l) was defined as deficiency, 10–29 ng/ml (25–74 nmol/l) has been accepted as insufficiency, and sufficient was when concentrations were between 30 and 100 ng/ml (75–250 nmol/l). In our previous study, we presented levels of serum vitamin D levels in all study subgroups [16].

2.2. Statistical Analyses. Statistical analyses were carried out with PQStat software, version 1.6. The significance of intergroup differences in sFlt-1 concentrations was verified with Mann-Whitney *U* test and Kruskal-Wallis test with Dunn's post hoc tests. Direction and power of relationships between serum sFlt-1, maternal age, pH of the umbilical cord blood, and birth weight were estimated based on Spearman's coefficients of rank correlation. Statistical significance of potential predictors of GH, PE, and GDM were verified in univariate and multivariate models of logistic regression. The roles of sFlt-1 and the sFlt-1 to 25(OH)D ratio as predictors of GH and PE were additionally verified on ROC analysis. The results of all the tests were considered significant at $p < 0.05$ and highly significant at $p < 0.01$.

The protocol of the study was approved by the Local Bioethics Committee at Ludwik Rydygier Collegium Medicum in Bydgoszcz (decision no. KB 502/2013), and written informed consent was sought from all participants.

3. Results

Patient age, parity, BMI, gestational age at delivery, route of delivery, birth weight, and pH of the umbilical cord blood were analyzed. The control group included 36 women with uncomplicated pregnancies, normal arterial blood pressure, and glucose concentrations. Baseline characteristics of study participants are presented in Table 1.

Women with GH differed significantly from the controls in terms of their sFlt-1 concentrations (5797 pg/ml vs. 3531 pg/ml, $p = 0.0014$; Table 2). Similarly, a significant difference was found between sFlt-1 concentrations in women with PE and the controls (6074 pg/ml vs. 3531 pg/ml, $p < 0.0001$; Table 3). However, no statistically significant differences were observed between sFlt-1 concentrations in women with GDM G1, women with GDM G2 and the controls (4301 pg/ml vs. 3704 pg/ml vs. 3531 pg/ml, $p = 1.0000$; Table 4).

Table 1: Baseline characteristics of the study participants.

Parameter	Study group ($N = 171$)	Control group ($N = 36$)	p
Age (years)	29.6 ± 5.2	29.4 ± 4.9	NS
BMI (kg/m^2)	27, 8 ± 2, 2	26, 9 ± 2, 4	NS
Parity	1.9 ± 1.1	1.8 ± 1.0	NS
pH of umbilical artery	7.35 ± 0, 09	7, 35 ± 0.07	NS
BMI (kg/m^2)	24, 8 ± 2, 0	25, 2 ± 2, 5	NS
Pregnancy (weeks)	38 ± 2, 96	40 ± 1, 08	NS
Caesarian sections (%)	43,3%	37,6%	NS
Weight of newborn (g)	3340 ± 680	3590 ± 430	NS
Systolic blood pressure (mmHg)	126,8 ± 13, 5	120,2 ± 9, 1	NS
Diastolic blood pressure (mmHg)	80, 3 ± 10, 3	76, 9 ± 8, 6	NS
GH status	$N = 45$	$N = 0$	—
Preeclampsia status	$N = 23$	$N = 0$	—
GDM status	$N = 103$	$N = 0$	—

Table 2: sFlt-1 concentration (pg/ml) in the group of patients with hypertension and the control group.

sFlt-1 (pg/ml)	Gestational hypertension ($N = 45$)	Control group ($N = 36$)	p value
Median range	5797 (4746-10277)	3531 (2672-4980)	$p = 0.0014$

Table 3: sFlt-1 concentration (pg/ml) in the group of women with preeclampsia and the control group.

sFlt-1 (pg/ml)	Preeclampsia ($N = 23$)	Control group ($N = 36$)	p value
Median range	6074 (5273-12448)	3531 (2672-4980)	$p < 0.0001$

While we must admit that our control group was relatively small ($N = 36$), the results for this group are consistent with those reported by other authors and fit within published reference limits for the third trimester [17].

Table 5 presents sFlt-1 concentrations stratified according to arterial pressure of the study participants. The levels of sFlt-1 increased with blood pressure and were the highest in the group of patients whose blood pressure exceeded 180/110 mmHg.

We also compared sFlt-1 levels in the groups of patients with adequate serum concentrations of 25(OH)D (≥20 ng/mL) and vitamin D deficiency. The results are presented in Table 6. The concentrations of sFlt-1 in patients with adequate serum levels of 25(OH)D (≥20 ng/ml) turned out to be significantly lower than in those with vitamin D insufficiency/deficiency (3356 pg/ml vs. 4452 pg/ml, $p = 0.0256$).

Table 4: sFlt-1 concentration (pg/ml) in the group of patients with gestational diabetes and the control group.

sFlt-1 (pg/ml)	GDM G1 ($N = 19$)	GDM G2 ($N = 84$)	Control group ($N = 36$)	p value
Median range	4301 (2384-5977)	3704 (2403-5153)	3531 (2673-4980)	$p = 1.0000$

Table 5: sFlt-1 concentration (pg/ml) in relation to blood pressure.

	sFlt-1 (pg/ml)			
	RR > 140/90	RR > 160/100	RR > 180/110	Control group
Median	5399	5880	6074	3531
Range	(4048–8232)	(4443–9239)	(5176–12325)	(2672–4980)
p value (vs. the control group)	0.0055	0.0015	0.0059	

Table 6: sFLT-1 levels in the group of patients with sufficient serum concentrations of 25(OH)D (>20 ng/ml) and with vitamin D insufficiency/deficiency (25(OH)D ≤ 20 ng/ml).

	sFlt-1 (pg/ml)	
	25(OH)D (ng/ml) ≤ 20	25(OH)D (ng/ml) > 20
Median	4452	3356
Range	(3137.5–6066.75)	(2447–5284)
p value	0.0256	

Then, we conducted a series of ROC analyses to verify whether sFlt-1 and the sFlt-1 to 25(OH)D ratio were significant predictors of GH and PE. The results are presented in Tables 7 and 8. Serum sFlt-1 turned out to be a significant predictor of GH ($p = 0.001$) and PE ($p < 0.0001$), with AUC equal 70.1% and 82.4, respectively (Figures 1 and 2). Also, the sFlt-1 to 25(OH)D ratio was identified as a significant predictor of both GH ($p < 0.0001$) and PE ($p < 0.0001$), with AUC amounting to 73.6% and 87.96%, respectively (Figures 3 and 4). In our present study, the serum sFlt-1 to 25(OH)D ratio (with the cutoff value of 652) was identified as a good predictor of GH on ROC analysis ($p < 0.0001$), with an AUC equal 73.6%. Moreover, the serum sFlt-1 to 25(OH)D ratio (with a similar cutoff value as above, 653) turned out to be a significant predictor of PE ($p < 0.0001$), with an AUC equal 87.96%.

Finally, multivariate logistic regression analysis was conducted to verify if serum sFlt-1 predicted GH and PE independently from other established risk factors (BMI ≥ 30 kg/m^2, age ≥ 35 years, primiparity) and low vitamin D levels. The results are presented in Tables 9 and 10. On multivariate logistic regression analysis, 25(OH)D was not identified as an independent predictor of either hypertension or preeclampsia ($p > 0.05$). The analysis identified serum sFlt-1 and BMI ≥ 30 kg/m^2 as independent predictors of GH. Furthermore, serum sFlt-1 turned out to be an independent predictor of PE on multivariate logistic regression analysis.

Table 7: Relationships between serum concentrations of sFlt-1 and the incidence of gestational hypertension (GH) and preeclampsia (PE); results of ROC (receiver operating characteristic) analysis.

Parameter	GH	PE
AUC	0.7012	0.8237
SE (AUC)	0.0489	0.0488
-95% CI	0.6055	0.7280
+95% CI	0.7970	0.9194
Z-statistic	3.9942	4.9837
p	0.0001	<0.0001
Cutoff value	9643	10488

Table 8: Relationship between serum concentrations of sFlt-1/25(OH)D index and the incidence of gestational hypertension (GH) and preeclampsia (PE); results of ROC analysis.

Parameter	GH	PE
AUC	0.7359	0.8796
SE (AUC)	0.0483	0.0354
-95% CI	0.6413	0.8101
+95% CI	0.8306	0.9490
Z-statistic	4.5472	5.6978
p	<0.0001	<0.0001
Cutoff value	652.37	653.19

4. Discussion

Impaired synthesis of placental biomarkers and vitamin D deficiency have been postulated as risk factors of many pregnancy pathologies; however, in the case of many such relationships, the exact pathogenic mechanisms are not fully understood. A growing body of evidence suggests that endothelial dysfunction may play an important role in the pathogenesis of many pregnancy complications [18].

VEGFs are essential for proper implantation of the placenta. Soluble type 1 receptor for VEGF (soluble fms-like tyrosine kinase 1 (sFlt-1)) probably plays an important role in many processes occurring during pregnancy, modulating function of VEGFs [19]. Placental ischemia was shown to be associated with the production of factors contributing to endothelial dysfunction, among them sFlt-1; the dysfunction of vascular endothelium can manifest as arterial hypertension and proteinuria [20–22].

Considering the results of many previous studies that documented the link between the sFlt-1 status and the occurrence of pregnancy pathologies, we verified whether a similar

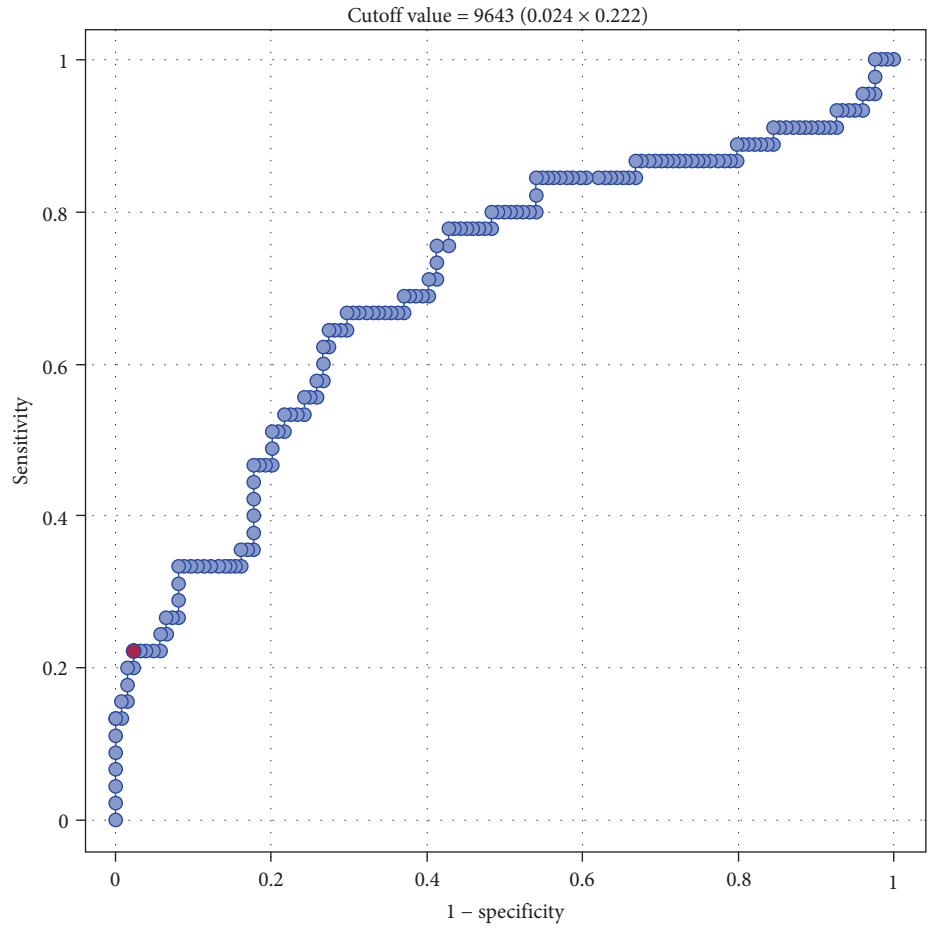

Figure 1: ROC curve—relationship between sFlt-1 concentrations (pg/ml) and occurrence of gestational hypertension (AUC 70.1%).

relationship existed in Polish women with GH. Our study showed that sFlt-1 concentrations in women with GH were significantly higher than in those with physiological pregnancies (5797 pg/ml vs. 3531 pg/ml, $p = 0.0014$) and serum sFlt-1 was identified as a significant predictor of GH on both logistic regression analysis and ROC analysis. On ROC analysis, serum sFlt-1 turned out to be a significant predictor of GH ($p = 0.001$), with an AUC equal 70.1%. Furthermore, multivariate logistic regression analysis identified elevated serum sFlt-1 and BMI $\geq 30\,kg/m^2$ as independent predictors of GH.

Our findings are consistent with the results published by Nanjo et al. [23] who demonstrated that prior to delivery, women with GH presented with significantly higher sFlt-1 levels than those without. Moreover, they found a significant correlation between the levels of circulating angiogenic factors shortly before delivery and the severity of hypertensive disorders in pregnancy [23]. Also, in our study, sFlt-1 concentrations increased with maternal blood pressure and were the highest in patients with arterial pressure exceeding 180/110 mmHg. This might be another argument for a role of sFlt-1 in endothelial damage. Possibly, the higher the blood pressure, the greater the endothelial damage and the more elevated the sFlt-1 levels. Our findings are consistent with the results of many previously published studies [24]. According to Verlohren et al., the sFlt-1/PlGF ratio allowed the identification of women at risk for imminent delivery and was a reliable tool to discriminate between various types of pregnancy-related hypertensive disorders [24].

Both available evidence and our present findings imply that sFlt-1 plays an important role in the pathogenesis of GH and PE, as well as in the clinical course of these conditions [25]. PE is diagnosed whenever a pregnant woman presents with hypertension and concomitant proteinuria. The proteinuria may be a consequence of glomerular damage which can be caused by binding sFlt-1 to VEGF and resultant destruction of vascular endothelium. The same mechanism may also be involved in glomerular damage in patients with GDM [26].

In this context, it is not surprising that patients with PE presented with the highest sFlt-1 concentrations of all pregnant women participating in our study. The concentration of sFlt-1 in the PE group turned out to be significantly higher than in the controls (6074 pg/ml vs. 3531 pg/ml, $p < 0.0001$). Furthermore, serum sFlt-1 was identified as a significant determinant of PE on ROC analysis ($p < 0.0001$), with AUC equal 82.4%. Serum sFlt-1 was also identified as an independent predictor of PE on multivariate logistic regression analysis. The elevated serum level of sFlt-1 was shown to be associated with higher risk of PE. sFlt-1 is known to

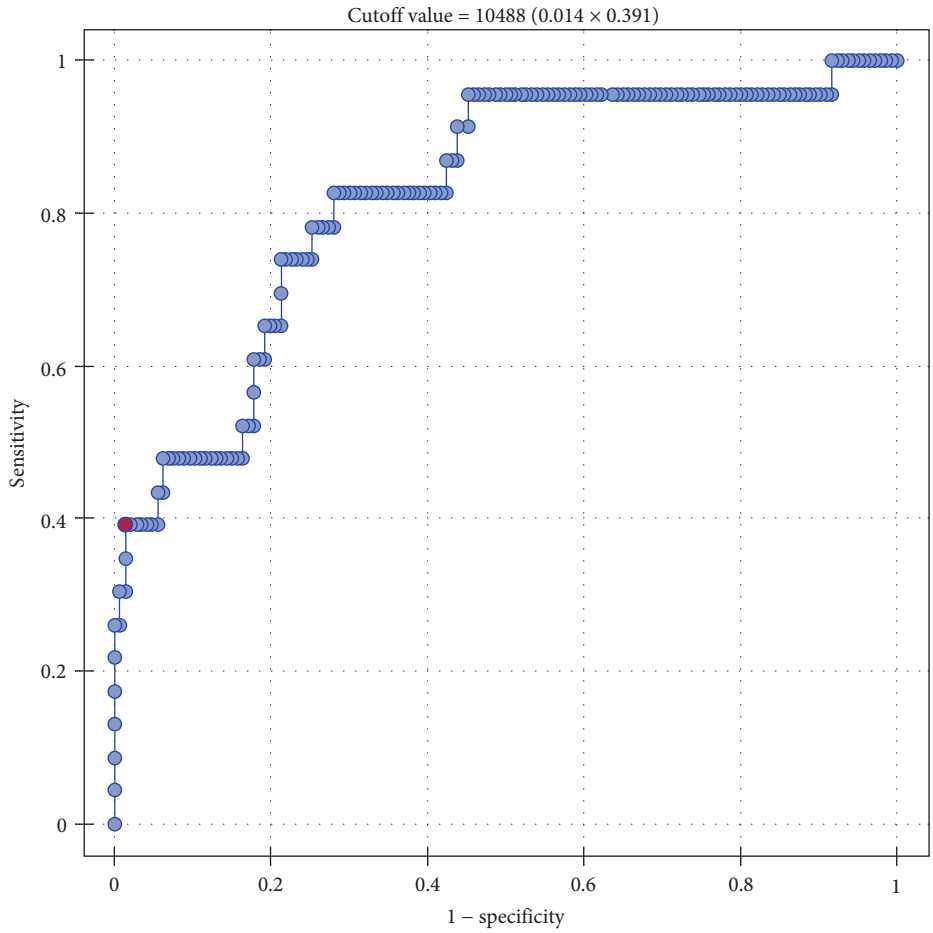

Figure 2: ROC curve—relationship between sFlt-1 concentrations (pg/ml) and occurrence of preeclampsia (AUC 82.4%).

contribute to endothelial damage, and hence, an increase in its concentration may negatively affect vascular integrity. The role of sFlt-1 in PE was a subject of many previous studies. Agrawal et al. conducted a meta-analysis to explore the predictive value of the sFlt-1/PlGF ratio in preeclampsia. The meta-analysis included 15 studies with a total of 534 cases of preeclampsia and 19587 controls. The sFlt-1/PlGF ratio had a pooled sensitivity of 80% (95% confidence interval, 0.68-0.88), specificity of 92% (95% confidence interval, 0.87-0.96), positive likelihood ratio of 10.5 (95% confidence interval, 6.2-18.0), and a negative likelihood ratio of 0.22 (95% confidence interval, 0.13-0.35) in predicting preeclampsia in both high- and low-risk patients. According to the authors of the meta-analysis, these findings imply that the sFlt-1/PlGF is a valuable screening tool for preeclampsia and might be helpful in decision-making, treatment stratification, and better resource allocation [27].

A recent prospective multicenter observational study PROGNOSIS (prediction of short-term outcome in pregnant women with suspected preeclampsia study) was designed to analyze the serum sFlt-1 to placental growth factor (PlGF) ratio as a predictor of PE during a short-term follow-up of women with singleton pregnancies (24 weeks and 0 days to 36 weeks and 6 days of gestation) suspected of this condition [28]. The study demonstrated that the sFlt-1 to PlGF ratio of 38 or less might be used to exclude PE in a short-term perspective in women suspected of this condition based on clinical presentation.

Although the role of the sFlt-1 to PlGF ratio raises no controversies, we still need more data about other potential predictors of GH and PE. Specifically, a reliable predictor of PE (and in particular the absence thereof) is needed in women with clinical suspicion of this pregnancy complication. Many women whose clinical presentation raises a suspicion of PE are hospitalized until this condition and other adverse outcomes have been excluded. At the same time, PE may be overlooked in other pregnant women who should be hospitalized. Although no preventive or therapeutic strategy for PE is yet available except low-dose acetylsalicylic acid treatment which was shown to exert a moderate preventive effect on high-risk pregnancies after the first trimester, clinical experience suggests that early detection and monitoring could be beneficial. Therefore, based on published evidence including the results of our previous study [16], we decided to verify whether sFlt-1 and 25(OH)D concentrations might be used as the measures of GH and pH risk. Our study demonstrated that women with adequate serum levels of 25(OH)D (≥20 ng/ml) presented with significantly lower levels of sFlt-1 than those with vitamin D deficiency (3356 pg/ml vs. 4452 pg/ml, $p = 0.0256$). This

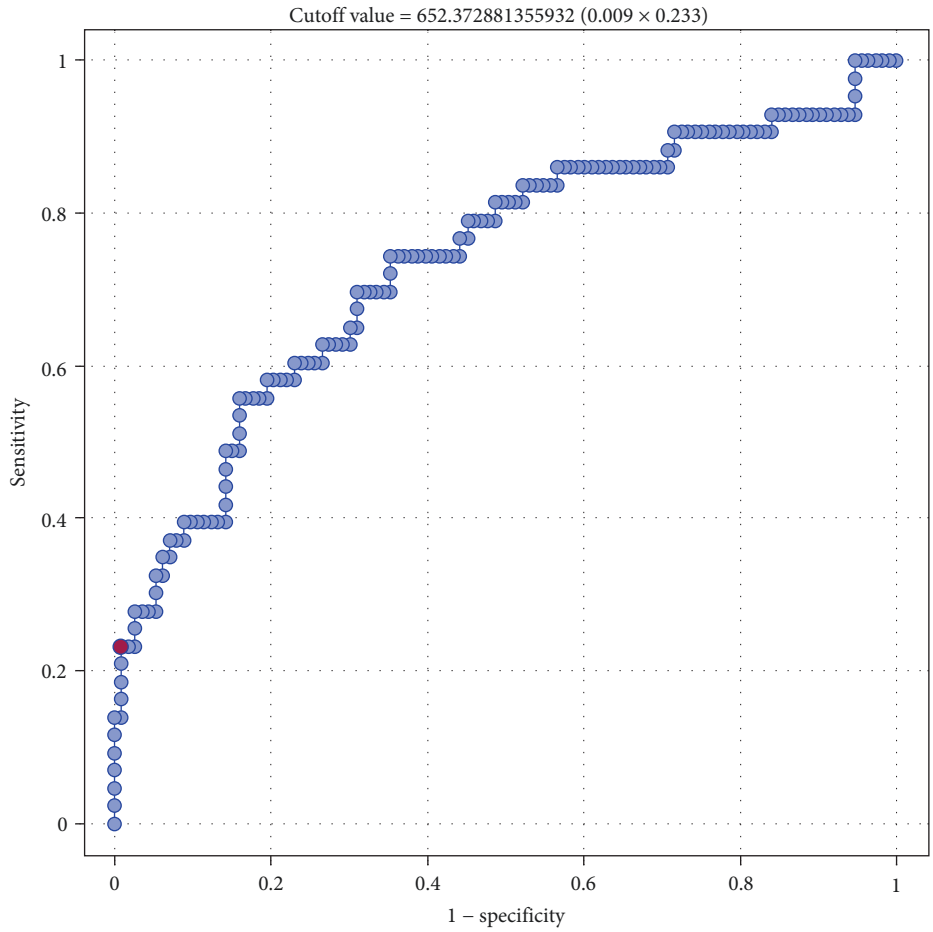

Figure 3: ROC curve—relationship between sFlt-1/25(OH)D index and occurrence of gestational hypertension (AUC 73.6%).

observation is consistent with the results published by Zeisler et al. [28]. According to those authors, 25(OH)D concentrations in women diagnosed with PE were significantly lower than those in patients without this condition and a low level of 25(OH)D was associated with increased risk of late-onset PE (odds ratio 4.6, 95% confidence interval 1.4-15). Interestingly, however, no similar association was found for early-onset PE. Furthermore, the study did not demonstrate a link between the 25(OH)D level and the sFlt-1 to PlGF ratio. Based on those findings, Álvarez-Fernández et al. concluded that low concentration of vitamin D in women with suspected late-onset PE is associated with increased risk of the imminent disease [29].

In our present study, the serum sFlt-1 to 25(OH)D ratio (with the cutoff value of 652) was identified as a good predictor of GH on ROC analysis ($p < 0.0001$), with an AUC equal 73.6%. Moreover, the serum sFlt-1 to 25(OH)D ratio (with a similar cutoff value as above, 653) turned out to be a significant predictor of PE ($p < 0.0001$), with an AUC equal 87.96%. Based on these findings, it can be speculated that sFlt-1 and 25(OH)D not only play an important role in the pathogenesis of GH and PE but can also be used as predictors thereof. A similar character of relationships between sFlt-1 and 25(OH)D levels and the risk of GH and PE might be explained by the fact that both those factors interfere with vascular endothelium [30]. However, in our present study, 25(OH)D did not turn out to be an independent predictor of either hypertension or preeclampsia on multivariate logistic regression analysis ($p > 0.05$).

The authors of one previous study, Ma et al. [31], verified whether vitamin D supplementation alleviated PE-associated endothelial dysfunction and explored the underlying mechanism of this relationship using a reduced uterine perfusion pressure (RUPP) rat model. 1,25(OH)2D turned out to significantly downregulate the expression of placental sFlt-1 in RUPP rats. Furthermore, circulating sFlt-1 levels in maternal serum correlated positively with the expression of placental sFlt-1 and returned to normal values after supplementation with vitamin D. Based on those findings, the authors concluded that vitamin D supplementation might have protected against the RUPP-induced endothelial dysfunction by downregulating placental sFlt-1, which could plausibly alleviate PE-related symptoms.

Another study, conducted by Song et al. [32], verified whether vitamin D supplementation could restore angiogenic balance and ameliorate inflammation in a rat model for PE. Animals from the supplemented group presented with significantly higher concentrations of VEGF and significantly lower sFlt-1 and TNF-α levels than untreated rats with PE. Therefore, the authors concluded that vitamin D

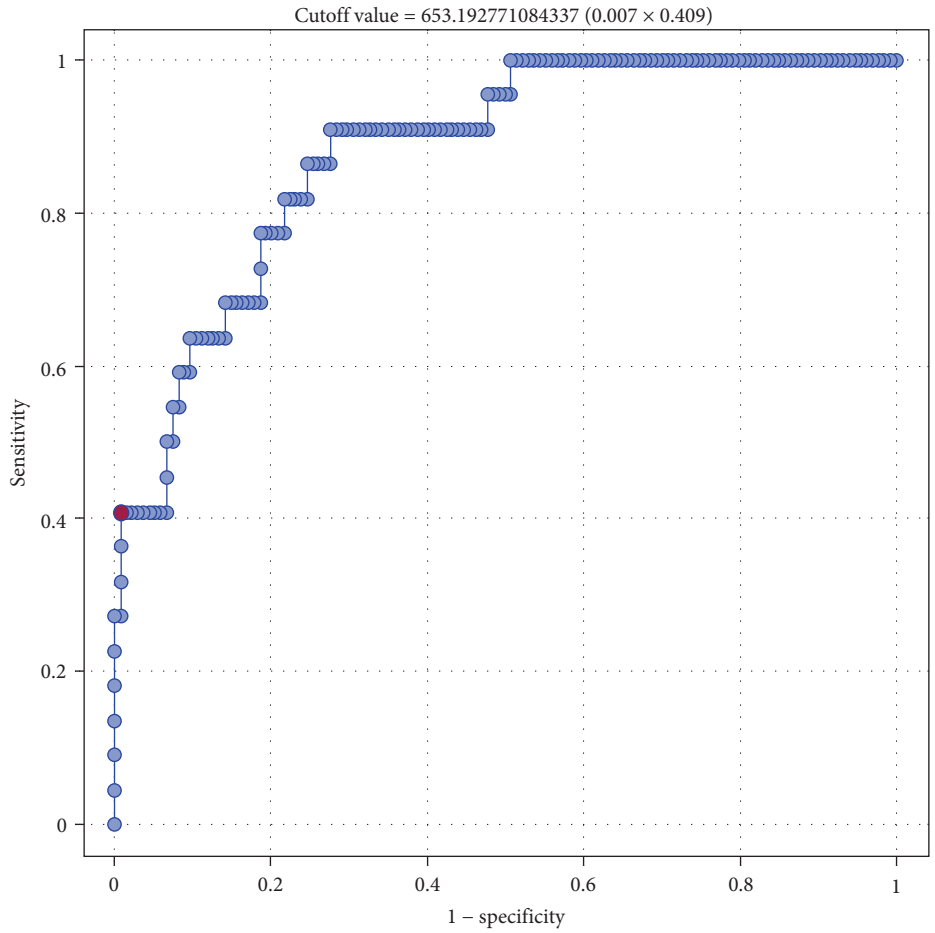

Figure 4: ROC curve—relationship between sFlt-1/25(OH)D index and occurrence of preeclampsia (AUC 87.96%).

Table 9: Results of multivariate logistic regression analyses examining the effects of serum sFlt-1 levels (pg/ml), BMI ≥ 30, age ≥ 35, primiparity, and 25(OH)D ≤ 20 ng/ml on the incidence of hypertension.

Parameter	*b*-coefficient	*p* value	Odds ratio	-95% CI	+95% CI
Intercept	-2.7821	0.0071	0.0619	0.0082	0.4687
sFlt-1 (pg/ml)	0.0004	0.0170	1.0004	1.0001	1.0007
BMI ≥ 30	2.7985	0.0003	16.4199	3.5615	75.7012
Age ≥ 35 years	-0.5656	0.5221	0.5680	0.1005	3.2093
Primiparity	0.6656	0.3842	1.9456	0.4345	8.7132
25(OH)D ≤ 20 ng/ml	0.1091	0.8875	1.1153	0.2459	5.0592

Table 10: Results of multivariate logistic regression analyses examining the effects of serum sFlt-1 levels (pg/ml), BMI ≥ 30, age ≥ 35, primiparity, and 25(OH)D ≤ 20 ng/ml on the incidence of preeclampsia.

Parameter	*b*-coefficient	*p* value	Odds ratio	-95% CI	+95% CI
Intercept	-5.6590	<0.0001	0.0035	0.0005	0.0250
sFlt-1 (pg/ml)	0.0004	0.0001	1.0004	1.0002	1.0006
BMI ≥ 30	0.6718	0.2829	1.9578	0.5745	6.6724
Age ≥ 35 years	-1.5500	0.2223	0.2122	0.0176	2.5585
Primiparity	0.9548	0.1540	2.5982	0.6991	9.6559
25(OH)D ≤ 20 ng/ml	1.0028	0.1331	2.7259	0.7365	10.0883

supplementation might play an important role in the restoration of angiogenic balance and attenuation of inflammation in pregnancy-induced hypertension [32].

Schulz et al. [33] demonstrated that sFlt-1 and VEGF gene expressions in the maternal subgroup with circulating $25(OH)D \geq 100$ ng/ml were significantly downregulated compared to the subgroup with $25(OH)D < 100$ ng/ml. Moreover, they found a significant association between the maternal vitamin D status and the expressions of sFlt-1 and VEGF at the mRNA level. Based on those findings, the authors stated that maternal supplementation with vitamin D3 may exert an effect on gene transcription in the placenta and, thus, may reduce the level of antiangiogenic factors that are implicated in vascular pregnancy complications [33].

Only few previous studies analyzed sFlt-1 levels in women with GDM, and their results are inconclusive. In our present study, we found no differences in sFlt-1 levels in the GDM G1 and GDM G2 groups and the controls (4301 pg/ml vs. 3704 pg/ml vs. 3532 pg/ml, $p = 1.00$). One potential explanation for this phenomenon might be the fact that our patients with GDM still did not develop an endothelial damage, and thus, their sFlt-1 concentrations remained within the normal range. In our opinion, no ultimate conclusions can be formulated on the role of sFlt in GDM and this issue needs to be addressed in further studies [34].

In conclusion, this study showed that determination of the sFlt-1 to 25(OH)D ratio may facilitate the identification of patients with preeclampsia and gestational hypertension and their qualification for intensive treatment, which can be reflected by better neonatal outcomes.

The results of our study, which can be considered preliminary findings, justify further clinical research on a larger group of patients, including measurements of vitamin D concentrations to calculate the ratio derived from this parameter aside from that based on sFLT-1 and PLGF levels.

Data Availability

The data used to support the findings of this study are available from the corresponding author upon request.

Ethical Approval

The protocol of the study was approved by the Local Bioethics Committee at Ludwik Rydygier Collegium Medicum in Bydgoszcz (decision no. KB 502/2013), and written informed consent was sought from all participants.

Conflicts of Interest

The authors declare that they have no competing interests.

References

[1] T. A. Buchanan, A. H. Xiang, and K. A. Page, "Gestational diabetes mellitus: risks and management during and after pregnancy," *Nature Reviews Endocrinology*, vol. 8, no. 11, pp. 639–649, 2012.

[2] C. Y. Su, H. C. Lin, H. C. Cheng, A. M. F. Yen, Y. H. Chen, and S. Kao, "Pregnancy outcomes of anti-hypertensives for women with chronic hypertension: a population-based study," *PLoS One*, vol. 8, no. 2, article e53844, 2013.

[3] T. E. R. Gillon, A. Pels, P. von Dadelszen, K. MacDonell, and L. A. Magee, "Hypertensive disorders of pregnancy: a systematic review of international clinical practice guidelines," *PLoS One*, vol. 9, no. 12, article e113715, 2014.

[4] R. M. Nilsen, E. S. Vik, S. A. Rasmussen et al., "Preeclampsia by maternal reasons for immigration: a population-based study," *BMC Pregnancy and Childbirth*, vol. 18, no. 1, p. 423, 2018.

[5] J. F. Plows, J. L. Stanley, P. N. Baker, C. M. Reynolds, and M. H. Vickers, "The pathophysiology of gestational diabetes mellitus," *International Journal of Molecular Sciences*, vol. 19, no. 11, article 3342, 2018.

[6] P. White, "Pregnancy complicating diabetes," *The American Journal of Medicine*, vol. 7, no. 5, pp. 609–616, 1949.

[7] A. Ferrara, "Increasing Prevalence of Gestational Diabetes Mellitus: A Public Health Perspective," *Diabetes Care*, vol. 30, Supplement 2, pp. S141–S146, 2007.

[8] *Confidental Enquiry into Maternal and Child Health: Pregancy in Women with Type 1 and Type 2 Diabetes in 2002-03 in England, Wales and Northern Ireland*, CEMACH London, 2005.

[9] A. Colatrella, V. Loguercio, L. Mattei et al., "Hypertension in diabetic pregnancy: impact and long-term outlook," *Best Practice & Research. Clinical Endocrinology & Metabolism*, vol. 24, no. 4, pp. 635–651, 2010.

[10] C. M. Failla, M. Carbo, and V. Morea, "Positive and negative regulation of angiogenesis by soluble vascular endothelial growth factor receptor-1," *International Journal of Molecular Sciences*, vol. 19, no. 5, p. 1306, 2018.

[11] G. Szalai, Y. Xu, R. Romero et al., "*In vivo* experiments reveal the good, the bad and the ugly faces of sFlt-1 in pregnancy," *PLoS One*, vol. 9, no. 11, article e110867, 2014.

[12] G. C. S. Smith, J. A. Crossley, D. A. Aitken et al., "Circulating angiogenic factors in early pregnancy and the risk of preeclampsia, intrauterine growth restriction, spontaneous preterm birth, and stillbirth," *Obstetrics & Gynecology*, vol. 109, no. 6, pp. 1316–1324, 2007.

[13] H. Stepan, I. Herraiz, D. Schlembach et al., "Implementation of the sFlt-1/PlGF ratio for prediction and diagnosis of preeclampsia in singleton pregnancy: implications for clinical practice," *Ultrasound in Obstetrics & Gynecology*, vol. 45, no. 3, pp. 241–246, 2015.

[14] M. Tabesh, A. Salehi-Abargouei, M. Tabesh, and A. Esmaillzadeh, "Maternal vitamin D status and risk of preeclampsia: a systematic review and meta-analysis," *The Journal of Clinical Endocrinology and Metabolism*, vol. 98, no. 8, pp. 3165–3173, 2013.

[15] W. Zhong, B. Gu, Y. Gu, L. J. Groome, J. Sun, and Y. Wang, "Activation of vitamin D receptor promotes VEGF and CuZn-SOD expression in endothelial cells," *The Journal of Steroid Biochemistry and Molecular Biology*, vol. 140, pp. 56–62, 2014.

[16] P. Domaracki, P. Sadlecki, G. Odrowaz-Sypniewska et al., "Serum 25(OH) vitamin D levels in Polish women during pregnancies complicated by hypertensive disorders and gestational diabetes," *International Journal of Molecular Sciences*, vol. 17, no. 10, article 1574, 2016.

[17] C. Birdir, L. Droste, L. Fox et al., "Predictive value of sFlt-1, PlGF, sFlt-1/PlGF ratio and PAPP-A for late-onset

preeclampsia and IUGR between 32 and 37 weeks of pregnancy," *Pregnancy Hypertension*, vol. 12, pp. 124–128, 2018.

[18] L. Huang, R. Sauve, N. Birkett, D. Fergusson, and C. van Walraven, "Maternal age and risk of stillbirth: a systematic review," *Canadian Medical Association Journal*, vol. 178, no. 2, pp. 165–172, 2008.

[19] H. Lehnen, N. Mosblech, T. Reineke et al., "Prenatal clinical assessment of sFlt-1 (soluble fms-like tyrosine kinase-1)/PlGF (placental growth factor) ratio as a diagnostic tool for pre-eclampsia, pregnancy-induced hypertension, and proteinuria," *Geburtshilfe und Frauenheilkunde*, vol. 73, no. 5, pp. 440–445, 2013.

[20] S. E. Maynard, J. Y. Min, J. Merchan et al., "Excess placental soluble fms-like tyrosine kinase 1 (sFlt1) may contribute to endothelial dysfunction, hypertension, and proteinuria in pre-eclampsia," *The Journal of Clinical Investigation*, vol. 111, no. 5, pp. 649–658, 2003.

[21] J. Pottecher, O. Huet, V. Degos et al., "*In vitro* plasma-induced endothelial oxidative stress and circulating markers of endothelial dysfunction in preeclampsia: an observational study," *Hypertension in Pregnancy*, vol. 28, no. 2, pp. 212–223, 2009.

[22] W. P. Mutter and S. A. Karumanchi, "Molecular mechanisms of preeclampsia," *Microvascular Research*, vol. 75, no. 1, pp. 1–8, 2008.

[23] S. Nanjo, S. Minami, M. Mizoguchi et al., "Levels of serum-circulating angiogenic factors within 1 week prior to delivery are closely related to conditions of pregnant women with pre-eclampsia, gestational hypertension, and/or fetal growth restriction," *The Journal of Obstetrics and Gynaecology Research*, vol. 43, no. 12, pp. 1805–1814, 2017.

[24] S. Verlohren, I. Herraiz, O. Lapaire et al., "The sFlt-1/PlGF ratio in different types of hypertensive pregnancy disorders and its prognostic potential in preeclamptic patients," *American Journal of Obstetrics and Gynecology*, vol. 206, no. 1, pp. 58.e1–58.e8, 2012.

[25] A. Leaños-Miranda, F. Méndez-Aguilar, K. L. Ramírez-Valenzuela et al., "Circulating angiogenic factors are related to the severity of gestational hypertension and preeclampsia, and their adverse outcomes," *Medicine*, vol. 96, no. 4, article e6005, 2017.

[26] C. H. Ku, K. E. White, A. Dei Cas et al., "Inducible overexpression of sFlt-1 in podocytes ameliorates glomerulopathy in diabetic mice," *Diabetes*, vol. 57, no. 10, pp. 2824–2833, 2008.

[27] S. Agrawal, A. S. Cerdeira, C. Redman, and M. Vatish, "Meta-analysis and systematic review to assess the role of soluble FMS-like tyrosine kinase-1 and placenta growth factor ratio in prediction of preeclampsia: the SaPPPhirE Study," *Hypertension*, vol. 71, no. 2, pp. 306–316, 2018.

[28] H. Zeisler, E. Llurba, F. Chantraine et al., "Predictive value of the sFlt-1:PlGF ratio in women with suspected preeclampsia," *The New England Journal of Medicine*, vol. 374, no. 1, pp. 13–22, 2016.

[29] I. Álvarez-Fernández, B. Prieto, V. Rodríguez, Y. Ruano, A. I. Escudero, and F. V. Álvarez, "Role of vitamin D and sFlt-1/PlGF ratio in the development of early- and late-onset pre-eclampsia," *Clinical Chemistry and Laboratory Medicine*, vol. 53, no. 7, pp. 1033–1040, 2015.

[30] Z. Xiao, S. Li, Y. Yu et al., "VEGF-A regulates sFlt-1 production in trophoblasts through both Flt-1 and KDR receptors," *Molecular and Cellular Biochemistry*, vol. 449, no. 1-2, pp. 1–8, 2018.

[31] S. L. Ma, X. Y. Tian, Y. Q. Wang, H. F. Zhang, and L. Zhang, "Vitamin D supplementation prevents placental ischemia induced endothelial dysfunction by downregulating placental soluble FMS-like tyrosine kinase-1," *DNA and Cell Biology*, vol. 36, no. 12, pp. 1134–1141, 2017.

[32] J. Song, Y. Li, and R. An, "Vitamin D restores angiogenic balance and decreases tumor necrosis factor-α in a rat model of pre-eclampsia," *The Journal of Obstetrics and Gynaecology Research*, vol. 43, no. 1, pp. 42–49, 2017.

[33] E. V. Schulz, L. Cruze, W. Wei, J. Gehris, and C. L. Wagner, "Maternal vitamin D sufficiency and reduced placental gene expression in angiogenic biomarkers related to comorbidities of pregnancy," *The Journal of Steroid Biochemistry and Molecular Biology*, vol. 173, pp. 273–279, 2017.

[34] F. Troncoso, J. Acurio, K. Herlitz et al., "Gestational diabetes mellitus is associated with increased pro-migratory activation of vascular endothelial growth factor receptor 2 and reduced expression of vascular endothelial growth factor receptor 1," *PLoS One*, vol. 12, no. 8, article e0182509, 2017.

Hindawi
Disease Markers
Volume 2019, Article ID 2568069, 9 pages
https://doi.org/10.1155/2019/2568069

Research Article

Links between High-Sensitivity C-Reactive Protein and Pulse Wave Analysis in Middle-Aged Patients with Hypertension and High Normal Blood Pressure

Ioana Mozos,[1,2] **Daniela Jianu**,[3,4] **Cristina Gug**,[5] **and Dana Stoian**[6]

[1]*Department of Functional Sciences, "Victor Babes" University of Medicine and Pharmacy, 300173 Timisoara, Romania*
[2]*Center for Translational Research and Systems Medicine, "Victor Babes" University of Medicine and Pharmacy, 300173 Timisoara, Romania*
[3]*1st Department of Internal Medicine, "Victor Babes" University of Medicine and Pharmacy, 300041 Timisoara, Romania*
[4]*Military Hospital, 300041 Timisoara, Romania*
[5]*Department of Microscopic Morphology, "Victor Babes" University of Medicine and Pharmacy, 300041 Timisoara, Romania*
[6]*2nd Department of Internal Medicine, "Victor Babes" University of Medicine and Pharmacy, 300723 Timisoara, Romania*

Correspondence should be addressed to Cristina Gug; dr.cristina.gug@gmail.com

Received 23 February 2019; Accepted 13 June 2019; Published 17 July 2019

Guest Editor: Zhongjie Shi

Arterial stiffness and arterial age provide valuable prognostic cardiovascular information. The present study aimed at assessing the levels of vitamin D, high-sensitivity C-reactive protein (hsCRP), low-density lipoprotein cholesterol (LDL), and oxidized LDL (oxLDL) in a group of middle-aged hypertensive patients and their relationship with pulse wave velocity (PWV), central blood pressure, and early arterial aging (EAA), respectively. A total of 56 patients, aged 48 ± 6 years, 57% males, with hypertension and high normal blood pressure (HNBP), were investigated using a Mobile-O-Graph, to assess central and peripheral blood pressure, PWV, and arterial age. Additionally, hsCRP, LDL, oxLDL, and 25-hydroxy vitamin D3 were assessed. PWV, 25-hydroxy vitamin D3, hsCRP, oxLDL, and LDL levels were 7.26 ± 0.69 m/s, 25.99 ± 11.17 microg/l, 0.48 ± 0.44 mg/dl, 261.37 ± 421 ng/ml, and 145.73 ± 39.53 mg/dl, respectively. Significant correlations were obtained between oxLDL and pulse pressure amplification (rS = −0.347, $p = 0.028$) and between hsCRP and LDL levels with PWV and EAA, respectively. ROC curve analysis revealed that hsCRP is a sensitive and specific predictor of EAA and increased PWV values. Concluding, vitamin D deficiency and increased hsCRP and LDL values are very common, and high oxidized LDL is related to pulse pressure amplification in patients with elevated blood pressure. Vitamin D level and high-sensitivity C-reactive protein and LDL provide valuable information in middle-aged hypertensive and HNBP patients related to arterial stiffness and early arterial aging, but only hsCRP is a sensitive predictor of EAA and PWV.

1. Introduction

Cardiovascular disorders are leading causes of death worldwide, and Romania was considered a high-cardiovascular-risk country according to the guidelines of the European Society of Cardiology [1]. Early detection of cardiovascular risk and subclinical atherosclerosis should represent a priority, along with the detection of new cardiovascular active substances. Arterial stiffness and arterial age provide valuable prognostic cardiovascular information [2]. Arterial stiffness, the expression of impaired arterial elasticity, may be assessed using pulse wave velocity (PWV) or the augmentation index (AI). AI is a wave reflection parameter and an indirect biomarker of arterial stiffening [3, 4], while arterial age represents the chronological age of a person with all risk factors at normal levels and the same 10-year predicted risk [5].

Vitamin D is essential not just for musculoskeletal health, considering that low 25-hydroxy vitamin D levels were frequently associated with an increased risk of cardiovascular events, including stroke and heart failure [6–9]. C-reactive

protein, an acute phase reactant and a marker of chronic low-grade inflammation, can predict cardiovascular events and was mentioned as the only circulating biomarker related to vascular wall biology [3, 10, 11]. High-sensitivity CRP (hsCRP) is a better predictor of vascular disorders than CRP. LDL cholesterol and oxidized LDL favor the formation of the foam cells and the development of the atherosclerotic plaque. There is a continuous relationship between blood pressure and cardiovascular events, and diagnosis of hypertension also requires evaluation of cardiovascular risk factors.

Considering the importance of prophylactic measures in hypertension, the present study aimed at assessing the levels of several laboratory biomarkers such as vitamin D, high-sensitivity C-reactive protein, LDL, and oxidized LDL (oxLDL) and their impact on pulse wave velocity, central blood pressure, and early arterial aging (EAA), respectively, in a group of middle-aged patients with hypertension and high normal blood pressure.

2. Materials and Methods

2.1. Study Population. A total of 56 consecutive hypertensive and HNBP patients, recruited from the Military Hospital Timisoara, were investigated during the period of July 2016–March 2017. All patients underwent investigation using a Mobil-O-Graph, and biochemical measurements were performed on the same day. Data about cardiovascular risk factors, diagnosis, and therapy were collected from medical records.

Patients aged between 18 and 55 years, with essential hypertension, both treated as well as uncontrolled patients, and high normal blood pressure, were included. Essential hypertension and high normal blood pressure were diagnosed according to the European criteria [12]. Cardiovascular risk in hypertensive patients was evaluated according to the criteria of the European Society of Cardiology, considering the number of cardiovascular risk factors, hypertension-mediated organ damage, and chronic kidney disease [12]. Patients with secondary hypertension, atrial fibrillation, diabetes mellitus, history of coronary heart disease, myocardial infarction, stroke, transient ischemic attack or peripheral arterial disease, systemic inflammatory processes, active infections, trauma, and therapy with statins were excluded.

The investigations conformed to the principles outlined in the Declaration of Helsinki and were approved by the "Victor Babes" University. Written informed consent was obtained from each study participant, and the objectives and procedures of the study were explained to each patient included in the study.

2.2. Biochemical Measurements. Blood was drawn after an overnight fast. Serum levels of 25-hydroxy-cholecalciferol, high-sensitivity C-reactive protein, LDL, and oxidized LDL were measured. LDL was assessed using a photometric method, a Siemens Advia 1800 analyzer, and Siemens LDL cholesterol reagents. An ELISA method and Immundiagnostik reagents were used for oxidized LDL. 25-Hydroxy-cholecalciferol and high-sensitivity C-reactive protein were assessed using liquid chromatography and immunophelometry, respectively. The thresholds used for defining normal/abnormal values for the various laboratory variables were provided by the laboratory.

2.3. Mobil-O-Graph. Pulse wave velocity (PWV), augmentation index and pressure (AI, AP), arterial (vascular) age, and central and peripheral blood pressure were assessed using a Mobil-O-Graph (IEM GmbH, Stolberg, Germany), a noninvasive, validated device.

The measurements were made after 10 minutes of rest, in supine position, using different cuff sizes, and considering the arm circumference. The participants were not allowed to smoke, eat, or drink coffee or alcohol 4 hours before the recording and speak or move during the measurements.

Mobil-O-Graph enables brachial blood pressure measurement, followed by the reinflation of the cuff and recording of pulse waves, with a high-fidelity pressure sensor [13]. After measuring systolic, diastolic, and mean arterial pressure, the software enabled the reconstruction of the aortic pulse wave using a generalized transfer function [13]. Wave separation analysis enabled decomposing the aortic pulse wave into forward-traveling (incident) and backward-traveling (reflected) pulse waves and allowed calculating the augmentation pressure (AP), augmentation index (AI), and PWV. AP was assessed as the difference in pressure of the reflected wave minus pressure of the forward-traveling wave of the systolic phase of the pulse wave [13]. Central systolic blood pressure (cSYS), central diastolic blood pressure (cDIA), and central pulse pressure (cPP) were also calculated by the device.

AI was defined as the ratio of AP to aortic pulse pressure, indicating the augmentation component of aortic SBP due to the premature arrival of the reflected wave [13]. PWV was estimated from the reconstructed aortic pulse waveform via mathematical models, considering impedance and age [13].

The significance of the variables was also described in previous studies [14]. PWV and AI were considered increased if they exceeded the normal values for the patients' ages according to the device manufacturer, and pathological values were shown by the device (Figure 1). Pulse pressure amplification, defined as cPP/PP [15], was calculated separately. Early arterial aging was considered when arterial age was higher than the biological age.

2.4. Statistical Analysis. Categorical data are given as numbers and percentages; continuous data are given as means ± standard deviation. Bravais-Pearson's, Kendall's, and Spearman's correlations and ROC curve analysis were used as statistical methods. Nonparametric correlations were used especially for assessing the correlation between a dichotomous variable and a continuous variable. Analyses were performed using IBM SPSS Base Edition.

3. Results

3.1. Characteristics of the Study Population. The subjects included in the study were middle-aged (48 ± 6 years), and most of them were male (57%). The baseline characteristics of the study population are included in Table 1.

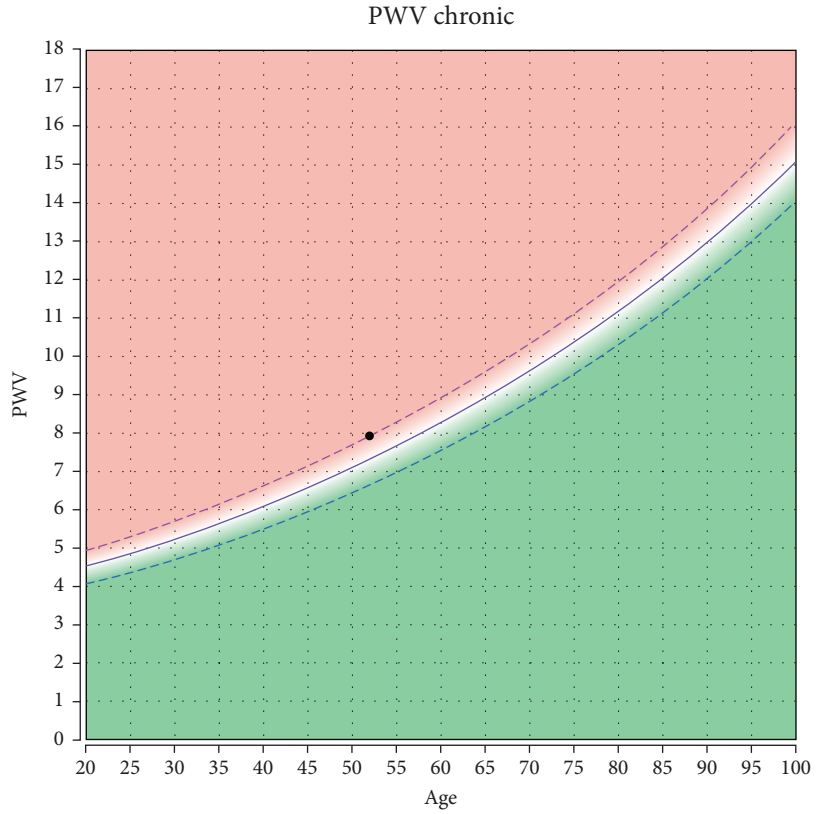

Figure 1: Pulse wave velocity (8 m/s) in a 52-year-old hypertensive patient. Within normal values considering age.

Vitamin D deficiency and insufficiency, defined as serum levels < 20 microg/l and <30 microg/l, respectively, were very common in the study population, as well as increased hsCRP and LDL values (Table 2). Vitamin D deficiency and insufficiency were defined according to the reference values provided by the laboratory.

3.2. Correlations. Correlations were calculated for all variables mentioned in the study objectives, both in a continuous fashion and after categorization. However, no significant correlations were obtained between vitamin D level and pulse wave and blood pressure variables. High-sensitivity C-reactive protein was significantly correlated with early arterial aging, PWV, and pulse pressure amplification (Table 3). LDL cholesterol levels correlated with central systolic and diastolic blood pressure, PWV values, and pulse pressure amplification (Table 3). No significant correlations were obtained between cardiovascular risk (low to very high) assessed according to the criteria of the European Society of Cardiology [12] and vitamin D level, high-sensitivity C-reactive protein, LDL cholesterol levels, and oxidized LDL.

3.3. Receiver-Operating Characteristic (ROC) Curve Analysis, Sensitivity, Specificity, and Positive and Negative Predictive Values. ROC curve analysis revealed hsCRP as a sensitive and specific test for EAA and pPWV (Figures 2 and 3). The cut-off value for hsCRP was higher for predicting an increased pulse wave velocity than early arterial aging (Table 4).

Vitamin D, LDL, and oxidized LDL were not revealed as sensitive markers for EAA or PWV according to ROC curve analysis (Table 5).

Further testing revealed important negative predictive values for low vitamin D, oxidized LDL, and hsCRP levels in predicting pathological PWV values and for hsCRP in predicting EAA (Table 6). Oxidized LDL showed good specificity in predicting PWV and EAA, and high-sensitivity C-reactive protein exceeding 0.100 mg/dl, also a good specificity (Table 6).

4. Discussion

The present study reports that low vitamin D levels and increased hsCRP and LDL values are very common in middle-aged hypertensive and HNBP patients; correlations were also found between pulse wave velocity and early arterial aging with high-sensitivity C-reactive protein and LDL cholesterol levels, respectively. However, only hsCRP was found as a sensitive predictor of early arterial aging.

Conflicting results have been previously published regarding the relationship between vitamin D level, vitamin D supplementation, and arterial stiffness [16, 17]. Several studies revealed associations between vitamin D level and PWV [18–21], but other authors found no significant association between vitamin D concentrations and markers of subclinical atherosclerosis [22, 23]. The present study found no significant correlation between vitamin D level and PWV but revealed a good negative predictive value of vitamin D

Table 1: Demographical and clinical characteristics of the study population ($n = 56$).

Characteristics	Means ± SD
Age (years)	48 ± 6
Gender (male)	32 (57%)
BMI (kg/m^2)	27.14 ± 6.01
SBP (mmHg)	137 ± 14
DBP (mmHg)	91 ± 11
MAP (mmHg)	111 ± 11
Heart rate (beats/minute)	69 ± 11
PP (mmHg)	45 ± 10
cSYS (mmHg)	127 ± 13
cDIA (mmHg)	93 ± 11
cPP (mmHg)	35 ± 9
TVR (s × mmHg/ml)	1.28 ± 0.18
Augmentation pressure (mmHg)	7.9 ± 6.5
Augmentation index (AI) (%)	20 ± 13.71
Pulse wave velocity (PWV) (m/s)	7.26 ± 0.69
PWV increased for age (pathological PWV)	12 (21.4%)
Early arterial aging	18 (32.1%)
Family history of cardiovascular disorders	13 (22.5%)
Cardiovascular risk	High: 17 (30%) Low: 14 (25%)
Hypertension (HT)	High normal: 21 (37.5%) HT grade 1: 16 (28.6%) HT grade 2: 13 (23.2%) HT grade 3: 6 (10.7%)
Therapy	ACEI: 17 (30%) Sartans: 10 (17.5%) Diuretics: 18 (32.5%) Beta blockers: 18 (32.5%) Calcium channel blockers: 4 (7.5%)

BMI=body mass index; SBP=systolic blood pressure; DBP=diastolic blood pressure; MAP=mean arterial pressure; PP=pulse pressure; cSYS=central systolic blood pressure; cDIA=central diastolic blood pressure; cPP=central pulse pressure; TVR=total vascular resistance; ACEI=angiotensin converting enzyme inhibitors; HT=hypertension.

Table 2: Biomarkers.

Biomarker	Means ± SD
Vitamin D (microg/l)	25.99 ± 11.17
Vitamin D < 20 microg/l	19 (34%)
Vitamin D < 30 microg/l	41 (73%)
hsCRP (mg/dl)	0.48 ± 0.44
hsCRP > 0.1 mg/dl	43 (77%)
hsCRP > 0.3 mg/dl	29 (52%)
LDL (mg/dl)	145.73 ± 39.53
LDL > 100 mg/dl	49 (88%)
LDL > 130 mg/dl	35 (62.5%)
LDL > 160 mg/dl	17 (30%)
Oxidized LDL (ng/ml)	261.37 ± 421

LDL=low-density lipoprotein; hsCRP=high-sensitivity C-reactive protein.

level for pathological PWV values. The link between vitamin D deficiency and hypertension can be explained by the activation of the renin-angiotensin-aldosterone system, increasing the vascular tone due to the release of angiotensin II [24]. Vitamin D is also involved in the downregulation of the renin gene expression [25]. Vitamin D has also pleiotropic effects on the immune system and suppresses the low-grade inflammation in the cardiovascular system [17, 26]. Other important pathophysiological vasculoprotective mechanisms by which vitamin D supplementation reduces arterial stiffness include improvement of the endothelial function, suppression of endothelin-induced vascular smooth muscle cell proliferation, effects on calcium metabolism and PTH level, counterbalancing of oxidative stress, and improvement of carbohydrate metabolism and insulin sensitivity [27–33]. Related to oxidative stress, vitamin D activates several genes encoding for antioxidant and detoxifying enzymes [25]. The accumulation of calcium in the vessel walls increases arterial tone and arterial stiffness in hypertension [34]. However, no significant correlations were obtained in our study between vitamin D level and hsCRP or oxidized LDL, respectively.

25-Hydroxy vitamin D and not 1,25-dihydroxy vitamin D was assessed in the present study because 25-hydroxy vitamin D is a nutritional parameter of vitamin D status, the primary circulating and storage form of vitamin D, and a reliable, available marker of low vitamin D levels able to bind to vitamin D receptors [18, 35].

Several mechanisms link inflammation and arterial stiffness, considering the effect of inflammation on the arterial endothelium, nitric oxide (NO), and smooth muscle cells and considering its ability to change the composition of the extracellular matrix, to breakdown elastin, and to enable the calcification of the vessel wall [36]. hsCRP was associated with arterial stiffness in some studies [3, 37–40], but other studies did not find any association [41]. Kim et al. reported significant associations between hsCRP and arterial stiffness independent of age, systolic blood pressure, gender, heart rate, glucose, lipid profiles, and therapy in treated hypertension [38]. The present study found significant correlations and associations between hsCRP and PWV, EAA and pulse pressure amplification, respectively. High-sensitivity C-reactive protein was the only sensitive predictor of early arterial aging and elevated PWV, with a higher cut-off value for predicting increased pulse wave velocity than early arterial aging (0.446 vs. 0.388). Significant correlations were obtained in the present study between hsCRP and LDL130 (exceeding 130 mg/dl) (rK = 0.219, $p = 0.049$; rS = 0.266, $p = 0.048$). High-sensitivity C-reactive protein, a marker of low-grade inflammation, was also associated with deep white matter lesions, ischemic stroke, and heart failure

Table 3: Correlations between variables of central hemodynamics and pulse wave analysis with high-sensitivity C-reactive protein (hsCRP), LDL, and oxidized LDL (oxLDL) cholesterol, respectively.

Correlated variables	Correlation coefficient	p
hsCRP-EAA	rP = 0.376	0.004
	rK = 0.332	0.003
	rS = 0.402	0.002
hsCRP-PWV	rK = 0.225	0.016
	rS = 0.308	0.021
hsCRP-pPWV	rP = 0.398	0.002
	rS = 0.378	0.004
hsCRP-EAA	rP = 0.358	0.007
CRP100-PWV	rP = 0.283	0.031
	rK = 0.242	0.032
	rS = 0.288	0.031
CRP100-cPP/PP	rP = 0.288	0.031
CRP100-EAA	rS = 0.288	0.031
CRP300-PWV	rP = 0.351	0.008
	rK = 0.357	0.002
	rS = 0.425	0.001
CRP300-EAA	rP = 0.358	0.007
	rK = 0.358	0.008
	rS = 0.358	0.007
LDL100-PWV	rP = 0.306	0.022
LDL130-cSYS	rP = −0.311	0.020
	rK = −0.248	0.028
	rS = −0.297	0.026
LDL130-cDIA	rP = −0.276	0.039
LDL130-PWV	rP = 0.303	0.023
LDL130-cPP/PP	rP = −0.285	0.033
oxLDL-cPP/PP	rK = −0.230	0.042
	rS = −0.347	0.028

rP=Bravais-Pearson's correlation coefficient; rK=Kendall's correlation; rS=Spearman's correlation; cPP/PP=pulse pressure amplification; EAA=early arterial aging; PWV=pulse wave velocity; pPWV=pathological pulse wave velocity (increased for age); cSYS=central systolic blood pressure; cDIA=central diastolic blood pressure; hsCRP=high-sensitivity C-reactive protein; CRP100=high-sensitivity C-reactive protein exceeding 0.100 mg/dl; CRP300=high − sensitivity C − reactive protein > 0.300 mg/dl; LDL100=LDL > 100 mg/dl; LDL130=LDL > 130 mg/dl; LDL160=LDL > 160 mg/dl; oxLDL=oxidized LDL.

[42, 43]. On the other hand, arterial stiffness was significantly associated with ischemic stroke after adjusting for cardiovascular risk factors [44].

Non-HDL cholesterol was reported as a good predictor of the risk of increased arterial stiffness in postmenopausal women in an urban Brazilian population [45]. Kim et al. reported a modest increase in arterial stiffness due to dyslipidemia only in women [46]. Increased LDL levels correlated with central systolic and diastolic blood pressure, PWV, and pulse pressure amplification in the present study, regardless of gender.

Oxidized LDL was associated with pulse wave velocity in patients with renal failure [47] and in healthy persons between 45 and 69 years old [48]; it was also associated with the augmentation index in obese children and adolescents [49]. In the present study, oxLDL correlated with pulse pressure amplification (rS = −0.347, $p = 0.028$). A high specificity and negative predictive value were obtained for oxidized LDL in predicting pathological PWV.

Pulse pressure amplification, the ratio between central and peripheral pulse pressure, is related to an increase of pulse pressure (PP) amplitude as pressure waves propagate distally in the vessel network and is a measure of arterial elasticity [50, 51]. Changes in PP amplification are associated with traditional cardiovascular risk factors, including hypertension [52]. In our study, oxLDL, elevated hsCRP, and LDL values significantly correlated with PP amplification.

The most important study limitations include the cross-sectional study design, which does not provide any data about the cause-effect relationship, the relatively small sample size, and not considering the duration of daily sun exposure, which is important for vitamin D synthesis. Further larger studies are needed to demonstrate if vitamin D level, hsCRP, LDL, and oxidized LDL play important roles in the development of increased arterial stiffness and early arterial aging in hypertensive patients and to reveal their relationship with cardiovascular events, such as stroke and heart failure in hypertensive patients. A power analysis, using PASS 2019, was conducted before the study to determine the sample size needed for the present study, and we do not expect changes in the results by increasing the sample size. A minimum sample size required for Bravais-Pearson's and Spearman's correlations was 35 participants (desired statistical power: 0.8; correlation coefficient: 0.4). The required sample size for an area under the curve (AUC) of 0.7 and power and alpha of 0.75 and 0.15, respectively, was 52. One reading was made for each study participant for PWV, AI, and AP using the Mobil-O-Graph, which might be considered as another study limitation; however, earlier measurements provided by the same device demonstrated good reproducibility. According to Table 1, average blood pressure values are not impressive (137/91 mmHg) and PWV is not very high (on average 7.26 m/s). However, the population is proper for the study purpose, considering that PWV was increased for age in 21.4% of the participants and high normal and grade 1-3 hypertension patients were included, with both high and low cardiovascular risks. The cut-off values for increased PWV were provided by the Mobil-O-Graph considering age, and they were lower than those recommended by the European Guidelines (a threshold of 10 m/s for pathological values) [53]. The latter should emphasize the prophylactic character of the present study.

Our study is the first one comparing the predictive value of vitamin D, LDL, oxidized LDL, and hsCRP for arterial stiffness and early arterial aging, demonstrating a high sensitivity only for hsCRP, and revealing, for the first time, as far as we know, a correlation between pulse pressure amplification and oxidized LDL level. The findings of the present

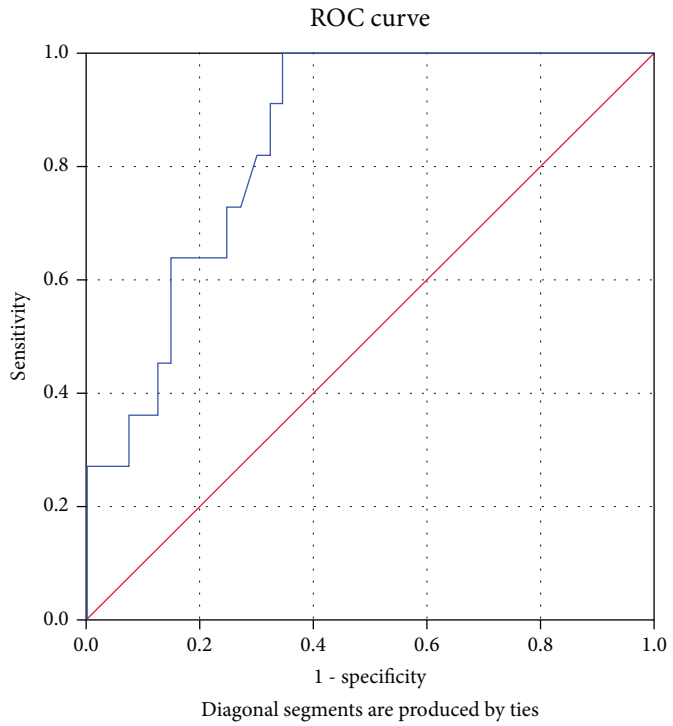

Figure 2: High-sensitivity C-reactive protein as a sensitive and specific predictor of increased pulse wave velocity. AUC = 0.766 (95% CI: 0.603-0.929), $p = 0.005$.

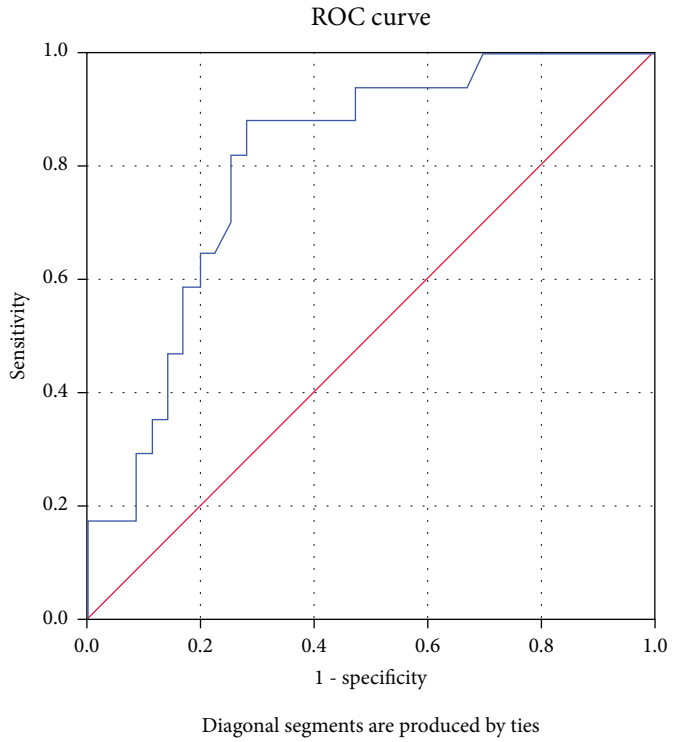

Figure 3: High-sensitivity C-reactive protein as a sensitive and specific predictor of early arterial aging. AUC = 0.749 (95% CI: 0.607-0.890), $p = 0.003$.

Table 4: Results of receiver-operating characteristic (ROC) curve analysis for high-sensitivity C-reactive protein (hsCRP).

Test variable	State variable	AUC (95% CI)	p	Cut-off value	Sensitivity	Specificity
hsCRP	EAA	0.749 (0.607-0.890)	0.003	0.388	83.3%	71.1%
hsCRP	pPWV	0.766 (0.603-0.929)	0.005	0.446	83.3%	65.6%

EAA=early arterial aging; PWV=pulse wave velocity; pPWV=pathological pulse wave velocity (increased for age).

Table 5: Results of receiver-operating characteristic (ROC) curve analysis for vitamin D, LDL, and oxidized LDL as predictors of pathological pulse wave velocity and early arterial aging.

Test variable	State variable	AUC (95% CI)	p
Vitamin D	pPWV	0.473 (0.274-0.673)	0.78
Vitamin D	EAA	0.487 (0.324-0.65)	0.875
LDL	pPWV	0.393 (0.227-0.559)	0.259
LDL	EAA	0.45 (0.291-0.608)	0.545
oxLDL	pPWV	0.547 (0.314-0.78)	0.685
oxLDL	EAA	0.484 (0.292-0.676)	0.874

pPWV=pathological pulse wave velocity (increased for age); EAA=early arterial aging; LDL=low-density lipoprotein; oxLDL=oxidized LDL.

Table 6: Sensitivity, specificity, and positive and negative predictive values.

Test variables	Sensitivity (95% CI)	Specificity (95% CI)	Positive predictive value (PPV) (95% CI)	Negative predictive value (NPV) (95% CI)
D20-pPWV	0.363 (0.123-0.683)	0.666 (0.509-0.795)	0.21 (0.069-0.46)	**0.81** (0.642-0.914)
D20-EAA	0.333 (0.143-0.588)	0.657 (0.485-0.798)	0.315 (0.135-0.565)	0.675 (0.501-0.814)
LDL160-pPWV	0.055 (0.002-0.293)	0.605 (0.434-0.755)	0.062 (0.003-0.322)	0.575 (0.41-0.725)
LDL160-EAA	0.166 (0.04-0.422)	0.631 (0.459-0.777)	0.176 (0.046-0.441)	0.615 (0.446-0.761)
oxLDL-pPWV	0.25 (0.044-0.644)	**0.843** (0.664-0.941)	0.285 (0.051-0.697)	**0.818** (0.639-0.923)
oxLDL-EAA	0.153 (0.027-0.463)	**0.814** (0.612-0.929)	0.285 (0.051-0.697)	0.666 (0.481-0.814)
CRP100-pPWV	**0.833** (0.508-0.97)	0.272 (0.154-0.43)	0.238 (0.125-0.398)	**0.857** (0.561-0.974)
CRP100-EAA	**0.944** (0.706-0.997)	0.315 (0.18-0.487)	0.395 (0.253-0.555)	**0.923** (0.62-0.995)
CRP300-pPWV	0.75 (0.428-0.933)	0.545 (0.389-0.693)	0.31 (0.159-0.509)	**0.888** (0.697-0.97)
CRP300-EAA	0777 (0.519-0.926)	0.605 (0.434-0.755)	0.482 (0.298-0.671)	**0.851** (0.653-0.951)

pPWV=pathological pulse wave velocity (increased for age); EAA=early arterial aging; oxLDL=oxidized LDL; LDL160=LDL > 160 mg/dl; CRP100=high-sensitivity C-reactive protein exceeding 0.100 mg/dl; CRP300=high-sensitivity C-reactive protein > 0.300 mg/dl; D20=vitamin D < 20 microg/l. The highest values for sensitivity, specificity, and NPV are in bold.

study have clinical implications, considering the prognostic importance of increased arterial stiffness and early arterial aging for cardiovascular risk. hsCRP, LDL, and oxidized LDL can provide valuable information related especially to large vessels, arterial age, and cardiovascular risk in treated hypertensive patients.

Hypertension is a state of low vitamin D level, oxidative stress, and low-grade inflammation. Further larger follow-up studies are needed in hypertensive patients to confirm the findings of the present study and to correlate the collagen content of the arterial wall with vitamin D level, high-sensitivity C-reactive protein, LDL, and oxidized LDL level, in order to confirm their role as cardiovascular active substances.

5. Conclusions

Concluding, low vitamin D levels and increased hsCRP and LDL values are very common in middle-aged hypertensive and high normal blood pressure patients, and they provide, along with oxidized LDL, valuable information about vascular function. However, only high-sensitivity C-reactive protein level is a sensitive predictor of increased arterial stiffness and early arterial aging.

Data Availability

The data used to support the findings of this study are available from the corresponding author upon request.

Disclosure

A part of the data were presented as an abstract at the 8th International Congress of Pathophysiology, 2018. The founding sponsors had no role in the design of the study; in the collection, analysis, or interpretation of data; in the writing of the manuscript; and in the decision to publish the results.

Conflicts of Interest

The authors declare no conflict of interest.

Acknowledgments

The present study was funded by the Bioclinica grant 9/2743/9.03.2016. No funds were received for covering the costs to publish in open access.

References

[1] M. F. Piepoli, A. W. Hoes, S. Agewall et al., "2016 European guidelines on cardiovascular disease prevention in clinical practice: the Sixth Joint Task Force of the European Society of Cardiology and Other Societies on Cardiovascular Disease Prevention in Clinical Practice (constituted by representatives of 10 societies and by invited experts) developed with the special contribution of the European Association for Cardiovascular Prevention and Rehabilitation (EACPR)," *Atherosclerosis*, vol. 252, pp. 207–274, 2016.

[2] I. Mozos and C. T. Luca, "Crosstalk between oxidative and nitrosative stress and arterial stiffness," *Current Vascular Pharmacology*, vol. 15, no. 5, pp. 446–456, 2017.

[3] C. Vlachopoulos, P. Xaplanteris, V. Aboyans et al., "The role of vascular biomarkers for primary and secondary prevention. A position paper from the European Society of Cardiology Working Group on peripheral circulation endorsed by the Association for Research into Arterial Structure and Physiology (ARTERY) Society," *Atherosclerosis*, vol. 241, no. 2, pp. 507–532, 2015.

[4] I. Mozos, "The link between ventricular repolarization variables and arterial function," *Journal of Electrocardiology*, vol. 48, no. 2, pp. 145–149, 2015.

[5] H. Y. Lee and B. H. Oh, "Aging and arterial stiffness," *Circulation Journal*, vol. 74, no. 11, pp. 2257–2262, 2010.

[6] T. J. Wang, M. J. Pencina, S. L. Booth et al., "Vitamin D deficiency and risk of cardiovascular disease," *Circulation*, vol. 117, no. 4, pp. 503–511, 2008.

[7] I. Mozos and O. Marginean, "Links between Vitamin D Deficiency and Cardiovascular Diseases," *BioMed Research International*, vol. 2015, 12 pages, 2015.

[8] I. Bressendorff, L. Brandi, M. Schou et al., "The effect of high dose cholecalciferol on arterial stiffness and peripheral and central blood pressure in healthy humans: a randomized controlled trial," *PLoS One*, vol. 11, no. 8, article e0160905, 2016.

[9] M. Craciunescu, D. Stoian, A. Schiller et al., "Study on 25-hydroxy-vitamin D for the assessment of bone mineral density," *Revista de Chimie*, vol. 67, no. 3, pp. 543–548, 2016.

[10] G. Liuzzo, L. M. Biasucci, J. R. Gallimore et al., "The Prognostic Value of C-Reactive Protein and Serum Amyloid A Protein in Severe Unstable Angina," *The New England Journal of Medicine*, vol. 331, no. 7, pp. 417–424, 1994.

[11] P. M. Ridker, N. Rifai, L. Rose, J. E. Buring, and N. R. Cook, "Comparison of C-reactive protein and low-density lipoprotein cholesterol levels in the prediction of first cardiovascular events," *The New England Journal of Medicine*, vol. 347, no. 20, pp. 1557–1565, 2002.

[12] G. Mancia, R. Fagard, K. Narkiewicz et al., "2013 ESH/ESC Guidelines for the management of arterial hypertension: The Task Force for the management of arterial hypertension of the European Society of Hypertension (ESH) and of the European Society of Cardiology (ESC)," *European Heart Journal*, vol. 34, no. 28, pp. 2159–2219, 2013.

[13] A. Karpetas, P. A. Sarafidis, P. I. Georgianos et al., "Ambulatory recording of wave reflections and arterial stiffness during intra- and interdialytic periods in patients treated with dialysis," *Clinical Journal of the American Society of Nephrology*, vol. 10, no. 4, pp. 630–638, 2015.

[14] I. Mozos, J. Maidana, D. Stoian, and M. Stehlik, "Gender differences of arterial stiffness and arterial age in smokers," *International Journal of Environmental Research and Public Health*, vol. 14, no. 6, p. 565, 2017.

[15] A. Benetos, F. Thomas, L. Joly et al., "Pulse Pressure Amplification: A Mechanical Biomarker of Cardiovascular Risk," *Journal of the American College of Cardiology*, vol. 55, no. 10, pp. 1032–1037, 2010.

[16] A. J. Rodriguez, D. Scott, V. Srikanth, and P. Ebeling, "Effect of vitamin D supplementation on measures of arterial stiffness: a systematic review and meta-analysis of randomized controlled trials," *Clinical Endocrinology*, vol. 84, no. 5, pp. 645–657, 2016.

[17] I. Mozos, D. Stoian, and C. T. Luca, "Crosstalk between vitamins A, B12, D, K, C, and E status and arterial stiffness," *Disease Markers*, vol. 2017, 14 pages, 2017.

[18] A. R. Patange, R. P. Valentini, W. Du, and M. D. Pettersen, "Vitamin D deficiency and arterial wall stiffness in children with chronic kidney disease," *Pediatric Cardiology*, vol. 33, no. 1, pp. 122–128, 2012.

[19] J. A. Reynolds, S. Haque, J. L. Berry et al., "25-Hydroxyvitamin D deficiency is associated with increased aortic stiffness in patients with systemic lupus erythematosus," *Rheumatology (Oxford, England)*, vol. 51, no. 3, pp. 544–551, 2012.

[20] R. Lieberman, R. P. Wadwa, N. Nguyen et al., "The association between vitamin D and vascular stiffness in adolescents with and without type 1 diabetes," *PLoS One*, vol. 8, no. 10, article e77272, 2013.

[21] P. Jha, L. M. Dolan, P. R. Khoury, E. M. Urbina, T. R. Kimball, and A. S. Shah, "Low serum vitamin D levels are associated with increased arterial stiffness in youth with type 2 diabetes," *Diabetes Care*, vol. 38, no. 8, pp. 1551–1557, 2015.

[22] M. C. Sachs, J. D. Brunzell, P. A. Cleary et al., "Circulating vitamin D metabolites and subclinical atherosclerosis in type 1 diabetes," *Diabetes Care*, vol. 36, no. 8, pp. 2423–2429, 2013.

[23] S. C. van Dijk, E. Sohl, C. Oudshoorn et al., "Non-linear associations between serum 25-OH vitamin D and indices of arterial stiffness and arteriosclerosis in an older population," *Age and Ageing*, vol. 44, no. 1, pp. 136–142, 2015.

[24] I. Al Mheid, R. S. Patel, V. Tangpricha, and A. A. Quyyumi, "Vitamin D and cardiovascular disease: is the evidence solid?," *European Heart Journal*, vol. 34, no. 48, pp. 3691–3698, 2013.

[25] D. Caccamo, S. Ricca, M. Currò, and R. Ientile, "Health Risks of Hypovitaminosis D: A Review of New Molecular Insights," *International Journal of Molecular Sciences*, vol. 19, no. 3, p. 892, 2018.

[26] E. K. Calton, K. N. Keane, P. Newsholme, and M. J. Soares, "The impact of vitamin D levels on inflammatory status: a systematic review of immune cell studies," *PLoS One*, vol. 10, no. 11, p. e0141770, 2015.

[27] S. Chen, C. S. Law, and D. G. Gardner, "Vitamin D-dependent suppression of endothelin-induced vascular smooth muscle cell proliferation through inhibition of CDK2 activity," *The*

Journal of Steroid Biochemistry and Molecular Biology, vol. 118, no. 3, pp. 135–141, 2010.

[28] Y. Dong, I. S. Stallmann-Jorgensen, N. K. Pollock et al., "A 16-Week Randomized Clinical Trial of 2000 International Units Daily Vitamin D3 Supplementation in Black Youth: 25-Hydroxyvitamin D, Adiposity, and Arterial Stiffness," *The Journal of Clinical Endocrinology and Metabolism*, vol. 95, no. 10, pp. 4584–4591, 2010.

[29] D. Martins, Y.-X. Meng, N. Tareen et al., "The effect of short term vitamin D supplementation on the inflammatory and oxidative mediators of arterial stiffness," *Health*, vol. 06, no. 12, pp. 1503–1511, 2014.

[30] K. J. Yun and K. H. Baek, "Is vitamin D supplementation really effective in patients with type 2 diabetes?," *The Korean Journal of Internal Medicine*, vol. 29, no. 5, pp. 574–576, 2014.

[31] A. Zaleski, G. Panza, H. Swales et al., "High-dose versus low-dose vitamin D supplementation and arterial stiffness among individuals with prehypertension and vitamin D deficiency," *Disease Markers*, vol. 2015, 7 pages, 2015.

[32] A. Caraba, V. Crisan, I. Romosan, I. Mozos, and M. Murariu, "Vitamin D status, disease activity, and endothelial dysfunction in early rheumatoid arthritis patients," *Disease Markers*, vol. 2017, 7 pages, 2017.

[33] G. Sypniewska, J. Pollak, P. Strozecki et al., "25-Hydroxyvitamin D, biomarkers of endothelial dysfunction and subclinical organ damage in adults with hypertension," *American Journal of Hypertension*, vol. 27, no. 1, pp. 114–121, 2014.

[34] R. M. Touyz, R. Alves-Lopes, F. J. Rios et al., "Vascular smooth muscle contraction in hypertension," *Cardiovascular Research*, vol. 114, no. 4, pp. 529–539, 2018.

[35] N. Chitalia, T. Ismail, L. Tooth et al., "Impact of vitamin D supplementation on arterial vasomotion, stiffness and endothelial biomarkers in chronic kidney disease patients," *PLoS One*, vol. 9, no. 3, article e91363, 2014.

[36] S. Jain, R. Khera, V. F. Corrales–Medina, R. R. Townsend, and J. A. Chirinos, "Inflammation and arterial stiffness in humans," *Atherosclerosis*, vol. 237, no. 2, pp. 381–390, 2014.

[37] P. Kampus, J. Kals, T. Ristim??e, K. Fischer, M. Zilmer, and R. Teesalu, "High-sensitivity C-reactive protein affects central haemodynamics and augmentation index in apparently healthy persons," *Journal of Hypertension*, vol. 22, no. 6, pp. 1133–1139, 2004.

[38] J. S. Kim, T. S. Kang, J. B. Kim et al., "Significant association of C-reactive protein with arterial stiffness in treated non-diabetic hypertensive patients," *Atherosclerosis*, vol. 192, no. 2, pp. 401–406, 2007.

[39] S. Park and E. G. Lakatta, "Role of inflammation in the pathogenesis of arterial stiffness," *Yonsei Medical Journal*, vol. 53, no. 2, pp. 258–261, 2012.

[40] A. Nurizal, D. Antono, I. P. Wijaia, and H. Shatri, "Correlation between high-sensitivity C reactive protein and local arterial stiffness measured by radio frequency echotracking system in type 2 diabetic patients," *Acta Medica Indonesiana*, vol. 46, no. 4, 2014.

[41] H. Tomiyama, T. Arai, Y. Koji et al., "The relationship between high-sensitive C-reactive protein and pulse wave velocity in healthy Japanese men," *Atherosclerosis*, vol. 174, no. 2, pp. 373–377, 2004.

[42] J. van Wezenbeek, J. M. Canada, K. Ravindra et al., "C-reactive protein and N-terminal pro-brain natriuretic peptide levels correlate with impaired cardiorespiratory fitness in patients with heart failure across a wide range of ejection fraction," *Frontiers in Cardiovascular Medicine*, vol. 5, p. 178, 2018.

[43] H. Yao, Y. Mizoguchi, A. Monji et al., "Low-Grade Inflammation Is Associated with Apathy Indirectly via Deep White Matter Lesions in Community-Dwelling Older Adults: The Sefuri Study," *International Journal of Molecular Sciences*, vol. 20, no. 8, p. 1905, 2019.

[44] E. Y. Yang, L. Chambless, A. R. Sharrett et al., "Carotid arterial wall characteristics are associated with incident ischemic stroke but not coronary heart disease in the Atherosclerosis Risk in Communities (ARIC) study," *Stroke*, vol. 43, no. 1, pp. 103–108, 2012.

[45] R. O. Alvim, J. Mourão, G. L. Magalhães et al., "Non-HDL cholesterol is a good predictor of the risk of increased arterial stiffness in postmenopausal women in an urban Brazilian population," *Clinics*, vol. 72, no. 2, pp. 106–110, 2017.

[46] J. Y. Kim, J. B. Park, D. S. Kim et al., "Gender difference in arterial stiffness in a multicenter cross-sectional study: the Korean arterial aging study (KAAS)," *Pulse*, vol. 2, no. 1-4, pp. 11–17, 2014.

[47] A. F. G. Cicero, M. Kuwabara, R. Johnson et al., "LDL-oxidation, serum uric acid, kidney function and pulse-wave velocity: data from the Brisighella Heart Study cohort," *International Journal of Cardiology*, vol. 261, pp. 204–208, 2018.

[48] M. Kim, M. Kim, H. J. Yoo, S. Y. Lee, S. H. Lee, and J. H. Lee, "Age-specific determinants of pulse wave velocity among metabolic syndrome components, inflammatory markers, and oxidative stress," *Journal of Atherosclerosis and Thrombosis*, vol. 25, no. 2, pp. 178–185, 2018.

[49] M. Manco, V. Nobili, A. Alisi, N. Panera, and A. Handberg, "Arterial stiffness, thickness and association to suitable novel markers of risk at the origin of cardiovascular disease in obese children," *International Journal of Medical Sciences*, vol. 14, no. 8, pp. 711–720, 2017.

[50] A. Wykretowicz, A. Rutkowska, T. Krauze et al., "Pulse pressure amplification in relation to body fatness," *British Journal of Clinical Pharmacology*, vol. 73, no. 4, pp. 546–552, 2012.

[51] M. R. Alfonso, R. L. Armentano, L. J. Cymberknop, A. R. Ghigo, F. M. Pessana, and W. E. Legnani, "A novel interpretation for arterial pulse pressure amplification in health and disease," *Journal of Healthcare Engineering*, vol. 2018, 9 pages, 2018.

[52] A. P. Avolio, L. M. Van Bortel, P. Boutouyrie et al., "Role of pulse pressure amplification in arterial hypertension: experts' opinion and review of the data," *Hypertension*, vol. 54, no. 2, pp. 375–383, 2009.

[53] L. Van Bortel, S. Laurent, P. Boutouyrie et al., "Expert consensus document on the measurement of aortic stiffness in daily practice using carotid-femoral pulse wave velocity," *Journal of Hypertension*, vol. 30, no. 3, pp. 445–448, 2012.

Hindawi
Disease Markers
Volume 2019, Article ID 7816438, 7 pages
https://doi.org/10.1155/2019/7816438

Research Article

Expression of B2 Receptor on Circulating CD34-Positive Cells and Outcomes of Myocardial Infarction

Cong Fu,[1,2] **Yuhan Cao**,[2,3] **Yuyu Yao**,[4] **Shengxing Tang**,[1] **Qun Fan**,[1] **and Yang Ling**[1]

[1]*Department of Cardiology, Yi Ji Shan Hospital Affiliated to Wan Nan Medical College, China*
[2]*Key Laboratory of Non-Coding RNA Transformation Research of Anhui Higher Education Institution (Wan Nan Medical College), China*
[3]*Department of Nephrology, Yi Ji Shan Hospital Affiliated to Wan Nan Medical College, China*
[4]*Department of Cardiology, Zhong Da Hospital Affiliated to Southeast University, China*

Correspondence should be addressed to Cong Fu; fucong7706@163.com

Received 14 January 2019; Revised 12 April 2019; Accepted 16 April 2019; Published 8 July 2019

Guest Editor: Zhongjie Shi

Background. Bradykinin B2 receptor (B2R) is a widely expressed cell surface receptor. The relationship between B2R expression on circulating CD34+ cells and prognosis of myocardial infarction remains unknown. *Methods*. We analyzed the expression of B2R on circulating CD34-positive cells and plasma VEGF concentration in 174 myocardial infarction patients. All involved patients were divided into two groups: high B2R group and low B2R group according to the median B2R expression percentage. 48 months of follow-up was performed. The endpoints were heart failure and revascularization. *Results*. The plasma level of VEGF in the low B2R group is 67 ± 12 pg/mL, whereas the high B2R group has significantly elevated VEGF levels of 145 ± 27 pg/mL ($P < 0.001$). The concentration of VEGF has correlated with expression of B2R ($r = 0.574$, $P < 0.001$). During the 48 months of follow-up, low expression of B2 receptor on circulating CD34-positive cells indicates the high incidence of heart failure (hazard ratio: 2.247; 95% confidence interval: 1.110-4.547; $P = 0.024$) and revascularization (hazard ratio: 2.335; 95% confidence interval: 1.075-5.074; $P = 0.032$). Kaplan-Meier survival analysis showed that the cumulative hazard of heart failure ($P = 0.014$) and revascularization ($P = 0.032$) has significant differences between low B2R and high B2R. *Conclusion*. Low expression of B2R on circulating progenitor cells indicated the poor outcomes of myocardial infarction.

1. Introduction

Cardiovascular disease is the major cause of death worldwide that frequently leads to irreversible heart failure [1]. Accompanied by the development of drug and invasive treatment, the mortality of ST-elevated myocardial infarction (STEMI) is lower than in the past. Despite the pathological process and inflammatory factors, the risk factors that influence the outcomes of STEMI remained not totally clear [2, 3].

Stem and progenitor cells derived from bone marrow get into circulating blood immediately when ischemic injury occur [4–7]. Stem and progenitor cells participated in repairing post-STEMI. Previous studies revealed that endothelial progenitor cells (EPCs) are capable of angiogenesis and differentiating into endothelial cells which are candidates for vascular regeneration [8, 9]. It can be concluded that the mobilization of stem cells and progenitor cells benefits the outcomes of ischemic damage. CD34 is a widely known marker of progenitor cells. CD34-positive cells can be found in peripheral blood [10]. However, it is unknown if CD34 have a relationship with the outcomes of myocardial ischemia damage.

B2 receptor (B2R) is the receptor of bradykinin which is important for the effect of bradykinin and is expressed on several cells including some progenitor cells, for example, EPCs. B2R has a key role in the angiogenesis [11]. We suggest a hypothesis that expression of B2R on circulating CD34-positive cells has the relationship to the prognosis of myocardial infarction.

2. Methods

2.1. Study Population. Between October 2013 and December 2014, 174 STEMI patients who consecutively underwent coronary angiography in Yi Ji Shan Hospital affiliated to Wan Nan Medical College were involved in the study. The definition of myocardial infarction was described previously [12]. Patients who have cancer, stroke, old myocardial infarction, severe liver dysfunction, chronic renal disease, heart failure (Killip III-IV), autoimmune diseases, and infection diseases, received stent implantation before, are receiving hormone and/or immunosuppressant therapy and hemodialysis, and died before discharge from the hospital were excluded. Also, lack of clinical document was excluded. All patients were asked to confirm their agreement to accept the 48 months of follow-up by providing written informed consent. This trial design was approved by the Ethics Committee in Yi Ji Shan Hospital (Approval number: 2013YJYSYLL108.1) and performed according to the Declaration of Helsinki.

2.2. Arterial Blood Sample Collected and Analyzed. Before revascularization, 20 mL of arterial blood sample was collected in EDTA-coated tubes. Mononuclear cells were isolated on a Lymphocyte Separation Solution (HaoYang, China) by centrifugation at 500 × g for 20 min according to standard protocols. Plasma was collected in EP tubes and stored at -40°C. The plasma VEGF level was determined by a Human VEGF ELISA Kit (BOSTER, Wuhan, China).

2.3. Flow Cytometry. For flow cytometry analysis, mononuclear cells were suspended in 200 μL of phosphate-buffered saline (PBS) containing 1% bovine serum albumin (BSA). Afterward, they were fixed in 1% paraformaldehyde and then permeabilized using 0.1% Triton X-100 containing 0.5% BSA. The cells were then incubated with specific rabbit anti-human B2R antibodies (Abcam, UK) on ice for 1 hour, followed by incubation with a PE-conjugated donkey anti-rabbit secondary antibody (Santa Cruz, USA) and a fluorescein isothiocyanate- (FITC-) conjugated anti-human CD34 antibody (BD Biosciences, USA) for 1 hour. Stained cells were washed 3 times with PBS and then analyzed using a FACScan flow cytometer (Becton Dickinson, USA) to detect B2R expression on CD34-positive cells (Figure 1). Firstly, mononuclear cells were gated. Secondly, the CD34-positive cells were gated; then, the B2R-positive cells were further analyzed. The proportion of B2R-positive cells among CD34-positive cells was calculated. The positive control and negative control were presented.

2.4. Angiography. Cardiac catheterization was performed according to the guidelines for coronary angiography of the American College of Cardiology and the American Heart Association [13]. The Gensini score was recorded according to a previous study [14].

2.5. Therapy Procedures. All the patients that participated in the study underwent coronary angiography, and 112 patients underwent percutaneous coronary intervention (PCI). Usage of platelet inhibitors or anticoagulants and other symptomatic treatments was left to the discretion of the treating physician according to the guideline and clinical condition. Clopidogrel and aspirin were administered at 600 mg and 300 mg after arrival in the hospital; and the patients were immediately transferred to the catheter room where CAG and/or PCI were performed. Clopidogrel and aspirin were administered at 75 mg and 100 mg per day after PCI, respectively. Beta receptor blocker, statin, and LMWH were administered according to the patients' status and guideline. Angiotensin-converting enzyme inhibitors/angiotensin receptor blocker (ACEI/ARB) was administered in patients who have a serum creatinine level less than 256 μmol/L.

2.6. Endpoints. Major adverse cardiovascular events (MACEs) were recorded. Coronary revascularization was defined as angioplasty, stenting, or coronary artery bypass grafting during the follow-up. Heart failure was defined as BNP measured in Yi Ji Shan Hospital at least one value above the 5 ∗ 99th percentile upper reference limit and having clinical symptoms in hospitalization during the follow-up. MACEs were verified by hospital medical records and telephone. No missing data was generated during the follow-up.

2.7. Statistical Analysis. The data were analyzed using the statistical software package of SPSS (SPSS Inc., Chicago, IL, USA, Version 17.0). Numerical variables were expressed as the mean ± standard deviation and categorical variables as percentages. Continuous variables between groups were compared by unpaired Student's t-test. Categorical variables were compared by the Chi-squared test. Kaplan-Meier survival analysis was performed. The hazard ratio (HR) and 95% confidence interval (CI) were calculated by the Cox proportional hazards model. Two-tailed P values < 0.05 were considered significant.

3. Results

3.1. The Number of Circulating CD34-Positive Cells and Expression of B2R. Flow cytometry showed that among the 174 patients, the proportion of circulating CD34-positive cells ranged from 0.89% to 1.36% (0.98 ± 0.12%). The expression of B2R on circulating CD34-positive cells ranged from 13.8% to 92.6% (median: 53.2%). The expression of B2R between two groups is shown in Figures 1(e) and 1(f).

3.2. Baseline Characteristics. According to the median level (53.2%) of B2R expression on CD34-positive cells, the patients were divided into two groups: low B2R (≤53.2%, $n = 87$) and high B2R group (>53.2%, $n = 87$). Detailed characteristics of the patients are listed in Table 1. The age, biochemical data, degree of coronary artery stenosis, and drug therapy were matched. WBC counts were associated with high B2R expression on CD34-positive cells ($P < 0.001$). The influence of clinical properties was further analyzed by multivariate analyses.

3.3. The Plasma Level of VEGF. As shown in Figure 2, the plasma level of VEGF in the low B2R group is 67 ± 12 pg/mL, whereas the high B2R group has significantly elevated VEGF levels (145 ± 27 pg/mL, $P < 0.001$) (Figure 2(a)).

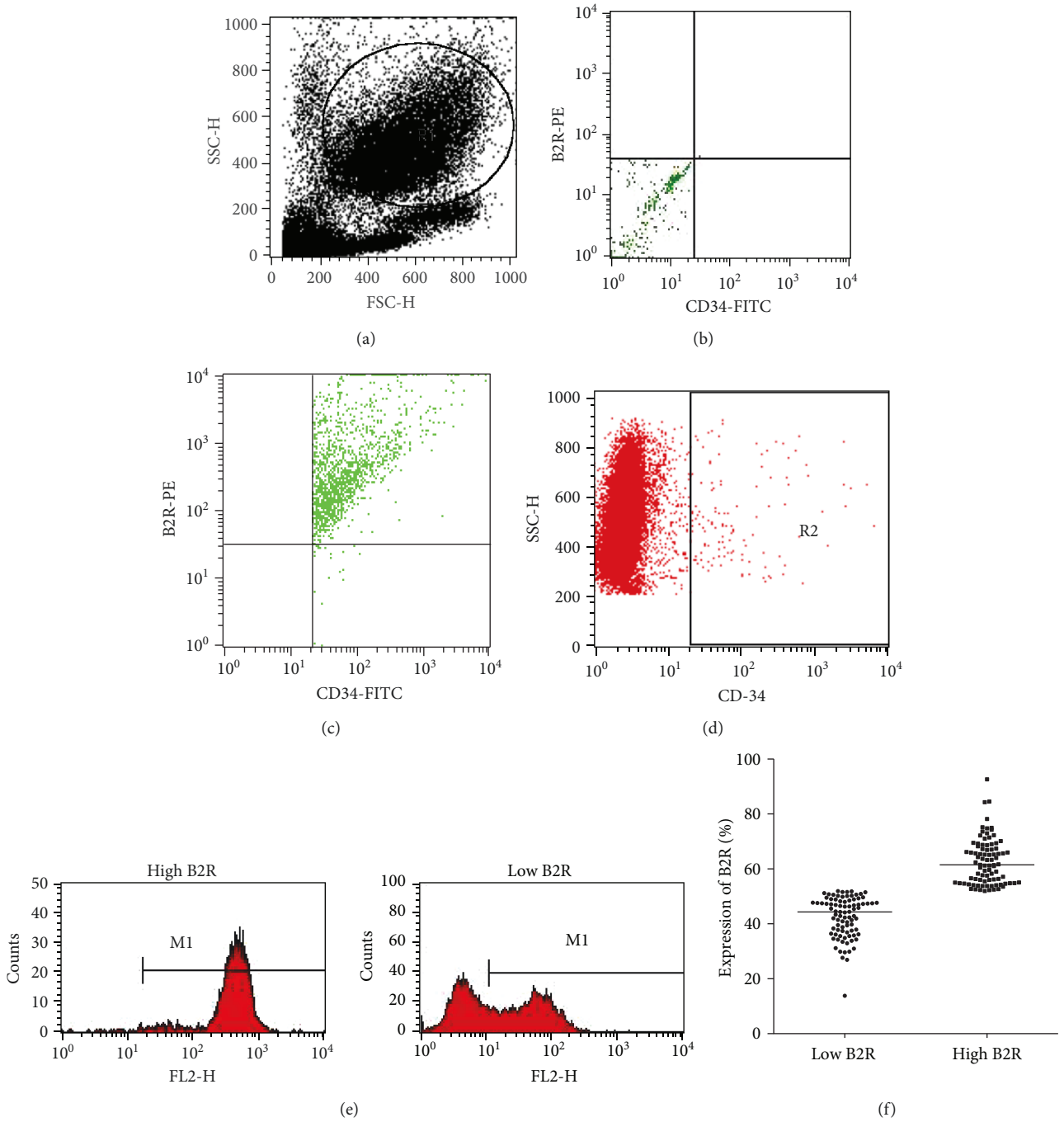

Figure 1: Representative figure of flow cytometry analysis: (a) the gating for mononuclear cells; (b) the negative control; (c) the CD34- and B2R-positive control; (d) R2 represents CD34-positive cells in all gating cells. (e) Representative FACS figure of B2R expression in two groups. M1 represents B2R-positive cells. (f) Scatter diagram shows the expression percentage of B2R between the low B2R and high B2R groups.

Pearson correlation analysis showed that the serum concentration of VEGF is correlated with B2R expression ($r = 0.574$, $P < 0.001$) (Figure 2(b)).

3.4. Incidence of MACEs. In univariate analyses, 25 patients in the low B2R group and 9 patients in the high B2R group have heart failure, respectively (HR: 2.501; 95% CI: 1.166-5.364; $P = 0.018$). Revascularization occurred in 26 patients in the low B2R group and 12 patients in the high B2R group, respectively (HR: 2.066; 95% CI: 1.042-4.096; $P = 0.038$).

In multivariate analyses, after adjusting for the age, sex, WBC, LM stenosis, PCI, plasma VEGF concentration, and drug treatment, the adjusted HR for heart failure is 2.247 (95% CI: 1.110-4.547, $P = 0.024$) and for revascularization is 2.335 (95% CI: 1.075-5.074, $P = 0.032$) (Table 2). The age,

Table 1: Baseline characteristics of myocardial infarction patients.

	Patients ($n = 174$)		
	Low B2R ($n = 87$)	High B2R ($n = 87$)	P
Sex (M/F)	68/19	70/17	0.500
Age (y)	69 ± 10	69 ± 11	0.718
WBC	7.2 ± 2.0	9.5 ± 3.9	<0.001
RBC	4.4 ± 0.5	4.5 ± 0.6	0.284
HB	133 ± 17	134 ± 17	0.972
Gensini score	81 ± 16	86 ± 23	0.684
B2R expression (%)	31.1 ± 4.6	76.5 ± 9.3	0.617
VEGF (pg/mL)	67 ± 12	145 ± 27	<0.001
cTnI	6.2 ± 2.7	14.0 ± 7.6	0.109
TC	4.3 ± 1.0	4.3 ± 1.2	0.058
TG	1.4 ± 0.7	1.3 ± 0.6	0.594
LDL	2.6 ± 0.8	2.7 ± 0.9	0.134
HDL	1.1 ± 0.2	1.1 ± 0.4	0.082
eGFR	78 ± 30	76 ± 34	0.775
Smoking, n (%)	26 (29.9)	17 (19.5)	0.080
HP, n (%)	71 (81.6)	65 (74.7)	0.180
DM, n (%)	26 (29.9)	26 (29.9)	NS
LM, n (%)	3 (3.4)	9 (10.3)	0.132
LAD, n (%)	53 (60.9)	58 (66.7)	0.528
LCX, n (%)	39 (44.8)	39 (44.8)	NS
RCA, n (%)	38 (43.7)	42 (48.3)	0.648
PCI, n (%)	53 (60.9)	59 (67.8)	0.429
Aspirin, n (%)	82 (94.3)	83 (95.4)	NS
Betaloc, n (%)	64 (73.6)	65 (74.7)	NS
ACEI/ARB, n (%)	49 (56.3)	48 (55.2)	NS
Statin, n (%)	76 (87.4)	79 (90.8)	0.628
LMWH, n (%)	45 (51.7)	52 (59.8)	0.360
Clopidogrel, n (%)	55 (63.2)	65 (74.7)	0.140

WBC: white blood cell ($*10^9$/L); HB: hemoglobin (g/L); Neutrophil: $*10^9$/L; cTnI: cardiac troponin I (ng/mL); RBC: red blood cell ($*10^{12}$/L); TC: total cholesterol (mmol/L); TG: triglyceride (mmol/L); LDL: low-density lipoprotein (mmol/L); HDL: high-density lipoprotein (mmol/L); eGFR: estimate glomerular filtration rate (mL/min/1.73m^2); HP: hypertension; DM: diabetes mellitus; LM: Left Main Artery; LAD: left anterior descending branch; LCX: Left Circumflex Artery; RCA: right coronary artery; PCI: percutaneous coronary intervention; ACEI/ARB: angiotensin-converting enzyme inhibitors/angiotensin receptor blocker; LMWH: low molecular weight heparins; NS: $P = 1.000$.

sex, WBC, LM stenosis, PCI, and plasma VEGF concentration are eliminated by the Cox proportional hazards model.

Kaplan-Meier survival analysis showed that the cumulative hazard of heart failure ($P = 0.014$) and revascularization ($P = 0.032$) has significant differences between the two groups (Figure 3).

4. Discussion

Our study indicated that low expression of B2R on circulating CD34-positive cells has a strong relation to the poor outcomes of STEMI. It is the first statement that the expression of B2R on progenitor cells has influenced the outcomes of ischemic damage.

CD34 is expressed on hematopoietic stem/progenitor cells as an adhesion molecule and disappeared gradually during the maturation of these cells. Progenitor cells own the ability to differentiate into several cells. Many experimental and clinical types of research showed that progenitor cells are involved in vascular repairing [15]. In particular, the transplantation of progenitor cells has clinical benefits in the treatment of vascular injury [16]. Moreover, Werner et al. found that the level of circulating $CD34^+KDR^+$ EPCs predicts the occurrence of cardiovascular events and death from cardiovascular causes. However, the predictability of the circulating CD34-positive cell number for the occurrence of cardiovascular events has yet to be reported in other cardiovascular diseases. According to a previous study [10] and this research, the proportion of CD34-positive cells is below 2%. In addition, if circulating CD34-positive cells have the ability to predict the outcomes of STEMI remains unknown. Thus, it is needed to find another way to identify the relation between circulating progenitor cells and outcomes in STEMI.

B2R is a member of the G protein-coupled receptor superfamily and a critical cell surface receptor molecule that is activated by BK and expressed on numerous cells, including EPCs that regulate cell proliferation and injury repair [11]. Spinetti et al. [17] had found that a B2R-dependent mechanism is involved in the invasive capacity of EPCs activated by tissue kallikrein which indicated that the B2R signal pathway is essential for the protective effect of EPCs. Previous researches have also shown that the B2R-mediated signaling pathway has suppressed the cell dysfunction through recruitment of circulating CD34-positive cells [11, 18]. Further, low B2R expression is associated with inhibition of cell proliferation [19]. In an animal model, age-related low B2R protein levels may leave the heart vulnerable to ischemic damage [20]. Recently, our previous study further demonstrated that B2R regulate the oxidative stress-induced premature senescence of EPCs [21]. In addition, B2R is strongly associated with P53 expression, as B2R knockout diabetic mice are resistant to oxidative stress-induced mitochondrial injury and show high expression of the tumor suppressor gene P53 [22]. In the ischemia disease model, activation of the B2R-associated signal pathway inhibits the development of myocardial infarction [23]. Besides, myocardial ischemia triggers B2 receptor upregulation in both the infarcted and noninfarcted areas of the heart [24]. Our data found that low B2R expression of circulating CD34-positive cells indicates the poor outcomes of STEMI. The possible reason is that high B2R expression triggers the protective effect of the B2R-associated signal pathway that further mobilizes the circulating EPCs.

VEGF is a classic factor that mediates angiogenesis [25]. Previous research indicated that plasma VEGF concentration is related to coronary collateral function in patients with CHD [26]. However, VEGF worked in many ways. The activation of B2R can further trigger the receptor of VEGF that promotes the angiogenesis. On the other side, VEGF may

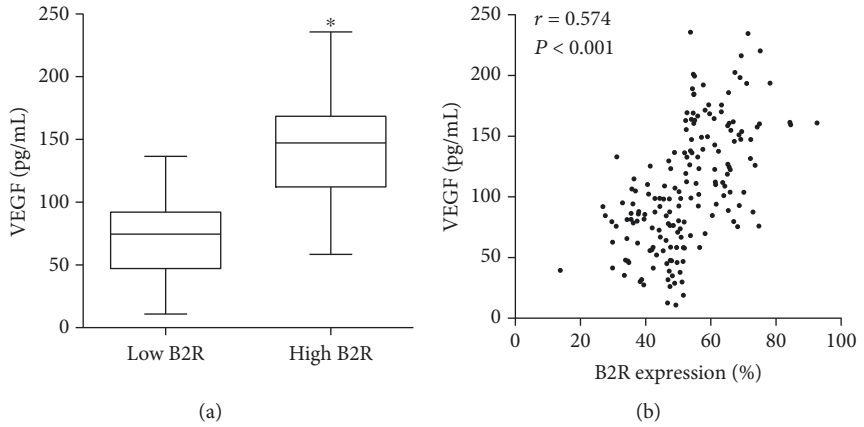

Figure 2: Plasma VEGF concentration of two groups and relationship with B2R expression. (a) Box plot shows the VEGF concentration of two groups. (b) Pearson correlation between the low and high B2R groups ($^*P < 0.001$).

Table 2: Multivariate analysis of the association between expression of B2R and outcomes.

Outcomes	Low B2R	High B2R	HR (95% CI)	*P*	Adjusted HR (95% CI)	*P*
Heart failure no./total no.	25/87	9/87	2.501 (1.166-5.364)	0.018	2.247 (1.110-4.547)	0.024
%	28.7	10.3				
Revascularization no./total no.	26/87	12/87	2.066 (1.042-4.096)	0.038	2.335 (1.075-5.074)	0.032
%	29.9	13.8				

HR: hazard ratio; CI: confidence interval.

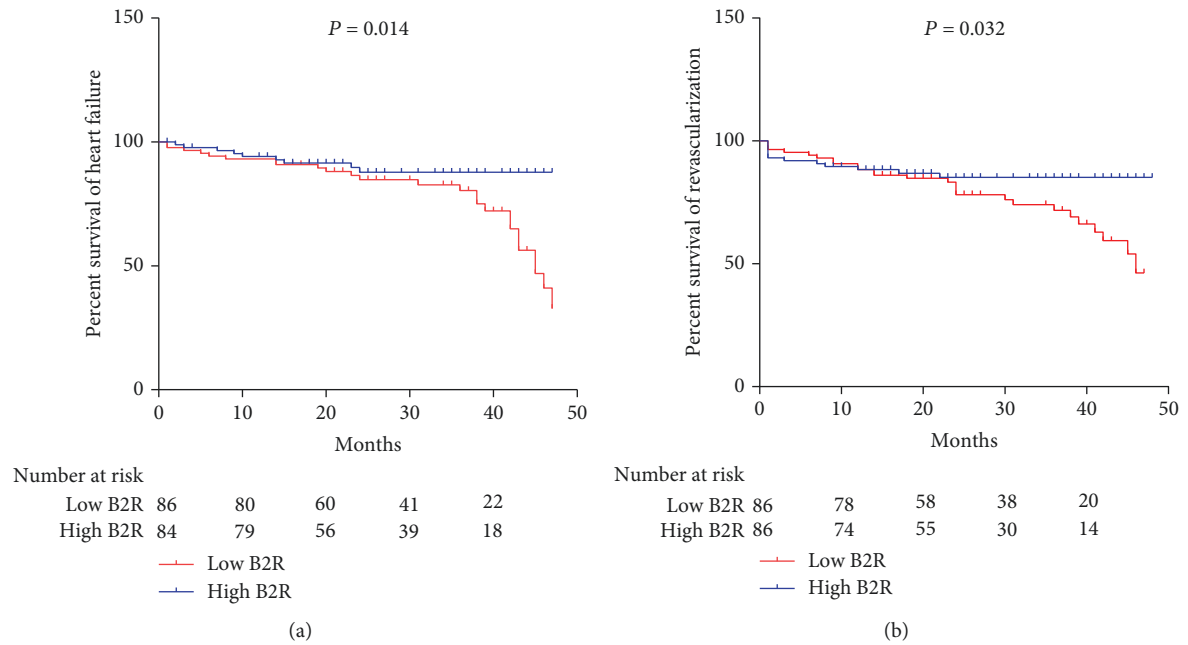

Figure 3: Kaplan-Meier survival analysis of MACEs: (a) percentage survival of heart failure between two groups; (b) percentage survival of revascularization between two groups.

lead to plaque instability as a proinflammation factor. Our study showed that the expression of B2R is related to plasma VEGF concentration. However, the Cox proportional hazards model eliminates plasma VEGF concentration. VEGF is not an effective single biomarker that indicates the prognosis of coronary artery disease. The poor outcomes in low B2R patients may have a relation to the poor angiogenesis after myocardial infarction.

Further, EPCs are a major source of CD34-positive cells. A previous study suggested that EPC transplantation has the potential to cure myocardial infarction via the activated B2R signal pathway [27]. The results from our cohort study

suggested that low B2R led to poor outcomes. We can further explain that low B2R expression failed to activate the B2R signal pathway when EPCs which mobilized to peripheral blood cannot be developed to exert its protective effects such as promoting cell proliferation and angiogenesis.

This research has several limitations. Firstly, the sample size is small, so the reliability of the results needs to be validated by a large sample trial. Secondly, the CD34 is not the unique marker of progenitor cells such as EPCs. Thirdly, if the increased incidence rate of MACEs is related to the failed activation of B2R that EPCs cannot develop its protective effect needs to be further studied by basic fundamental research.

5. Conclusion

Low expression of B2R on circulating progenitor cells indicated the poor outcomes of STEMI.

Data Availability

The datasets used and/or analyzed in the current study are available from the corresponding author on reasonable request.

Disclosure

The abstract of this manuscript has been presented in the Journal of the American College of Cardiology, Volume 72, Issue 16, Supplement, 16 October 2018, Page C77.

Conflicts of Interest

The authors declare that they have no conflicts of interest.

Authors' Contributions

Cong Fu and Yuhan Cao contributed equally to this work.

Acknowledgments

The sources of funding are National Natural Science Foundation of China (81700265 to Cong Fu and 81702092 to Yuhan Cao) and Colleges and Universities Natural Science Fund of Anhui (KJ2017A270 to Cong Fu and KJ2017A269 to Yuhan Cao).

References

[1] G. A. Roth, C. Johnson, A. Abajobir et al., "Global, regional, and national burden of cardiovascular diseases for 10 causes, 1990 to 2015," *Journal of the American College of Cardiology*, vol. 70, no. 1, pp. 1–25, 2017.

[2] J. C. Choy, D. J. Granville, D. W. C. Hunt, and B. M. McManus, "Endothelial cell apoptosis: biochemical characteristics and potential implications for atherosclerosis," *Journal of Molecular and Cellular Cardiology*, vol. 33, no. 9, pp. 1673–1690, 2001.

[3] M. Gill, S. Dias, K. Hattori et al., "Vascular trauma induces rapid but transient mobilization of $VEGFR2^{+}AC133^{+}$ endothelial precursor cells," *Circulation Research*, vol. 88, no. 2, pp. 167–174, 2001.

[4] T. Asahara, T. Murohara, A. Sullivan et al., "Isolation of putative progenitor endothelial cells for angiogenesis," *Science*, vol. 275, no. 5302, pp. 964–966, 1997.

[5] C. Kalka, H. Masuda, T. Takahashi et al., "Transplantation of *ex vivo* expanded endothelial progenitor cells for therapeutic neovascularization," *Proceedings of the National Academy of Sciences of the United States of America*, vol. 97, no. 7, pp. 3422–3427, 2000.

[6] A. Kawamoto, H. C. Gwon, H. Iwaguro et al., "Therapeutic potential of ex vivo expanded endothelial progenitor cells for myocardial ischemia," *Circulation*, vol. 103, no. 5, pp. 634–637, 2001.

[7] S. Rafii and D. Lyden, "Therapeutic stem and progenitor cell transplantation for organ vascularization and regeneration," *Nature Medicine*, vol. 9, no. 6, pp. 702–712, 2003.

[8] U. M. Gehling, S. Ergün, U. Schumacher et al., "In vitro differentiation of endothelial cells from AC133-positive progenitor cells," *Blood*, vol. 95, no. 10, pp. 3106–3112, 2000.

[9] E. Gunsilius, H. C. Duba, A. L. Petzer, C. M. Kähler, and G.. A. Gastl, "Contribution of endothelial cells of hematopoietic origin to blood vessel formation," *Circulation Research*, vol. 88, no. 1, article E1, 2001.

[10] N. Werner, S. Kosiol, T. Schiegl et al., "Circulating endothelial progenitor cells and cardiovascular outcomes," *The New England Journal of Medicine*, vol. 353, no. 10, pp. 999–1007, 2005.

[11] N. Kränkel, R. G. Katare, M. Siragusa et al., "Role of kinin B_2 receptor signaling in the recruitment of circulating progenitor cells with neovascularization potential," *Circulation Research*, vol. 103, no. 11, pp. 1335–1343, 2008.

[12] K. Thygesen, J. S. Alpert, A. S. Jaffe, M. L. Simoons, B. R. Chaitman, and H. D. White, "Third universal definition of myocardial infarction," *Global Heart*, vol. 7, no. 4, pp. 275–295, 2012.

[13] P. J. Scanlon, D. P. Faxon, A. M. Audet et al., "ACC/AHA guidelines for coronary angiography: executive summary and recommendations. A report of the American College of Cardiology/American Heart Association Task Force on Practice Guidelines (Committee on Coronary Angiography) developed in collaboration with the Society for Cardiac Angiography and Interventions," *Circulation*, vol. 99, no. 17, pp. 2345–2357, 1999.

[14] G. G. Gensini, "A more meaningful scoring system for determining the severity of coronary heart disease," *The American Journal of Cardiology*, vol. 51, no. 3, p. 606, 1983.

[15] D. Kong, L. G. Melo, M. Gnecchi et al., "Cytokine-induced mobilization of circulating endothelial progenitor cells enhances repair of injured arteries," *Circulation*, vol. 110, no. 14, pp. 2039–2046, 2004.

[16] N. Werner, S. Junk, U. Laufs et al., "Intravenous transfusion of endothelial progenitor cells reduces neointima formation after vascular injury," *Circulation Research*, vol. 93, no. 2, pp. e17–e24, 2003.

[17] G. Spinetti, O. Fortunato, D. Cordella et al., "Tissue kallikrein is essential for invasive capacity of circulating proangiogenic cells," *Circulation Research*, vol. 108, no. 3, pp. 284–293, 2011.

[18] H. Oeseburg, D. Iusuf, P. van der Harst, W. H. van Gilst, R. H. Henning, and A. J. M. Roks, "Bradykinin protects against

oxidative stress-induced endothelial cell senescence," *Hypertension*, vol. 53, no. 2, pp. 417–422, 2009.

[19] M. Kakoki, C. M. Kizer, X. Yi et al., "Senescence-associated phenotypes in Akita diabetic mice are enhanced by absence of bradykinin B2 receptors," *The Journal of Clinical Investigation*, vol. 116, no. 5, pp. 1302–1309, 2006.

[20] E. Kintsurashvili, A. Duka, I. Ignjacev, G. Pattakos, I. Gavras, and H. Gavras, "Age-related changes of bradykinin B_1 and B_2 receptors in rat heart," *American Journal of Physiology. Heart and Circulatory Physiology*, vol. 289, no. 1, pp. H202–H205, 2005.

[21] C. Fu, B. Li, Y. Sun, G. Ma, and Y. Yao, "Bradykinin inhibits oxidative stress-induced senescence of endothelial progenitor cells through the B2R/AKT/RB and B2R/EGFR/RB signal pathways," *Oncotarget*, vol. 6, no. 28, pp. 24675–24689, 2015.

[22] S. S. El-Dahr and Z. Saifudeen, "Interactions between *BdkrB2* and *p53* genes in the developing kidney," *Biological Chemistry*, vol. 394, no. 3, pp. 347–351, 2013.

[23] H. Ito, I. Hayashi, T. Izumi, and M. Majima, "Bradykinin inhibits development of myocardial infarction through B_2 receptor signalling by increment of regional blood flow around the ischaemic lesions in rats," *British Journal of Pharmacology*, vol. 138, no. 1, pp. 225–233, 2003.

[24] C. Tschope, S. Heringer-Walther, M. Koch et al., "Myocardial bradykinin B2-receptor expression at different time points after induction of myocardial infarction," *Journal of Hypertension*, vol. 18, no. 2, pp. 223–228, 2000.

[25] Y. Wang, M. Nakayama, M. E. Pitulescu et al., "Ephrin-B2 controls VEGF-induced angiogenesis and lymphangiogenesis," *Nature*, vol. 465, no. 7297, pp. 483–486, 2010.

[26] R. S. Ripa, E. Jorgensen, F. Baldazzi et al., "The influence of genotype on vascular endothelial growth factor and regulation of myocardial collateral blood flow in patients with acute and chronic coronary heart disease," *Scandinavian Journal of Clinical and Laboratory Investigation*, vol. 69, no. 6, pp. 722–728, 2009.

[27] Z. L. Sheng, Y. Y. Yao, Y. F. Li, C. Fu, and G. S. Ma, "Transplantation of bradykinin-preconditioned human endothelial progenitor cells improves cardiac function via enhanced Akt/eNOS phosphorylation and angiogenesis," *American Journal of Translational Research*, vol. 7, no. 7, pp. 1214–1226, 2015.

Hindawi
Disease Markers
Volume 2019, Article ID 7676189, 10 pages
https://doi.org/10.1155/2019/7676189

Research Article

Metabolic Disturbances Identified in Plasma Samples from ST-Segment Elevation Myocardial Infarction Patients

Vânia Aparecida Mendes Goulart,[1] **Anderson Kenedy Santos**,[1] **Valéria Cristina Sandrim**,[2] **Josimar Marques Batista**,[3] **Mauro Cunha Xavier Pinto**,[4] **Luiz Cláudio Cameron**,[5] **and Rodrigo Ribeiro Resende**[1]

[1]*Departamento de Bioquímica e Imunologia, Instituto de Ciências Biológicas, Universidade Federal de Minas Gerais, Belo Horizonte, MG, Brazil*
[2]*Instituto de Ensino e Pesquisa da Santa Casa de BH, Belo Horizonte, MG, Brazil*
[3]*Departamento de Química, Universidade Federal de Minas Gerais, Belo Horizonte, MG, Brazil*
[4]*Departamento de Farmacologia, Instituto de Ciências Biológicas, Universidade Federal de Goiás, Goiânia, GO, Brazil*
[5]*Laboratório de Bioquímica de Proteínas, Centro de Inovação de Espectrometria de Massas, Universidade Federal do Rio de Janeiro, Rio de Janeiro, RJ, Brazil*

Correspondence should be addressed to Vânia Aparecida Mendes Goulart; vaniagoulartbio@gmail.com
and Rodrigo Ribeiro Resende; rrresende@hotmail.com

Received 21 January 2019; Revised 7 May 2019; Accepted 16 May 2019; Published 1 July 2019

Guest Editor: Zhongjie Shi

ST-segment elevation myocardial infarction (STEMI) is the most severe form of myocardial infarction (MI) and the main contributor to morbidity and mortality caused by MI worldwide. Frequently, STEMI is caused by complete and persistent occlusion of a coronary artery by a blood clot, which promotes heart damage. STEMI impairment triggers changes in gene transcription, protein expression, and metabolite concentrations, which grants a biosignature to the heart dysfunction. There is a major interest in identifying novel biomarkers that could improve the diagnosis of STEMI. In this study, the phenotypic characterization of STEMI patients ($n = 15$) and healthy individuals ($n = 19$) was performed, using a target metabolomics approach. Plasma samples were analyzed by UPLC-MS/MS (ultra-high-performance liquid chromatography-tandem mass spectrometry) and FIA-MS (MS-based flow injection analysis). The goal was to identify novel plasma biomarkers and metabolic signatures underlying STEMI. Concentrations of phosphatidylcholines, lysophosphatidylcholines, sphingomyelins, and biogenic amines were altered in STEMI patients in relation to healthy subjects. Also, after multivariate analysis, it was possible to identify alterations in the glycerophospholipids, alpha-linolenic acid, and sphingolipid metabolisms in STEMI patients.

1. Introduction

Myocardial infarction (MI) is a heart blood flow disruption that leads to tissue damage and cell death in the heart muscle. This pathology presents a high incidence worldwide, and it is a common cause of death and disability in humans [1]. MI has two major clinical manifestations: non-ST-segment elevation myocardial infarction (NSTEMI) and ST-segment elevation myocardial infarction (STEMI), which is the more severe form and main contributor to morbidity and mortality by MI [2–4]. STEMI results from the abrupt occlusion of an epicardial coronary artery; as a consequence, the myocardium distal to the occlusion site becomes ischemic [5, 6].

During the ischemic process, oxygen supply is interrupted, and mitochondrial oxidative phosphorylation rapidly stops, with a massive reduction of ATP production from energy metabolism. A compensatory increase in anaerobic glycolysis for ATP production leads to the accumulation of hydrogen ions and lactate, resulting in intracellular acidosis and inhibition of glycolysis, as well as mitochondrial fatty

acid and residual energy metabolism. Impaired contraction with persistent electrical activity (excitation-contraction uncoupling) is developed in association with alterations in ion transport systems in the sarcolemma and organellar membranes [6–8].

In addition to the osmotic and ionic imbalance, the membrane depolarization also activates the voltage-dependent Ca^{2+} channels, raising levels of intracellular Ca^{2+}. The rapid increase of intracellular calcium is due to the influx through the membrane and by the release of Ca^{2+} present in the mitochondria and in the cytoplasmic reticulum. Excessive cytosolic Ca^{2+} leads to the activation of calcium-dependent proteases, phospholipases, lipases, ATPases, and endonucleases. Activation of these enzymes alters cell function, destabilizes the structure of plasma membrane and cytoskeleton, increases lipolysis by free fatty acid metabolism, induces superoxide radical production, promotes DNA damage, and ultimately leads to cell death [9–12].

STEMI injury triggers changes in gene transcription, protein expression, and metabolite concentrations, which grant a biosignature of the heart dysfunction [13–15]. Detection of these biochemical changes has resulted in the discovery of emerging biomarkers, such as myoglobin, total creatine kinase (CK), CK-myocardial band, troponin I (cTnI), and troponin T (cTnT) [16]. However, the efficacy of these STEMI biomarkers is questionable because of the low sensitivity (35% for CK-MB and cTnI) and specificity (85 and 86% for CK-MB and cTnI, respectively) in the first 8 h after injury [15, 17].

The low sensitivity and specificity of biomarkers added to the fact that they can only be detected at least six hours after symptoms onset and that the MI diagnosis is based, besides other factors, in symptoms, that can vary individually, lay emphasis on the importance of the improvement of a biochemical diagnosis of MI [3, 5, 18].

The metabolomics approach has demonstrated great utility in the biomarker discovery field, as well as in detecting changes in biological pathways and in providing information on the mechanisms underlying various conditions, including cardiovascular diseases [19–21]. It is based on the global quantitative measurement of low molecular weight endogenous metabolites in tissues or biological fluids [22]. In this study, a target metabolomics approach was used to characterize the phenotypes of STEMI patients and healthy individuals. The overarching goal was to identify novel plasma biomarkers and metabolic signatures underlying STEMI.

2. Methods

2.1. Study Population. The study was conducted according to the Declaration of Helsinki, and its protocol was approved by the Ethics Committee in Research of Santa Casa Misericórdia of Belo Horizonte under number 064/2009. All subjects that agreed to participate prior to their inclusion in the study have signed an informed consent form. STEMI patients were screened based on the following inclusion criteria: age 40-80 years, gender-balanced, chest pain above 20 minutes, and electrocardiographic (ECG) features consistent with STEMI: coronary stenosis with minimal commitment of 70% of the arterial lumen in at least one coronary artery, based on the angiography results (Table 1). The exclusion criteria were as follows: prior history of myocardial infarction or stroke, non-ST-segment elevation myocardial infarction, or other acute coronary syndromes.

Table 1: The number of cases and affected arteries in patients with STEMI.

Affected arteries*	Cases (%)
One artery	
Left anterior descending coronary artery (LAD)	5 (33.3)
Right coronary artery (RCA)	1 (6.6)
Left circumflex coronary artery (LCX)	1 (6.6)
Two arteries	
Right coronary artery+left anterior descending coronary artery	3 (20)
Right coronary artery+left circumflex coronary artery	3 (20)
Left anterior descending coronary artery+posterior descending artery	2 (13.3)

*Information obtained through coronary angiography.

The control group was compound on 19 individuals who had never had heart disease or stroke. All participants were recruited from the Clinics Hospital of the Federal University of Minas Gerais (Belo Horizonte, MG, Brazil) and Santa Casa of BH (Belo Horizonte, MG, Brazil). The demographic characteristics of the patients and controls are shown in Table 2.

2.2. Sample Analysis. Blood samples were collected using tubes from the Vacuette® system, and 4 mL were stored in anticoagulant ethylenediaminetetraacetic acid (EDTA) to obtain plasma. The blood samples obtained were rapidly centrifuged at 3.000 rotations per minute (RPM) for 10 minutes to separate the plasma samples and then were distributed in several aliquots into microtubes and immediately stored at -80°C. Plasma samples ($n = 15$) were obtained up to seven hours after hospitalization.

A targeted metabolomics approach was used to analyze plasma samples from STEMI patients and controls. The sample preparation and analysis procedures were performed according to the AbsoluteIDQp180 kit (Biocrates Life Sciences AG, Innsbruck, Austria). This kit allows the measurement of metabolites by UPLC-MS/MS (ultra-high performance liquid chromatography-tandem mass spectrometry) and FIA-MS (MS-based flow injection analysis). Briefly, the samples were added to the center of a filter on the upper 96-well plate in 10 μL aliquots per well and dried using a nitrogen evaporator. Subsequently, 50 μL of a 5% solution of phenyl isothiocyanate was added for derivatization of the amino acids and biogenic amines. After incubation, the filter spots were dried again using the nitrogen evaporator.

The metabolites were extracted using 300 μL of 5 mM ammonium acetate in methanol solution and transferred by centrifugation into the lower 96-deep well plate. From the obtained extract, 150 μL was diluted with the same volume of H_20 and submitted to UPLC-MS/MS for amino acid and biogenic amine measurements. The remainder of the extract was diluted with 400 μL of mass spectrometry running

Table 2: Demographic data of patients and controls.

Patients		Age*	SAH** (%)	Smoking (%)	Dyslipidemia (%)	Type 2 diabetes mellitus (%)
STEMI	$n = 15$					
Male	8	66.72 (±4.92)	50.0	62.5	12.5	12.5
Female	7	69.43 (±9.95)	57.2	28.5	28.5	42.8
Controls	$n = 19$					
Male	9	55.56 (±12.07)	44.4	44.4	—	—
Female	10	58.30 (±7.70)	70.0	30.0	—	—

*Mean (±SD). **SAH: systemic arterial hypertension.

solvent for further MS analysis lipid detection. The UPLC-MS/MS system was equipped with an Acquity UPLC BEH C18 column (1.7 μm, 2.1 × 50 mm) (Waters Chromatography, Dublin, Ireland) connected to Xevo TQ-S mass spectrometers (Waters Technologies, Massachusetts, USA), and the samples were analyzed in positive mode.

The identification and quantification of the metabolites were achieved using internal standards and multiple reaction monitoring (MRM) detection. FIA-MS analysis was performed using the tandem quadrupole mass spectrometer Xevo-TQ-S (Waters Technologies, Massachusetts, USA) also in positive mode. The data analysis and calculation of the metabolite concentrations analyzed by FIA (acylcarnitines, glycerophospholipids, sphingolipids, and hexoses) were automated using MetIDQ software (Biocrates Life Sciences AG, Innsbruck, Austria), an integral part of the kit that imports Waters' raw data files. The peaks obtained by UPLC (amino acids and biogenic amines) were analyzed using the Target Lynx Application Manager (Waters Technologies, Massachusetts, USA).

2.3. Statistical Analysis. The dataset was analyzed by univariate and multivariate methods. IBM SPSS (International Business Machines, New York, USA) software and the web server MetaboAnalyst 3.0 (http://www.metaboanalyst.ca) were used to develop the univariate analyses, specifically the Wilcoxon-Mann-Whitney test. These methods were used to identify the variables (metabolites) that presented statistically significant differences ($p < 0.05$) in concentrations between the groups studied.

For the multivariate analysis, the software SIMCA 14.0 (Umetrics, Umeå, Sweden) was used. The dataset containing the statistically significant variables were submitted to normalization by unit variance (UV) scaling and then to principal component analysis (PCA), partial least squares discriminant analysis (PLS-DA), and orthogonal projection to latent structure discriminant analysis (OPLS-DA) [23]. The unsupervised method, principal component analysis (PCA), was performed to verify the trends of separation between groups. Then, PLS-DA was performed. This classification technique finds the components or latent variables which discriminate as much as possible between two or more different groups of samples (X block), according to their maximum covariance with target classes (concentrations of metabolites) defined in the Y data block [24]. By relating a data matrix containing independent variables from samples

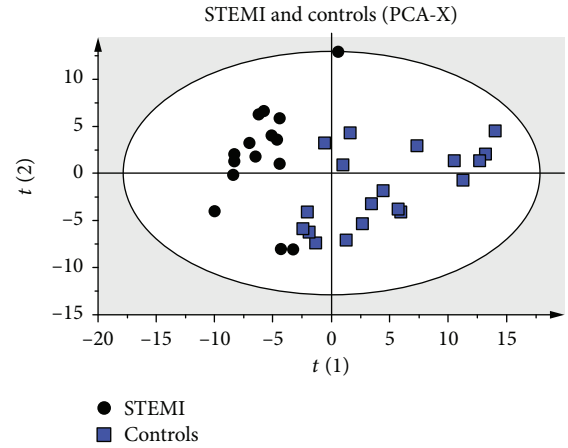

Figure 1: Score plots of principal component analysis (PCA) results. Score plots discriminating the metabolic profiles in plasma samples between patients with STEMI and controls. The parameters of the models were as follows: 4 PCs, $R^2 = 0.679$, and $Q^2 = 0.47$.

(concentration values) to a matrix containing dependent variables (classes) for these samples, OPLS-DA can remove variations from the independent variables that are not correlated to the dependent variables and enables reducing the model complexity with preserved prediction ability [25].

The models were evaluated using the goodness-of-fit parameter (R^2) and the predictive ability parameter (Q^2). R^2 represents the proportion of variance explained by a given component in the model, whereas Q^2 is defined as the proportion of variance in the data predictable model under cross-validation [26]. The R^2 ranges from 0 to 1, with higher levels indicating more predictive accuracy, whereas $Q^2 = 1$ indicates perfect predictability [26, 27]. OPLS-DA models were examined to determine which variables were more responsible for any observed separation between groups.

To identify which variables were responsible for this separation, the variable influence on the projection (VIP) parameter was used to select variables that have the more significant contribution in discriminating between metabolomics profiles of ischemic stroke patients, STEMI, and controls. VIP scores indicate the importance of the variable to the whole model [28]. The independent variable evaluation contributes to predictions, and it is an important aspect in the multivariate classification models [29]. In our work, the independent variables were metabolite concentrations

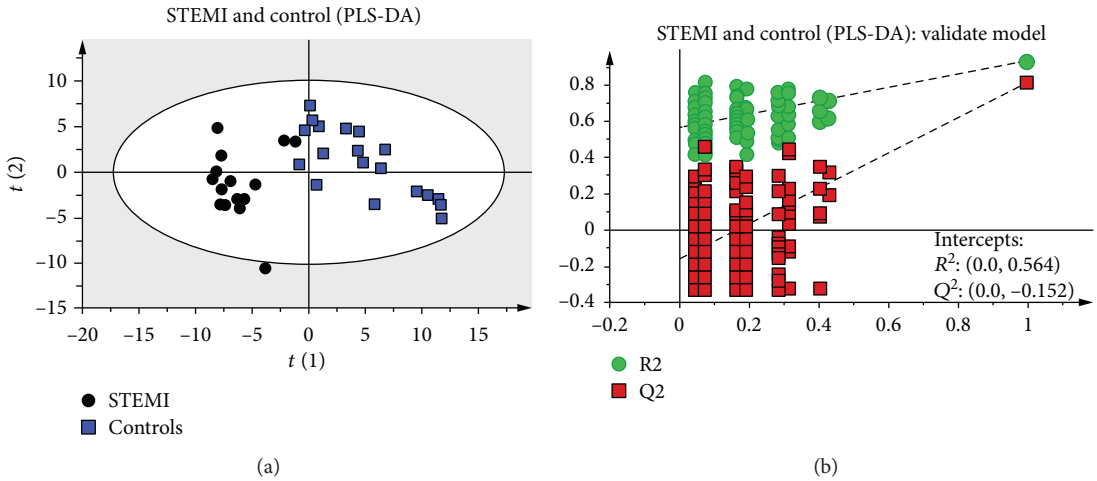

Figure 2: Score plots of partial least squares discriminant analysis (PLS-DA) and validation of the model. Score plots discriminating the metabolic profiles in plasma samples between patients with STEMI versus controls (a). The model's parameters were as follows: 3 latent variables, $R^2 = 0.93$, and $Q^2 = 0.811$. The plot of the permutation test of PLS-DA of STEMI versus the control group (b). Model validation with the number of permutations equaling 200.

and the observation of the regression coefficients allowed us to identify which ones were more positively (high content) or negatively (low content) related to a predicted class. The web server MetaboAnalyst 3.0 (http://www.metaboanalyst.ca) was used for the construction of heatmaps and for the analysis of metabolic pathways.

3. Results

Concentrations of 184 metabolites were analyzed in plasma samples from STEMI patients and healthy volunteers (controls). The unsupervised PCA was first applied to explore correlations between healthy subjects and STEMI patients. According to the PCA analysis of score plots, there was a tendency towards the separation of the STEMI patients and controls (Figure 1).

In addition to PCA analysis, we used the same dataset for PLS-DA analyses. Permutation testing and seven-fold cross-validation, two established methods of internal validation, were used to confirm model validity. Permutation tests involve the random assignment of class labels to cases and controls [26]. The seven-fold cross-validation step involves omitting a portion of the data from model development, developing parallel models from the reduced data, predicting the omitted data from the different models, and then comparing predicted with actual values, providing an estimate of overall predictive power [30]. The obtained results demonstrated evident discrimination between the metabolic profiles (Figure 2(a)). The PLS-DA model presented high predictive and adjustment capacity ($Q^2 = 0.42$, $R^2 = 0.93$) through cross-validation. Additionally, the permutation test plot ($n = 200$) showed intercepts: $R^2 = 0.0$ and 0.564; $Q^2 = 0.0$ and 0.152, indicating that this PLS-DA model is not overfitting and is valid for this metabolomics profiling (Figure 2(b)).

The best visualization of the discrimination between STEMI and controls was obtained through the construction of the model by OPLS-DA (Figure 3). This model, as well as PLS-DA, was validated using a seven-fold cross-validation step as internal validation. After validation, the quality parameters obtained were $R^2 = 0.93$ and $Q^2 = 0.771$.

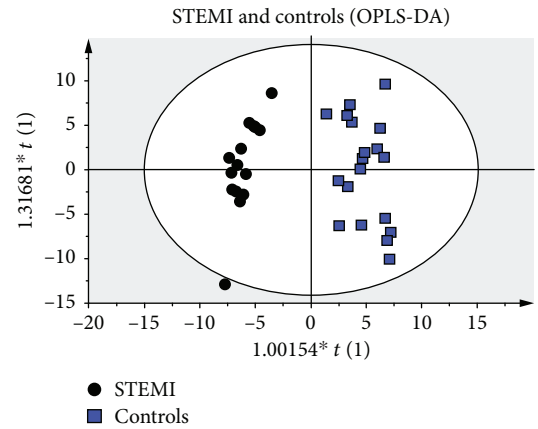

Figure 3: Score plots of orthogonal projection to latent structures discriminant analysis (OPLS-DA) results. Score plots discriminating the metabolic profiles in plasma samples between patients with STEMI versus controls. The parameters of the model were as follows: 2 PCs, $R^2 = 0.93$, and $Q^2 = 0.771$.

To verify which independent variables (metabolites) were more important for the classification between the groups using OPLS-DA, the VIP scores were calculated. By combining the VIP values > 1 with the results from the univariate statistical analysis, we could select the differential metabolites between STEMI patients and controls. Sixty metabolites with VIP scores > 1 were found; among them, 44 presented a statistical difference ($p < 0.05$) between STEMI and controls (Table 3). Of these metabolites, 41 had an identification record in the HMDB (Human Metabolome Database, http://www.hmdb.ca/). The differences in concentration of these metabolites among the samples are demonstrated in the heatmaps (Figure 4(a)), and the difference between groups is demonstrated in Figure 4(b) and in the graphic of

Table 3: Differentiating metabolites between STEMI and healthy individuals (controls).

No.	Metabolites	Classes	VIP[a]	FC[b]	p value[c]	q value[d]	STEMI	Controls
1	PC ae C36:4	Phosphatidylcholines	1,49	-3.69	**0.0003**	0.0049	Up	Down
2	PC ae C36:3	Phosphatidylcholines	1,48	1.98	**0.0021**	0.0140	Down	Up
3	PC ae C34:2	Phosphatidylcholines	1,47	1.05	0.8082	0.8841	Down	Up
4	PC ae C38:5	Phosphatidylcholines	1,44	-3.65	**0.0014**	0.0119	Up	Down
5	PC ae C38:6	Phosphatidylcholines	1,42	2.27	**< 0.0001**	0.0000	Down	Up
6	PC ae C34:3	Phosphatidylcholines	1,39	1.92	**0.0020**	0.0140	Down	Up
7	PC aa C34:4	Phosphatidylcholines	1,39	-2.4	**0.0076**	0.0285	Up	Down
8	PC ae C40:3	Phosphatidylcholines	1,38	-2.29	**0.0442**	0.0913	Up	Down
9	PC aa C40:2	Phosphatidylcholines	1,37	1.22	0.5324	0.6310	Down	Up
10	PC ae C40:6	Phosphatidylcholines	1,35	1.64	**0.0022**	0.0142	Down	Up
11	lysoPC a C14:0	Lysophosphatidylcholines	1,35	1.68	**0.0004**	0.0049	Down	Up
12	PC aa C36:1	Phosphatidylcholines	1,33	1.7	**< 0.0001**	0.0017	Down	Up
13	PC aa C36:3	Phosphatidylcholines	1,33	-3.29	**0.0302**	0.0729	Up	Down
14	PC ae C36:5	Phosphatidylcholines	1,32	-1.21	0.7157	0.8035	Up	Down
15	PC ae C32:1	Phosphatidylcholines	1,32	1.14	**0.0076**	0.0285	Down	Up
16	PC aa C36:0	Phosphatidylcholines	1,32	-1.44	**0.0136**	0.0426	Up	Down
17	PC aa C40:3	Phosphatidylcholines	1,30	3.0	**0.0264**	0.0663	Down	Up
18	PC ae C38:4	Phosphatidylcholines	1,29	-3.69	**0.0003**	0.0049	Up	Down
19	PC aa C38:3	Phosphatidylcholines	1,29	1.54	**0.0003**	0.0049	Down	Up
20	PC aa C42:4	Phosphatidylcholines	1,28	-1.6	**0.0045**	0.0190	Up	Down
21	SM C26:0	Sphingomyelins	1,27	2.42	**0.0002**	0.0036	Down	Up
22	lysoPC a C18:2	Lysophosphatidylcholines	1,25	1.58	**0.0045**	0.0190	Down	Up
23	PC aa C30:0	Phosphatidylcholines	1,23	1.82	**0.0004**	0.0049	Down	Up
24	PC ae C42:1	Phosphatidylcholines	1,22	-1.35	0.1401	0.2330	Up	Down
25	PC ae C38:3	Phosphatidylcholines	1,22	2.23	0.0860	0.1594	Down	Up
26	PC ae C36:2	Phosphatidylcholines	1,21	-4.02	**0.0315**	0.0733	Up	Down
27	PC ae C34:1	Phosphatidylcholines	1,20	1.05	0.5324	0.6310	Down	Up
28	Nitro-Tyr	Biogenic amines	1,20	-2.18	**0.0008**	0.0075	Up	Down
29	PC aa C38:5	Phosphatidylcholines	1,20	1.87	**<0.0001**	0.0017	Down	Up
30	SM (OH) C24:1	Sphingomyelins	1,19	-1.14	0.1760	0.2715	Down	Down
31	lysoPC a C20:3	Lysophosphatidylcholines	1,19	1.04	0.3764	0.4824	Down	Up
32	PC ae C38:1	Phosphatidylcholines	1,17	-2.11	**0.0183**	0.0533	Up	Down
33	PC ae C44:3	Phosphatidylcholines	1,16	-1.32	0.3488	0.4603	Down	Down
34	Ac-Orn	Biogenic amines	1,16	1.82	**0.0039**	0.0190	Down	Up
35	PC aa C40:5	Phosphatidylcholines	1,15	-2.44	**0.0201**	0.0548	Up	Down
36	PC ae C32:2	Phosphatidylcholines	1,15	1.55	**0.0005**	0.0052	Down	Up
37	PC ae C30:1	Phosphatidylcholines	1,15	1.98	**0.0159**	0.0474	Down	Up
38	PC ae C40:4	Phosphatidylcholines	1,14	-1.68	**0.0044**	0.0190	Down	Down
39	PC aa C40:1	Phosphatidylcholines	1,13	-1.44	**0.0376**	0.0829	Up	Down
40	SM (OH) C14:1	Sphingomyelins	1,13	1.07	0.2746	0.3779	Down	Up
41	PC ae C34:0	Phosphatidylcholines	1,13	-1.42	0.9171	0.9403	Up	Down
42	SM C24:0	Sphingomyelins	1,13	1.41	**0.0001**	0.0035	Down	Up
43	PC aa C38:4	Phosphatidylcholines	1,13	-2.04	0.1600	0.2561	Up	Down
44	lysoPC a C16:1	Phosphatidylcholines	1,12	1.59	**0.0080**	0.0293	Down	Up
45	PC aa C40:6	Phosphatidylcholines	1,11	-1.02	**0.0329**	0.0738	Up	Down
46	SM (OH) C22:1	Sphingomyelins	1,11	1.55	**0.0119**	0.0391	Down	Up
47	PC aa C38:0	Phosphatidylcholines	1,11	1.29	**0.0113**	0.0388	Down	Up
48	SM (OH) C22:2	Sphingomyelins	1,11	1.62	**0.0018**	0.0136	Down	Up
49	PC aa C42:2	Phosphatidylcholines	1,10	-1.44	**0.0201**	0.0548	Up	Down

Table 3: Continued.

No.	Metabolites	Classes	VIP[a]	FC[b]	p value[c]	q value[d]	STEMI	Controls
50	PC ae C44:5	Phosphatidylcholines	1,10	-1.58	0.2382	0.3397	Up	Down
51	PC ae C44:6	Phosphatidylcholines	1,07	-1.72	0.3580	0.4675	Up	Down
52	lysoPC a C18:1	Lysophosphatidylcholines	1,07	1.27	**0.0329**	0.0738	Down	Up
53	PC aa C24:0	Phosphatidylcholines	1,07	-1.77	**0.0090**	0.0321	Up	Down
54	PC aa C38:6	Phosphatidylcholines	1,06	1.69	**0.0009**	0.0084	Down	Up
55	PC aa C28:1	Phosphatidylcholines	1,03	1.48	**0.0263**	0.0663	Down	Up
56	PC ae C30:0	Phosphatidylcholines	1,03	1.58	0.1761	0.2715	Down	Up
57	PC ae C38:2	Phosphatidylcholines	1,02	-1.81	**0.0033**	0.0184	Up	Down
58	lysoPC a C18:0	Lysophosphatidylcholines	1,01	1.21	**0.0315**	0.0733	Down	Up
59	PC aa C40:4	Phosphatidylcholines	1,01	1.41	**0.0040**	0.0190	Down	Up
60	PC aa C32:0	Phosphatidylcholines	1,01	-1.5	0.9862	0.9862	Up	Down

[a]Variable importance in the projection (VIP) was obtained from OPLS-DA with a threshold of 1.0. [b]The fold change (FC) was calculated by the average value of the STEMI group to that of the control group. [c]p value was calculated by the Wilcoxon-Mann-Whitney test. p values < 0.05 are in bold. [d]q value was the adjusted p value with the false discovery rate (FDR).

concentrations (Figure 1S of the Supplementary Material). In the heatmaps, metabolites were clustered according to their Pearson correlation coefficients.

This panel containing 41 metabolites was used to investigate the metabolic pathways associated with STEMI. Significantly altered pathways ($p < 0.05$) that also had high impact values include glycerophospholipid metabolism, alpha-linolenic acid metabolism, and sphingolipid metabolism (Figure 5). Pathway significance was determined from pathway enrichment analysis and based upon the values for each compound in the dataset. The impact value, on the other hand, was determined by pathway topology analysis. Impact represents the importance of a metabolite within a pathway; a metabolite that is found at a junction point within a pathway may have a greater impact on the pathway function if the level is altered.

The phosphatidylcholines were the main group of metabolites that showed a difference between STEMI and controls: 15 were in lower concentration and 16 in higher concentration in patients with STEMI. Four lysophosphatidylcholines and four sphingomyelins showed a lower concentration in patients with STEMI. Two biogenic amines showed a difference in STEMI: one showed high concentration and the other lower concentration (Figure 4(b)). Differences in amino acid, acylcarnitines, and hexoses concentrations between the two groups were not found.

According to the statistical model, there were no significant differences between groups related to the quantified metabolites, coronary arteries committed, and comorbidities (systemic arterial hypertension, type II diabetes mellitus, and dyslipidemia) (Tables 1 and 2). Patients with STEMI presented similar metabolic profiles, despite these variables.

4. Discussion

For more than three decades, the glycerophospholipid hydrolysis in a cardiomyocyte membrane during ischemia has been linked to the pathogenesis of myocardial infarction [31, 32]. The contribution of phospholipid metabolism to plasma membrane disruption in necrotic cell death induced by hypoxia or ischemia has been classically attributed to the action of phospholipases, loss of asymmetry, or the accumulation of bilayer-disrupting amphiphilic lipids, such as lysophospholipid [12]. In general, alterations in myocardial lipid metabolism during ischemia/reperfusion can be classified into two groups: (1) changes in fatty acid β-oxidation and (2) changes mediated by the activation of phospholipases and other lipid catabolic enzymes (e.g., ceramidase and sphingomyelinase) that target the structurally important lipid constituents of cellular membrane structures of the heart [8].

The major lipids present in the eukaryotic cell membrane are glycerophospholipids, sterols, and sphingolipids [15]. According to our results, the main metabolic pathway associated with STEMI is the metabolism of glycophospholipids, followed by alpha-linoleic acid metabolism and sphingolipid metabolism. The major classes of glycerophospholipid include phosphatidylcholine, phosphatidylethanolamine, phosphatidylserine, phosphatidylinositol, and phosphatidic acid [14]. Plasmalogens are unique phospholipid species particularly derived from phosphatidylcholine (PC) or phosphatidylethanolamine (PE); they are characterized by the presence of a vinyl-ether bond and an ester bond at the *sn*-1 and *sn*-2 positions, respectively, of the glycerol backbone [33]. On the basis of their polar head groups at the *sn*-3 position, plasmalogens are mainly classified into either choline plasmalogens or ethanolamine plasmalogens [34].

Glycerophospholipids have received special attention in research on myocardial infarction and its causes [19, 22]. Phosphatidylcholine is the principle phospholipid in the mammalian heart [21]. The human cardiomyocytes are composed of approximately 40% of phosphatidylcholines [20, 21]. Compared to the control group, we found 15 phosphatidylcholines in a lower concentration in the plasma of STEMI patients. In a cardiac tissue, previous studies reported the inhibition of phosphatidylcholine synthesis during hypoxia or ischemia. Hatch and Choy described the inhibition of phosphatidylcholine synthesis in perfused hearts

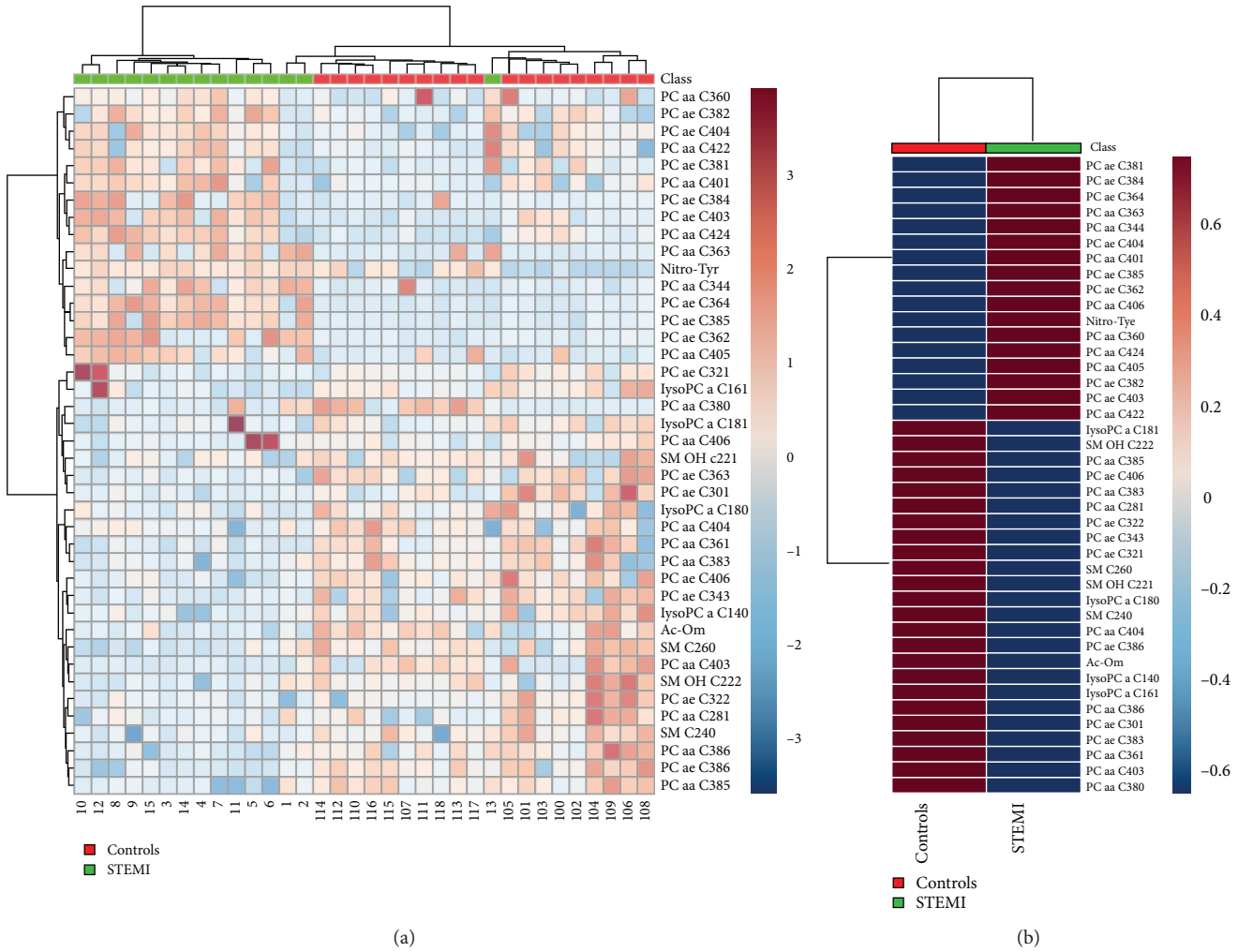

Figure 4: Heatmap of the metabolomics dataset. The colors represent the mean concentration of metabolites. In (a), individual samples (horizontal axis) and metabolites (vertical axis) are represented; they are separated using hierarchical clustering (Ward's algorithm), with the dendrogram being scaled to represent the distance between branches (distance measure: Euclidean). In (b), the contrast in metabolite concentrations between the patient's group with STEMI and healthy individuals is presented.

undergoing hypoxia [35], phosphatidylcholine synthesis was also impaired by hypoxia in isolated rat ventricular myocytes [36], and a net loss of choline after global ischemia has been recently demonstrated in reperfused rat hearts [37]. In this context, several authors suggested that the depletion of ATP and CTP was the cause of the reduced phosphatidylcholine synthesis [35, 38, 39].

Recently, it has been shown in two apparently healthy middle-aged adult cohorts that serum concentrations of four sphingomyelins and six phosphatidylcholines were associated with a higher risk of STEMI, regardless of several risk factors for cardiovascular disease. These are PC aa C38:3, PC aa C40:4, PC ae C36:3, PC ae C38:3, PC ae C38:4, and PC ae C40:3, as well as sphingomyelins C16:0, C24:0, and C16:1 and hydroxy-sphingomyelin C22:1 [21]. According to our results, seven of these markers prevailed after STEMI, two in higher concentrations in relation to the control group (PC ae C38:4 and PC ae C40:3) and five in lower concentrations (PC aa C38:3, PC aa C40, and PC ae C36:3; sphingomyelins C24:0 and hydroxy-sphingomyelin C22:1). Some biologically active substances during ischemia, for example, tumor necrosis factor-α (TNF-α), may induce the synthesis of ceramide from sphingomyelin via sphingomyelinase. Ceramide, in turn, may act as a second messenger, promoting cardiomyocyte apoptosis [40, 41]. This may be an explanation for the decrease of sphingomyelins in STEMI patients.

Substantial evidence accumulated in the last decade indicates that glycerophospholipids, specifically plasmalogens, could represent a major lipid-soluble antioxidant component [42–44]. This proposal is based on the ability of the plasmalogens to scavenge several reactive oxygen species, their relatively high concentrations in cardiac tissue, and their subcellular and extracellular locations in close vicinity to the oxidizable substrates [34, 39]. In this way, oxidative stress can be a justification for the decrease of phosphatidylcholines (choline plasmalogens) in myocardial infarction.

On the other hand, we found 16 phosphatidylcholines in higher concentration in STEMI patients. Furthermore, orthogonal partial least squares discriminant analysis

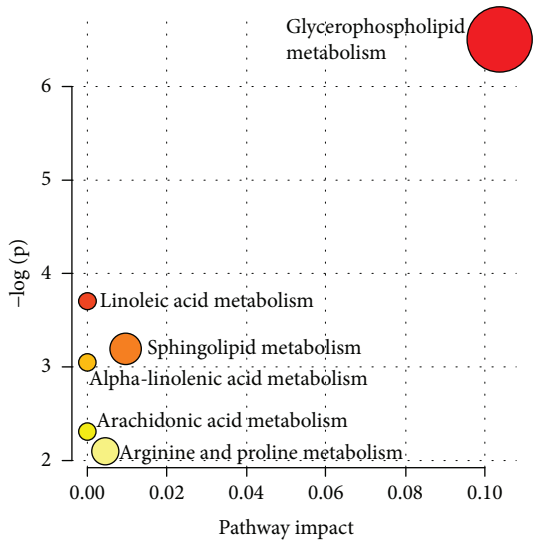

Figure 5: Metabolic pathways associated with STEMI. In the metabolome view, each circle represents a different pathway; circle size and color shade are based on the pathway impact and p value (red being the most significant), respectively.

(OPLS-DA) indicated that STEMI patients can be differentiated from healthy volunteers by the phosphatidylcholine PC ae C36:4. Some hypotheses may be suggested to justify these results: the wide variety of phospholipase A and their selectivity to certain substrates [45, 46] and the activation enzyme kinetics [47]. Using Langdorf rabbits as an experimental model of global myocardial ischemia, Hazen and colleagues analyzed the action of the calcium-independent plasmalogen-selective phospholipases A_2 enzyme. It was reported that membrane-associated calcium-independent plasmalogen-selective phospholipase A_2 activity increased over 400% during 2 min of global ischemia, was nearly maximally activated (greater than 10-fold) after only 5 min of ischemia, and remained activated throughout the entire ischemic interval examined (2-60 min). The activation of membrane-associated plasmalogen-selective phospholipase A_2 after 5 min of myocardial ischemia was rapidly reversible during reperfusion of ischemic tissue [8]. This example suggests that after reperfusion, past the process of injury and inflammation, phospholipid biosynthesis may increase during the repair process in the same way as it occurs with cholesterol and other biomolecules [48].

A reduction in four lysophospholipids was also observed in STEMI patients (lysoPC a C18:1, lysoPC an 18:0, lysoPC a C14:0, and lysoPC a C16:1) when compared to healthy volunteers. The results of Zhu and colleagues corroborate our findings [49]. Using the UHPLC method, they observed a reduction of three lysophospholipids (lysoPC a C18:2, lysoPC a C16:0, and lysoPC a C18:1) in serum concentration from MI patients. The difference between our works lies in the fact that their samples were collected in the period of 1-6 months after the infarction [49]. Interestingly, it can be observed that one of the potential markers found in STEMI patients in the acute phase (lysoPC an 18:1) are also present in the chronic phase of the disease.

Nitrotyrosine is produced by the modification of protein tyrosine residues by peroxynitrite generated from the reaction of nitric oxide (NO) and superoxide [50]. In our study, it was found to be increased in STEMI patients. This increase has already been reported in patients with cardiovascular pathologies, being considered a transient change during myocardial ischemia [51, 52]. Regarding acetylornithine, its decrease was reported in the early stages of cardiotoxicity induced by a potent chemotherapeutic agent, doxorubicin in male B6C3F1 mice, but its implication on human myocardial infarction is described here for the first time [53].

In this study, we did not find a significant difference between STEMI patients and controls in the metabolic classes: amino acids, acylcarnitines, and hexoses. It has been reported that the amino acid concentration increasing is related to the major risk of adverse events and death in STEMI patients after primary percutaneous coronary intervention [9, 10]. Elevated levels of acylcarnitines were associated with a higher risk of myocardial infarction and diabetes mellitus. Despite this, in this work, we did not find metabolic differences between STEMI patients with diabetes mellitus and STEMI patients without this disease, and neither did we observe alterations in hexoses concentrations. Other works with bigger samples have demonstrated that glycemic alterations can be related to worse prognosis and with a smaller capacity of myocardial regeneration/-healing [54, 55].

5. Conclusion

In conclusion, the present study suggests that there are significant alterations in the metabolism of glycerophospholipids, alpha-linolenic acid metabolism, and sphingolipid metabolism in STEMI patients. These changes were observed in the concentrations of 31 phosphatidylcholines, four lysophosphatidylcholines, four sphingomyelins, and two biogenic amines. Although this work had a limitation in the number of samples, the results confirm trends exhibited in previous studies. In addition, this work points to metabolites with a great potential to be biomarkers for STEMI and for the study of new pharmacological targets.

Data Availability

The data used to support the findings of this study are available from the corresponding authors upon request.

Conflicts of Interest

The authors declare that they have no conflicts of interest.

Acknowledgments

This study was supported by the National Council for Scientific and Technological Development (CNPq, Brazil) and Nanocell Institute. The authors would like to thank the Universidade Federal de Minas Gerais and Waters Technologies of Brazil.

Supplementary Materials

Figure 1S: mean of metabolic concentrations. All presented metabolites have a p value < 0.05 and VIP scores (variable influence on the projection) greater than 1. *(Supplementary Materials)*

References

[1] E. J. Benjamin, S. S. Virani, C. W. Callaway et al., "Heart disease and stroke statistics—2018 update: a report from the American Heart Association," *Circulation*, vol. 137, no. 12, pp. e67–e492, 2018.

[2] B. Ibanez, S. James, S. Agewall et al., "2017 ESC Guidelines for the management of acute myocardial infarction in patients presenting with ST-segment elevation: the task force for the management of acute myocardial infarction in patients presenting with ST-segment elevation of the European Society of Cardiology (ESC)," *European Heart Journal*, vol. 39, no. 2, pp. 119–177, 2018.

[3] A. Kumar and C. P. Cannon, "Acute coronary syndromes: diagnosis and management, part I," *Mayo Clinic Proceedings*, vol. 84, no. 10, pp. 917–938, 2009.

[4] D. J. Hausenloy, H. E. Botker, T. Engstrom et al., "Targeting reperfusion injury in patients with ST-segment elevation myocardial infarction: trials and tribulations," *European Heart Journal*, vol. 38, no. 13, pp. 935–941, 2017.

[5] B. Ibáñez, G. Heusch, M. Ovize, and F. van de Werf, "Evolving therapies for myocardial ischemia/reperfusion injury," *Journal of the American College of Cardiology*, vol. 65, no. 14, pp. 1454–1471, 2015.

[6] A. Deshpande and Y. Birnbaum, "ST-segment elevation: distinguishing ST elevation myocardial infarction from ST elevation secondary to nonischemic etiologies," *World Journal of Cardiology*, vol. 6, no. 10, pp. 1067–1079, 2014.

[7] D. C. Crossman, "The pathophysiology of myocardial ischaemia," *Heart*, vol. 90, no. 5, pp. 576–580, 2004.

[8] G. Heusch and B. J. Gersh, "The pathophysiology of acute myocardial infarction and strategies of protection beyond reperfusion: a continual challenge," *European Heart Journal*, vol. 38, no. 11, pp. 774–784, 2016.

[9] X. du, H. You, Y. Li et al., "Relationships between circulating branched chain amino acid concentrations and risk of adverse cardiovascular events in patients with STEMI treated with PCI," *Scientific Reports*, vol. 8, no. 1, article 15809, 2018.

[10] A. Vignoli, L. Tenori, B. Giusti et al., "NMR-based metabolomics identifies patients at high risk of death within two years after acute myocardial infarction in the AMI-Florence II cohort," *BMC Medicine*, vol. 17, no. 1, p. 3, 2019.

[11] M. Neri, I. Riezzo, N. Pascale, C. Pomara, and E. Turillazzi, "Ischemia/reperfusion injury following acute myocardial infarction: a critical issue for clinicians and forensic pathologists," *Mediators of Inflammation*, vol. 2017, Article ID 7018393, 14 pages, 2017.

[12] C. F. Yang, "Clinical manifestations and basic mechanisms of myocardial ischemia/reperfusion injury," *Tzu Chi Medical Journal*, vol. 30, no. 4, pp. 209–215, 2018.

[13] M. Cheng, S. An, and J. Li, "Identifying key genes associated with acute myocardial infarction," *Medicine*, vol. 96, no. 42, article e7741, 2017.

[14] S. E. Ali, M. A. Farag, P. Holvoet, R. S. Hanafi, and M. Z. Gad, "A comparative metabolomics approach reveals early biomarkers for metabolic response to acute myocardial infarction," *Scientific Reports*, vol. 6, no. 1, article 36359, 2016.

[15] V. N. Silbiger, A. D. Luchessi, R. D. C. Hirata et al., "Time course proteomic profiling of human myocardial infarction plasma samples: an approach to new biomarker discovery," *Clinica Chimica Acta*, vol. 412, no. 11-12, pp. 1086–1093, 2011.

[16] S. Mythili and N. Malathi, "Diagnostic markers of acute myocardial infarction," *Biomedical Reports*, vol. 3, no. 6, pp. 743–748, 2015.

[17] A. H. Wu, Y. J. Feng, J. H. Contois, and S. Pervaiz, "Comparison of myoglobin, creatine kinase-MB, and cardiac troponin I for diagnosis of acute myocardial infarction," *Annals of Clinical and Laboratory Science*, vol. 26, no. 4, pp. 291–300, 1996.

[18] E. Danese and M. Montagnana, "An historical approach to the diagnostic biomarkers of acute coronary syndrome," *Annals of translational medicine*, vol. 4, no. 10, pp. 194–194, 2016.

[19] G. D. Lewis, A. Asnani, and R. E. Gerszten, "Application of metabolomics to cardiovascular biomarker and pathway discovery," *Journal of the American College of Cardiology*, vol. 52, no. 2, pp. 117–123, 2008.

[20] V. T. Dang, A. Huang, and G. H. Werstuck, "Untargeted metabolomics in the discovery of novel biomarkers and therapeutic targets for atherosclerotic cardiovascular diseases," *Cardiovascular & Hematological Disorders Drug Targets*, vol. 18, no. 3, pp. 166–175, 2018.

[21] A. Floegel, T. Kühn, D. Sookthai et al., "Serum metabolites and risk of myocardial infarction and ischemic stroke: a targeted metabolomic approach in two German prospective cohorts," *European Journal of Epidemiology*, vol. 33, no. 1, pp. 55–66, 2018.

[22] X. Gao, C. Ke, H. Liu et al., "Large-scale metabolomic analysis reveals potential biomarkers for early stage coronary atherosclerosis," *Scientific Reports*, vol. 7, no. 1, article 11817, 2017.

[23] J. Bartel, J. Krumsiek, and F. J. Theis, "Statistical methods for the analysis of high-throughput metabolomics data," *Computational and Structural Biotechnology Journal*, vol. 4, no. 5, article e201301009, 2013.

[24] S. Wold, M. Sjöström, and L. Eriksson, "PLS-regression: a basic tool of chemometrics," *Chemometrics and Intelligent Laboratory Systems*, vol. 58, no. 2, pp. 109–130, 2001.

[25] H. Gu, Z. Pan, B. Xi, V. Asiago, B. Musselman, and D. Raftery, "Principal component directed partial least squares analysis for combining nuclear magnetic resonance and mass spectrometry data in metabolomics: application to the detection of breast cancer," *Analytica Chimica Acta*, vol. 686, no. 1-2, pp. 57–63, 2011.

[26] M. N. Triba, L. le Moyec, R. Amathieu et al., "PLS/OPLS models in metabolomics: the impact of permutation of dataset rows on the K-fold cross-validation quality parameters," *Molecular BioSystems*, vol. 11, no. 1, pp. 13–19, 2015.

[27] J. F. Hair, G. T. M. Hult, C. M. Ringle, and M. Sarstedt, *A Primer on Partial Least Squares Structural Equation Modeling (PLS-SEM)*, Sage, Thousand Oaks, CA, USA, 2nd edition, 2017.

[28] B. Galindo-Prieto, L. Eriksson, and J. Trygg, "Variable influence on projection (VIP) for orthogonal projections to latent

structures (OPLS)," *Journal of Chemometrics*, vol. 28, no. 8, pp. 623–632, 2014.

[29] B. Xi, H. Gu, H. Baniasadi, and D. Raftery, "Statistical analysis and modeling of mass spectrometry-based metabolomics data," *Methods in Molecular Biology*, vol. 1198, pp. 333–353, 2014.

[30] J. A. Westerhuis, H. C. J. Hoefsloot, S. Smit et al., "Assessment of PLSDA cross validation," *Metabolomics*, vol. 4, no. 1, pp. 81–89, 2008.

[31] A. T. Turer, "Using metabolomics to assess myocardial metabolism and energetics in heart failure," *Journal of Molecular and Cellular Cardiology*, vol. 55, pp. 12–18, 2013.

[32] M. Nam, Y. Jung, D. H. Ryu, and G. S. Hwang, "A metabolomics-driven approach reveals metabolic responses and mechanisms in the rat heart following myocardial infarction," *International Journal of Cardiology*, vol. 227, pp. 239–246, 2017.

[33] N. E. Braverman and A. B. Moser, "Functions of plasmalogen lipids in health and disease," *Biochimica et Biophysica Acta (BBA) - Molecular Basis of Disease*, vol. 1822, no. 9, pp. 1442–1452, 2012.

[34] J. Lessig and B. Fuchs, "Plasmalogens in biological systems: their role in oxidative processes in biological membranes, their contribution to pathological processes and aging and plasmalogen analysis," *Current Medicinal Chemistry*, vol. 16, no. 16, pp. 2021–2041, 2009.

[35] G. M. Hatch and P. C. Choy, "Effect of hypoxia on phosphatidylcholine biosynthesis in the isolated hamster heart," *Biochemical Journal*, vol. 268, no. 1, pp. 47–54, 1990.

[36] P. C. Choy, M. Chan, G. Hatch, and R. Y. K. Man, "Phosphatidylcholine metabolism in ischemic and hypoxic hearts," *Molecular and Cellular Biochemistry*, vol. 116, no. 1-2, pp. 53–58, 1992.

[37] A. Bruhl, G. Hafner, and K. Loffelholz, "Release of choline in the isolated heart, an indicator of ischemic phospholipid degradation and its protection by ischemic preconditioning: no evidence for a role of phospholipase D," *Life Sciences*, vol. 75, no. 13, pp. 1609–1620, 2004.

[38] A. Lochner and M. de Villiers, "Phosphatidylcholine biosynthesis in myocardial ischaemia," *Journal of Molecular and Cellular Cardiology*, vol. 21, no. 2, pp. 151–163, 1989.

[39] I. Sutter, R. Klingenberg, A. Othman et al., "Decreased phosphatidylcholine plasmalogens–a putative novel lipid signature in patients with stable coronary artery disease and acute myocardial infarction," *Atherosclerosis*, vol. 246, pp. 130–140, 2016.

[40] M. Knapp, M. Żendzian-Piotrowska, A. Błachnio-Zabielska, P. Zabielski, K. Kurek, and J. Górski, "Myocardial infarction differentially alters sphingolipid levels in plasma, erythrocytes and platelets of the rat," *Basic Research in Cardiology*, vol. 107, no. 6, p. 294, 2012.

[41] S. Borodzicz, K. Czarzasta, M. Kuch, and A. Cudnoch-Jedrzejewska, "Sphingolipids in cardiovascular diseases and metabolic disorders," *Lipids in Health and Disease*, vol. 14, no. 1, p. 55, 2015.

[42] B. Engelmann, "Plasmalogens: targets for oxidants and major lipophilic antioxidants," *Biochemical Society Transactions*, vol. 32, no. 1, pp. 147–150, 2004.

[43] R. A. Zoeller, A. C. Lake, N. Nagan, D. P. Gaposchkin, M. A. Legner, and W. Lieberthal, "Plasmalogens as endogenous antioxidants: somatic cell mutants reveal the importance of the vinyl ether," *Biochemical Journal*, vol. 338, no. 3, Part 3, pp. 769–776, 1999.

[44] D. Reiss, K. Beyer, and B. Engelmann, "Delayed oxidative degradation of polyunsaturated diacyl phospholipids in the presence of plasmalogen phospholipids *in vitro*," *Biochemical Journal*, vol. 323, no. 3, Part 3, pp. 807–814, 1997.

[45] A. M. Astudillo, M. A. Balboa, and J. Balsinde, "Selectivity of phospholipid hydrolysis by phospholipase A2 enzymes in activated cells leading to polyunsaturated fatty acid mobilization," *Biochimica et Biophysica Acta - Molecular and Cell Biology of Lipids*, vol. 1864, no. 6, pp. 772–783, 2019.

[46] E. Diez, F. H. Chilton, G. Stroup, R. J. Mayer, J. D. Winkler, and A. N. Fonteh, "Fatty acid and phospholipid selectivity of different phospholipase A_2 enzymes studied by using a mammalian membrane as substrate," *The Biochemical Journal*, vol. 301, no. 3, Part 3, pp. 721–726, 1994.

[47] S. L. Hazen, D. A. Ford, and R. W. Gross, "Activation of a membrane-associated phospholipase A2 during rabbit myocardial ischemia which is highly selective for plasmalogen substrate," *Journal of Biological Chemistry*, vol. 266, no. 9, pp. 5629–5633, 1991.

[48] M. Pfohl, I. Schreiber, H. M. Liebich, H. U. Häring, and H. M. Hoffmeister, "Upregulation of cholesterol synthesis after acute myocardial infarction–is cholesterol a positive acute phase reactant?," *Atherosclerosis*, vol. 142, no. 2, pp. 389–393, 1999.

[49] M. Zhu, Y. Han, Y. Zhang et al., "Metabolomics study of the biochemical changes in the plasma of myocardial infarction patients," *Frontiers in Physiology*, vol. 9, p. 1017, 2018.

[50] R. Radi, "Protein tyrosine nitration: biochemical mechanisms and structural basis of functional effects," *Accounts of Chemical Research*, vol. 46, no. 2, pp. 550–559, 2012.

[51] K. Tanabe, Y. Kawai, M. Kitayama et al., "Increased levels of the oxidative stress marker, nitrotyrosine in patients with provocation test-induced coronary vasospasm," *Journal of Cardiology*, vol. 64, no. 2, pp. 86–90, 2014.

[52] G. Peluffo and R. Radi, "Biochemistry of protein tyrosine nitration in cardiovascular pathology," *Cardiovascular Research*, vol. 75, no. 2, pp. 291–302, 2007.

[53] L. K. Schnackenberg, L. Pence, V. Vijay et al., "Early metabolomics changes in heart and plasma during chronic doxorubicin treatment in $B6C3F_1$ mice," *Journal of Applied Toxicology*, vol. 36, no. 11, pp. 1486–1495, 2016.

[54] R. Marfella, M. R. Rizzo, M. Siniscalchi et al., "Peri-procedural tight glycemic control during early percutaneous coronary intervention up-regulates endothelial progenitor cell level and differentiation during acute ST-elevation myocardial infarction: effects on myocardial salvage," *International Journal of Cardiology*, vol. 168, no. 4, pp. 3954–3962, 2013.

[55] C. Sardu, M. Barbieri, M. L. Balestrieri et al., "Thrombus aspiration in hyperglycemic ST-elevation myocardial infarction (STEMI) patients: clinical outcomes at 1-year follow-up," *Cardiovascular Diabetology*, vol. 17, no. 1, p. 152, 2018.

Hindawi
Disease Markers
Volume 2019, Article ID 8945974, 9 pages
https://doi.org/10.1155/2019/8945974

Research Article

Integrated Microfluidic Device for Enrichment and Identification of Circulating Tumor Cells from the Blood of Patients with Colorectal Cancer

Wentao Su,[1,2] **Hao Yu**,[1] **Lei Jiang**,[1,2] **Wenwen Chen**,[1,2] **Hongjing Li**,[3] **and Jianhua Qin**[1,2,4,5]

[1]*Division of Biotechnology, Dalian Institute of Chemical Physics, Chinese Academy of Sciences, Dalian, China*
[2]*University of Chinese Academy of Sciences, Beijing, China*
[3]*First Affiliated Hospital of Dalian Medical University, Dalian, China*
[4]*CAS Centre for Excellence in Brain Science and Intelligence Technology, Chinese Academy of Sciences, Shanghai, China*
[5]*Institute for Stem Cell and Regeneration, Chinese Academy of Sciences, Beijing, China*

Correspondence should be addressed to Jianhua Qin; jhqin@dicp.ac.cn

Received 21 February 2019; Accepted 8 April 2019; Published 1 July 2019

Guest Editor: Zhongjie Shi

Integrated device with high purity for circulating tumor cell (CTC) identification has been regarded as a key goal to make CTC analysis a "bench-to-bedside" technology. Here, we have developed a novel integrated microfluidic device that can enrich and identify the CTCs from the blood of patients with colorectal cancer. To enrich CTCs from whole blood, microfabricated trapping chambers were included in the miniaturized device, allowing for the isolation of tumor cells based on differences in size and deformability between tumor and normal blood cells. Microvalves were also introduced sequentially in the device, enabling automatic CTC enrichment as well as immunostaining reagent delivery. Under optimized conditions, the whole blood spiked with caco-2 cells passing through the microfluidic device after leukocyte depletion and approximately 73% of caco-2 cells were identified by epithelial cell adhesion molecule (EpCAM) staining. In clinical samples, CTCs were detectable from all patients with advanced colorectal cancer within 3 h. In contrast, the number of CTCs captured on the device from the blood of healthy donors was significantly lower than that from the patients, suggesting the utilization of the integrated device for further molecular analyses of CTCs.

1. Introduction

The spread of cancer, either by lymphatic drainage or distant metastasis through the peripheral bloodstream, could increase the death risk [1]. Although treated with surgical resection, approximately 20%–45% of colorectal cancer (CRC) patients developed local tumor recurrence or metastasis at distant sites [2]. Traditional serological tests offered limited information for early clinical symptom diagnosis and therapeutic response monitoring in a real-time manner. It is urgent to develop a reliable method to screen the early CRC patients and monitor antitumor response continuously [3].

Circulating tumor cells (CTCs), which are shed from the primary tumor and circulated in the bloodstream, may indicate the severity of metastatic progression. Identification, enumeration, and characterization of CTCs may provide a minimally invasive method for assessing the cancer status of patients and prescribing personalized anticancer therapy [4]. However, it is difficult to enrich CTCs from whole blood of patients, owing to their low quantity (about 1 CTC among ten million white blood cells and billions of red blood cells per milliliter) [5]. A variety of immuoaffinity-based approaches have been developed for enrichment of CTCs from peripheral blood, including immunomagnetic bead separation and flow cytometry [6–11]. For example, CellSearch™ system showed clinical validity regarding the monitoring of metastatic breast, prostate, and colon cancer [4, 5, 12, 13]. This approach relies on the enrichment of cancer cells from blood using EpCAM-

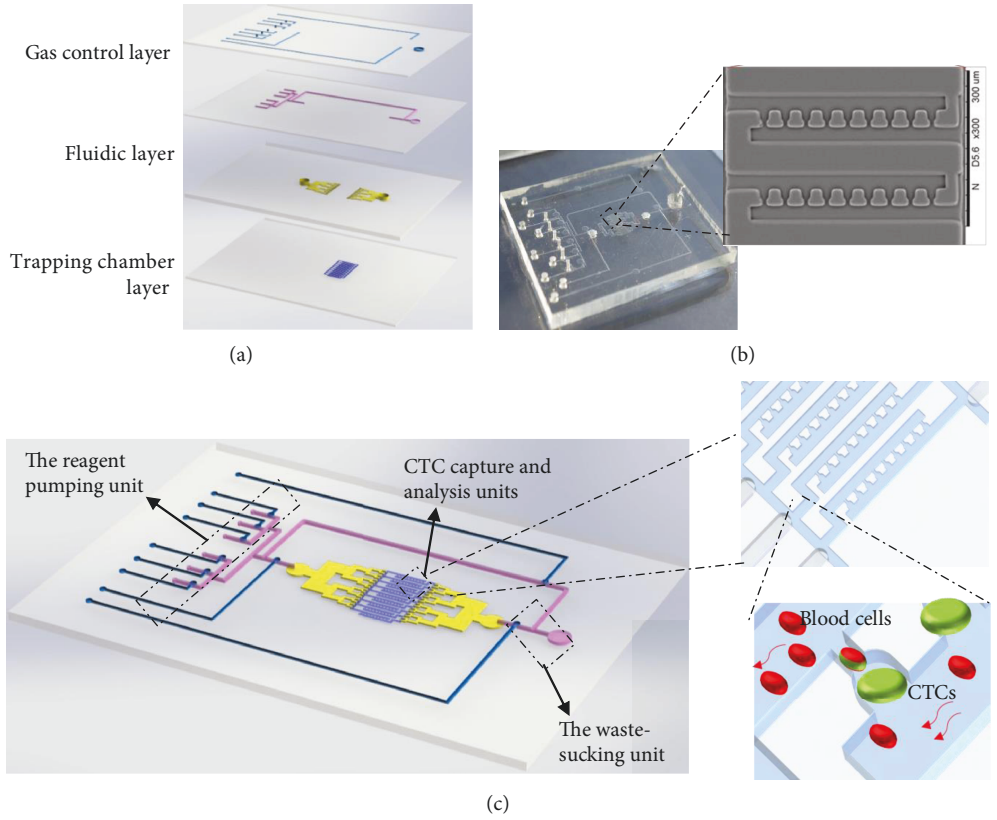

Figure 1: Schematic drawing of the integrated microfluidic device for CTC enrichment and analysis. (a) Layout of the integrated microfluidic device. It was composed of four layers, in which the top layer was a gas control layer containing microvalve and micropump channels. The two middle layers were fluidic microchannels, and the bottom layer contained microfeatures leading to multiple-cell trapping chambers with individual pore channels. (b) Photograph of the prototype microfluidic device. (c) A schematic representing how larger cancer cells got trapped in the trapping chamber while other blood cells with the smaller size escaped.

coated magnetic nanoparticles combined with cell fixation and staining for visual CTC enumeration and identification. However, some invasive tumor cells may lose their EpCAM by an epithelial-mesenchymal transition (EMT) process [14, 15]. CTC enrichment based on targeting specific surface markers often leads to confused results and thus remains a point of controversy. Therefore, novel label-free technologies are desirable with a good precision for isolating CTCs from the circulated bloodstream of cancer patients.

Microfluidic technologies have come of age in the last 10–15 years and offer many advantages for the label-free separation and analysis of CTCs. Various microfluidic devices have been used to separate CTCs from a liquid biopsy. According to the physical property differences, these label-free techniques can be further divided into two subcategories: hydrophoresis (based on the cell size, density, shape, and deformability properties) [16–21] and dielectrophoresis (based on the cell dielectric property) [22, 23]. Among these technologies, the size- and deformability-based cell capture system is a commonly used label-free hydrophoresis technique because it is a relatively straightforward approach for cell separation mainly based on their size property. The size of microcavities is usually less than 10 μm, and because of the larger size of tumor cells than red blood cells (RBCs), the blood cells can be filtered out while tumor cells are left behind. The pores of microcavity array can be also designed as many shapes, such as circular [24], oval [25], and rectangular [26]. However, these methods still lack the capabilities to realize CTC capture and analysis in a real-time or automatic manner.

In this report, we present the novel integrated microfluidic device for rapid isolation of CTCs with high purity in an automated manner. To isolate CTCs selectively based on size differences between CTCs and normal blood cells, multiple-cell trapping chambers with specific dimensions are fabricated on the microfluidic chip. Also, several microvalves are integrated to actuate the fluid flow, allowing to reduce manual operation procedures and integrate the CTC separation, staining, and detection processes. Spike-in tests and clinical tests were performed with the whole blood from healthy donors or patients to verify the practicability of the device for the isolation and detection of CTCs.

2. Materials and Methods

2.1. Microfluidic Device Fabrication. The multilayer CTC microfluidic device consists of four polymer layers as shown in Figure 1(a). The top layer is gas control layer that contains micropump channels and microvalves. The two middle layers are fluidic microchannels (~75 μm deep), and the bottom layer contains multiple-cell trapping chambers ($20 \times 25 \times 30$ μm) with separated pore channels. The corresponding master

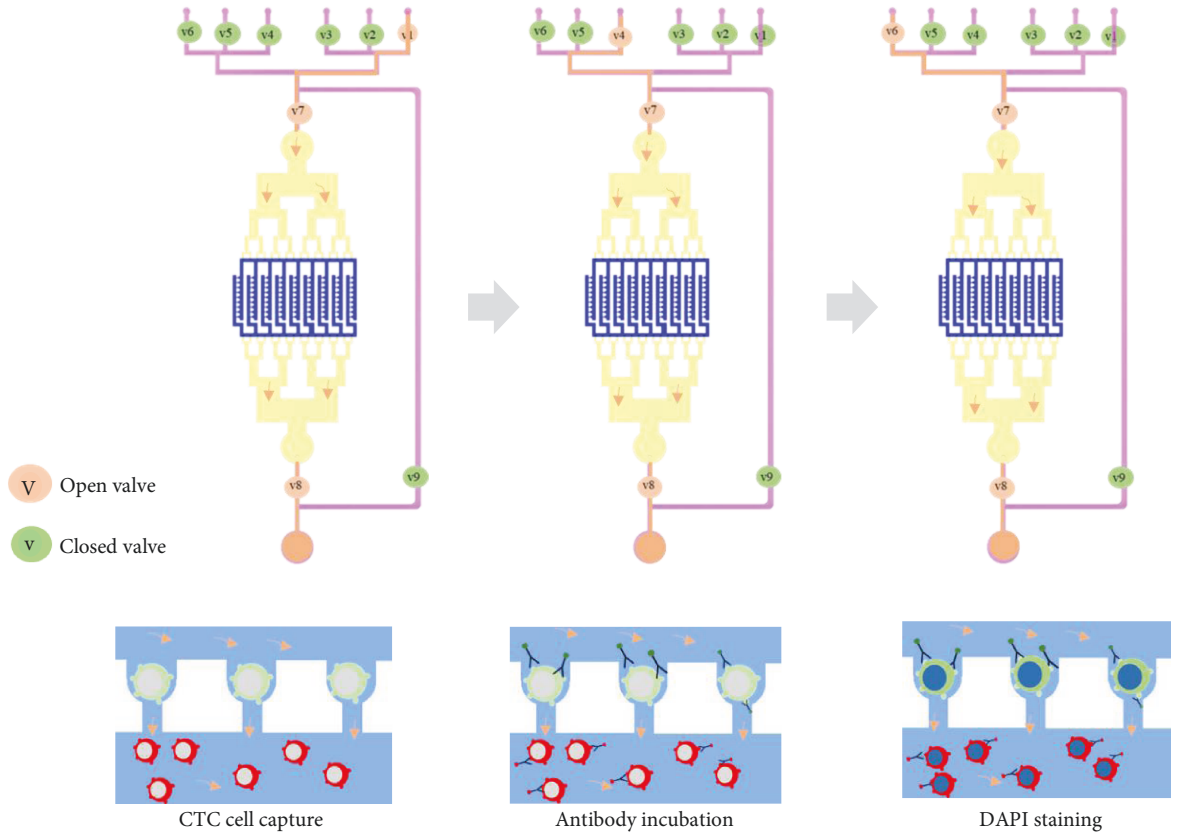

Figure 2: Schematic drawing of CTC enrichment and identification on the microfluidic device. The lysed samples, washing buffer (1x PBS), 4% PFA, blocking buffer, EpCAM-FITC, CD45-PE, and DAPI were loaded into the microchannel device in correct sequence by opening the microvalves in a simple manner.

mold was designed by the AutoCAD software (Autodesk, USA) and prepared using soft photolithography techniques. SU-8 photoresist (Microlithography Chemical Co., USA) was spin coated onto clean glass wafer and then exposed to UV light (mask aligner UV-KUB-2, France) using the photomask described above. After removing the uncured photoresist, the glass wafer was put in a 180°C oven for 2 h to hard bake and be treated by chlorotrimethylsilane to reduce adhesion. The device were molded using a PDMS prepolymer (Dow Corning, USA) with a curing agent at 10 : 1 (*w*/*w*). The molded prepolymer was then cured by thermal curing at 80°C for 1 h and peeled off from the plates.

2.2. Cancer Cell Culture and Sample Preparation. Human colorectal carcinoma cell lines caco-2 (ATCC HTB-37) were used for spiked-in tests. The caco-2 were cultured in DMEM with 10% (*v*/*v*) fetal bovine serum (Gibco, USA) and 1% penicillin/streptomycin (HyClone, USA). The condition for the culture was maintained at 37°C with humidified atmosphere. The medium was changed every 48 h. When the cell lines reached 75 to 90% confluency, they were dissociated using 0.25% trypsin solution (Gibco, USA).

For sample preparation, peripheral blood samples from healthy donors or patients with colorectal cancer were received from the First Affiliated Hospital of Dalian Medical University. Samples were collected in Eppendorf tubes with ethylenediaminetetraacetic acid to prevent blood coagulation. 2 mL blood samples were collected from 7 colorectal cancer patients. For spike-in tests, a known amount of cancer cells were obtained using a microscope and dissociated by trypsin solution for each experiment. For the lysed blood samples, red blood cells were removed following the procedure of the red blood cell lysis kit (Beyotime Biotechnology, China), at a ratio of 10 mL lysis buffer to 1 mL of blood. Dissociated cells were directly added to 2 mL of PBS or lysed whole blood samples, which were loaded into the integrated device for CTC enrichment.

2.3. Device Operation for CTC Enrichment and Identification. Special buffer was pumped into the microfluidic device to remove bubbles before sample introduction, which consist of 1x PBS, ethylenediamine tetraacetic acid, and 0.5 % bovine serum albumin. Sample loading was conducted by applying pressure to the device through controlling the open or close of microvalves. The compressor and vacuum pump were used for controlling microvalves. In brief, the valves were closed by loading pressure (5 kPa) and opened by a vacuum (50 kPa) through the gas microchannels. The computer program was written by VC++ for the solenoid valve controlling [27]. CTCs with the bigger size were captured by trapping

chambers, while other leukocytes with smaller size passed through pore channels and collected at the outlet reservoir. Larger leukocytes such as macrophages could be distinguished by their surface markers in the trapping chambers.

2.4. CTC Imaging and Analysis. For analysis of the captured cells, the immunostaining method was used. In order to identify and count the captured CTCs, CTC determination criteria EpCAM positive, CD45 negative, and DAPI positive were used. In each test, positive or negative controls were included for antibody staining and performance. Cells were incubated with a staining solution containing 4′,6-diamidino-2-phenylindole (DAPI) (Sigma-Aldrich, St. Louis, MO), EpCAM-FITC (VU-1D9, Abcam, UK), and CD45-PE (clone HI30, eBioscience, San Diego, CA). After immunostaining, the integrated device was monitored on a fluorescence inverted microscope (DMI 3000B, Leica, Germany). The enriched cells were enumerated and analyzed by the NIH ImageJ software. For scanning electron microscope (SEM) analysis of the microfluidic device, the surface of the capture chambers were coated with the Au layer (10 nm in thickness). The resulting samples were also conducted and imaged under 10 kV condition using SEM (HITACHI TM3000, Japan). The results were expressed as mean ± standard deviation (SD), and each experiment was performed in triplicate.

3. Results

3.1. Microfluidic Chip Design and Fabrication for CTC Capture and Analysis. In this study, we developed a novel integrated microfluidic device that can enrich and characterize CTCs in an automated manner. The design of the microfluidic device was shown in Figure 1(a), which composed of four layers. The top layer was a gas control layer containing microvalves and micropumps. The two middle layers were fluidic control layers with microchannels, and the bottom layer contains microfeatures leading to multiple-cell trapping chambers with individual pore channels. The photograph of the fabricated microfluidic device was shown in Figure 1(b) for size-selective CTC isolation and identification.

For CTC capture and analysis, several functional units were integrated on the single chip, including a CTC analysis unit, a reagent pumping unit, and a waste-sucking unit (Figure 1(c)). The CTC analysis unit had the function for CTC enrichment and identification. The unit consisted of about 5600 cell trapping chambers and a parallel network of individual pore microchannels (~$10 \times 8\,\mu$m). The design of pore microchannel ensured that larger cancer cells got trapped in the trapping chamber while other blood cells with the smaller size escaped. Moreover, the single-cell trapping chamber integrated on the microfluidic device showed potential for downstream molecular analysis (e.g., PCR and FISH assays) at the single-cell level. The reagent pumping unit was designed for sample and immunostaining reagent loading. Six microvalves were designed to form micropump in the reagent channel, which delivered the required reagents from each reagent reservoir to the CTC analysis unit. The waste-sucking unit consisted with a microvalve in the waste channel, which was used for waste solution sucking. Using such chip design, the whole process for recovery, staining, washing, and detection of CTCs could be accomplished in an automated and simple fashion.

3.2. Microfluidic Operation for CTC Capture and Analysis. For integrated CTC microfluidic capture and identification, the lysed samples, washing buffer (1x PBS), 4% PFA, 0.1% Triton X-100, blocking buffer, EpCAM-FITC, CD45-PE, and DAPI were loaded into the microchannel device in correct sequence by simply opening the microvalves (Figure 2). (a) The lysed samples were pumped from the sample reservoirs to the CTC analysis unit by valves 1, 7, and 8. Cancer cells with the bigger size were captured by trapping chambers. Sample loading time was 10 min at approximately 0.2 mL/min volumetric flow rate. (b) The PBS washing buffer was introduced into the CTC analysis units by valves 6, 7, and 8 to wash the trapping chambers for 5 min. (c) The 4% PFA solution was pumped into trapping chambers by valves 2, 7, and 8 to fix the captured cells for 10 min. Washing step was repeated. (d) The blocking solution with 5% goat serum (Life Technologies) was pumped into the trapping chambers by valves 3, 7, and 8 for 25 min. (e) Then, the monoclonal antibodies EpCAM-FITC and CD45-PE (1 : 100 dilution) were pumped into the trapping chambers by valves 4, 7, and 8 for 50 min. Washing step was repeated. (f) DAPI (Life Technologies) was finally pumped into the trapping chambers by valves 5, 7, and 8 for 5 min. After washing, the microfluidic device was ready for CTC identification.

3.3. Enumeration and Enrichment Efficiency of CTCs. To examine the performance of the integrated microfluidic device, the samples of caco-2 cell lines which spiked in 1x PBS were firstly used for the CTC enrichment test (Figure 3(a)). Caco-2 cells were dyed with CellTracker CM-Dil fluorescent dye in the concentration ranging from 0 to 60 cells per 0.5 mL 1x PBS. The efficiency of cell enrichment ranged between 80 and 90% with average cell enrichment efficiency of 80%. The variation coefficient varied between 0.5 and 3.8 with three independent experiments ($n = 3$), suggesting high reproducibility of cell capture using this device.

To test the cell enrichment efficiency under physiological conditions, the samples of caco-2 cell lines which spiked into healthy peripheral blood were further conducted. As demonstrated in Figure 3(b), the cell capture efficiency in the spike-in samples ranging from 65 to 82% for caco-2 cells with the average cell capture efficiency of 73% depended on the amount of spiked cells. The result showed that the low variation coefficient varied from 1.2 to 4.9 with three independent experiments ($n = 3$). The results further demonstrated the high experimental reproducibility and enrichment efficiency using the integrated device, which were consistent with the results of spike-in experiment in PBS buffer.

3.4. CTC Analysis with Fluorescence Microscopy. To further test the performance of the integrated microfluidic device, the enriched cells were characterized with fluorescence antibody staining. A series of immunostaining experiments were conducted to analyze the expression of colorectal cancer-

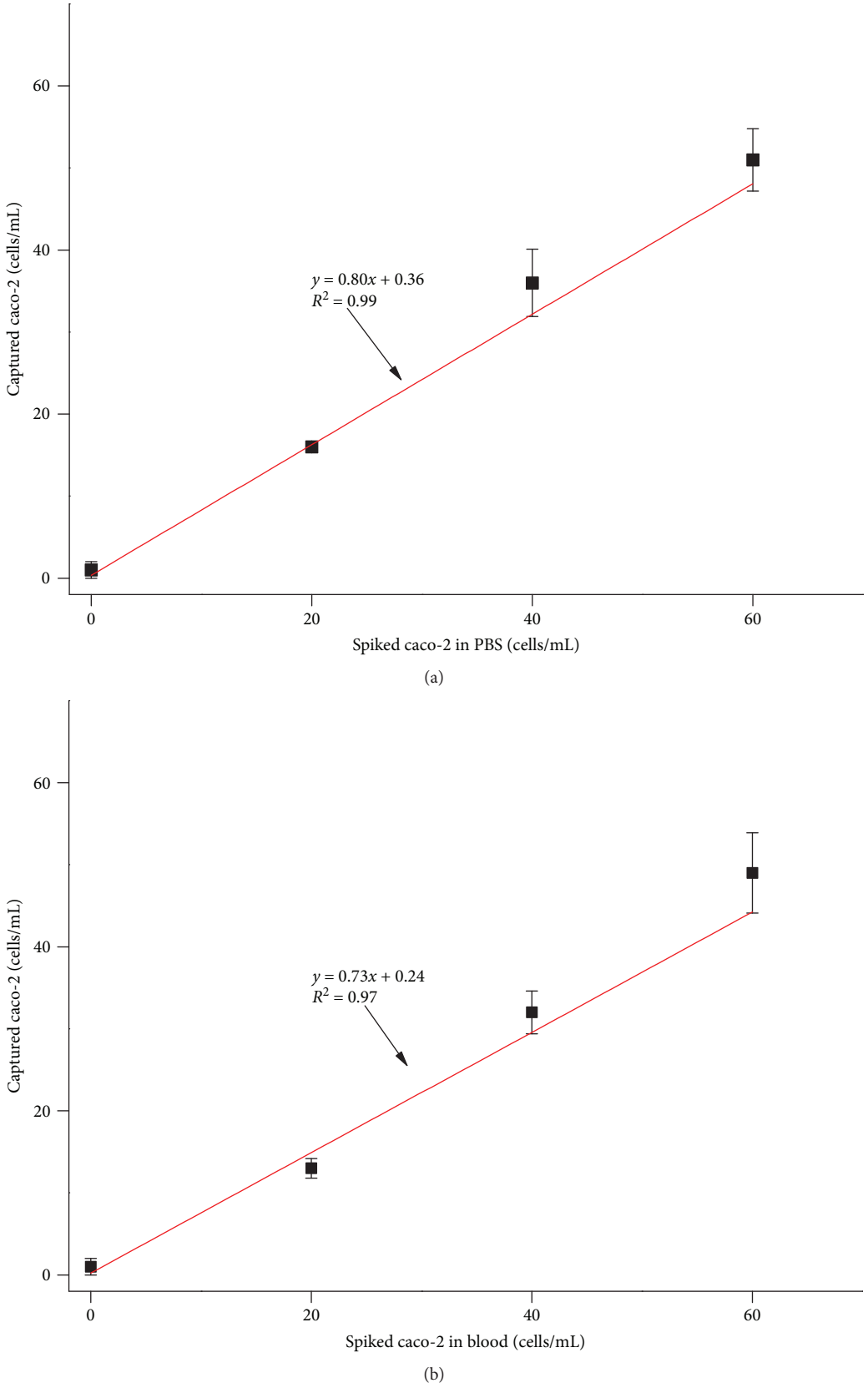

Figure 3: Capture efficiency of colorectal cancer lines spiked in PBS or the healthy donor blood. (a) The capture efficiency of cells using different cell lines in 1x PBS was used to show the performance of the device. (b) To assess cell capture efficiency under physiological conditions, a series of spike-in experiments in which a certain number of colorectal cancer were spiked into peripheral blood samples from healthy donors.

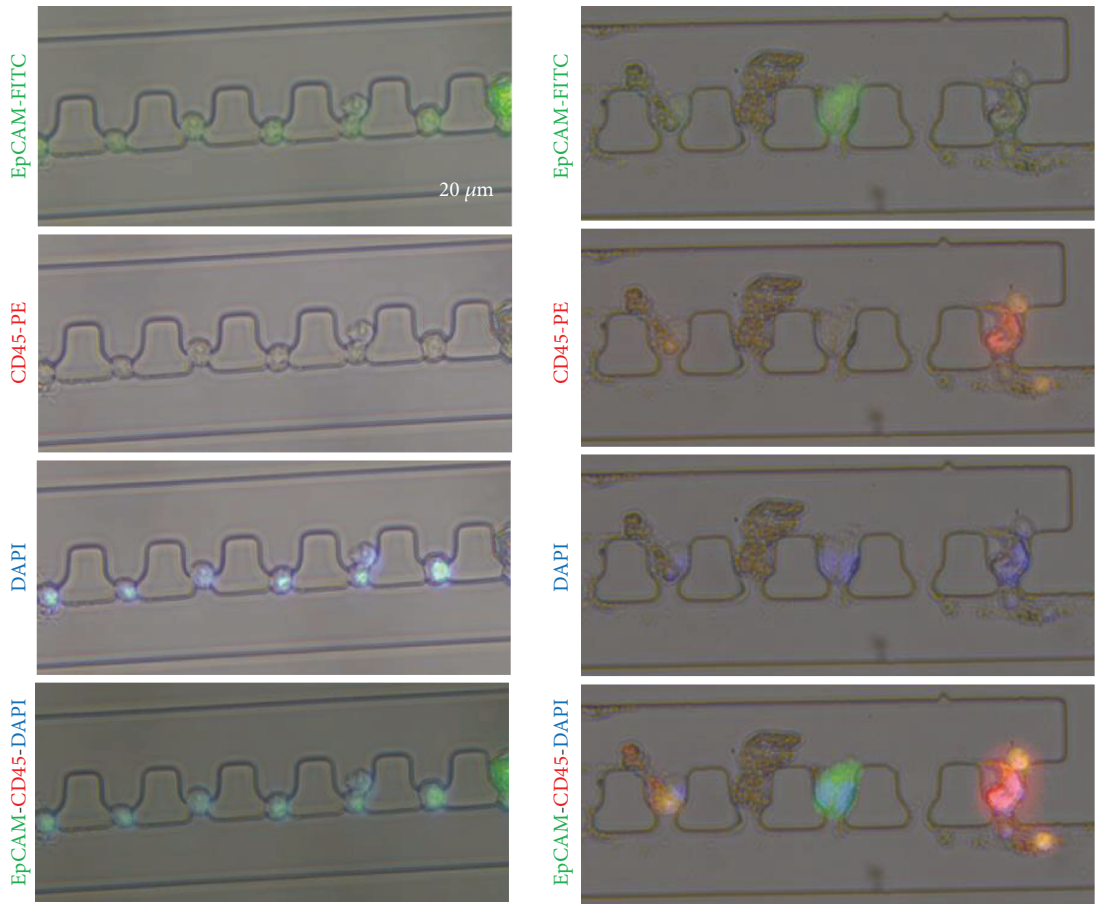

Figure 4: Immunostaining of captured cells in PBS or in human blood. A certain amount of caco-2 cell lines were first spiked into 2 mL (a) 1x PBS or (b) spiked into peripheral blood samples from healthy donors and then stained with either EpCAM-FITC or CD45-PE after being captured by microchambers. The cell nuclei were also stained by DAPI in all cases.

specific biomarkers. A known amount of caco-2 cells were firstly spiked into 2 mL 1x PBS and introduced into the integrated device. The captured cells by the pore channels were then stained with EpCAM-FITC, CD45-PE, and DAPI (Figure 4(a)). The result revealed that caco-2 cell lines were positively stained with EpCAM antibody but negatively stained with CD45. Similar analysis had been performed using the spike-in samples into peripheral blood. The captured cancer cells and leucocytes were stained separately in Figure 4(b). CD45-PE was used as a marker for leukocyte staining to distinguish background leukocyte cells from the captured cancer cells. The results were highly consistent with those from the caco-2 with EpCAM positive and CD45 negative. The result suggested that the integrated microfluidic device was able to identify the differential phenotype of captured cells using specific biomarkers.

3.5. Enrichment of CTCs in Patient Clinical Samples. For clinical evaluation of the CTC isolation and analysis in the integrated microfluidic chip, 7 colorectal cancer patients and 7 healthy donors were enrolled in the study. For blood samples, 2 mL of whole blood was lysed by 20 mL of lysis buffer and directly pumped into the microfluidic device. The lysed blood sample loading as well as captured cell immunostaining were then conducted and generated in correct sequence by simply opening the microvalves. The data of actual CTC counts from colorectal cancer patients and healthy donors were provided in Figure 5. According to the results of immunofluorescence detection, CD45-positive hematologic cells (leukocytes) in majority of the blood samples were not captured by the device, which indicated that our integrated device showed a stronger specificity for CTC enrichment. Only 2 of the 7 healthy subjects in the control group had their cells detected by the device, and the number of detected cells was 1 and 1, respectively. These false positively stained cells were probably epithelial cells or leukocytes with EpCAM attached to the surface in whole blood [28]. In contrast, all the 7 tumor patients in the experimental group had their cells successfully detected. The actual number of isolated CTCs from colorectal cancer patients ranged from 2 to 13 CTCs. The results proved that the fabricated device could effectively detect CTCs in peripheral blood.

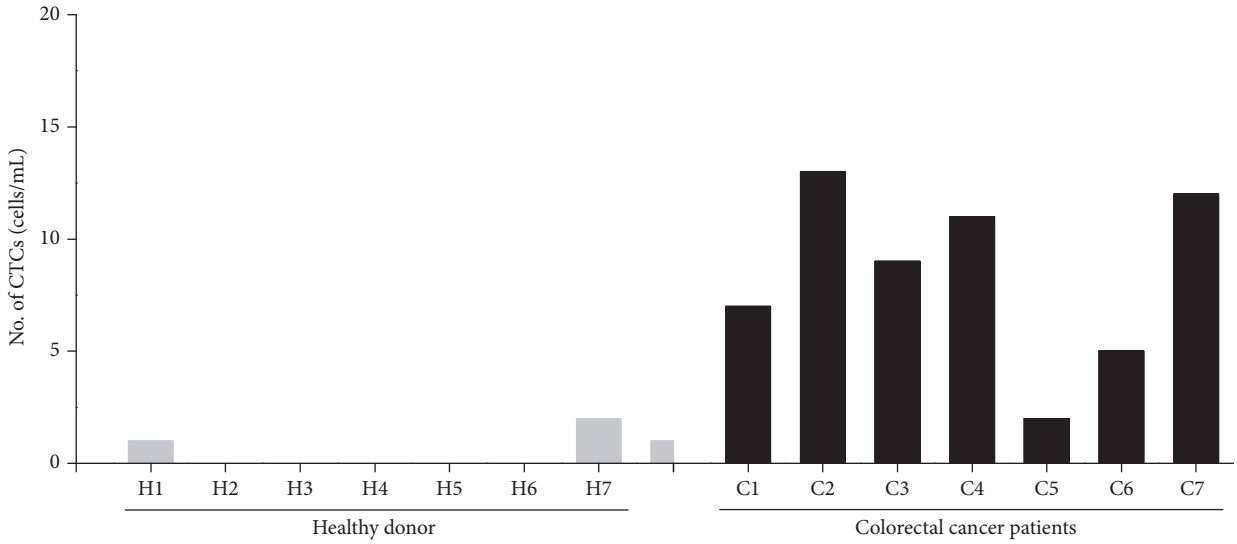

Figure 5: Results showing the performance of the CTC isolation microfluidic chip integrated with microvalves in colorectal cancer patient samples and healthy donors. The sample usage for CTC counts was normalized to 2 mL. CTC enumeration following antibody labeling was performed manually. EpCAM+/CD45-nucleated cells were identified as CTCs.

4. Discussion

In this study, we developed a novel integrated microfluidic device that can enrich and identify the CTCs from the blood of patients with colorectal cancer. This integrated microfluidic device had the ability for recovery, staining, washing, and detection of CTCs in an automated and simple fashion. Under optimized conditions, the enrichment efficiency for CTCs was greater than 73% in the cell-spiking experiment. In clinical study, CTCs were identified in all 7 patients with advanced colorectal cancer by epithelial cell adhesion molecule (EpCAM) staining. Thus, our device has potential as an efficient yet simple manner for fully automated CTC enrichment and identification.

Cancer metastasis and tumor recurrence are the main cause of cancer-related death, and dissemination of CTCs through the blood circulation is an important intermediate step [1, 8]. In contrast to invasive tissue biopsies that may impose a high risk to patients, CTC enrichment and analysis from circulating blood is considered as the real-time "liquid biopsy" in a noninvasive manner. CTCs show a great promise for potential clinical implications, including assessing prognosis of cancer and monitoring the therapeutic treatment, as well as serving as a surrogate biomarker for early diagnosis of cancer [8, 29, 30]. For those studies, the FDA-approved CellSearch system was regarded as the gold standard as the diagnostic tool, which worked for metastatic breast, prostate, and colon cancer. Despite its sensitivity, the CellSearch™ system highly relies on cell surface marker detection, which is not necessary, or low expression by CTCs [15]. Also, we should note that a population of CTCs may undergo the epithelial-mesenchymal transition (EMT) process to invade surrounding tissues and trigger distant metastasis [31]. In order to improve CTC detection sensitivity, it is essential to incorporate enrichment methods other than EpCAM-based ones.

Recently, several membrane filter devices are available for CTC enrichment based on the differential cellular size, including ScreenCell®, CellSieve™, and CellOptics [32–35]. Most of these filtering devices in common are provided solely for CTC capture, and the method and criteria for CTC recognition need to be established by researchers. On the other hand, our integrated microfluidic device covers all the steps from capturing the cells to staining them, resulting in much less manual effort and less turnaround time. The incorporated microvalves were used to realize the automatic CTC loading as well as immunostaining reagent delivery. Sample loading into the capture chambers and immunostaining of the captured cells on the microchannel device were then conducted and generated in correct sequence by simply opening the microvalves. Our microfluidics-based CTC detection platform may dramatically promote the current approaches for cancer diagnosis and prognosis. A further study would focus on a larger cohort to clarify the correlation between CTC count and clinicopathologic factors.

Data Availability

The data used to support the findings of this study are available from the corresponding author upon request.

Conflicts of Interest

The authors declare that they have no conflicts of interest.

Authors' Contributions

Wentao Su, Hao Yu, and Jianhua Qin equally contributed to this work.

Acknowledgments

This research was supported by the National Key R&D Program of China (No. 2017YFB0405404), the National Nature Science Foundation of China (Nos. 21607151, 81573394, and 31671038), the Strategic Priority Research Program of the Chinese Academy of Sciences (Grant Nos. XDA16020900, XDB29050301, and XDB32030200), the National Science and Technology Major Project (No. 2018ZX09201017-001-001), and the Innovation Program of Science and Research from the DICP, CAS (DICP TMSR201601).

References

[1] S. A. Stacker, C. Caesar, M. E. Baldwin et al., "VEGF-D promotes the metastatic spread of tumor cells via the lymphatics," *Nature Medicine*, vol. 7, no. 2, pp. 186–191, 2001.

[2] W. Chen, R. Zheng, P. D. Baade et al., "Cancer statistics in China, 2015," *Ca-a Cancer Journal for Clinicians*, vol. 66, no. 2, pp. 115–132, 2016.

[3] J. F. Linnekamp, X. Wang, J. P. Medema, and L. Vermeulen, "Colorectal cancer heterogeneity and targeted therapy: a case for molecular disease subtypes," *Cancer Research*, vol. 75, no. 2, pp. 245–249, 2015.

[4] M. Cristofanilli, "Circulating tumor cells, disease progression, and survival in metastatic breast cancer," *Seminars in Oncology*, vol. 33, pp. 9–14, 2006.

[5] M. Cristofanilli, D. F. Hayes, G. T. Budd et al., "Circulating tumor cells: a novel prognostic factor for newly diagnosed metastatic breast cancer," *Journal of Clinical Oncology*, vol. 23, no. 7, pp. 1420–1430, 2005.

[6] Y. Dong, A. M. Skelley, K. D. Merdek et al., "Microfluidics and circulating tumor cells," *Journal of Molecular Diagnostics*, vol. 15, no. 2, pp. 149–157, 2013.

[7] Z. Zhang and S. Nagrath, "Microfluidics and cancer: are we there yet?," *Biomedical Microdevices*, vol. 15, no. 4, pp. 595–609, 2013.

[8] S. Nagrath, L. V. Sequist, S. Maheswaran et al., "Isolation of rare circulating tumour cells in cancer patients by microchip technology," *Nature*, vol. 450, no. 7173, pp. 1235–1239, 2007.

[9] S. L. Stott, C.-H. Hsu, D. I. Tsukrov et al., "Isolation of circulating tumor cells using a microvortex-generating herringbone-chip," *Proceedings of the National Academy of Sciences of the United States of America*, vol. 107, no. 43, pp. 18392–18397, 2010.

[10] P. Li, Z. S. Stratton, M. Dao, J. Ritz, and T. J. Huang, "Probing circulating tumor cells in microfluidics," *Lab on a Chip*, vol. 13, no. 4, pp. 602–609, 2013.

[11] M. E. Warkiani, G. Guan, K. B. Luan et al., "Slanted spiral microfluidics for the ultra-fast, label-free isolation of circulating tumor cells," *Lab on a Chip*, vol. 14, no. 1, pp. 128–137, 2014.

[12] E. A. Punnoose, S. K. Atwal, J. M. Spoerke et al., "Molecular biomarker analyses using circulating tumor cells," *Plos One*, vol. 5, no. 9, p. e12517, 2010.

[13] S. Riethdorf, H. Fritsche, V. Muller et al., "Detection of circulating tumor cells in peripheral blood of patients with metastatic breast cancer: a validation study of the CellSearch system," *Clinical Cancer Research*, vol. 13, no. 3, pp. 920–928, 2007.

[14] J. P. Thiery, "Epithelial-mesenchymal transitions in tumour progression," *Nature Reviews Cancer*, vol. 2, no. 6, pp. 442–454, 2002.

[15] M. Mego, M. Mego, M. Mego et al., "Circulating tumor cells (CTCs) and epithelial mesenchymal transition (EMT) in breast cancer: describing the heterogeneity of microscopic disease," *Cancer Research*, vol. 69, 24 Supplement, p. 3011, 2009.

[16] X. Chen, C. Xue, L. Zhang, G. Hu, X. Jiang, and J. Sun, "Inertial migration of deformable droplets in a microchannel," *Physics of Fluids*, vol. 26, no. 11, p. 112003, 2014.

[17] P. Baptista, E. Pereira, P. Eaton et al., "Gold nanoparticles for the development of clinical diagnosis methods," *Analytical and Bioanalytical Chemistry*, vol. 391, no. 3, pp. 943–950, 2008.

[18] M. Zhao, P. G. Schiro, J. S. Kuo et al., "An automated high-throughput counting method for screening circulating tumor cells in peripheral blood," *Analytical Chemistry*, vol. 85, no. 4, pp. 2465–2471, 2013.

[19] M. Zhao, W. C. Nelson, B. Wei et al., "New generation of ensemble-decision aliquot ranking based on simplified microfluidic components for large-capacity trapping of circulating tumor cells," *Analytical Chemistry*, vol. 85, no. 20, pp. 9671–9677, 2013.

[20] C. Liu, G. Hu, X. Jiang, and J. Sun, "Inertial focusing of spherical particles in rectangular microchannels over a wide range of Reynolds numbers," *Lab on a Chip*, vol. 15, no. 4, pp. 1168–1177, 2015.

[21] M. G. Lee, J. H. Shin, C. Y. Bae, S. Choi, and J. K. Park, "Label-free cancer cell separation from human whole blood using inertial microfluidics at low shear stress," *Analytical Chemistry*, vol. 85, no. 13, pp. 6213–6218, 2013.

[22] J. Sun, Y. Gao, R. J. Isaacs et al., "Simultaneous on-chip DC dielectrophoretic cell separation and quantitative separation performance characterization," *Analytical Chemistry*, vol. 84, no. 4, pp. 2017–2024, 2012.

[23] P. Li, Z. Mao, Z. Peng et al., "Acoustic separation of circulating tumor cells," *Proceedings of the National Academy of Sciences of the United States of America*, vol. 112, no. 16, pp. 4970–4975, 2015.

[24] M. Hosokawa, T. Hayata, Y. Fukuda et al., "Size-selective microcavity array for rapid and efficient detection of circulating tumor cells," *Analytical Chemistry*, vol. 82, no. 15, pp. 6629–6635, 2010.

[25] S. Zheng, H. Lin, J.-Q. Liu et al., "Membrane microfilter device for selective capture, electrolysis and genomic analysis of human circulating tumor cells," *Journal of Chromatography A*, vol. 1162, no. 2, pp. 154–161, 2007.

[26] M. Hosokawa, T. Yoshikawa, R. Negishi et al., "Microcavity array system for size-based enrichment of circulating tumor cells from the blood of patients with small-cell lung cancer," *Analytical Chemistry*, vol. 85, no. 12, pp. 5692–5698, 2013.

[27] B. Li, L. Jiang, H. Xie, Y. Gao, J. Qin, and B. Lin, "Development of micropump-actuated negative pressure pinched injection for parallel electrophoresis on array microfluidic chip," *Electrophoresis*, vol. 30, no. 17, pp. 3053–3057, 2009.

[28] X. Huang, J. Tang, L. Hu et al., "Arrayed microfluidic chip for detection of circulating tumor cells and evaluation of drug potency," *Analytical Biochemistry*, vol. 564-565, pp. 64–71, 2019.

[29] P. Zuo, X. Li, D. C. Dominguez, and B. C. Ye, "A PDMS/paper/glass hybrid microfluidic biochip integrated with

aptamer-functionalized graphene oxide nano-biosensors for one-step multiplexed pathogen detection," *Lab on a Chip*, vol. 13, no. 19, pp. 3921–3928, 2013.

[30] K. Pantel, R. H. Brakenhoff, and B. Brandt, "Detection, clinical relevance and specific biological properties of disseminating tumour cells," *Nature Reviews Cancer*, vol. 8, no. 5, pp. 329–340, 2008.

[31] D. Marrinucci, K. Bethel, A. Kolatkar et al., "Fluid biopsy in patients with metastatic prostate, pancreatic and breast cancers," *Physical Biology*, vol. 9, no. 1, p. 016003, 2012.

[32] V. Hofman, E. Long, M. Ilie et al., "Morphological analysis of circulating tumour cells in patients undergoing surgery for non-small cell lung carcinoma using the isolation by size of epithelial tumour cell (ISET) method," *Cytopathology*, vol. 23, no. 1, pp. 30–38, 2012.

[33] V. J. Hofman, M. I. Ilie, C. Bonnetaud et al., "Cytopathologic detection of circulating tumor cells using the isolation by size of epithelial tumor cell method promises and pitfalls," *American Journal of Clinical Pathology*, vol. 135, no. 1, pp. 146–156, 2011.

[34] V. Hofman, C. Bonnetaud, M. I. Ilie et al., "Preoperative circulating tumor cell detection using the isolation by size of epithelial tumor cell method for patients with lung cancer is a new prognostic biomarker," *Clinical Cancer Research*, vol. 17, no. 4, pp. 827–835, 2011.

[35] V. Souza e Silva, L. Chinen, E. Abdallah et al., "Early detection of poor outcome in patients with metastatic colorectal cancer: tumor kinetics evaluated by circulating tumor cells," *Oncotargets and Therapy*, vol. Volume 9, pp. 7503–7513, 2016.

Hindawi
Disease Markers
Volume 2019, Article ID 6487152, 8 pages
https://doi.org/10.1155/2019/6487152

Research Article

Hypertrophic Cardiomyopathy: The Time-Synchronized Relationship between Ischemia and Left Ventricular Dysfunction Assessed by Highly Sensitive Troponin I and NT-proBNP

Renata Rajtar-Salwa,[1] Adam Gębka,[1] Artur Dziewierz,[1,2] and Paweł Petkow Dimitrow[1,2]

[1]*Second Department of Cardiology and Cardiovascular Interventions, University Hospital, Krakow, Poland*
[2]*Second Department of Cardiology, Jagiellonian University Collegium Medicum, Krakow, Poland*

Correspondence should be addressed to Paweł Petkow Dimitrow; dimitrow@mp.pl

Received 22 January 2019; Revised 22 March 2019; Accepted 15 April 2019; Published 20 June 2019

Guest Editor: Zhongjie Shi

The aim of this study was to compare NT-proBNP using the absolute values and NT-proBNP/ULN values that were standardized by age and gender between three subgroups: those without ischemia (negative hs-troponin I and no anginal pain (hsTnI-/AP-)), those with painless ischemia (hsTnI+/AP-), and those with painful ischemia (hsTnI+/AP+). Additionally, echocardiographic parameters were compared in these three subgroups. The absolute value of NT-proBNP was significantly higher in the painful ischemia subgroup (hsTnI-/AP- vs. hsTnI+/AP- vs. hsTnI+/AP+: 502 (174-833) vs. 969 (363-1346) vs. 2053 (323-3283) pg/ml; $p = 0.018$ for the whole-model analysis). The standardized value of NT-proBNP/ULN was gradually increased (hsTnI-/AP- vs. hsTnI+/AP- vs. hsTnI+/AP+: $3.61 + 0.63$ vs. $6.90 + 1.31$ vs. $9.35 + 1.87$; $p = 0.001$ for the whole-model analysis). In the comparison between subgroups (hsTnI-/AP- vs. hsTnI+/AP- vs. hsTnI+/AP+), two echocardiographic parameters increased significantly. The left ventricular maximum wall thickness (LVMWT) at diastole was 1.99 ± 0.08 cm vs. 2.28 ± 0.13 cm vs. 2.49 ± 0.15 cm ($p = 0.004$ for the whole-model analysis). The maximal gradient of the provoked left ventricular outflow tract (LVOT) gradient increased significantly in only the painful-ischemia subgroup (11 (7-30) mmHg vs. 12 (9.35-31.5) mmHg vs. 100 (43-120) mmHg). In conclusion, both painless ischemia and painful ischemia are associated with a gradual, significant increase in NT-proBNP/ULN in comparison to the double-negative hsTnI/AP subgroup. In contrast, NT-proBNP is significantly higher in only the subgroup with painful ischemia.

1. Introduction

It is proposed [1, 2] that routine measurement biomarkers especially including [1] both N-terminal pro-B-type NT-pronatriuretic peptide (NT-proBNP) and cardiac troponin (Tn) may be useful in the clinical evaluation and management of patients with HCM. NT-proBNP is predominantly secreted from the ventricles in response to increased myocyte stretching from increased stress and pressure at the LV wall. It is plausible that microvascular ischemia directly stimulates the release of NT-proBNP in HCM. In clinical studies, there is little information about the combined use of Tn and plasma BNP as prognostic biomarkers for adverse events mediated by myocardial ischemia with LV dysfunction [3].

In a study by Kubo et al. [3] on 167 patients with HCM, TnI and BNP were measured only once at the initial examination without control measurements during a follow-up period of more than 3 years (mean value). Patients with elevated TnI values had more frequent adverse events. Similarly, the risk of adverse events was higher in patients with high BNP (≥200 pg/ml). Importantly, TnI used in combination with BNP further improved the prognostic value, as patients with high values of both cTnI and BNP had nearly 12 times higher risk of cardiovascular events than patients with a combination of low cTnI/BNP values. However, this study had some important limitations because there was a long time between the initial biomarker measurement and the final event.

In contrast, we studied the direct short-term relationship between angina pectoris and the levels of both hsTnI and NT-proBNP after a 24-hour monitoring period. Taking into account methodological aspects, we compared NT-proBNP using absolute values and NT-proBNP/ULN values that were standardized by age and gender between three subgroups: those without ischemia (negative hs-troponin I/no anginal pain (hsTnI-/AP-)), those with painless ischemia (hsTnI +/AP-), and those with painful ischemia (hsTnI+/AP+).

2. Methods

A total of 64 patients with HCM were recruited (mean age 37 ± 6 years, 33 men and 31 women). The study protocol was approved by the local institutional review board (Komisja Bioetyki Jagiellonian University KBET/119/B/2017). Informed consent was obtained from each participant. All patients met the standard diagnostic criteria for HCM [4]. In adults, HCM is defined by a wall thickness ≥ 15 mm in one or more LV myocardial segments that is not explained solely by loading conditions and measured by any imaging technique (echocardiography (our method), cardiac magnetic resonance imaging (CMR), or computed tomography (CT)) [4]. Patients on current pharmacotherapy or without pharmacotherapy (newly diagnosed patients referred to our ambulatory clinic) were examined by echocardiography with LVOT gradient provocation by a combination of two natural stimuli (orthostatic test and the Valsalva test).

The exclusion criteria were myocardial infarction with ST-segment or non-ST-segment elevation (current or previous), previous alcohol septal ablation, significant coronary stenosis in recent coronary angiography, diabetes mellitus, regular sports activity, dilated LV cavity and decreased LV contractibility (we included only patients with LVEF > 50%), atrial fibrillation, and elevated serum creatinine levels resulting in eGFR < 60 ml/min. We included only patients with coronary microvessel disease, which is a common abnormality in HCM at any age (inclusion criteria: normal/near-normal coronary arteries or no indication of coronary arteriography).

The minority of patients did not have coronary angiography performed (young, without AP, without risk factors for CAD—especially without diabetes mellitus—see below). The risk for CAD was minimal and coronary angiography was not indicated. Diabetes mellitus is usually linked with silent ischemia from epicardial coronary arteries (so it is necessary to exclude painless macrovascular stenosis).

Renal failure is a typical extracardiac factor related to TnI elevation. Frequent sports activity may be responsible for repetitive myocardial ischemia in some patients [5]. Patients were asked to report presence or absence of angina pectoris episodes before the 24-hour period. Next, an echocardiographic examination was performed. Just after, hsTnI and NT-proBNP (absolute or upper limit of normal (ULN)) were measured. There were 38 patients in subgroup 0 (i.e., the double-negative group; hsTnI-/AP-). Subgroup 1 (hsTnI+/AP-) was composed of 12 patients, and subgroup 2 (double positive) consisted of 14 patients. A cut-off value of 19 ng/l was used according to the manufacturer's instructions (bioMerieux VIDAS® High sensitive Troponin I). This value represents the 99th percentile of a presumably healthy population.

Table 1: TNHS test repeatability and intralaboratory precision.

High-sensitivity troponin (pg/ml; ng/l)	Assay output requirements	
	Repeatability (within the same series) (CV (%))	Intralaboratory precision (total) (CV (%))
9-20	≤10%	≤12%
>20	≤10%	≤10%

Precision was assessed in accordance with the EP05-A3 protocol of the Clinical and Laboratory Standards Institute (CLSI): "Evaluation of Precision of Quantitative Measurement Procedures; Approved Guidelines—Third Edition" (CLSI Document EP05-A3).

Table 2: NT-proBNP test repeatability and intralaboratory precision.

NT-proBNP		Assay output requirements	
pg/ml	pmol/l	Repeatability (within the same series) (CV (%))	Intralaboratory precision (total) (CV (%))
100-500	11.8–59.0	≤5%	≤8%
>500	>59,0	≤7%	≤10%

Precision was assessed in accordance with the EP05-A3 protocol of the Clinical and Laboratory Standards Institute (CLSI): "Evaluation of Precision of Quantitative Measurement Procedures; Approved Guidelines—Third Edition" (CLSI Document EP05-A3).

High-sensitivity troponin tests were performed with the use of the VIDAS High sensitive Troponin I (TNHS). The test is capable of measuring cardiac troponin I concentration in the range of 4.9-40,000.00 pg/ml (ng/1) without the need for dilution. The TNHS test was designed to meet the following criteria of repeatability and intralaboratory precision (Table 1).

The NT-proBNP tests were performed with use of an Elecsys proBNP II Cobas e601 system. The test is capable of measuring the NT-proBNP concentration in the range of 5–35,000 pg/ml without the need for dilution.

The proBNP II test was designed to meet the following criteria of repeatability and intralaboratory precision (Table 2).

The NT-proBNP levels were presented as absolute values and transformed values that were standardized according to sex and age based on the manufacturer's guidelines. (http://www.rochecanada.com/content/dam/roche_canada/en_CA/documents/package_inserts/ProBNPII-04842464190-EN-V9-CAN.pdf). Values NT-proBNP greater than the 95th percentile for age and gender (the ULN) were considered abnormal.

Therefore, the results were expressed as the ratio of the NT-proBNP to age and sex-matched ULN. Ratios > 1.0 were considered abnormal [6]. This standardization of NT-proBNP provides a normal distribution of data, whereas absolute values were distributed abnormally. In this situation, we do not need to perform a logarithmic transformation for artificial calculation.

For the statistical analysis, continuous variables were presented as the mean (±standard deviation (SD)) or median (interquartile range (IQR)). NT-proBNP levels were

Table 3: The baseline characteristics of HCM patients.

(a)

Mean age	37 ± 6 years
Males/females	33/31
The ICD implantation	8 patients
EF %	59 ± 8%
hsTnI value	73.74 ± 232.9
Medications	Patients
Beta-blockers	43
Verapamil	17
Diuretics	3
ACE inhibitors	4
Past history of AP in years	4.1 + 1.2 years

(b)

		Total ($N = 64$)	Subgroup 0 ($N = 38$)	Subgroup 1 ($N = 12$)	Subgroup 2 ($N = 14$)
Baseline characteristics of subgroups of patients with HCM					
NYHA	Class I (n (%))	12 (19%)	9 (24%)	3 (25%)	0*,**
	Class II (n (%))	33 (51%)	20 (52%)	6 (50%)	7 (50%)
	Class III (n (%))	19 (30%)	9 (24%)	3 (25%)	7 (50%)*
CCS	Class I (n (%))	24 (38%)	18 (47%)	5 (42%)	1 (7%)*,**
	Class II (n (%))	29 (45%)	16 (42%)	5 (42%)	8 (57%)
	Class III (n (%))	11 (17%)	4 (11%)	2 (8%)	5 (36%)*
Syncope (n (%))		25 (39%)	13 (34%)	5 (42%)	7 (50%)
Sudden death in family history (n (%))		23 (36%)	14 (37%)	4 (33%)	5 (36%)
All patients had Holter					
NSVT in Holter (n (%))		26 (41%)	15 (39%)	5 (42%)	6 (43%)
LV maximal wall thickness (LVMWT) at diastole (cm)		2.23 ± 0.57	Detailed calculation in Figure 3		
Resting LVOT gradient, ≥30 mmHg (n (%))		14 (22%)	6 (16%)	3 (25%)	5 (36%)
Provocable LVOT gradient, ≥30 mmHg (n (%))		14 (22%)	5 (13%)	3 (25%)	6 (43%)*
Left atrial diameter (cm)		4.78 ± 0.64	Detailed calculation in Figure 5		

Abbreviations: CCS: Canadian Cardiovascular Society; LVOT: left ventricular outflow tract; LV: left ventricular; NSVT: nonsustained ventricular tachycardia; NYHA: New York Heart Association. *$p < 0.05$ subgroup 0 vs. 2; **$p < 0.05$ subgroup 1 vs. 2.

compared between the three subgroups of patients using the Kruskal–Wallis test, which was also used to compare the maximal LVOT gradient. The values of standardized NT-proBNP/ULN had a normal distribution according to the Kolmogorov-Smirnov test and were compared using ANOVA for comparison, which was also used to compare the LV maximum wall thickness (LVMWT) and left atrial diameter (LAD). *Stepwise multiple linear regression analysis was used to identify factors independently correlated with NT-proBNP levels. Patients' age, gender, troponin level, presence of angina, and several echocardiographic parameters (max LVH, resting LVOT gradient, maximal LVOT gradient, and LAD) were tested as possible candidates.* A p value of <0.05 was considered statistically significant (Statistica 12.0).

3. Results

Demographics, relevant echocardiographic information, medical history, and treatment data are presented in Table 3.

Among all patients, chest pain was present more than 10 hours (during daily physical activity on the first day) before the blood sampling at 8.00 a.m. on the second day in the morning. There were no chest pains during the night.

The absolute value of NT-proBNP was significantly higher in the painful ischemia subgroup (hsTnI-/AP- vs. hsTnI+/AP- vs. hsTnI+/AP+: 502 (174-833) vs. 969 (363-1346) vs. 2053 (323-3283) pg/ml; $p = 0.0178$ for the whole model, Figure 1).

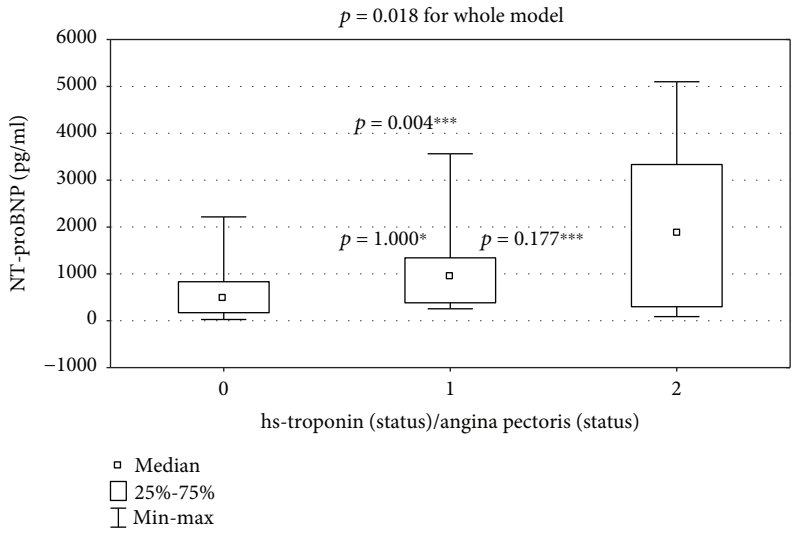

Figure 1: Comparison of NT-proBNP between subgroup 0 (hsTnI-/AP-), subgroup 1 (hsTnI+/AP-), and subgroup 2 (hsTnI+/AP+); $p = 0.018$ for the whole model. For inter-subgroup comparison: *subgroup 0 vs. 1: $p = 1.000$; **subgroup 1 vs. 2: $p = 0.177$; ***subgroup 0 vs. 2: $p = 0.004$.

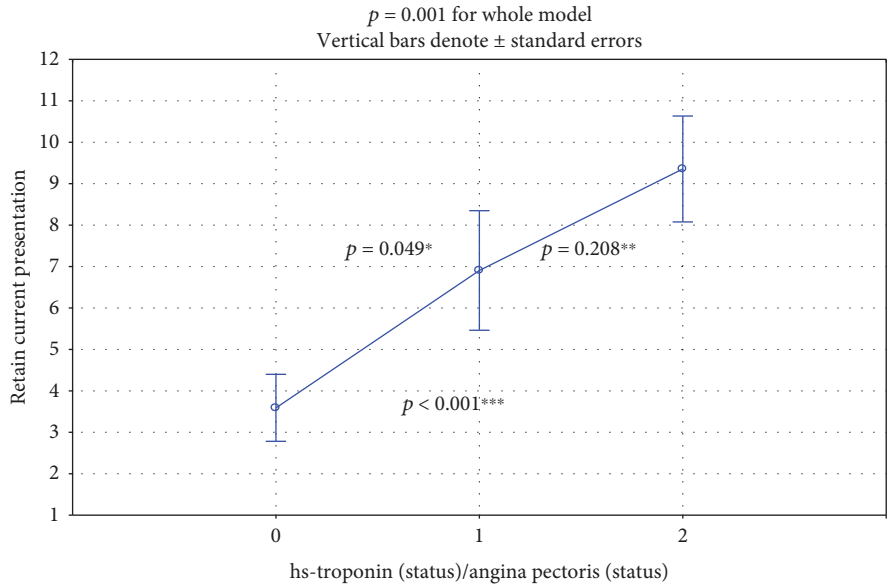

Figure 2: Comparison of NT-proBNP standardized according to age and sex between subgroup 0 (hsTnI-/AP-), subgroup 1 (hsTnI+/AP-), and subgroup 2 (hsTnI+/AP+). $p = 0.001$ for the whole model. Inter-subgroup comparison: *subgroup 0 vs. 1: $p = 0.049$; **subgroup 1 vs. 2: $p = 0.208$; ***subgroup 0 vs. 2: $p < 0.001$.

The standardized value of NT-proBNP/ULN showed a gradual significant increase (hsTnI-/AP- vs. hsTnI+/AP- vs. hsTnI+/AP+: 3.59 + 0.63 vs. 6.90 + 1.31 vs. 9.35 + 1.87; $p = 0.001$ for the whole model in ANOVA; Figure 2).

In the comparison between subgroups (hsTnI-/AP- vs. hsTnI+/AP- vs. hsTnI+/AP+), two echocardiographic parameters increased significantly. The LV maximum wall thickness (LVMWT) at diastole was 1.99 ± 0.08 cm vs. 2.28 ± 0.13 cm vs. 2.49 ± 0.15 cm (Figure 3, normal distribution, ANOVA test, $p = 0.004$ in the whole-model analysis).

The maximal provoked LVOT gradient increased significantly in only the painful-ischemia subgroup: 11 (7-30) mmHg vs. 12 (9.35-31.5) mmHg vs. 100 (43-120) mmHg (Figure 4; abnormal distribution: Kruskal–Wallis test, $p < 0.001$ for the whole model).

The increase of LAD from subgroup to subgroup was nonstatistically significant (4.28 ± 0.16 vs. 4.64 ± 0.28 vs. 4.95 ± 0.15; $p = 0.051$ for the whole model, Figure 5).

NT-proBNP/ULN was more strongly correlated with echocardiographic parameters than NT-proBNP (Table 4).

In multiple linear regression analysis, resting LVOT gradient, LAD, and the presence of angina were identified as independent factors affecting NT-proBNP levels in patients with HCM (Table 5).

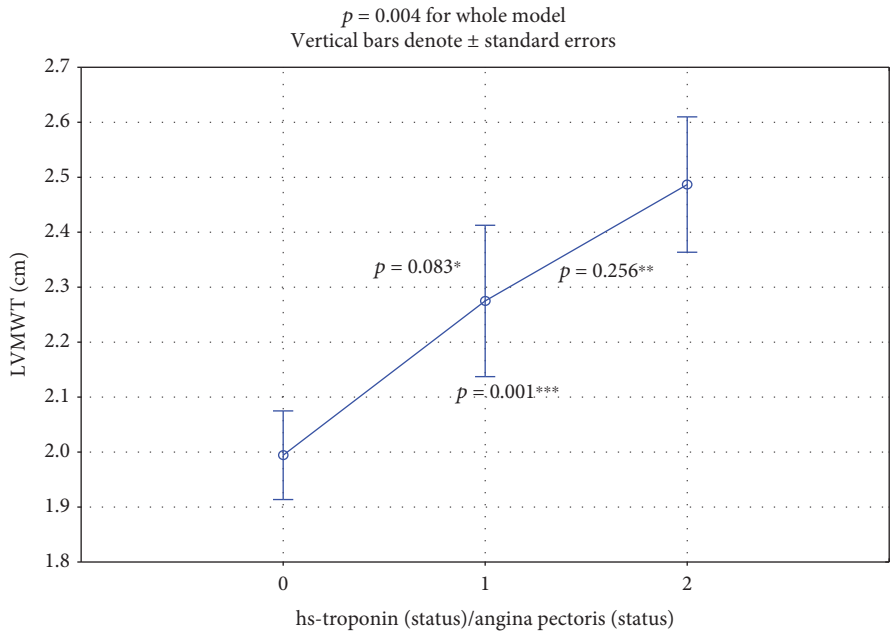

Figure 3: Significant increase ($p = 0.004$) of LVMWT in the whole model. Inter-subgroup comparison: *subgroup 0 vs.1: $p = 0.083$; **subgroup 1 vs. 2: $p = 0.256$; ***subgroup 0 vs. 2: $p = 0.001$.

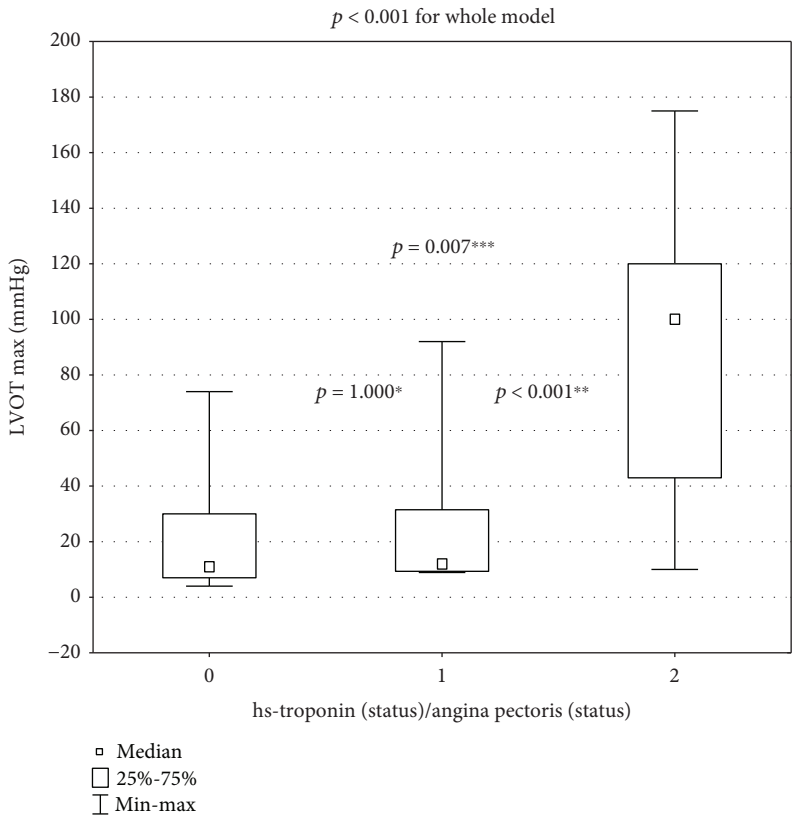

Figure 4: Significant increase ($p < 0.001$ for the whole model) of provocable LVOT gradient. Inter-subgroup comparison: *subgroup 0 vs. 1: $p = 1.000$; **subgroup 1 vs. 2: $p < 0.001$; ***subgroup 0 vs. 2: $p = 0.007$.

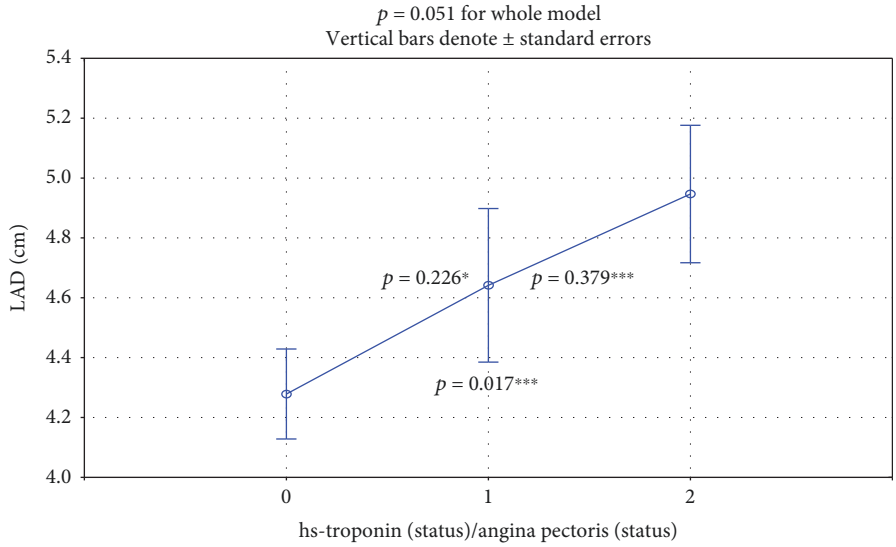

Figure 5: There was a nonsignificant increase in LAD ($p = 0.051$ for the whole model). *Subgroup 0 vs. 1: $p = 0.226$; **subgroup 1 vs. 2: $p = 0.379$; ***subgroup 0 vs. 2: $p = 0.017$.

Table 4: Correlations between NT-proBNP(/ULN) and echocardiographic parameters.

	NT-proBNP	NT-proBNP/ULN
LVMWT	$r = 0.24^*$	$r = 0.36$
LVOTG max	$r = 0.44$	$r = 0.54$
LAD	$r = 0.41$	$r = 0.42$

*Nonsignificant; remaining correlations were significant; $p < 0.05$.

4. Discussion

hsTnI is a precise and very useful biomarker for the detection of even small, focal, subendocardial myocardial injury caused by ischemia in patients with HCM. In recent investigations, measurements of hsTnI levels were synchronized with a non-invasive assessment of clinical and hemodynamic parameters within a short time, similar with previous studies [7–11]. We have documented that levels of both NT-proBNP and NT-proBNP/ULN were the highest in the most ischemic subgroup (painful angina pectoris; hsTnI+/AP+). Both biomarkers and echocardiographic parameters have not been investigated previously using currently proposed models of analysis [12–15].

In the hsTnI+/AP+ subgroup, both LVMWT at diastole and the provocable LVOT gradient had significantly higher values. In the subgroup of painless ischemia, the LVMWT at diastole had an intermediate value and differed significantly from the values of the nonischemic and painful ischemic subgroups (Figure 3). Our findings are rational because both increased myocardial mass and LVOT gradient induce myocardial ischemia through an increase in oxygen demand. LAD is the third echocardiographic risk factor for sudden death included in the guideline calculator from the European Society of Cardiology [4, 10, 11]. This value was increased in subgroups, but the differences were only on the statistical borderline ($p = 0.052$, Figure 5).

In an experimental protocol for HCM with more physiological conditions [15], biomarkers were measured before exercise testing with only one control point at 4 hours post-exercise. NT-proBNP increased by 27% after exercise. Similarly, hsTnI increased by 24% 4 hours after exercise, but the differences were not statistically significant. The 4-hour check-point in the postexercise recovery seems to be too long for peak NT-proBNP and too short for peak hsTnI values. In small study with 7 young HCM patients without symptomatic coronary artery disease, authors [16] detected elevated troponin levels after physical exercise in 5 patients. In serial measurement, the peak concentration had been reached between 6 and 9 hours and levels returned to preexercise values within 24 hours. Troponin release was consistently diminished after use of a beta-blocker. We tried to study this problem by using a 24-hour spectrum of time and with a more physiological approach. We monitored the 24-hour physical activity and occurrence of angina. It has been proposed that moderate, fluctuating exercise during daily physical activity may be more appropriate to detect abnormalities in cardiac biomarker release, rather than maximum symptom-limited exercise [15]. To support the theory about the link with postexercise prolonged myocardial ischemia, we need a larger study, with many points in time to measure hsTnI (24-hour profile of release). Tesic et al. [17] recently found that the coronary flow reserve in the left anterior descending artery appeared to be an independent predictor of NT-proBNP. Thus, elevated NT-proBNP might be the result of cardiac ischemia indicated by low coronary flow reserve.

4.1. Limitations. The main limitation of study is the relatively small number of patients due to several exclusion criteria. Not all of the patients underwent coronary arteriograms, which was only performed on patients with the appropriate indications. The minority of patients did not have coronary angiography performed (young, without AP, and without

Table 5: Results of linear regression analysis.

Independent variable	Coefficient	Standard error	Standardized coefficient	p value
Resting LVOT gradient	19.76	5.29	0.41	<0.001
LAD	314.44	123.30	0.26	0.013
Angina	658.35	297.13	0.25	0.031

risk factors for CAD). The risk for CAD was minimal and coronary angiography was not indicated. The strategy of noninvasive identification of subgroups with low likelihood of obstructive CAD [18] is effective.

The next limitation of the study was the following problem. We measured biomarkers simultaneously, once in time, and we do not have a sufficient period of follow-up with prognostic findings.

5. Conclusions

Both painless ischemia and painful ischemia are associated with a gradual, significant increase in NT-proBNP/ULN in comparison to the double-negative hsTnI/AP subgroup. In contrast, NT-proBNP was significantly higher in only the subgroup with painful ischemia. In the comparison between subgroups (hsTnI-/AP- vs. hsTnI+/AP- vs. hsTnI+/AP+), two echocardiographic parameters increased significantly: LVMWT at diastole (in the whole-model analysis) and the maximal provoked LVO T gradient (only in the painful subgroup in both analysis models).

Data Availability

The data used to support the findings of this study are available from the corresponding author upon request.

Additional Points

Clinical Perspective. The study documented the evidence that positive troponin status is timely related with higher biomarker value NT-proBNP reflecting LV myocardial dysfunction. From the clinical perspective, monitoring of these 2 biomarkers may improve pharmacological and nonpharmacological treatments and safety of exercise training.

Conflicts of Interest

The authors declare that they have no conflicts of interest.

Authors' Contributions

RR-S performed the conceptualization, formal analysis, investigation, writing of the reviews, and editing. AG performed formal analysis, investigation, writing of the reviews, and editing. AD performed some analysis, investigation, and editing, and PPD performed the conceptualization, formal analysis, investigation, draft writing, writing of the reviews, and editing. RR-S and AG contributed equally to this work.

References

[1] D. W. Kehl, A. Buttan, R. J. Siegel, and F. Rader, "Clinical utility of natriuretic peptides and troponins in hypertrophic cardiomyopathy," *International Journal of Cardiology*, vol. 218, no. 2, pp. 252–258, 2016.

[2] M. Gawor, M. Śpiewak, J. Janas et al., "The usefulness of sST2 and galectin-3 as novel biomarkers for better risk stratification in hypertrophic cardiomyopathy," *Kardiologia Polska*, vol. 75, no. 10, pp. 997–1004, 2017.

[3] T. Kubo, H. Kitaoka, M. Okawa et al., "Combined measurements of cardiac troponin I and brain natriuretic peptide are useful for predicting adverse outcomes in hypertrophic cardiomyopathy," *Circulation Journal*, vol. 75, no. 4, pp. 919–926, 2011.

[4] Authors/Task Force members, P. M. Elliott, A. Anastasakis et al., "2014 ESC guidelines on diagnosis and management of hypertrophic cardiomyopathy: The task force for the diagnosis and management of hypertrophic cardiomyopathy of the European Society of Cardiology (ESC)," *European Heart Journal*, vol. 35, no. 39, pp. 2733–2779, 2014.

[5] A. Pelliccia, E. Lemme, V. Maestrini et al., "Does sport participation worsen the clinical course of hypertrophic cardiomyopathy? Clinical outcome of hypertrophic cardiomyopathy in athletes," *Circulation*, vol. 137, no. 5, pp. 531–533, 2018.

[6] J. L. Blackshear, R. E. Safford, C. S. Thomas et al., "Platelet function analyzer 100 and brain natriuretic peptide as biomarkers in obstructive hypertrophic cardiomyopathy," *The American Journal of Cardiology*, vol. 121, no. 6, pp. 768–774, 2018.

[7] A. Gębka, R. Rajtar-Salwa, A. Dziewierz, and P. Petkow-Dimitrow, "Painful and painless myocardial ischemia detected by elevated level of high-sensitive troponin in patients with hypertrophic cardiomyopathy," *Advances in Interventional Cardiology*, vol. 14, no. 2, pp. 195–198, 2018.

[8] R. Rajtar-Salwa, R. Hładij, and P. P. Dimitrow, "Elevated level of troponin but not N-terminal probrain natriuretic peptide is associated with increased risk of sudden cardiac death in hypertrophic cardiomyopathy calculated according to the ESC Guidelines 2014," *Disease Markers*, vol. 2017, Article ID 9417908, 5 pages, 2017.

[9] R. Hładij, R. Rajtar-Salwa, and P. Petkow Dimitrow, "Associaton of elevated troponin levels with increased heart rate and higher frequency of nonsustained ventricular tachycardia in hypertrophic cardiomyopathy," *Polish Archives of Internal Medicine*, vol. 126, no. 6, pp. 445–447, 2017.

[10] R. Hładij, R. Rajtar-Salwa, and P. P. Dimitrow, "Troponin as ischemic biomarker is related with all three echocardiographic risk factors for sudden death in hypertrophic cardiomyopathy (ESC Guidelines 2014)," *Cardiovascular Ultrasound*, vol. 15, no. 1, p. 24, 2017.

[11] C. M. McGorrian, S. Lyster, A. Roy et al., "Use of a highly-sensitive cardiac troponin I assay in a screening population

for hypertrophic cardiomyopathy: a case-referent study," *BMC Cardiovascular Disorders*, vol. 13, no. 1, p. 70, 2013.

[12] S. W. Kim, S. W. Park, S. H. Lim et al., "Amount of left ventricular hypertrophy determines the plasma N-terminal pro-brain natriuretic peptide level in patients with hypertrophic cardiomyopathy and normal left ventricular ejection fraction," *Clinical Cardiology*, vol. 29, no. 4, pp. 155–160, 2006.

[13] G. Kahveci, F. Bayrak, B. Mutlu, and Y. Basaran, "Determinants of elevated NT-proBNP levels in patients with hypertrophic cardiomyopathy: an echocardiographic study," *Heart, Lung and Circulation*, vol. 18, no. 4, pp. 266–270, 2009.

[14] Y. Sato, R. Taniguchi, K. Nagai et al., "Measurements of cardiac troponin T in patients with hypertrophic cardiomyopathy," *Heart*, vol. 89, no. 6, pp. 659-660, 2003.

[15] J. E. Ho, L. Shi, S. M. Day et al., "Biomarkers of cardiovascular stress and fibrosis in preclinical hypertrophic cardiomyopathy," *Open Heart*, vol. 4, no. 2, article e000615, 2017.

[16] G. A. Pop, E. Cramer, J. Timmermans, H. Bos, and F. W. Verheugt, "Troponin I release at rest and after exercise in patients with hypertrophic cardiomyopathy and the effect of betablockade," *Archivos de Cardiologia de Mexico*, vol. 76, no. 4, pp. 415–418, 2006.

[17] M. Tesic, J. Seferovic, D. Trifunovic et al., "N-terminal pro-brain natriuretic peptide is related with coronary flow velocity reserve and diastolic dysfunction in patients with asymmetric hypertrophic cardiomyopathy," *Journal of Cardiology*, vol. 70, no. 4, pp. 323–328, 2017.

[18] J. Reeh, C. B. Therming, M. Heitmann et al., "Prediction of obstructive coronary artery disease and prognosis in patients with suspected stable angina," *European Heart Journal*, vol. 40, no. 18, pp. 1426–1435, 2019.

Hindawi
Disease Markers
Volume 2019, Article ID 4823156, 9 pages
https://doi.org/10.1155/2019/4823156

Research Article

Effects of Apelin on Left Ventricular-Arterial Coupling and Mechanical Efficiency in Rats with Ischemic Heart Failure

Qiufang Ouyang,[1] **Tao You**,[1] **Jinjian Guo**,[2] **Rong Xu**,[1] **Quehui Guo**,[1] **Jiqin Lin**,[1] **and Hongjia Zhao**[3]

[1]*Department of Ultrasonography, Second Affiliated People's Hospital of Fujian Traditional Chinese Medicine University, Fuzhou, Fujian, China*
[2]*Department of Cardiology, Second Affiliated People's Hospital of Fujian Traditional Chinese Medicine University, Fuzhou, Fujian, China*
[3]*Department of Cardiology, First Affiliated People's Hospital of Fujian Traditional Chinese Medicine University, Fuzhou, Fujian, China*

Correspondence should be addressed to Hongjia Zhao; hongjiafz@163.com

Received 3 October 2018; Accepted 6 December 2018; Published 17 June 2019

Guest Editor: Zhongjie Shi

Apelin plays important roles in cardiovascular homeostasis. However, its effects on the mechanoenergetics of heart failure (HF) are unavailable. We attempted to investigate the effects of apelin on the left ventricular-arterial coupling (VAC) and mechanical efficiency in rats with HF. HF was induced in rats by the ligation of the left coronary artery. The ischemic HF rats were treated with apelin or saline for 12 weeks. The sham-operated animals served as the control. The left ventricular (LV) afterload and the systolic and diastolic functions, as well as the mechanoenergetic indices were estimated from the pressure-volume loops. Myocardial fibrosis by Masson's trichrome staining, myocardial apoptosis by TUNEL, and collagen content in the aorta as well as media area in the aorta and the mesenteric arteries were determined. Our data indicated that HF rats manifested an increased arterial load (Ea), a declined systolic function (reduced ejection fraction, $+dP/dt_{max}$, end-systolic elastance, and stroke work), an abnormal diastolic function (elevated end-diastolic pressure, τ, and declined $-dP/dt_{max}$), and decreased mechanical efficiency. Apelin treatment improved those indices. Concomitantly, increased fibrosis in the LV myocardium and the aorta and enhanced apoptosis in the LV were partially restored by apelin treatment. A declined wall-to-lumen ratio in the mesenteric arteries of the untreated HF rats was further reduced in the apelin-treated group. We concluded that the rats with ischemic HF were characterized by deteriorated LV mechanoenergetics. Apelin improved mechanical efficiency, at least in part, due to the inhibiting cardiac fibrosis and apoptosis in the LV myocardium, reducing collagen deposition in the aorta and dilating the resistant artery.

1. Introduction

The interaction between the left ventricle (LV) and the arterial system, usually termed ventricular-arterial coupling (VAC), is recognized nowadays as a key determinant of global cardiovascular performance [1]. The cardiovascular system is structured to provide adequate pressure and flow to the tissues. Aortic elastic properties and total arterial compliance are important determinants of the left ventricular function and coronary blood flow. Studying the LV efficiency requires investigating not only the performance of the LV itself but also the properties of the arterial system.

Heart failure (HF) following myocardial infarction (MI) is associated with cardiac and vascular alterations. The cardiac remodeling is characterized by LV dilation and pump dysfunction, indicating decreased LV end-systolicelastance (Ees) and stroke work (SW). Meanwhile, the vascular changes are manifested as the compliance decreased, which led to an increase in effective arterial elastance (Ea). Accordingly, VAC and mechanical efficiency in the LV were altered during ischemic HF [30].

Apelin is the endogenous ligand of the G protein-coupled receptor APJ. Now, a second ligand for the apelin receptor has been discovered in the fish Danio, called Elabela [2] or Toddler [3]. Elabela/Toddler has also been shown to be present in humans and act as the apelin receptor and is downregulated like apelin in cardiovascular diseases. The Toddler/apelin/APJ system plays important roles in adjusting the blood pressure, the pulmonary artery pressure, and the cardiac function [4–6]. Compelling evidence indicated that the exogenous apelin treatment significantly increased the LV stroke volume [7], enhanced the cardiac contractility [8], reduced the ventricular preload and afterload [9], or caused vasodilation [10] in various *in vivo* models. However, the effect of apelin on the interaction of LV and the arterial system in HF rats has not been reported yet.

Therefore, the aim of this work was to investigate the effects of apelin on VAC and mechanical efficiency with pressure-volume (P-V) analysis in a model of ischemic HF. Then, the morphological changes of LV and the artery were investigated, trying to elucidate the mechanism underlying these effects from the perspective of histomorphology.

2. Materials and Methods

2.1. Animal Experiment Protocol. All of the procedures and protocols were approved by the Animal Care Committee of Fujian Traditional Chinese Medicine University and followed the guidelines of the Animal Management Rules of the Chinese Ministry of Health.

The heart failure model was established in 10-week-old male Wistar rats (Shanghai Laboratory Animal Center, Chinese Academy Sciences) by left anterior descending (LAD) ligation, as described previously [11]. Briefly, rats were anesthetized with a combination of 80 mg/kg ketamine and 5 mg/kg acepromazine (both form Sigma-Aldrich, St. Louis, MO, USA), and the left thoracotomy was performed. The heart was exteriorized, and the LAD was ligated 2 mm from its origin with a Prolene 6-0 suture. In the sham-operated animals, the suture was passed but not tied. After the procedure, the animals were closed in 3 layers. Immediately after surgery, the left ventricular dimensions, the ejection fraction (EF), and the MI size were assessed by echocardiography. Following echocardiography, the rats with similar MI size (both average in size and variance) were divided into two groups: the apelin group ($n = 20$) received (Pyr1)-apelin-13 (GL Biochem Ltd., Shanghai, China), 200 μg/kg/day intraperitoneal injection, initiated after echocardiography, once a day for 12 weeks; and the control group ($n = 20$) as well as the sham-operated rats ($n = 15$), treated with isovolume saline. At the end of the treatment, the rats were weighed and the hemodynamics was analyzed. Then, these animals were killed for morphologic study.

2.2. Assessment of the Hemodynamics and the Left Ventricular Function by Pressure-Volume Analysis. 12 weeks after the treatment, the cardiac hemodynamic parameters were determined. For this, the rats were anesthetized with the method as mentioned above and ventilated. A small incision was made to the right of the midline in the neck. A polyethylene catheter was inserted into the left external jugular vein for fluid administration. A 2-Fr microtip pressure-conductance catheter (SPR-838, Millar Instruments, Houston, TX) was inserted into the right carotid artery and advanced into the ascending aorta. After stabilization for 5 min, the mean arterial pressure (MAP) and the heart rate (HR) were recorded by the PowerLab data acquisition system (ADInstruments, Australia). Then, the catheter was advanced into the LV under pressure control. With the use of a special pressure-volume (P-V) analysis program, the traditional load-dependent hemodynamic indices, such as LV end-systolic pressure (ESP), LV end-diastolic pressure (EDP), the maximal slopes of LV systolic pressure increment ($+dP/dt_{max}$) and diastolic pressure decrement ($-dP/dt_{max}$), and the isovolumic relaxation time constant (τ) were determined. The slope of the LV end-diastolic PV relationship (EDPVR) was calculated as a reliable indicator of LV stiffness [12]. Meanwhile, the load-independent indices, i.e., the end-systolic elastance (Ees), the arterial elastance (Ea, calculated as ESP/SV), the stroke work (SW), and the P-V area (PVA, the specific area in the P-V plane bounded by the end-systolic and end-diastolic P-V relationship lines and the systolic segment of the P-V loop), were calculated by transient occlusion of the inferior caval vein. Then, the VAC ratio (as Ea/Ees) and the mechanical efficiency (as SW/PVA) were calculated to assess the LV mechanoenergetics [13].

2.3. Determination of Myocardial Fibrosis with Masson Staining and Apoptosis with Terminal dUTP Nick End Labeling Assay. The hearts of the rats in each group were harvested, fixed in 4% paraformaldehyde, embedded in paraffin, and cut into 5 μm sections. Subsequently, the LV myocardial sections from the midpapillary muscle level were subjected to hematoxylin and eosin, Masson's trichrome, and terminal dUTP nick end labeling (TUNEL) staining. MI size was expressed as an average percentage of the LV endocardial and epicardial circumferences that was identified as infarct in the Masson's trichrome staining sections. Myocardial fibrosis was expressed as a percentage of fibrotic area to the left ventricular area (% of LV) in an average of 5 sections in each heart. The number of TUNEL-positive cardiomyocyte nuclei was counted manually in whole, noninfarcted myocardium, including the LV posterior wall and septum, under light microscopy from each LV short-axis section. Only the nuclei clearly located within cardiomyocytes were counted and expressed as a percentage of total myocytes in a given LV section.

2.4. Histology and Morphometric Analysis of the Aorta and the Mesenteric Artery. The thoracic aorta and mesenteric artery specimens were collected and stained with hematoxylin and eosin staining. The media cross-sectional area (CSA, defined as the area between the internal and external elastic laminae) and the media-to-lumen ratio (defined as the ratio of the medial area and the lumen area times 100%) in the aorta and the mesenteric artery were determined. Meanwhile, the collagen deposition in the aorta was determined by Masson's trichrome staining. The collagen content was

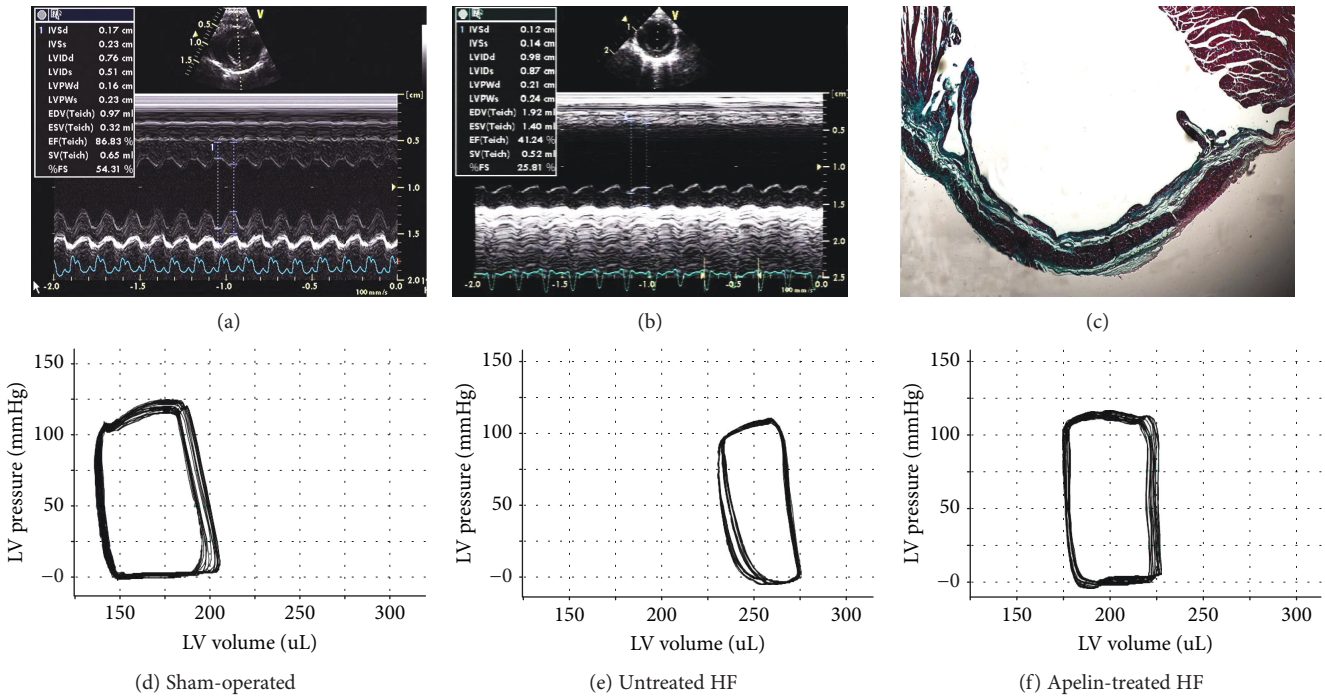

Figure 1: Representative short-axis echocardiographic images at midpapillary muscle level before treatment, gross left ventricular morphology, and pressure-volume loops at the study termination.

represented by collagen area/media area in order to normalize the vessels with different sizes. Photos were taken by a microscope (BX52, Olympus, Tokyo, Japan), and the data were analyzed by the Image-Pro Plus 5.0 analysis software (Media Cybernetics, USA).

2.5. Statistical Analysis. All the values were expressed as the mean ± standard deviation unless otherwise indicated. The group comparisons were performed with one-way ANOVAs, followed by a Bonferroni test. The Mann-Whitney U test was used if the variance was not normally distributed significantly. The statistical analysis was performed using the SPSS 17.0 software. A value of $P < 0.05$ was considered statistically significant.

3. Results

3.1. Apelin-13 Improved the Left Ventricular Dysfunction in Rats with Ischemic Heart Failure. There was no mortality in the sham-operated group and apelin-treated HF group. In the untreated HF group, two rats were excluded from further study due to a myocardial infarction size less than 20%. And four rats died 24 hours after coronary ligation surgery. Additionally, two rats died during the assessment of hemodynamics. And so, only 12 animals remained alive in the untreated HF group at the study termination. Therefore, 12 rats were eventually included in each group for the following experiments.

In rats following LAD ligation, the LV dimensions enlarged, the EF dropped, the motion of the anterior wall attenuated, and the systolic thickening rate of the anterior wall disappeared, indicating a successful ischemic HF model (Figure 1(b)). Obvious fibrosis in the myocardial infarction region was observed in the untreated HF rats at the study termination as indicated by Masson's trichrome staining (Figure 1(c)). In comparison with the sham-operated rat (Figure 1(d)), the rightward shift of the end-systolic pressure-volume relationship and the narrowed P-V loop (Figure 1(e)) in the HF animals were partially reversed by apelin treatment (Figure 1(f)).

LVSP in the untreated HF was significantly lower than that in the sham-operated group (105.56 ± 12.49 mmHg vs 136.81 ± 9.06 mmHg). Apelin treatment induced a further significant reduction of LVSP by 11.7% compared to the untreated HF animals. The heart rate differed insignificantly among the three groups (Table 1). Increased vascular afterload parameters (Ea) in the untreated HF group was partially restored by apelin treatment (0.51 ± 0.04 mmHg/μl in the sham, 0.74 ± 0.08 mmHg/μl in the untreated, and 0.46 ± 0.05 mmHg/μl in the apelin group).

EF, $+dP/dt_{max}$, Ees, and SW were lower in the untreated HF group than those in the sham-operated group, indicating a significant decline of the LV systolic function. Apelin treatment increased those indices by 27.4% for EF, 18.4% for $+dP/dt_{max}$, 57.5% for Ees, and 64.5% for SW.

Meanwhile, as compared to the sham-operated rats, an impaired diastolic function was observed in the untreated HF group as evidenced by the elevated EDP and the slopes of the EDPVR and τ as well as by the reduced $-dP/dt_{min}$. Apelin treatment improved the diastolic function as evidenced by reduced EDP (16.19 ± 5.92 mmHg vs 25.65 ± 4.93 mmHg) and the slopes of the end-diastolic

Table 1: Hemodynamic and histological measurements among the groups.

	Sham-operated ($n = 12$)	Untreated HF ($n = 12$)	Apelin-treated HF ($n = 12$)
Final body weight (g)	542.58 ± 38.29	525.16 ± 24.45	538.65 ± 29.48
Hemodynamics			
LVSP (mmHg)	136.81 ± 9.06	105.56 ± 12.49*	93.28 ± 11.64#
Ea (mmHg/μl)	0.51 ± 0.04	0.74 ± 0.08*	0.46 ± 0.05#
Ejection fraction (%)	68.64 ± 4.55	43.13 ± 6.09*	54.96 ± 5.24#
$+dP/dt_{max}$ (mmHg/s)	8514.12 ± 745.83	5950.74 ± 729.60*	7047.67 ± 635.58#
Ees (mmHg/μl)	1.06 ± 0.25	0.40 ± 0.08*	0.63 ± 0.15#
SW (mmHg/ml)	9.16 ± 10.24	6.02 ± 1.18*	7.35 ± 0.93#
$-dP/dt_{max}$ (mmHg/s)	8129.41 ± 802.95	5150.77 ± 629.05*	6746.29 ± 714.83#
EDP (mmHg)	5.84 ± 1.47	25.65 ± 4.93*	16.19 ± 5.92#
Slope of EDPVR (mmHg/μl)	0.035 ± 0.003	0.056 ± 0.008*	0.044 ± 0.003#
τ (msec)	9.14 ± 0.49	13.91 ± 1.78*	10.42 ± 0.78#
Ea/Ees	0.52 ± 0.08	1.62 ± 0.13*	0.93 ± 0.05#
Pressure-volume area (mmHg/ml)	16.44 ± 1.18	17.70 ± 10.24	16.62 ± 0.93
Heart rate (bpm)	405.43 ± 20.41	412.15 ± 54.26	378.26 ± 56.64
SW/PVA	0.56 ± 0.08	0.34 ± 0.04*	0.48 ± 0.05#
Histology			
Collagen density in LV (%)	1.92 ± 0.03	4.51 ± 0.08*	3.14 ± 0.05#
TUNEL (+) per 10^5 myocytes	45 ± 4	629 ± 91*	316 ± 46#
Myocardial infarction size (%)	NA	41.39 ± 5.24*	28.26 ± 4.55#

Data were expressed as % or mean ± standard deviation. LVSP: left ventricular systolic pressure; Ea: effective arterial elastance; $+dP/dt_{max}$: maximal rate of pressure increase; Ees: end-systolic elastance; SW: stroke work; $-dP/dt_{max}$: maximal rate of pressure decline; EDP: end-diastolic pressure; EDPVR: end-diastolic pressure-volume relationship; τ: isovolumic relaxation time constant; PVA: pressure-volume area; LV: left ventricle; TUNEL: terminal dUTP nick end labeling; NA: not applicable. *$P < 0.05$ vs the sham-operated group and #$P < 0.05$ vs the untreated heart failure group.

pressure-volume relationship (0.044 ± 0.003 mmHg/μl vs 0.056 ± 0.008 mmHgμl) and τ (10.42 ± 0.78 msec vs 13.91 ± 1.78 msec) whereas elevated $-dP/dt_{min}$ (6746.29 ± 714.83 mmHg/s vs 5150.77 ± 629.05 mmHg/s) when compared to the untreated HF group.

In comparison with the sham-operated animals, Ea/Ees rose markedly in the untreated HF group, suggesting a deterioration of VAC (1.62 ± 0.13 vs 0.52 ± 0.08). Concurrently, SW/PVA dropped obviously due to decreased SW and slightly elevated PVA. As a consequence, mechanical efficiency remained significantly impaired at 0.34 ± 0.04, as compared with the sham-operated group (0.56 ± 0.08). Following the treatment with apelin-13, VAC and mechanical efficiency were significantly improved by 42.6% and 41.2%, respectively, as compared to the untreated HF rats.

3.2. Apelin-13 Improved the Structural Disorder and Myocardial Fibrosis in Rats with Ischemic Heart Failure. Hematoxylin and eosin staining was used to evaluate the morphological changes. The left ventricle in the sham-operated group (Figure 2(a)) exhibited normal cardiomyocyte structure, with a clear texture and vein, and plump cytoplasm (less gaps and spaces between the myofilaments). However, myocardium in the untreated HF group (Figure 2(b)) showed disordered structure. The myofilaments were rougher with wave-like changes and the boundary of textures and veins was unclear. While in the apelin-treated group (Figure 2(c)), the above histopathological changes were ameliorated as compared with the untreated group.

Cardiac fibrosis was evaluated by Masson's trichrome staining. The LV myocardium in the untreated HF group (Figure 2(e)) exhibited numerous collagen fiber (blue) compared with the sham-operated group (Figure 2(d)). However, following the treatment with apelin-13 (Figure 2(f)), the percentage of fibrosis was significantly attenuated by 31.1% compared with the untreated HF group (Table 1).

3.3. Apelin-13 Inhibited Cardiac Cell Apoptosis in Rats with Ischemic Heart Failure. Representative slices of myocardium in the LV posterior wall of TUNEL staining (Figure 3) and the average number of positively stained nuclei for each group were shown (Table 1). After 12 weeks of treatment, the number of TUNEL-positive nuclei in the apelin-treated group (316 ± 46 per 10^5 myocytes) was significantly lower than that in the model group (629 ± 91 per 10^5 myocytes). And sparse apoptotic nuclei were observed in the sham-operated group.

3.4. Effect of Apelin on Morphological Characteristics of the Aorta and the Mesenteric Arteries. Compared with the

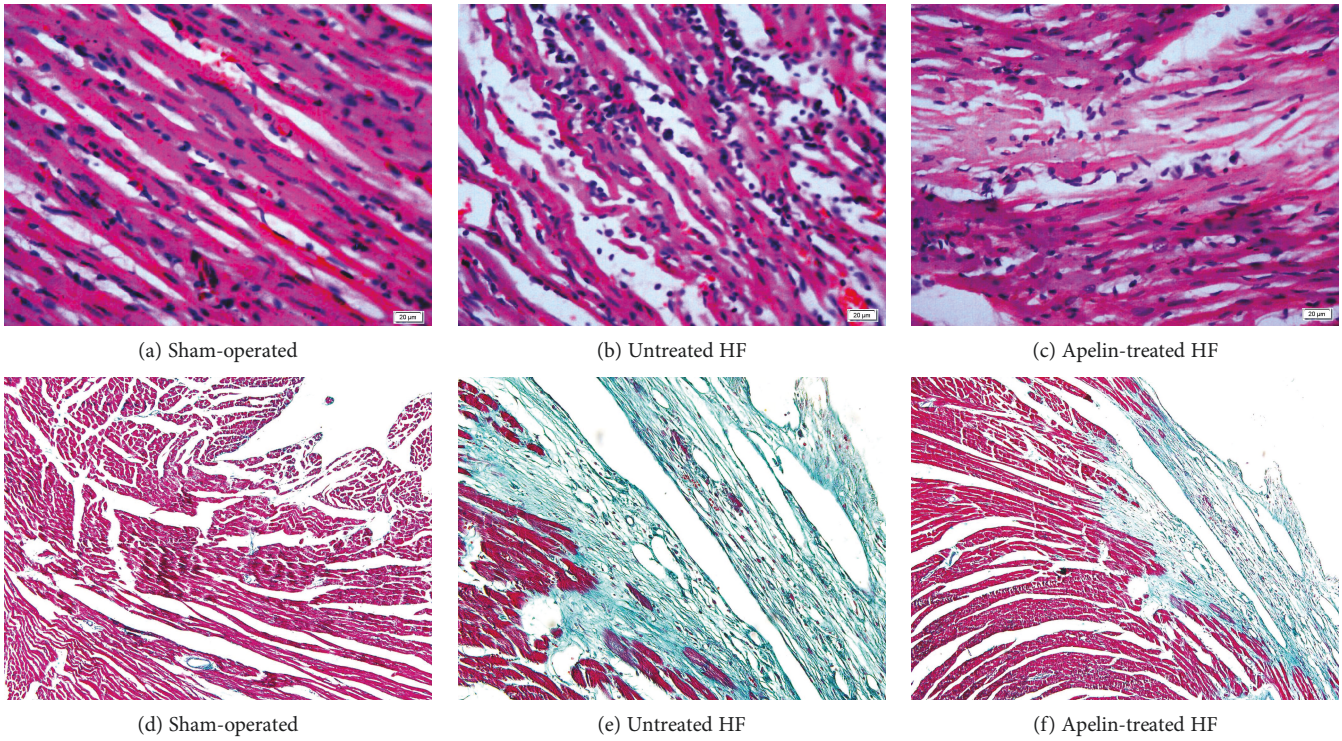

(a) Sham-operated (b) Untreated HF (c) Apelin-treated HF

(d) Sham-operated (e) Untreated HF (f) Apelin-treated HF

Figure 2: The morphological changes as illustrated by hematoxylin and eosin staining and Masson's trichrome staining. For Masson's trichrome staining, fibrosis was stained blue, whereas cytoplasm red. Untreated HF animals displayed disorder structure and fibrotic myocardium, which were ameliorated by apelin treatment.

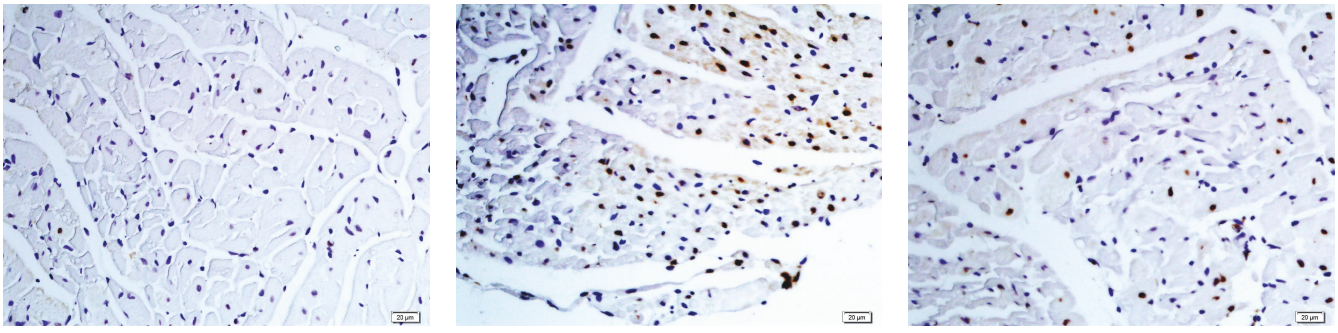

(a) Sham-operated (b) Untreated HF (c) Apelin-treated HF

Figure 3: Representative TUNEL staining slices for left ventricular myocardium. TUNEL: terminal dUTP nick end labeling. Apoptotic nuclei were stained brown. Apelin alleviated myocardial apoptosis induced by coronary artery ligation.

sham-operated animals (Figure 4(a)), media thickness reduced significantly and lumen diameter augmented slightly in the mesenteric arteries from rats of the untreated HF group (Figure 4(b)). Those resulted in a smaller media-to-lumen ratio in untreated HF rats. There was no significant difference in CSA between the untreated HF and sham-operated groups. Apelin treatment attenuated CSA by 19.2% and media-to-lumen ratio by 16.3% when compared with the untreated HF animals (Figures 4(c) and 4(j)).

In the thoracic aorta, no statistically significant changes of the layers of the elastic lamina, the media CSA, the lumen diameter, the media thickness, or the wall-to-lumen ratio were observed among the groups (Figures 4(d), 4(e), 4(f), and 4(k)). However, higher collagen deposition was present in the untreated HF group (Figure 4(h)) compared with sham-operated rats (Figure 4(g)) (9.35%±0.81% vs 10.91%±1.25%) as demonstrated by Masson's trichrome staining. Apelin alleviated aorta collagen density without a change in the elastin area (data not shown), leading to a declined collagen/elastin ratio in the aorta (Figure 4(i)).

4. Discussion

This study provides evidence that deteriorated LV mechanoenergetics (mechanical efficiency and ventricular-arterial

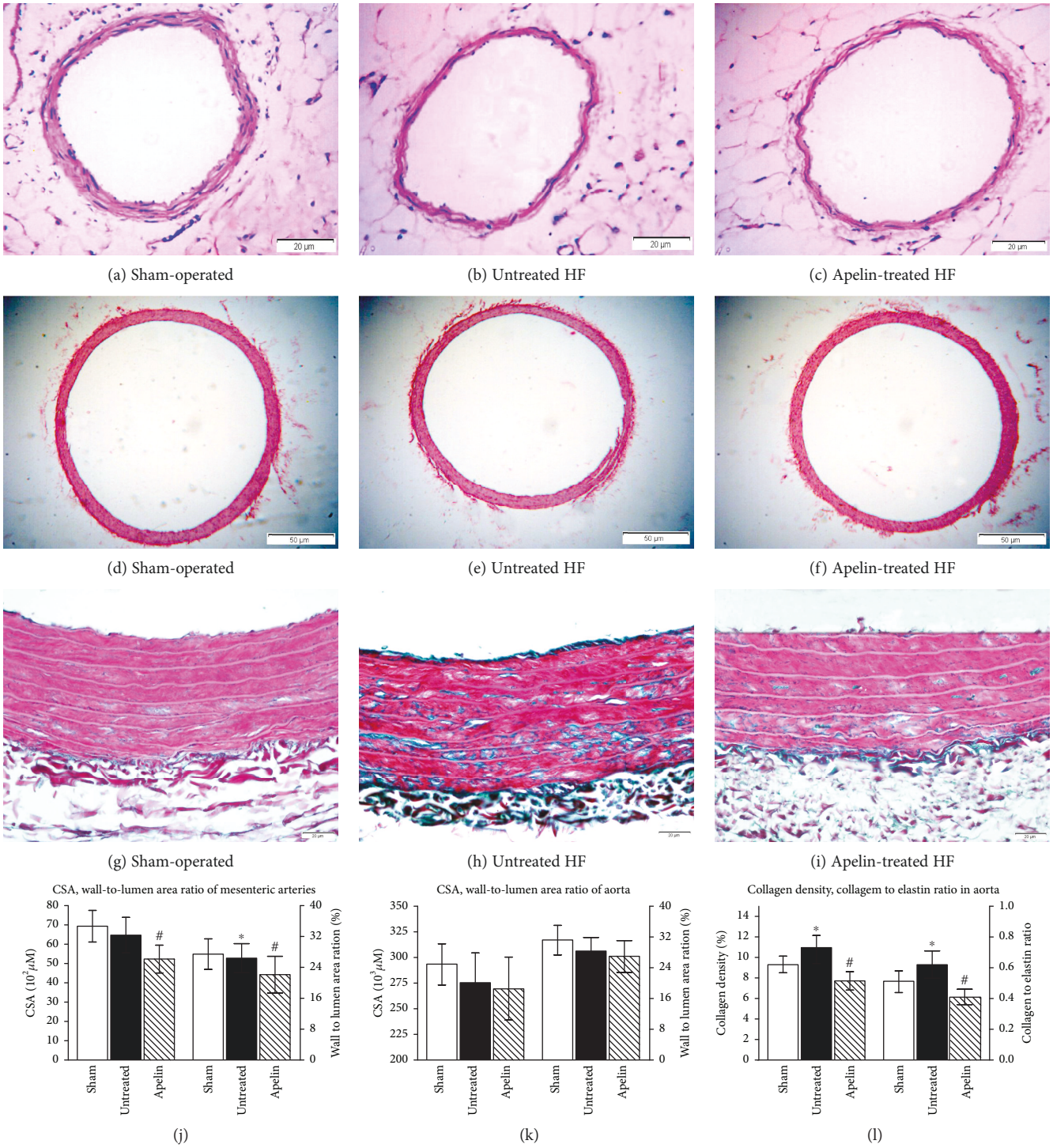

FIGURE 4: The media cross-sectional area in thoracic and mesenteric arteries depicted by hematoxylin and eosin staining and the collagen density in thoracic aorta indicated by Masson's trichrome staining. Representative transverse sections of the complete mesenteric arteries (a, b, and c) and aortas (d, e, and f) stained with hematoxylin and eosin. Aortic collagen deposition was shown by Masson's trichrome staining. Collagen was stained green while muscle and cytoplasm were red (g, h, and i). Quantitative analysis of media cross-sectional area in the mesenteric and thoracic arteries (j, k) and collagen in the aortas (l). CSA: media cross-sectional area. Apelin reduced media CSA and wall-to-lumen ratio in the mesenteric arteries and alleviated aorta collagen accumulation, but it did not affect media CSA and wall-to-lumen ratio in the aortas.

coupling) in HF rats can be improved by apelin treatment via elevating Ees and SW, decreasing Ea, and unaltering PVA. And this effect is, at least in part, due to the inhibiting cardiac fibrosis and apoptosis in LV myocardium, reducing collagen deposition in the aorta and dilating the resistant artery.

4.1. Apelin Modified the Arterial Properties in Rats with Ischemic Heart Failure. The aorta functions not only as a conduit delivering blood to tissues but also as an important modulator of the entire cardiovascular system, buffering the intermittent pulsatile output from the heart to provide steady flow to the capillary beds. The arterial compliance is an important determinant of the left ventricular function and coronary blood flow. Arterial system stiffness can be characterized by Ea, an integrative index that incorporates the principal elements of arterial load, including peripheral vascular resistance, total arterial compliance, and characteristic impedance [14]. Accordingly, the elevated Ea can result from either peripheral vasoconstriction or decrease in arterial compliance or a combination of both. Elastic and collagen fibers and their normal arrangement primarily determine the arterial compliance. The increase of collagen/elastin ratio represented the decline in arterial compliance. In this study, our data showed that increased Ea in the untreated HF rats was reversed by apelin treatment. In parallel, our result suggested that higher collagen deposition in the aortas was present in the untreated HF group, which can be alleviated by apelin treatment. And our result was partially substantiated by the observation that collagen area increased by 59% in the carotid artery of MI rats at 3 weeks of post-LAD ligation [15]. This was somewhat at odds with the report that media collagen density was not different between the sham-operated and untreated HF animals, either in the abdominal aorta, the femoral, or the mesenteric arteries at 90 days following LAD ligation [16]. The inconsistency may be partly explained by the difference in the disease course of HF or the type of artery studied.

There are also conflicting results on morphologic changes of mesenteric arteries in rats with ischemic HF. Several studies show that no morphologic changes were seen at 3 and 5 weeks of postoperation [17, 18], whereas others demonstrated an increased lumen diameter and reduced media thickness in the mesenteric arteries at 12 weeks of postinfarct [19]. Our results confirm the latter finding that the media-to-lumen ratio of the mesenteric arteries was lower in the untreated HF than that in the sham-operated animals. Additionally, our data indicated that apelin attenuated CSA and media-to-lumen ratio in the mesenteric arteries in the HF animals. To the best of our knowledge, no investigation has elaborated the effect of apelin on the remodeling of the mesenteric arteries in HF rats as yet.

In brief, apelin may reduce Ea by inhibiting the collagen deposition in the aorta and by dilating the resistance vessels. Presumably, the molecular mechanism may be related to the activation of nitric oxide (NO) pathways [20].

4.2. Apelin Improved LV Structural and Functional Characteristics. EF, $+dP/dt_{max}$, and SW were elevated in the apelin-treated rats, suggesting an increased LV systolic performance. Myocardial contractile dysfunction in heart failure is characterized by a decrease in contraction and prolonged relaxation. These alterations are mainly due to the changes in intracellular Ca^{2+} transients (CaT), Ca^{2+} sensitivity of the contractile elements, and/or contractile proteins [21]. Although the molecular mechanisms underlying its inotropic effect are not clarified in this investigation, activation of protein kinase Cε (PKCε) and extracellular signal-regulated kinase (ERK1/2) signaling might be involved [22].

Additionally, apoptosis is also responsible for the decline of pump function. The present data indicated that the numbers of TUNEL-positive nuclei in the apelin group were significantly lower compared to the untreated HF group. This observation is supported by the report that apelin-13 exerts antiapoptotic effects in the rats with myocardial infarction [23]. The possible mechanisms are related to the phosphatidylinositol-3-kinase (PI3K)/Akt, ERK1/2, caspase signaling, and autophagy pathways [24].

The impaired active relaxation and the increased myocardial stiffness are both responsible for the diastolic dysfunction. LV active relaxation is an active, energy-consuming process and depends mostly on calcium uptake by the sarcoplasmic reticulum during diastole [25], while the main determinant of myocardial stiffness is the collagen accumulation in the extracellular matrix [26]. In our investigation, EDP, slope of EDPVR, τ, and $-dP/dt_{max}$ were partially reversed by apelin treatment, suggesting improved active relaxation and end-diastolic stiffness. This observation was precisely reflected by our investigation, since the slope of EDPVR (the index of myocardial stiffness), along with the Masson's score, significantly increased in the HF model group and regressed by apelin treatment.

4.3. Apelin Ameliorated Mechanoenergetic Indices of Ventricular-Arterial Coupling and Mechanical Efficiency. Imbalance between energy production and consumption was observed in heart failure [27]. In this investigation, mechanoenergetic changes were determined by the ratios of Ea/Ees and SW/PVA via P-V analysis [28]. Ahmet et al. [29] reported that the rats with ischemic heart failure manifested mismatched VAC due to increased Ea and decreased Ees. Another study corroborated this finding that VAC and mechanical efficiency were severely deteriorated in pigs with myocardial infarct [13]. Similarly, our investigation indicated that LAD ligation induced inefficient VAC. In addition, our data demonstrated that apelin improved VAC, suggesting its optimal efficiency of blood transfer from the heart to the arterial system.

SW is the external mechanical work performed by the LV during a single heart cycle. PVA represents the total mechanical energy generated by ventricular contraction. PVA is an index of LV total energy expenditure mechanical energy and linearly related to total myocardial oxygen consumption [30]. We found that SW was enhanced while PVA was altered insignificantly by apelin treatment, indicating that apelin increased cardiac contractility with no significant change of metabolic needs of viable myocardium. Thus, apelin is a potential innovative treatment for heart failure.

Most studies hitherto have focused on the effects of apelin treatment on the single aspect of the heart or the vessels. And there is a paucity of information on the effects of apelin on the interrelationship between these two aspects. Our study suggested myocardial infarction resulted in structural and functional alterations at both the arterial level and the cardiac level, which is valuable for the global understanding of the

pathophysiological phenomena in the development of HF. Furthermore, our result provided novel morphological evidences concerning the cardiovascular protective potential of apelin on heart failure. Treatment of HF should therefore not only be directed to increase LV contractility but also to reduce arterial elastance.

Further research at the endothelial function, renin-angiotensin system, or intracellular Ca^{2+} may facilitate our understanding of the effects of apelin on mechanoenergetics in rats with HF. Additionally, caution is needed in translating these results into clinical practice.

5. Conclusions

LV performance and arterial properties are impaired in tandem in rats with ischemic heart failure, which resulted in ventricular-arterial mismatch and mechanical efficiency deterioration. Apelin improved mechanoenergetics, at least in part, due to its inhibiting cardiac fibrosis and apoptosis in LV myocardium, reducing collagen deposition in the aorta and dilating the resistant artery.

Data Availability

The data used to support the findings of this study are available from the corresponding author upon request.

Conflicts of Interest

The authors state no conflict of interest.

Acknowledgments

This study was supported by grants from Youth Scientific Research Project of Fujian Health and Family Planning Commission (2018-ZQN-71), the Natural Science Foundation of Fujian (2019J01480 and 2013J01321), and the Key Cooperative Project on the University Industry Education by Fujian Science and Technology Commission (2011Y4004).

References

[1] J. A. Chirinos and N. Sweitzer, "Ventricular–arterial coupling in chronic heart failure," *Cardiac Failure Review*, vol. 3, no. 1, pp. 12–18, 2017.

[2] S. C. Chng, L. Ho, J. Tian, and B. Reversade, "ELABELA: a hormone essential for heart development signals via the apelin receptor," *Developmental Cell*, vol. 27, no. 6, pp. 672–680, 2013.

[3] A. Pauli, M. L. Norris, E. Valen et al., "Toddler: an embryonic signal that promotes cell movement via apelin receptors," *Science*, vol. 343, no. 6172, article 1248636, 2014.

[4] K. Tatemoto, K. Takayama, M. X. Zou et al., "The novel peptide apelin lowers blood pressure via a nitric oxide-dependent mechanism," *Regulatory Peptides*, vol. 99, no. 2-3, pp. 87–92, 2001.

[5] P. Yang, C. Read, R. E. Kuc et al., "Elabela/toddler is an endogenous agonist of the apelin APJ receptor in the adult cardiovascular system, and exogenous administration of the peptide compensates for the downregulation of its expression in pulmonary arterial hypertension," *Circulation*, vol. 135, no. 12, pp. 1160–1173, 2017.

[6] Z. Chen, D. Wu, L. Li, and L. Chen, "Apelin/APJ system: a novel therapeutic target for myocardial ischemia/reperfusion injury," *DNA and Cell Biology*, vol. 35, no. 12, pp. 766–775, 2016.

[7] M. Wang, R. C. Gupta, S. Rastogi et al., "Effects of acute intravenous infusion of apelin on left ventricular function in dogs with advanced heart failure," *Journal of Cardiac Failure*, vol. 19, no. 7, pp. 509–516, 2013.

[8] Y. X. Jia, C. S. Pan, J. Zhang et al., "Apelin protects myocardial injury induced by isoproterenol in rats," *Regulatory Peptides*, vol. 133, no. 1–3, pp. 147–154, 2006.

[9] E. A. Ashley, J. Powers, M. Chen et al., "The endogenous peptide apelin potently improves cardiac contractility and reduces cardiac loading in vivo," *Cardiovascular Research*, vol. 65, no. 1, pp. 73–82, 2005.

[10] X. Cheng, X. S. Cheng, and C. C. Y. Pang, "Venous dilator effect of apelin, an endogenous peptide ligand for the orphan APJ receptor, in conscious rats," *European Journal of Pharmacology*, vol. 470, no. 3, pp. 171–175, 2003.

[11] S. Cheng, P. Yu, L. Yang et al., "Astragaloside IV enhances cardioprotection of remote ischemic conditioning after acute myocardial infarction in rats," *American Journal of Translational Research*, vol. 8, no. 11, pp. 4657–4669, 2016.

[12] M. S. Maurer, I. Kronzon, and D. Burkhoff, "Ventricular pump function in heart failure with normal ejection fraction: insights from pressure-volume measurements," *Progress in Cardiovascular Diseases*, vol. 49, no. 3, pp. 182–195, 2006.

[13] P. Kolh, B. Lambermont, A. Ghuysen et al., "Alteration of left ventriculo-arterial coupling and mechanical efficiency during acute myocardial ischemia," *International Angiology*, vol. 22, no. 2, pp. 148–158, 2003.

[14] K. Sunagawa, W. L. Maughan, D. Burkhoff, and K. Sagawa, "Left ventricular interaction with arterial load studied in isolated canine ventricle," *American Journal of Physiology-Heart and Circulatory Physiology*, vol. 245, no. 5, pp. H773–H780, 1983.

[15] M. A. Gaballa, T. E. Raya, and S. Goldman, "Large artery remodeling after myocardial infarction," *American Journal of Physiology-Heart and Circulatory Physiology*, vol. 268, no. 5, pp. H2092–H2103, 1995.

[16] P. Mulder, P. Compagnon, B. Devaux et al., "Response of large and small vessels to alpha and beta adrenoceptor stimulation in heart failure: effect of angiotensin converting enzyme inhibition," *Fundamental & Clinical Pharmacology*, vol. 11, no. 3, pp. 221–230, 1997.

[17] F. R. M. Stassen, G. E. Fazzi, P. J. A. Leenders, J. F. M. Smits, and J. G. R. De Mey, "Coronary arterial hyperreactivity and mesenteric arterial hyporeactivity after myocardial infarction in the rat," *Journal of Cardiovascular Pharmacology*, vol. 29, no. 6, pp. 780–788, 1997.

[18] F. R. M. Stassen, M. J. J. M. F. Willemsen, G. M. J. Janssen et al., "Reduced responsiveness of rat mesenteric resistance artery smooth muscle to phenylephrine and calcium following myocardial infarction," *British Journal of Pharmacology*, vol. 120, no. 8, pp. 1505–1512, 1997.

[19] S. Heeneman, P. J. A. Leenders, P. J. J. W. Aarts, J. F. M. Smits, J. W. Arends, and M. J. A. P. Daemen, "Peripheral vascular alterations during experimental heart failure in the rat," *Arteriosclerosis, Thrombosis, and Vascular Biology*, vol. 15, no. 9, pp. 1503–1511, 1995.

[20] X. H. Yu, Z. B. Tang, L. J. Liu et al., "Apelin and its receptor APJ in cardiovascular diseases," *Clinica Chimica Acta*, vol. 428, pp. 1–8, 2014.

[21] M. F. Berry, T. J. Pirolli, V. Jayasankar et al., "Apelin has in vivo inotropic effects on normal and failing hearts," *Circulation*, vol. 110, no. 11, Supplement 1, pp. II187–II193, 2004.

[22] Á. Perjés, R. Skoumal, O. Tenhunen et al., "Apelin increases cardiac contractility via protein kinase Cε- and extracellular signal-regulated kinase-dependent mechanisms," *PLoS One*, vol. 9, no. 4, article e93473, 2014.

[23] Y. Azizi, M. Faghihi, A. Imani, M. Roghani, and A. Nazari, "Post-infarct treatment with [Pyr1]-apelin-13 reduces myocardial damage through reduction of oxidative injury and nitric oxide enhancement in the rat model of myocardial infarction," *Peptides*, vol. 46, pp. 76–82, 2013.

[24] J. Liu, M. Liu, and L. Chen, "Novel pathogenesis: regulation of apoptosis by apelin/APJ system," *Acta Biochimica et Biophysica Sinica*, vol. 49, no. 6, pp. 471–478, 2017.

[25] W. Zhao, J. H. Choi, G. R. Hong, and M. A. Vannan, "Left ventricular relaxation," *Heart Failure Clinics*, vol. 4, no. 1, pp. 37–46, 2008.

[26] C. H. Conrad, W. W. Brooks, J. A. Hayes, S. Sen, K. G. Robinson, and O. H. L. Bing, "Myocardial fibrosis and stiffness with hypertrophy and heart failure in the spontaneously hypertensive rat," *Circulation*, vol. 91, no. 1, pp. 161–170, 1995.

[27] P. Knaapen, T. Germans, J. Knuuti et al., "Myocardial energetics and efficiency: current status of the noninvasive approach," *Circulation*, vol. 115, no. 7, pp. 918–927, 2007.

[28] D. A. Kass and R. P. Kelly, "Ventriculo-arterial coupling: concepts, assumptions, and applications," *Annals of Biomedical Engineering*, vol. 20, no. 1, pp. 41–62, 1992.

[29] I. Ahmet, M. Krawczyk, P. Heller, C. Moon, E. G. Lakatta, and M. I. Talan, "Beneficial effects of chronic pharmacological manipulation of β-adrenoreceptor subtype signaling in rodent dilated ischemic cardiomyopathy," *Circulation*, vol. 110, no. 9, pp. 1083–1090, 2004.

[30] H. Suga, "Cardiac energetics: from E(max) to pressure-volume area," *Clinical and Experimental Pharmacology & Physiology*, vol. 30, no. 8, pp. 580–585, 2003.

Hindawi
Disease Markers
Volume 2019, Article ID 7583690, 14 pages
https://doi.org/10.1155/2019/7583690

Review Article

Biomarkers of Inflammation in Left Ventricular Diastolic Dysfunction

Mihaela Mocan,[1,2] **Larisa Diana Mocan Hognogi**,[1,3] **Florin Petru Anton**,[1,3] **Roxana Mihaela Chiorescu**,[1,3] **Cerasela Mihaela Goidescu**,[1,3] **Mirela Anca Stoia**,[1,3] **and Anca Daniela Farcas**[1,3]

[1]*"Iuliu Hatieganu" University of Medicine and Pharmacy, Department of Internal Medicine, Cluj-Napoca, Romania*
[2]*Emergency Clinical County Hospital, Department of Internal Medicine, Cluj-Napoca, Romania*
[3]*Emergency Clinical County Hospital, Department of Cardiology, Cluj-Napoca, Romania*

Correspondence should be addressed to Larisa Diana Mocan Hognogi; dyi_larisa@yahoo.com

Received 22 February 2019; Revised 21 April 2019; Accepted 7 May 2019; Published 2 June 2019

Guest Editor: Agata M. Bielecka-Dabrowa

Left ventricular diastolic dysfunction (LVDD) is an important precursor to many different cardiovascular diseases. Diastolic abnormalities have been studied extensively in the past decade, and it has been confirmed that one of the mechanisms leading to heart failure is a chronic, low-grade inflammatory reaction. The triggers are classical cardiovascular risk factors, grouped under the name of metabolic syndrome (MetS), or other systemic diseases that have an inflammatory substrate such as chronic obstructive pulmonary disease. The triggers could induce myocardial apoptosis and reduce ventricular wall compliance through the release of cytokines by multiple pathways such as (1) immune reaction, (2) prolonged cell hypoxemia, or (3) excessive activation of neuroendocrine and autonomic nerve function disorder. The systemic proinflammatory state causes coronary microvascular endothelial inflammation which reduces nitric oxide bioavailability, cyclic guanosine monophosphate content, and protein kinase G (PKG) activity in adjacent cardiomyocytes favoring hypertrophy development and increases resting tension. So far, it has been found that inflammatory cytokines associated with the heart failure mechanism include TNF-α, IL-6, IL-8, IL-10, IL-1α, IL-1β, IL-2, TGF-β, and IFN-γ. Some of them could be used as diagnosis biomarkers. The present review aims at discussing the inflammatory mechanisms behind diastolic dysfunction and their triggering conditions, cytokines, and possible future inflammatory biomarkers useful for diagnosis.

1. Introduction

Left ventricular diastolic dysfunction (LVDD) is a preclinical condition defined as the inability of LV to fill an adequate end-diastolic volume (preload volume) at an acceptable pressure [1]. LVDD is an important precursor to many different cardiovascular diseases. It represents the dominant mechanism (2/3 of patients) in the development of heart failure (HF) with preserved ejection fraction (HFpEF), which shows a rising prevalence in older population (by 2020, more than 8% of people over 65 are estimated to have HFpEF) and is associated with a poor prognosis [2]. Diastolic abnormalities have been studied extensively in the past decade, and it has been confirmed that chronic low-grade inflammatory reaction is the key mechanism leading to HF [3].

A new paradigm of LVDD development was recently proposed. Classical cardiovascular risk factors, grouped under the name of metabolic syndrome (MetS), or other systemic diseases that have an inflammatory substrate such as chronic obstructive pulmonary disease (COPD), atrial fibrillation (AF), anemia, or chronic kidney disease (CKD) induce myocardial structural and functional abnormalities through low-grade systemic and endothelial inflammation (IF). IF triggers oxidative stress (OS) cascade in the coronary microvascular endothelial cells and reduces nitric oxide (NO) bioavailability in the myocardial cells. Following NO decreased

availability, myocardial cyclic guanosine monophosphate-(cGMP-) protein kinase G (PKG) signaling is reduced, causing maladaptive hypertrophy and increased cardiomyocyte stiffness [4].

The newly published joined European and American guidelines underline the diagnosis difficulties of LVDD [5], as echocardiographic measurements are considered partly nonsensitive or inconclusive [6]. Therefore, it is of utmost importance to find biomarkers and risk scores that enable us to have an early diagnosis and enhance the prognosis of HF patients.

Baring these in mind, the present review aims at discussing the inflammatory mechanisms behind LVDD and their triggering conditions, cytokines, and possible future inflammatory biomarkers useful for diagnosis.

2. Pathological Mechanisms of Left Diastolic Dysfunction

The diastole is the part of the cardiac cycle that includes the isovolumetric relaxation phase and the filling phases and has passive and active components. The filling of the LV is divided into rapid filling during early diastole, diastasis, and rapid contraction phase during the late contraction phase. LVDD can be the consequence of abnormalities during any phase of the diastole. Thus, impaired relaxation, high filling pressure, increased LV operating stiffness, mechanical asynchronism, increased peripheral artery stiffness, and the loss of atrial contraction at higher heart rates are just some of the underlying mechanisms in LVDD [7].

Patients with LVDD are generally older, more often female, and have a high prevalence of CVD and other morbid conditions, such as obesity, metabolic syndrome, diabetes mellitus type 2, salt-sensitive hypertension, atrial fibrillation, COPD, anemia, and/or renal dysfunction. Each one of these pathologies were proved to be linked to LVDD and could lead to LVDD through different pathways.

The incidence of LVDD associated to HFpEF is increasing with *global aging*. LVDD, left atrial remodeling, and cardiac fibrosis along with vascular changes such as endothelial dysfunction, arterial stiffening, and vascular IF are all the attributes of the advanced age [8]. The effect of aging on ECM was nicely synthesised by Meschiari et al. [9]. In brief, senescence modifications of the cardiovascular system increase afterload and impair vasodilation, which increases LV's wall stress leading to cardiomyocyte hypertrophy. Hypertrophic cardiomyocytes have increased oxygen needs, and the imbalance between supply and demand of oxygen favors reactive oxygen species (ROS) production with toxic effect on cardiomyocytes. In response to hypoxemia, cardiomyocytes release proinflammatory cytokines and chemokines promoting IF and recruiting macrophage in the LV [10]. Macrophages are a rich source of matrix metalloproteinases (MMP) which are linked to myocardial aging status and LVDD. Moreover, aging favors amyloid deposit in LV, which increases myocardial thickening, described as senile amyloidosis. The possible mechanism is still under debate but may be linked to posttranscriptional biochemical alterations of transthyretin or its chaperones [11].

Metabolic syndrome (*MetS*) has been associated with LVDD with preserved systolic function. With cardiovascular risk factors clustered in the MetS, as triggers, IF favors pathological changes in the myocardium leading to relaxation abnormalities [12].

The key mechanism responsible for LVDD in MetS patients is not entirely understood. In animal models with diet-provoked MetS, the hypertrophy and fibrosis of the myocardial cells were caused by accelerated OS. In mouse models of dyslipidemia, high blood pressure, or insulin resistance IF, along with endothelial dysfunction played an important role in the development of cardiac fibrosis and increased myocardial stiffness [13].

In previous studies, our group demonstrated that IF biomarkers have a good predictive potential for LVDD [14, 15] showing a strong association between LVDD and IL-6 levels, independent of MetS components and NT-proBNP. Thus, IL-6 could be useful in identifying asymptomatic patients with MetS and LVDD and applying lifestyle measures to prevent overt heart failure development. Others have reported an association between IF biomarkers and LVDD in patients with symptomatic heart failure [16], and studies on animal models showed that pathological elevations of IL-6 [5] result in extensive cardiac fibrosis, by regulating cell function through a cell surface receptor. Our results come to add knowledge to this two-step model of LVDD in MetS patients by pointing out IL-6 as the IF biomarker with the best predictive capacity for LVDD.

The systemic proinflammatory state present in *chronic obstructive pulmonary disease* (*COPD*) patients might contribute to vascular and myocardial abnormalities leading to an increased risk of cardiovascular morbidity, especially during acute exacerbations. López-Sánchez et al. demonstrated that a systemic inflammatory pattern characterized by increasing IL-6 and CRP was associated with LVDD in a homogeneous population of severe stable COPD patients [6]. Development of LV alterations manifested through LVDD is found in more than 90% of the subgroup of severe COPD patients, independently of age and the presence of systemic hypertension [7]. The IF was present, mostly in sedentary and obese patients, and could be more closely related to obesity or lower physical activity than to the degree of airway obstruction. On the other hand, extracellular matrix (ECM) proteins such as MMP can act as IF stimuli by modulating the proinflammatory response of the heart, synthetizing cytokines and growth factors. In patients with myocardial injuries such as ischemia, myocarditis, and advanced heart failure, tenascin-C (Tn-C), an ECM glycoprotein, was transiently expressed in myocardial tissue, in association with immediate tissue repair response and the final deposit of collagen in the damaged tissue [17].

The role of *chronic kidney disease* (CKD) in the development of LVDD was elegantly summarized recently by ter Maaten et al. [18]. In brief, CKD causes metabolic and systemic abnormalities in circulating factors, inducing an activated systemic IF (CRP, TNF-α, IL-6, sST2, and pentraxin-3) and microvascular dysfunction (favored by chemokines, adhesion molecules, and cytokines), which may lead to cardiomyocyte stiffening, hypertrophy, and interstitial

fibrosis via cross-linking between the microvascular and cardiomyocyte compartments [19]. As for common biomarkers, galectin-3 has proved its utility in identifying both early CKD [20] and incident cardiac fibrosis [21].

A high prevalence of *atrial fibrillation* (AF) in association with LVDD and HFpEF (up to 60%) is reported by numerous studies (CHARM programme, ADHERE Core, and SwedeHF) [22, 23]. This could potentially be explained by shared pathological conditions (MetS, obesity, hypertension, coronary artery diseases, and atrial myocardial injury) promoting low-grade systemic IF and leading to simultaneous development of AF and LVDD [24]. The same mediator molecules are found in both AF and LVDD: CRP, TNF-α, IL-6, IL-8, IL-10, IL-1α, IL-1β, IL-2, TGF-β, and IFN-γ, along with MMP and ROS [19].

Several neurohormonal and mechanistic hypotheses have been proposed for the IF-LVDD continuum: (1) the activation of the renin-angiotensin-aldosterone system (RAAS) stimulating the production of proinflammatory cytokines (such as IL-6, IL-8, and TNF-α), directly activating immune cells and increasing the expression of adhesion molecules such as vascular cell adhesion protein 1, intercellular adhesion molecule 1, selectins, or MCP-1 and (2) elevated LV diastolic pressure might induce cardiac apoptosis, and OS, which can subsequently induce regional IF thereby increasing production of IL-1, IL-6, and TNF-α [19].

The neurohormonal hypothesis of RAAS activating OS was verified by Negi et al. in a well-performed clinical study [25], trying to explain the negative results from RAAS inhibitor therapy in HFpEF patients. The authors found that HFpEF was not associated with RAAS activation or systemic OS [25]. On the other hand, preclinical studies showed that angiotensin-II induces mitochondrial dysfunction, OS, reducing eNOS bioavailability and impairing myocardial relaxation [26]. Some possible explanations are available so far. First of all, OS may take place only in the affected myocardium (OS "signaling is compartmentalized") explaining the absence of systemic OS markers in patients with HFpEF [27]. Secondly, OS in the myocardium may appear earlier than systemic OS. At last, other mechanism may be responsible of LVDD progression, given the polymorphism of etiological and trigger factors.

The *activation of mineralocorticoid receptors* through aldosterone may be an important factor in the pathogenesis of HFpEF through multiple mechanisms such as cardiac fibrosis or endothelial dysfunction [1, 28]. In this respect, mineralocorticoid receptor agonists (MRA) have been studied in patients with HFpEF or ischemic HFpEF (after myocardial infarction). Although in some of the studies MRA failed to improve mortality in HFpEF (such as the TOPCAT trial), others showed that MRA could improve LVDD and reduce cardiac remodeling having positive impact on the quality of life. These studies were analyzed by Chen et al. [29] in an extensive meta-analysis which concluded that "MRA treatment may exert beneficial effects, including reduced hospitalizations due to HFpEF, improved life quality and diastolic function, and cardiac remodeling reversal, without an effect on all-cause mortality." These are indirect evidence that RAAS is implicated in pathogenesis of LVDD and HFpEF.

Another mechanism proposed in LVDD was myocardial *microvascular dysfunction* [30]. Mohammed et al. performed in 124 myocardial autopsy specimens of patients with HFpEF. The authors found out that microvascular density and myocardial fibrosis are more frequent in patients with HFpEF and are not related to the severity of epicardial coronary stenosis, supporting the hypothesis of microvascular endothelium IF in LVDD pathogenesis. Moreover, there was an inverse relation between fibrosis and microvessel density [31]. In this respect, Kato et al. conducted an imagistic study (cardiac magnetic resonance (CMR)) and calculated the coronary flow reserve (CFR) in hypertensive patients with LVDD. They proved that CFR was decreased in these patients and correlated significantly with NT-proBNP values. Both pathological and imagistic data indicate that myocardial microvascular impairment might contribute to the development and progression of LVDD [32]. Despite the evidence of microvascular dysfunction, the therapy aiming vasodilation (*angiotensin-converting enzyme inhibitors*, *angiotensin-II receptor blockers*, and *phosphodiesterase-5 inhibitors*) that had had promising results in experimental studies yielded negative or neutral results in large clinical trials.

Thus, a meta-analysis of the clinical trials of *angiotensin-converting enzyme inhibitors and angiotensin-II receptor blockers* (CHARM-Preserved, I-Preserve, and PEP-CHF) showed no effect of these drugs on mortality or hospitalization rate in patients with HFpEF. The beta-blocker and spironolactone trials arrived at neutral conclusions [33]. The potential effects of *phosphodiesterase-5 inhibitors* were assessed in a randomized, double-blind, placebo-controlled clinical trial of 216 patients with stable HFpEF who showed no improvement in exercise capacity or clinical status, after 8 months [34].

With regard to *molecular basis* of LVDD, the data about IF are scarce. Westermann et al. investigated LVDD mechanisms by performing endomyocardial biopsy samples and analyzing the inflammatory cells and their inflammatory products, in vitro. The authors elegantly showed that CD3-, CD11a-, and CD45-marked inflammatory cells had higher concentrations in LVDD myocardial tissue as compared with controls. Moreover, the VCAM-1 adhesion molecule and TGF-β, along with oxygen radical production, were found to be increased in LVDD patients but with no significant change in serum concentration of CRP [3].

Any mechanism that interferes with actin-myosin cross-bridge detachment, intracellular changes in titin or microtubules, extracellular changes in collagen, and infiltration was proved to be responsible for LVDD [35].

Recent studies on both animal and human models showed that titin isoform shift, ROS, nitric oxide synthetase (NOS) dysfunction that results in decreased nitric oxide (NO), and myosin-binding protein C (MyBP-C) are implicated in LVDD [35]. Increased titin N2B isoform expression and the reduced phosphorylation of titin were linked to elevated cardiomyocyte stiffness in endomyocardial biopsy samples of patients with LVDD [2]. ROS resulted from OS, and *advance glycation end products* cause LVDD in diabetic

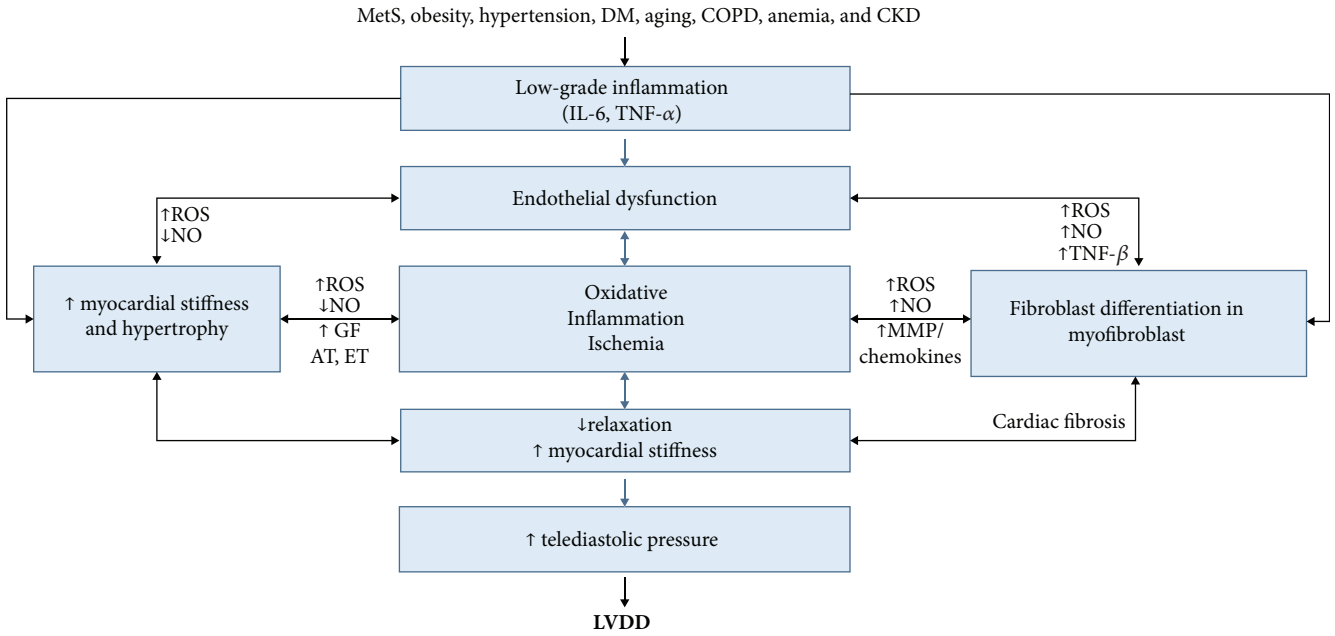

Figure 1: Scheme showing the interrelation between trigger conditions and LVDD via systemic IF (adapted after von Bibra et al. [52]). IL-6: interleukin-6; hsCRP: high-sensitivity C reactive protein; ROS: reactive oxygen species; NO: nitric oxide; MMP: matrix metalloproteinases; GF: growth factors; AT: angiotensin; ET: endothelin; TNF-β: tumor necrosis factor beta.

patients [36]. Jeong et al. showed in an experimental mouse model that high-fat diet leads to mitochondrial ROS production and LVDD through insulin resistance and glucose intolerance. The mitochondria-targeted antioxidant administration to the high-fat diet mouse model prevented LVDD development and progression [37]. This study proved that mitochondrial OS actively participates to development and progression of LVDD, and its inhibition represents a potential therapy target. In this same study, low-carb diet or glycemic control was unable to reverse LVDD [38].

In clinical settings, a meta-analysis showed an obvious trend of reduction in mortality rates in *HMGCoA reductase inhibitor* users from 2005 to 2013, as a consequence of their pleiotropic and antioxidant effects [39], supporting the hypothesis that HMGCoA reductase inhibitors may improve survival in HFpEF [40].

Advanced glycation end products (AGEs) result from glucose interactions with proteins via nonenzymatic ways and accumulate in a variety of pathological conditions such as hypertension or diabetes mellitus [41]. AGE accumulation in the myocardium was found in patients with diabetes mellitus [42]. Serum concentrations of some AGE might be predictive for mortality and hospitalization rates in HFpEF patients [41]. Thus, AGE became a potential therapeutic target. Alagebrium is a cross-link breaker that showed promising results in small studies but discouraging conclusions in larger ones [43].

NOS is an important modulator of cardiac nitroso-redox balance and function. Uncoupled NOS in hypertensive mouse models results in decrease in NO that are consistent with increased cytosolic calcium and LVDD [44]. In human studies, G894T polymorphism of the eNOS gene and MetS was related to arterial stiffness and can be a connection pathway between MetS and the increased cardiovascular risk [45]. Finally, *MyBP-C* is a thick protein localized in the striated muscle sarcomeres, and it plays an important role in cardiac contraction and relaxation. Experimental studies showed that phosphorylation of MyBP-C leads to impaired cardiac muscle contraction and subsequent LVDD [36]. Further, cMyBP-C decrease LV remodeling in response to pressure overload [46]. Thoonen et al. identified MyBP-C as a cGMP-dependent protein kinase I leucine zipper (PKGIα LZ) binding partner and kinase substrate, with great importance for the possible therapeutic targets in HFpEF [47]. The experimental study of Jeong et al. showed that preventing glutathionylation of MyBP-C using cofactor tetrahydrobiopterin ameliorates diastolic dysfunction through reversing changes of myofilaments [48]. These data "provide evidence that cardiac relaxation could be modified by posttranslational changes of myofilament proteins." In clinical studies, MyBP-C had both diagnosis and prognosis properties in patients with HFpEF. Tong et al. observed that cMyBP-C is a potential screening biomarker for the existence of severe cardiovascular diseases [49]. Jeong et al. considered it as a novel biomarker in HF patients, with the capacity to discriminate between HFpEF, having higher values than in HFrEF (4.02 ± 1.4 vs. 2.01 ± 0.61) [50].

At last, fibroblasts differentiate into myofibroblasts and secrete collagen into ECM. Shifts in the collagen type (from type III to type I) could impair the cardiac biomechanism by contributing to increased LV stiffness [9]. These mechanisms are synthetized in Figure 1.

Given these data, we can state that IF is an important link in the pathogenesis of LVDD, and thus, it is conceivable that treatments targeting IF will require the development of new treatment modalities in patients with LVDD. Studies using

targeted immunomodulating therapy in HF were elegantly reviewed by [51].

3. Inflammatory Biomarkers for Diastolic Dysfunction

In this pathological chain, activation of persistent immune response is currently considered to stay at the origin of inflammatory cytokine secretion. In LVDD with or without HFpEF, the current hypothesis is that the associated conditions (described above) are the triggers to immune reaction with the production of a vast amount of proinflammatory cytokines. These cytokines could be a measurement of the risk of LVDD development rather than quantification of severity [53]. In HF patients, on the other hand, IF biomarkers are closely associated with pathogenesis, poor functional state, and adverse prognosis.

Natriuretic peptides, especially N-terminal pro-BNP (NT-proBNP), have been extensively studied as a diagnosis biomarker of HFpEF, showing lower cut-off values than those in HFrEF [54]. In the ESC guideline (2016) for the diagnosis of HFpEF, along with echocardiographic criteria, the elevations in BNP or NT-proBNP are recommended for the identification of elevated LV filling pressures. Moreover, the guideline stipulates that "the negative predictive values are very similar and high (94-98%) in both the nonacute and acute settings, but the positive predictive values are lower both in the nonacute setting (44-57%) and in the acute setting (66-67%)." To this point, the ESC's guidelines recommend that the diagnosis of HFpEF should be based on structural and Doppler findings of LVDD, and elevated NT-proBNP should be used to rule out HF [55]. Even though, at the moment, NT-proBNP represents a standard biomarker for HFpEF, one can only wonder whether it is trustful enough for the positive diagnosis in HFpEF. The initial results from the large registries such as DIAST-CHF (Diastolic Congestive Heart Failure) which showed a sensitivity of 65% for the diagnosis of HFpEF only increased mistrust and stimulate the search for other biomarkers to increase diagnostic accuracy [56]. In contrast to brain natriuretic peptides, inflammatory biomarkers used independently or associated with multimarker scores raise high expectations both for positive diagnosis and prognosis of HFpEF [4, 57].

Proinflammatory cytokines involved in LVDD (both with and without HFpEF) are interleukins (IL-6, IL-8, IL-10, IL-11, IL-1α, IL-1β, and IL-2), tumoral necrosis factors (TNF-α, TGF-β), and interferon (IFN-γ). Other biomarkers quantifying IF in LVDD are MCP-1, galectin-3, sST2, and GDF-15.

3.1. CRP, IL-6, IL-8, IL-11, and TNF-α. CRP, TNF-α, and IL-6 were among the first to be described as having multiple sites of action both on the vascular endothelium and at the myocyte level, where they enhance apoptosis, inducing hypertrophy or dilation [53]. Additionally, cytokine levels in LVDD are the result of a complex dysregulation of the cytokine. This could include activation of mediators involved in both IF and myocardial fibrosis such as IL-6, as well as a lack of overall regulation of the immune response by impaired function of regulatory T cells [51].

CRP is considered a biomarker of diagnosis and severity rather than a key player in LVDD. Michowitz et al. showed that hsCRP was higher in patients with LVDD and HFpEF, as compared with healthy patients. Moreover, in these patients, levels of hsCRP correlated with NYHA class (and therefore the severity of HFpEF), and the main predictors of hsCRP levels are NYHA class and diabetes mellitus [58]. In the study performed by our group, hsCRP proved to be a predictive marker for LVDD in MetS patients [14].

IL-6 is playing a central role in IF initiation and progression in cardiovascular diseases [59]. IL-6 infusion in rats results in LV hypertrophy, increased collagen volume fraction, and increased myocardial stiffness. Studies have shown that IL-6 could be linked to the increased number of major cardiac events and cardiomyocyte hypoxic stress [60]. In our study, IL-6 proved to be an independent predictive biomarker for LVDD in MetS patients [14]. IL-6 and hsCRP proved to be biomarkers of prognosis in MetS associated with LVDD [61]. Moreover, increased levels of IL-6 correlate with the severity of HF and are strongly prognostic of 1-year mortality [62].

IL-8 has been demonstrated to increase the expression and production of osteopontin, which stimulates interstitial fibrosis, and TGF-β, which stimulates collagen synthesis, and inhibit matrix degradation by reducing MMP. Collier et al. have shown that IL-8 and MCP-1 [57] also play a role in the development and worsening of LVDD as it has been shown in different studies [63].

IL-11 has pleomorphic actions and is capable of upregulating or downregulating inflammatory processes according to different states of the microenvironment [64]. One of the mechanisms through which IF induces LVDD is fibrosis. This is a common process in the pathology of cardiovascular disease, and it seems that IL-11 targets cardiac myocytes thorough pathways that could either protect or be deleterious for them. Also, research has shown that fibroblasts express IL-11 required for the synthesis of fibrogenic proteins. Research has shown that fibroblast expressing IL-11 was responsible for fibrosis, but deletion of IL-11RA$_1$ provided protection against this condition [65]. Aside from the effect on myocardial fibrosis, the other pathways through which it acts are still unknown and under research.

A study which observed patients with CAD showed that IL-11 was mainly secreted by macrophages and may be related to cardiac atherosclerotic disease initiation and progress, being found in high concentration in plasma and aorta of patients with aortic dissection [66]. If we focus on the effects of IL-11 on patients with HF, studies have shown that its plasma concentrations are significantly increased and related to the severity of HF and to the number of cardiovascular events. Furthermore, bearing in mind its protective effects, IL-11 might become a new target for the therapy and prevention in HF patients [64].

TNF-α induces myocardial apoptosis and myocardial stiffness, playing a major role in the progression of LVDD. The myocardial apoptosis is a consequence of activating p38 mitogen-activated protein kinase, stimulating iNOS to transform NO to ONOO-, and of increased ROS synthesis. Myocardial stiffness is aggravated by the imbalance of

MMP activity, with an increased ratio of MMP/TIMP and changes in collagen fibers, favored by TNF-α secretion [67]. The increased production and reduced degradation of collagen and increased activation of lysyl oxidase-1, resulting in a cross-linked and insoluble collagen network, may in turn result in LVDD. In another study performed by our group, LVDD in coronary disease patients did not show a good correlation with TNF-α levels but with leptin levels [68]. TNF-α was reported to have both an involvement in cardiac dysfunction and a protective effect on ischemic myocardium. The expression of the two TNF-α receptors might be responsible for TNF-α conflicting actions, and ischemic myocardium remodeling is a consequence of the balance between TNF-α actions [68]. Dunlay et al. in the Olmsted County study found that mortality in HF patients is directly correlated with TNF-α and not influenced by EF value [69]. Thus, TNF-α could be useful for the prognosis of LVDD. TNF-α receptors (sTNFR1 and sTNFR2) were found to be higher in HFpEF patients [51].

Furthermore, assessing these cytokines in large populations of well-characterized patients may provide insight information regarding the pathophysiology of LVDD. Unfortunately, cytokines circulate at low levels, thus requiring high-sensitivity assays and large population studies, which represents the main disadvantage of using them as biomarkers for LVDD. More reliable biomarkers could be the corresponding soluble receptors of soluble ligands which are frequently detected in high concentrations in serum and plasma [51].

3.2. Pentraxin-3. Pentraxin-3 belongs to a superfamily of proteins together with CRP and serum amyloid-associated protein, but it differs from the latter through the monomer constitute. Pentraxin-3 has five long monomers, and their role is primarily at the interface of the immune system IF and ECM [70]. There are several types of cells that produce pentraxin-3: immune system cells such as mononuclear cells and neutrophils and also adipocytes, fibroblasts, and smooth muscle cells. In one study they conducted, Matsubara et al. proved that pentraxin-3 is produced in the coronary circulation in patients with LVDD. When they compared patients with HFpEF to healthy individuals, they found a direct and positive correlation between pentraxin-3 and LVDD. Pentraxin-3 was produced in the coronary circulation in patients with LVDD. Furthermore, pentraxin-3 levels were higher than those of hsCRP, IL-6, or TNF-α levels in patients with LVDD [71]. Even though pentraxin-3 proved to be a good diagnosis biomarker, assessing pentraxin-3 in relation to LVDD prognosis was not established until recently. The same group showed that high plasma pentraxin-3 levels, but not other inflammatory markers, are correlated with future cardiovascular events in patients with HFpEF. The authors concluded that pentraxin-3 may be a useful biomarker for assessment of risk stratification in HFpEF [72]. The impossibility of this biomarker to distinguish HFpEF of HFrEF is an important pitfall.

3.3. MCP-1. Monocyte chemoattractant protein 1 (MCP-1) has been shown in animal studies to be required for macrophage infiltration, the induction of TGF-β and the development of reactive fibrosis, and LVDD progression [73]. Cardiomyocyte-targeted expression of MCP-1 in mice caused death by heart failure at 6 months of age. MCP-induced protein expression increased in parallel with the development of ventricular dysfunction. In situ hybridization showed that the presence of MCP-induced protein transcripts in the cardiomyocytes was associated with apoptosis [74]. MCP-1 could be a potential therapeutic target as gene therapy with an MCP-1 antagonist was recently found to attenuate the development of ventricular remodeling in a mouse model for ischemic HF [51].

In human studies, MCP-1 was increased, along with other IF biomarkers (IL-6, IL-8) in hypertensive patients with LVDD, without proving to be an independent diagnosis marker or prognosis factor [57]. Additional research in ischemic HF patients showed that both lower and higher MCP-1 levels are associated with an increased risk of all-cause and cardiovascular mortality [75], but further research is need to confirm these findings.

3.4. Galectin-3. Galectin-3 is a beta-galactosidase binding lectin, with a wide variety of biological functions in IF, immunity, and cancer. It has recently been proposed to be a novel biomarker of LVDD. It was found to be involved in cell adhesion, growth, and differentiation, but also, it is involved in the process of fibroblast activation with known chemoattractant and proapoptotic roles [51].

The axis galectin-3/cardiotrophin-1 (Gal-3/CT-1) was found to be one of the mechanisms through which these properties are manifested. Martínez-Martínez et al. found in a study completed on Wistar rats that once treated with CT-1, they presented a higher cardiac Gal-3 level and a higher degree of myocardial fibrosis and also perivascular fibrosis. They concluded that an elevation of both molecules in HF patients could mean higher cardiovascular mortality and that the axes CT-1/Gal-3 might become a therapeutic target and also a HF biomarker [76]. Other data suggests that Gal-3 could also enhance a pathway through myocardial fibrosis, by activating RAAS. This might have therapeutic aim in the near future [77].

In HF patients, Gal-3 may be a biomarker of poor prognosis related to excessive and potentially irreversible myocardial fibrosis, which again may be related to enhanced IF. In this respect, a comprehensive review about the predictive value of Gal-3 was written by Coburn et al., in 2014 [77]. In brief, Gal-3 was repeatedly shown to be elevated in the setting of IF processes underlying HF and proved to be a better prognosis biomarker in HF than other conventional IF markers currently in use, such as natriuretic peptides or hsCRP. Besides that, it is worth mentioning that De Boer et al. showed that predictive value of Gal-3 appeared to be stronger in patients with HFpEF and correlated with echocardiographic measurements of LVDD [78]. Recently, van Vark et al. in the TRIUMPH (Translational Initiative on Unique and Novel Strategies for Management of Patients with Heart Failure) clinical cohort study, composed of 496 acute HF patients, evaluated the levels of circulating Gal-3. Elevated circulating Gal-3 appeared to be a strong predictor of outcome in acute HF patients, independent

of N-terminal probrain natriuretic peptide. Hence, galectin-3 may be helpful in the clinical practice for prognostication and treatment monitoring [79].

3.5. Soluble ST2. ST2 is a part of the IL-1 receptor family with an important role in regulating IF and immunity. This protein has two isoforms—ST2L which is a receptor and sST2 which responds to myocardial stretching in relation to elevation of filling pressure. When IL-33 binds to sST2-L, it produces a cascade of events that prevent the progression of myocardial hypertrophy and fibrosis. But in contrast, circulating plasma sST2 limits this binding, therefore promoting alterations in the myocardial structure [80]. Given the apparent contribution of static and pulsatile hemodynamic overload to the pathophysiology of LVDD, sST2 may be a particularly relevant marker of diagnosis, disease progression, and prognosis [54].

Our group showed, recently, a positive and strong correlation between the LV mass and severity of LVDD and the plasma level of sST2, in hypertensive patients with LV hypertrophy. The pathogenic hypothesis in this case is that sST2 might be also produced by the vascular endothelial cells as a consequence to the diastolic load. Another interesting observation is that the increased plasma level of ST2 performed better in predicting LV hypertrophy in hypertensive patients, than NT-proBNP [81]. Moreover, ST2 levels were correlated with the risk of adverse cardiovascular outcome in hypertensive patients with LVDD and increased filling pressure and may represent a useful prognostic marker in these patients [82]. The studies regarding sST2 predictive capacity in HF have been elegantly synthetized by Dattagupta and Immaneni [83], by Bayés-Genís et al. [84], and very recently by Dieplinger and Mueller [85]. In summary, there are large studies such as the Pro-BNP Investigation of Dyspnea in the Emergency Department (PRIDE) study, PROTECT study, SHOP study, and Val-HEFT study showing that ST2 values predict prognosis in chronic HF patients and over time were significantly and independently associated with mortality [83]. ST2 has been recently added in the American College of Cardiology/American Heart Association guidelines with a class II indication for the prognosis in HF [86].

As LVDD and HFpEF are a complex syndrome, only one biomarker is not enough for the diagnosis and prognosis. Thus, a HF risk calculator has been recently developed, the Barcelona bioHF, which comprises sST2 along with brain natriuretic peptide and troponin, to stratify the mortality risk and hospitalization within 5 years. Another score focusing on remodeling and sudden death in HF patients is the ST2-R2 score, which includes sST2 along with several other clinical parameters and which has a high accuracy in predicting reverse remodeling of LVDD [84]. Unfortunately, the aspect of how determining sST2 correlates with LVDD and HFpEF in order to become a diagnosis or prognostic biomarker is still not entirely known. However, ST2 levels appeared to be lower in decompensated HFrEF than in HFpEF, even though not related to 1-year mortality [87].

3.6. GDF-15. Growth differentiation factor 15 (GDF-15) was first named macrophage inhibitory cytokine-1 and is a member of the TGF-β cytokine superfamily which links it to IF, increased filling pressures, and tissue injury [88]. Under normal, physiological conditions, this hormone is underexpressed, but ischemia-reperfusion injury, oxygen reactive species, and pressure overload upregulate its production. Apparently, GDF-15 plays a protective role in the above conditions by inhibiting apoptosis, hypertrophy, and adverse remodeling via PI3K-Akt, ERK1/2, and SMAD 2/3, thus having a positive impact on the fractional shortening [89]. HF is a condition that was found to be in association with plasma levels of this biomarker, especially in patients with ischemic heart disease [90].

Besides diagnostic capacity, GDF-15 might have screening capacity for unmasking the risk of developing LVDD in a healthy elderly and increasing diagnosis accuracy of asymptomatic LVDD [91]. Thus, Stahrenberg et al. demonstrated that GDF-15 has similar concentrations in both HFpEF and HFrEF. It is independently associated with exercise capacity impairment and quality of life in HFpEF. Diagnostic precision of GDF-15 is at least as good as natriuretic peptide, and the combining signification of NT-proBNP and GDF-15 could increase HFpEF diagnostic accuracy [92]. Moreover, Santhanakrishnan et al. revealed similar results in an Asian population, concluding that GDF-15 distinguished HFpEF patients at least as well as NT-proBNP and the combination of both the biomarkers, providing a useful screening and diagnosis tool for LVDD [93]. Later on, Chan et al. performed a similar study on a large Asian population—Singapore Heart Failure Outcomes and Phenotypes (SHOP) study—and proved that GDF-15, unlike NT-proBNP, was similarly elevated in both types of HF. Thus, GDF-15 has additional prognostic utility over NT-proBNP and hsTnT in both HFpEF and HFrEF. Moreover, serial measurements of GDF-15 provided additional predictive information for outcomes, making GDF-15 a reliable prognosis and risk stratification biomarker [94].

The information regarding novel IF biomarkers in LVDD or HFpEF are synthetized in Table 1. Unfortunately, most studies have sought for prognosis biomarkers in HF rather than diagnosis biomarkers for LVDD; thus, the information regarding specificity and sensibility for the diagnosis of LVDD or HFpEF is not available in all the cited studies. Some authors focused on the correlation between IF biomarker concentrations and echocardiographic criteria for LVDD, while others sought the differences between HFrEF and HFpEF. Moreover, some of the cited studies have small sample size and lack full adjustment. Furthermore, some of the studied biomarkers are at low levels, thus increasing analytical variation and requiring expensive high-sensitivity assays that should be tested on large sample population. Larger trials are clearly needed to obtain pathophysiological information. A future meta-analysis of previous data regarding the diagnosis role of IF biomarkers in HFpEF could be of help to deconvolute markers of HF in general from markers of isolated LVDD.

4. Conclusions and Future Trends

LVDD or impaired ventricular relaxation is one of the multiple mechanisms underlying the complex syndrome of

Table 1: Novel inflammatory biomarkers for diagnosis and/or prognosis in LVDD and HFpEF.

Biomarker	Authors	Clinical study	Population (n)	Diagnosis biomarker	Prognosis biomarker
			Single marker		
CRP	Sciarretta et al. [95]		128	Correlated with LVMI and E/E'	
	Koller et al. [96]	LURIC study	459		HR: 1.32 (95% CI 1.08–1.62), CV mortality at 5 years
	Sinning et al. [97]	GHS study	5000	AUC 0.66 (95% CI: 0.61–0.71)	HR: 1.5 (95% CI: 1.3–1.7)
IL-6	DuBrock et al. [98]	RELAX study	214	Higher levels in LVDD	
	Haugen et al. [62]		72	Higher levels in LVDD	Cut – off value > 10 ng/L, 1-year mortality
	Mocan et al. [14]		72	AUC 0.73 (95% CI: 0.61–0.83)	
	Kloch et al. [99]	EPOGH study	303	Correlated with E' ($r = 0.039$)	
IL-8	Collier et al. [57]		275	Higher values in HFpEF hypertensive patients	
	Phelan et al. [100]		41	Higher levels with greater LVMI and LAVI	
TNF-α	Sciarretta et al. [95]		128	Correlated with LVMI and E/E'	
	Dunlay et al. [69]	Olmsted County study	486		HR: 2.10 (95% CI: 1.30–3.38)
Pentraxin-3	Matsubara et al. [71]		82	OR: 1.49 (95% CI: 1.11-1.98)	
MCP-1	Ding et al. [75]	Guangdong Coronary Artery Disease Cohort	1411		HR: 1.5-2.11 C-index +12,6%
Galectin-3	Shah et al. [101]	PRIDE study	115	Correlated with E/E' ($r = 0.035$)	
	De Boer et al. [78]	COACH study	592		HR: 1.97 (1.62–2.42), better for HFpEF than for HFrEF
	Edelmann et al. [102]	Aldo-DHF trial	422		HR: 3.319 (95% CI: 1.214-9.07), all-cause death or hospitalization at 6 or 12 months
Soluble ST2	Bartunek et al. [103]		163	ST2 mARN higher in LVDD, correlated with LVEDP	
	Shah et al. [104]		134	Correlated with E amplitude	
	Manzano-Fernández et al. [105]		447		Cut-off 0.35 ng/mL HR: 3.26 (95% CI: 1.50–7.05), prediction of 1-year mortality

Table 1: Continued.

Biomarker	Authors	Clinical study	Population (n)	Diagnosis biomarker	Prognosis biomarker
	Shah et al. [106]		387		HR: 2.85 (95% CI: 2.04–3.99), prediction of 1-year mortality
	Santhanakrishnan et al. [93]	SHOP study	151	Cut-off 26.47 ng/mL, AUC 0.662 (95% CI: 0.554–0.770) Se 70%, Sp 48% for HFpEF	
	Wang et al. [107]			Cut-off 13.5 ng/mL OR: 11.7 (95% CI: 2.9-47.4) for HFpEF	
	Anand et al. [108]	VAL-HEFT study	1650		Cut – off sST2 ≤ 33.2 ng/mL Cox logHR: 0.048 (0.031-0.065), 1-year mortality
	Sinning et al. [97]	GHS study	5000	AUC 0.62 (95% CI: 0.56–0.67)	HR: 1.4 (95% CI: 1.2–1.6)
	Farcas et al. [82]		76		OR: 2.43 (95% CI: 1.32-7.24) at baseline predicts the CV events for 1 year
	Farcas et al. [81]		88	Cut-off 28.14 ng/mL (Se 94.4%, Sp 69.1%) for LVDD Cut-off 14 04 ng/mL (Se 82.1%, Sp 53.8%) for LVH	AUC: 0.732 (95% CI: 0.613–0.850)
	Najjar et al. [109]		193		HR: 6.62 (95% CI: 1.04–42.28) for mortality or rehospitalization
	Stahrenberg et al. [92]		1935	Cut-off 1.16 ng/mL, AUC 0.891 (95% CI: 0.850-0.932)	
GDF-15	Santhanakrishnan et al. [93]	SHOP study	151	Cut-off 879 pg/mL (Se 92%, Sp 84%) Cut-off 1120 pg/mL (Sp 92%, Se 82%)	
	Sinning et al. [97]	GHS study	5000	AUC 0.79 (95% CI: 0.75–0.83)	HR: 1.7 (95% CI: 1.6–1.9)
	Chan et al. [94]	SHOP study	488		HR: 1.68 (95% CI: 1.15–2.45) CV events at 6 months
	Jeong et al. [50]			Higher values in HFpEF than in HFrEF (4.02 ± 1.4 vs. 2.01 ± 0.61)	
MyBP-C	Tong et al. [49]		158		Prestress cut-off 127 ng/mL, HR: 8.1 (95% CI: 1.09-60.09) Poststress cut-off 214 ng/mL, HR: 4.77 (95% CI: 1.75-12.98)

Table 1: Continued.

Biomarker	Authors	Clinical study	Population (n)	Diagnosis biomarker	Prognosis biomarker
			Multimarker score		
CRP+GDF-15+sST2/ NT-proBNP and GDF-15/NT-proBNP	Sinning et al. [97]	GHS study	5000	Discrimination between HFpEF and HFrEF	
NT-proBNP+GDF-15	Stahrenberg et al. [92]		1935	AUC 0.942 (0.912-0.972) GDF − 15 ≥ 1.16 ng/mL + NT − proBNP ≥ 200.7 ng/L (Se 56.6%, Sp 98.9%)	
	Chan et al. [94]		488	AUC: 0.891 (95% CI: 0.850-0.932) for GDF-15	HR: 1.68 (95% CI: 1.15–2.45), risk for composite outcome (mortality and rehospitalization)

AUC: area under the curve; CI: confidence interval; CRP: C reactive protein; CV: cardiovascular; EPOGH: European Project on Genes in Hypertension; GDF-15: growth differentiation factor 15; GHS: Gothenburg Heart Study; IL: interleukin; HFrEF: heart failure with reduced ejection fraction; HFpEF: heart failure with preserved ejection fraction; HR: hazard ratio; LAVI: left atrial volume index; LVDD: left ventricular diastolic dysfunction; LVED: left ventricular end-diastolic pressure; LVMI: left ventricular mass index; MCP-1: monocyte chemoattractant protein 1; MyBP-C: myosin-binding protein C; NT-proBNP: N-terminal probrain natriuretic peptide; OR: odds ratio; PRIDE: Pro-BNP Investigation of Dyspnea in the Emergency Department; RELAX: Phosphodiesterase-5 Inhibition to Improve Clinical Status and Exercise Capacity in Diastolic Heart Failure; SHOP: Singapore Heart Failure Outcomes and Phenotypes; TNF-α: tumor necrosis factor alpha; sST2: soluble ST2; VAL-HEFT: Valsartan Heart Failure Trial.

HFpEF. Multiple comorbidities are the triggers of LVDD progression to HFpEF. LVDD diagnosis is nowadays based solely on echocardiography, even though it is characterized by multiple pathogenic factors and is associated with a plethora of biomarkers. In the future, the association of these three diagnosis tools (clinical identification of comorbidities, echocardiography, and IF biomarkers) in risk scores that could allow patients' risk stratification and detection of LVDD in early asymptomatic phases would reduce significantly the burden of HFpEF.

Many of the IF biomarkers are currently under investigation. Until now, they did not enter the clinical practice and had similar or lower diagnosis and prognosis capacity as compared to natriuretic peptides. Further research is needed to identify the most reliable biomarker for the early diagnosis, progression monitoring, and prognosis in patients with LVDD.

The development of molecular target immunotherapy that enhances ventricular-vascular coupling, cardiomyocyte stiffness at the level of the myofilaments, or other inflammatory and immunopathogenic pathways could have a benefit in preventing LVDD progression to HFpEF.

Conflicts of Interest

The authors declare that there is no conflict of interest regarding the publication of this paper.

References

[1] S. M. Dunlay, V. L. Roger, and M. M. Redfield, "Epidemiology of heart failure with preserved ejection fraction," *Nature Reviews Cardiology*, vol. 14, no. 10, pp. 591–602, 2017.

[2] L. van Heerebeek and W. J. Paulus, "Understanding heart failure with preserved ejection fraction: where are we today?," *Netherlands Heart Journal*, vol. 24, no. 4, pp. 227–236, 2016.

[3] D. Westermann, D. Lindner, M. Kasner et al., "Cardiac inflammation contributes to changes in the extracellular matrix in patients with heart failure and normal ejection fraction," *Circulation: Heart Failure*, vol. 4, no. 1, pp. 44–52, 2011.

[4] W. J. Paulus and C. Tschöpe, "A novel paradigm for heart failure with preserved ejection fraction," *Journal of the American College of Cardiology*, vol. 62, no. 4, pp. 263–271, 2013.

[5] C. Y. Wong, T. O'Moore-Sullivan, R. Leano, N. Byrne, E. Beller, and T. H. Marwick, "Alterations of left ventricular myocardial characteristics associated with obesity," *Circulation*, vol. 110, no. 19, pp. 3081–3087, 2004.

[6] M. López-Sánchez, M. Muñoz-Esquerre, D. Huertas et al., "High prevalence of left ventricle diastolic dysfunction in severe COPD associated with a low exercise capacity: a cross-sectional study," *PLoS ONE*, vol. 8, no. 6, p. e68034, 2013.

[7] A. Deswal, "Diastolic dysfunction and diastolic heart failure: mechanisms and epidemiology," *Current Cardiology Reports*, vol. 7, no. 3, pp. 178–183, 2005.

[8] B. Upadhya, B. Pisani, and D. W. Kitzman, "Evolution of a geriatric syndrome: pathophysiology and treatment of heart failure with preserved ejection fraction," *Journal of the American Geriatrics Society*, vol. 65, no. 11, pp. 2431–2440, 2017.

[9] C. A. Meschiari, O. K. Ero, H. Pan, T. Finkel, and M. L. Lindsey, "The impact of aging on cardiac extracellular matrix," *GeroScience*, vol. 39, no. 1, pp. 7–18, 2017.

[10] A. B. Gevaert, H. Shakeri, A. J. Leloup et al., "Endothelial senescence contributes to heart failure with preserved ejection fraction in an aging mouse model," *Circulation: Heart Failure*, vol. 10, no. 6, 2017.

[11] M. P. van den Berg, B. A. Mulder, S. H. C. Klaassen et al., "Heart failure with preserved ejection fraction, atrial

fibrillation, and the role of senile amyloidosis," *European Heart Journal*, vol. 40, no. 16, pp. 1287–1293, 2019.

[12] C.-K. Wu, C. Y. Yang, J. W. Lin et al., "The relationship among central obesity, systemic inflammation, and left ventricular diastolic dysfunction as determined by structural equation modeling," *Obesity*, vol. 20, no. 4, pp. 730–737, 2012.

[13] N. Ayalon, D. M. Gopal, D. M. Mooney et al., "Preclinical left ventricular diastolic dysfunction in metabolic syndrome," *The American Journal of Cardiology*, vol. 114, no. 6, pp. 838–842, 2014.

[14] M. Mocan, F. Anton, S. Suciu, R. Rahaian, S. N. Blaga, and A. D. Farcas, "Multimarker assessment of diastolic dysfunction in metabolic syndrome patients," *Metabolic Syndrome and Related Disorders*, vol. 15, no. 10, pp. 507–514, 2017.

[15] M. Mocan, T. Popa, and S. N. Blaga, "The influence of metabolic syndrome components on N-terminal pro B-type natriuretic peptide concentrations: the role of left ventricular diastolic dysfunction," *Acta Endocrinologica*, vol. 9, no. 2, pp. 229–240, 2013.

[16] F. Kuwahara, H. Kai, K. Tokuda et al., "Hypertensive myocardial fibrosis and diastolic dysfunction: another model of inflammation?," *Hypertension*, vol. 43, no. 4, pp. 739–745, 2004.

[17] J. Gu, F. Zhao, Y. Wang et al., "The molecular mechanism of diastolic heart failure," *Integrative Medicine International*, vol. 2, no. 3-4, pp. 143–148, 2015.

[18] J. M. ter Maaten, K. Damman, M. C. Verhaar et al., "Connecting heart failure with preserved ejection fraction and renal dysfunction: the role of endothelial dysfunction and inflammation," *European Journal of Heart Failure*, vol. 18, no. 6, pp. 588–598, 2016.

[19] Y. F. Hu, Y. J. Chen, Y. J. Lin, and S. A. Chen, "Inflammation and the pathogenesis of atrial fibrillation," *Nature Reviews Cardiology*, vol. 12, no. 4, pp. 230–243, 2015.

[20] C. Drechsler, G. Delgado, C. Wanner et al., "Galectin-3, renal function, and clinical outcomes: results from the LURIC and 4D studies," *Journal of the American Society of Nephrology*, vol. 26, no. 9, pp. 2213–2221, 2015.

[21] J. E. Ho, C. Liu, A. Lyass et al., "Galectin-3, a marker of cardiac fibrosis, predicts incident heart failure in the community," *Journal of the American College of Cardiology*, vol. 60, no. 14, pp. 1249–1256, 2012.

[22] L. G. Olsson, K. Swedberg, A. Ducharme et al., "Atrial fibrillation and risk of clinical events in chronic heart failure with and without left ventricular systolic dysfunction," *Journal of the American College of Cardiology*, vol. 47, no. 10, pp. 1997–2004, 2006.

[23] Z. J. Eapen, M. A. Greiner, G. C. Fonarow et al., "Associations between atrial fibrillation and early outcomes of patients with heart failure and reduced or preserved ejection fraction," *American Heart Journal*, vol. 167, no. 3, pp. 369–375.e2, 2014.

[24] U. Sartipy, G. Savarese, U. Dahlström, M. Fu, and L. H. Lund, "Association of heart rate with mortality in sinus rhythm and atrial fibrillation in heart failure with preserved ejection fraction," *European Journal of Heart Failure*, vol. 21, no. 4, pp. 471–479, 2019.

[25] S. I. Negi, E. M. Jeong, I. Shukrullah et al., "Renin-angiotensin activation and oxidative stress in early heart failure with preserved ejection fraction," *BioMed Research International*, vol. 2015, 7 pages, 2015.

[26] R. B. Neuman, H. L. Bloom, I. Shukrullah et al., "Oxidative stress markers are associated with persistent atrial fibrillation," *Clinical Chemistry*, vol. 53, no. 9, pp. 1652–1657, 2007.

[27] T. Inoue, T. Ide, M. Yamato et al., "Time-dependent changes of myocardial and systemic oxidative stress are dissociated after myocardial infarction," *Free Radical Research*, vol. 43, no. 1, pp. 37–46, 2009.

[28] F. Edelmann, A. Tomaschitz, R. Wachter et al., "Serum aldosterone and its relationship to left ventricular structure and geometry in patients with preserved left ventricular ejection fraction," *European Heart Journal*, vol. 33, no. 2, pp. 203–212, 2012.

[29] Y. Chen, H. Wang, Y. Lu, X. Huang, Y. Liao, and J. Bin, "Effects of mineralocorticoid receptor antagonists in patients with preserved ejection fraction: a meta-analysis of randomized clinical trials," *BMC Medicine*, vol. 13, no. 1, 2015.

[30] G. Giamouzis, E. B. Schelbert, and J. Butler, "Growing evidence linking microvascular dysfunction with heart failure with preserved ejection fraction," *Journal of the American Heart Association*, vol. 5, no. 2, pp. 1–4, 2016.

[31] S. F. Mohammed, S. Hussain, S. A. Mirzoyev, W. D. Edwards, J. J. Maleszewski, and M. M. Redfield, "Coronary microvascular rarefaction and myocardial fibrosis in heart failure with preserved ejection fraction," *Circulation*, vol. 131, no. 6, pp. 550–559, 2015.

[32] S. Kato, N. Saito, H. Kirigaya et al., "Impairment of Coronary Flow Reserve Evaluated by Phase Contrast Cine-Magnetic Resonance Imaging in Patients With Heart Failure With Preserved Ejection Fraction," *Journal of the American Heart Association*, vol. 5, no. 2, 2016.

[33] R. V. Shah, A. S. Desai, and M. M. Givertz, "The effect of renin-angiotensin system inhibitors on mortality and heart failure hospitalization in patients with heart failure and preserved ejection fraction: a systematic review and meta-analysis," *Journal of Cardiac Failure*, vol. 16, no. 3, pp. 260–267, 2010.

[34] M. M. Redfield, H. H. Chen, B. A. Borlaug et al., "Effect of phosphodiesterase-5 inhibition on exercise capacity and clinical status in heart failure with preserved ejection fraction," *Journal of the American Medical Association*, vol. 309, no. 12, pp. 1268–1277, 2013.

[35] S. H. Wan, M. W. Vogel, and H. H. Chen, "Pre-clinical diastolic dysfunction," *Journal of the American College of Cardiology*, vol. 63, no. 5, pp. 407–416, 2014.

[36] A. R. Aroor, C. H. Mandavia, and J. R. Sowers, "Insulin resistance and heart failure: molecular mechanisms," *Heart Failure Clinics*, vol. 8, no. 4, pp. 609–617, 2012.

[37] E. M. Jeong, J. Chung, H. Liu et al., "Role of mitochondrial oxidative stress in glucose tolerance, insulin resistance, and cardiac diastolic dysfunction," *Journal of the American Heart Association*, vol. 5, no. 5, 2016.

[38] E.-M. Jeong and S. C. Dudley Jr, "New diagnostic and therapeutic possibilities for diastolic heart failure," *Rhode Island Medical Journal*, vol. 97, no. 2, pp. 35–37, 2014.

[39] S. A. Chang, Y. J. Kim, H. W. Lee et al., "Effect of rosuvastatin on cardiac remodeling, function, and progression to heart failure in hypertensive heart with established left ventricular hypertrophy," *Hypertension*, vol. 54, no. 3, pp. 591–597, 2009.

[40] G. Liu, X. X. Zheng, Y. L. Xu, J. Ru, R. T. Hui, and X. H. Huang, "Meta-analysis of the effect of statins on mortality in patients with preserved ejection fraction," *The American Journal of Cardiology*, vol. 113, no. 7, pp. 1198–1204, 2014.

[41] S. Willemsen, J. W. L. Hartog, D. J. van Veldhuisen et al., "The role of advanced glycation end-products and their receptor on outcome in heart failure patients with preserved and reduced ejection fraction," *American Heart Journal*, vol. 164, no. 5, pp. 742–749.e3, 2012.

[42] F. A. Zouein, L. E. de Castro Brás, D. V. da Costa, M. L. Lindsey, M. Kurdi, and G. W. Booz, "Heart failure with preserved ejection fraction: emerging drug strategies," *Journal of Cardiovascular Pharmacology*, vol. 62, no. 1, pp. 13–21, 2013.

[43] N. Fujimoto, J. L. Hastings, G. Carrick-Ranson et al., "Cardiovascular effects of 1 year of alagebrium and endurance exercise training in healthy older individuals," *Circulation: Heart Failure*, vol. 6, no. 6, pp. 1155–1164, 2013.

[44] G. A. Silberman, T. H. M. Fan, H. Liu et al., "Uncoupled cardiac nitric oxide synthase mediates diastolic dysfunction," *Circulation*, vol. 121, no. 4, pp. 519–528, 2010.

[45] A. Cozma, A. S. Taut, O. Orasan, L. M. Procopciuc, and A. D. Farcas, "The relationship between eNOS (G894T) gene polymorphism and arterial stiffness in patients with metabolic syndrome," *Revista de Chimie*, vol. 69, pp. 2351–2356, 2018.

[46] P. C. Rosas, Y. Liu, M. I. Abdalla et al., "Phosphorylation of cardiac myosin binding protein-C is a critical mediator of diastolic function," *Circulation: Heart Failure*, vol. 8, no. 3, pp. 582–594, 2015.

[47] R. Thoonen, S. Giovanni, S. Govindan et al., "Molecular Screen Identifies Cardiac Myosin–Binding Protein-C as a Protein Kinase G-Iα Substrate," *Circulation: Heart Failure*, vol. 8, no. 6, pp. 1115–1122, 2015.

[48] E. M. Jeong, M. M. Monasky, L. Gu et al., "Tetrahydrobiopterin improves diastolic dysfunction by reversing changes in myofilament properties," *Journal of Molecular and Cellular Cardiology*, vol. 56, pp. 44–54, 2013.

[49] C. W. Tong, G. F. Dusio, S. Govindan et al., "Usefulness of released cardiac myosin binding protein-C as a predictor of cardiovascular events," *The American Journal of Cardiology*, vol. 120, no. 9, pp. 1501–1507, 2017.

[50] E.-M. Jeong, L. Zhou, A. Xie et al., "Plasma cardiac myosin binding protein-C maybe a novel biomarker for heart failure," *Journal of the American College of Cardiology*, vol. 65, no. 10, p. A993, 2015.

[51] L. Gullestad, T. Ueland, L. E. Vinge, A. Finsen, A. Yndestad, and P. Aukrust, "Inflammatory cytokines in heart failure: mediators and markers," *Cardiology*, vol. 122, no. 1, pp. 23–35, 2012.

[52] H. von Bibra, W. Paulus, and M. St John Sutton, "Cardiometabolic Syndrome and Increased Risk of Heart Failure," *Current Heart Failure Reports*, vol. 13, no. 5, pp. 219–229, 2016.

[53] J. M. Cheng, K. M. Akkerhuis, L. C. Battes et al., "Biomarkers of heart failure with normal ejection fraction: a systematic review," *European Journal of Heart Failure*, vol. 15, no. 12, pp. 1350–1362, 2013.

[54] N. Parekh and A. S. Maisel, "Utility of B-natriuretic peptide in the evaluation of left ventricular diastolic function and diastolic heart failure," *Current Opinion in Cardiology*, vol. 24, no. 2, pp. 155–160, 2009.

[55] P. Ponikowski, A. A. Voors, S. D. Anker et al., "2016 ESC Guidelines for the diagnosis and treatment of acute and chronic heart failure," *European Heart Journal*, vol. 37, no. 27, pp. 2129–2200, 2016.

[56] S. Werhahn, C. Becker, M. Mende, F. Edelmann, R. Wachter, and KNHI study group, "P2640NT-proBNP is a more sensitive and specific biomarker for the prediction of future atrial fibrillation than for forthcoming onset of heart failure: results from the observational DIAST-CHF study," *European Heart Journal*, vol. 38, suppl_1, p. 1094, 2017.

[57] P. Collier, C. J. Watson, V. Voon et al., "Can emerging biomarkers of myocardial remodelling identify asymptomatic hypertensive patients at risk for diastolic dysfunction and diastolic heart failure?," *European Journal of Heart Failure*, vol. 13, no. 10, pp. 1087–1095, 2011.

[58] Y. Michowitz, Y. Arbel, D. Wexler et al., "Predictive value of high sensitivity CRP in patients with diastolic heart failure," *International Journal of Cardiology*, vol. 125, no. 3, pp. 347–351, 2008.

[59] J. Danesh, S. Kaptoge, A. G. Mann et al., "Long-term interleukin-6 levels and subsequent risk of coronary heart disease: two new prospective studies and a systematic review," *PLoS Medicine*, vol. 5, no. 4, p. e78, 2008.

[60] G. C. Meléndez, J. L. McLarty, S. P. Levick, Y. Du, J. S. Janicki, and G. L. Brower, "Interleukin 6 mediates myocardial fibrosis, concentric hypertrophy, and diastolic dysfunction in rats," *Hypertension*, vol. 56, no. 2, pp. 225–231, 2010.

[61] M. Mocan, R. Rahaian, B. Mocan, and S. N. Blaga, "Multimarker evaluation of the cardio-metabolic risk," *Atherosclerosis*, vol. 263, pp. e201–e202, 2017.

[62] E. Haugen, L.-M. Gan, A. Isic, T. Skommevik, and M. Fu, "Increased interleukin-6 but not tumour necrosis factor-alpha predicts mortality in the population of elderly heart failure patients," *Experimental and Clinical Cardiology*, vol. 13, no. 1, pp. 19–24, 2008.

[63] L. D. Mocan Hognogi, C. M. Goidescu, and A. D. Farcaș, "usefulness of the adipokines as biomarkers of ischemic cardiac dysfunction," *Disease Markers*, vol. 2018, Article ID 3406028, 8 pages, 2018.

[64] J. Ye, Z. Wang, D. Ye et al., "Increased interleukin-11 levels are correlated with cardiac events in patients with chronic heart failure," *Mediators of Inflammation*, vol. 2019, 8 pages, 2019.

[65] S. Schafer, S. Viswanathan, A. A. Widjaja et al., "IL-11 is a crucial determinant of cardiovascular fibrosis," *Nature*, vol. 552, no. 7683, pp. 110–115, 2017.

[66] Y. Xu, J. Ye, M. Wang et al., "Increased interleukin-11 levels in thoracic aorta and plasma from patients with acute thoracic aortic dissection," *Clinica Chimica Acta*, vol. 481, pp. 193–199, 2018.

[67] W. Dinh, R. Füth, W. Nickl et al., "Elevated plasma levels of TNF-alpha and interleukin-6 in patients with diastolic dysfunction and glucose metabolism disorders," *Cardiovascular Diabetology*, vol. 8, no. 1, p. 58, 2009.

[68] A. D. Farcas, A. Rusu, M. A. Stoia, and L. A. Vida-Simiti, "Plasma leptin but not resistin TNF-α and adiponectin is associated with echocardiographic parameters of cardiac remodeling in patients with coronary artery disease," *Cytokine*, vol. 103, pp. 46–49, 2018.

[69] S. M. Dunlay, S. A. Weston, M. M. Redfield, J. M. Killian, and V́. L. Roger, "Tumor Necrosis Factor-α and Mortality in Heart Failure," *Circulation*, vol. 118, no. 6, pp. 625–631, 2008.

[70] B. M. Kaess and R. S. Vasan, "Pentraxin 3—a marker of diastolic dysfunction and HF?," *Nature Reviews Cardiology*, vol. 8, no. 5, pp. 246–248, 2011.

[71] J. Matsubara, S. Sugiyama, T. Nozaki et al., "Pentraxin 3 is a new inflammatory marker correlated with left ventricular diastolic dysfunction and heart failure with normal ejection fraction," *Journal of the American College of Cardiology*, vol. 57, no. 7, pp. 861–869, 2011.

[72] J. Matsubara, S. Sugiyama, T. Nozaki et al., "Incremental prognostic significance of the elevated levels of pentraxin 3 in patients with heart failure with normal left ventricular ejection fraction," *Journal of the American Heart Association*, vol. 3, no. 4, pp. 1–11, 2014.

[73] S. Matsuda, S. Umemoto, K. Yoshimura et al., "Angiotensin II Activates MCP-1 and Induces Cardiac Hypertrophy and Dysfunction via Toll-like Receptor 4," *Journal of Atherosclerosis and Thrombosis*, vol. 22, no. 8, pp. 833–844, 2015.

[74] L. Zhou, A. Azfer, J. Niu et al., "Monocyte chemoattractant protein-1 induces a novel transcription factor that causes cardiac myocyte apoptosis and ventricular dysfunction," *Circulation Research*, vol. 98, no. 9, pp. 1177–1185, 2006.

[75] D. Ding, D. Su, X. Li et al., "Serum levels of monocyte chemoattractant protein-1 and all-cause and cardiovascular mortality among patients with coronary artery disease," *PLoS ONE*, vol. 10, no. 3, article e0120633, 2015.

[76] E. Martínez-Martínez, C. Brugnolaro, J. Ibarrola et al., "CT-1 (cardiotrophin-1)-Gal-3 (galectin-3) axis in cardiac fibrosis and inflammation," *Hypertension*, vol. 73, no. 3, pp. 602–611, 2019.

[77] E. Coburn and W. Frishman, "Comprehensive review of the prognostic value of galectin-3 in heart failure," *Cardiology in Review*, vol. 22, no. 4, pp. 171–175, 2014.

[78] R. A. de Boer, D. J. A. Lok, T. Jaarsma et al., "Predictive value of plasma galectin-3 levels in heart failure with reduced and preserved ejection fraction," *Annals of Medicine*, vol. 43, no. 1, pp. 60–68, 2011.

[79] L. C. van Vark, I. Lesman-Leegte, S. J. Baart et al., "Prognostic Value of Serial ST2 Measurements in Patients With Acute Heart Failure," *Journal of the American College of Cardiology*, vol. 70, no. 19, pp. 2378–2388, 2017.

[80] S. K. Nadar and M. M. Shaikh, "Biomarkers in routine heart failure clinical care," *Cardiac Failure Review Journal*, vol. 5, pp. 1–7, 2019.

[81] A. D. Farcas, F. P. Anton, C. M. Goidescu, I. L. Gavrilă, L. A. Vida-Simiti, and M. A. Stoia, "Serum soluble ST2 and diastolic dysfunction in hypertensive patients," *Disease Markers*, vol. 2017, 8 pages, 2017.

[82] A. D. Farcas, F. P. Anton, M. A. Stoia, C. M. Goidescu, D. L. Mocan Hognogi, and L. A. Vida-Simiti, "P1866Plasma levels of ST2 - predictive factor of unfavourable outcome in hypertensive patients," *European Heart Journal*, vol. 39, suppl_1, 2018.

[83] A. Dattagupta and S. Immaneni, "ST2: current status," *Indian Heart Journal*, vol. 70, pp. S96–101, 2018.

[84] A. Bayés-Genís, J. Núñez, and J. Lupón, "Soluble ST2 for prognosis and monitoring in heart failure," *Journal of the American College of Cardiology*, vol. 70, no. 19, pp. 2389–2392, 2017.

[85] B. Dieplinger and T. Mueller, "Soluble ST2 in heart failure," *Clinica Chimica Acta*, vol. 443, pp. 57–70, 2015.

[86] C. W. Yancy, M. Jessup, B. Bozkurt et al., "2013 ACCF/AHA guideline for the management of heart failure: a report of the American College of Cardiology Foundation/American Heart Association Task Force on practice guidelines," *Circulation*, vol. 128, no. 16, pp. e240–e327, 2013.

[87] A. Bayes-Genis, J. L. Januzzi, H. K. Gaggin et al., "ST2 pathogenetic profile in ambulatory heart failure patients," *Journal of Cardiac Failure*, vol. 21, no. 4, pp. 355–361, 2015.

[88] E. O'Meara, S. de Denus, J. L. Rouleau, and A. Desai, "Circulating biomarkers in patients with heart failure and preserved ejection fraction," *Current Heart Failure Reports*, vol. 10, no. 4, pp. 350–358, 2013.

[89] K. C. Wollert, T. Kempf, and L. Wallentin, "Growth differentiation factor 15 as a biomarker in cardiovascular disease," *Clinical Chemistry*, vol. 63, no. 1, pp. 140–151, 2017.

[90] J.-F. Lin, S. Wu, S.-Y. Hsu et al., "Growth-differentiation factor-15 and major cardiac events," *The American Journal of the Medical Sciences*, vol. 347, no. 4, pp. 305–311, 2014.

[91] J. Meluzín and J. Tomandl, "Can biomarkers help to diagnose early heart failure with preserved ejection fraction?," *Disease Markers*, vol. 2015, Article ID 426045, 9 pages, 2015.

[92] R. Stahrenberg, F. Edelmann, M. Mende et al., "The novel biomarker growth differentiation factor 15 in heart failure with normal ejection fraction," *European Journal of Heart Failure*, vol. 12, no. 12, pp. 1309–1316, 2010.

[93] R. Santhanakrishnan, J. P. C. Chong, T. P. Ng et al., "Growth differentiation factor 15 , ST2 , high-sensitivity troponin T , and N-terminal pro brain natriuretic peptide in heart failure with preserved vs . reduced ejection fraction," *European Journal of Heart Failure*, vol. 14, no. 12, pp. 1338–1347, 2012.

[94] M. M. Y. Chan, R. Santhanakrishnan, J. P. C. Chong et al., "Growth differentiation factor 15 in heart failure with preserved vs. reduced ejection fraction," *European Journal of Heart Failure*, vol. 18, no. 1, pp. 81–88, 2016.

[95] S. Sciarretta, A. Ferrucci, G. Ciavarella et al., "Markers of inflammation and fibrosis are related to cardiovascular damage in hypertensive patients with metabolic syndrome," *American Journal of Hypertension*, vol. 20, no. 7, pp. 784–791, 2007.

[96] L. Koller, M. Kleber, G. Goliasch et al., "C-reactive protein predicts mortality in patients referred for coronary angiography and symptoms of heart failure with preserved ejection fraction," *European Journal of Heart Failure*, vol. 16, no. 7, pp. 758–766, 2014.

[97] C. Sinning, T. Kempf, M. Schwarzl et al., "Biomarkers for characterization of heart failure – distinction of heart failure with preserved and reduced ejection fraction," *International Journal of Cardiology*, vol. 227, pp. 272–277, 2017.

[98] H. M. DuBrock, O. F. AbouEzzeddine, and M. M. Redfield, "High-sensitivity C-reactive protein in heart failure with preserved ejection fraction," *PLoS ONE*, vol. 13, no. 8, p. e0201836, 2018.

[99] M. Kloch, K. Stolarz-Skrzypek, A. Olszanecka et al., "Inflammatory markers and left ventricular diastolic dysfunction in a family-based population study," *Kardiologia Polska*, vol. 77, no. 1, pp. 33–39, 2019.

[100] D. Phelan, C. Watson, R. Martos et al., "Modest elevation in BNP in asymptomatic hypertensive patients reflects subclinical cardiac remodeling, inflammation and extracellular matrix changes," *PLoS ONE*, vol. 7, no. 11, p. e49259, 2012.

[101] R. V. Shah, A. A. Chen-Tournoux, M. H. Picard, R. R. J. Van Kimmenade, and J. L. Januzzi, "Galectin-3, cardiac structure and function, and long-term mortality in patients with acutely decompensated heart failure," *European Journal of Heart Failure*, vol. 12, no. 8, pp. 826–832, 2010.

[102] F. Edelmann, V. Holzendorf, R. Wachter et al., "Galectin-3 in patients with heart failure with preserved ejection fraction: results from the Aldo-DHF trial," *European Journal of Heart Failure*, vol. 17, no. 2, pp. 214–223, 2015.

[103] J. Bartunek, L. Delrue, F. van Durme et al., "Nonmyocardial production of ST2 protein in human hypertrophy and failure is related to diastolic load," *Journal of the American College of Cardiology*, vol. 52, no. 25, pp. 2166–2174, 2008.

[104] R. V. Shah, A. A. Chen-Tournoux, M. H. Picard, R. R. J. van Kimmenade, and J. L. Januzzi, "Serum levels of the interleukin-1 receptor family member ST2, cardiac structure and function, and long-term mortality in patients with acute dyspnea," *Circulation: Heart Failure*, vol. 2, no. 4, pp. 311–319, 2009.

[105] S. Manzano-Fernández, T. Mueller, D. Pascual-Figal, Q. A. Truong, and J. L. Januzzi, "Usefulness of soluble concentrations of interleukin family member ST2 as predictor of mortality in patients with acutely decompensated heart failure relative to left ventricular ejection fraction," *The American Journal of Cardiology*, vol. 107, no. 2, pp. 259–267, 2011.

[106] K. B. Shah, W. J. Kop, R. H. Christenson et al., "Prognostic utility of ST2 in patients with acute dyspnea and preserved left ventricular ejection fraction," *Clinical Chemistry*, vol. 57, no. 6, pp. 874–882, 2011.

[107] Y.-C. Wang, C.-C. Yu, F.-C. Chiu et al., "Soluble ST2 as a biomarker for detecting stable heart failure with a normal ejection fraction in hypertensive patients," *Journal of Cardiac Failure*, vol. 19, no. 3, pp. 163–168, 2013.

[108] I. S. Anand, T. S. Rector, M. Kuskowski, J. Snider, and J. N. Cohn, "Prognostic value of soluble ST2 in the Valsartan Heart Failure Trial," *Circulation: Heart Failure*, vol. 7, no. 3, pp. 418–426, 2014.

[109] E. Najjar, U. L. Faxén, C. Hage et al., "ST2 in heart failure with preserved and reduced ejection fraction," *Scandinavian Cardiovascular Journal*, vol. 53, no. 1, pp. 21–27, 2019.

Hindawi
Disease Markers
Volume 2019, Article ID 6984845, 11 pages
https://doi.org/10.1155/2019/6984845

Research Article

Glutathione Transferase P1 Polymorphism Might Be a Risk Determinant in Heart Failure

Dejan Simeunovic,[1,2] Natalija Odanovic,[3] Marija Pljesa-Ercegovac,[2,4] Tanja Radic,[2,4] Slavica Radovanovic,[5] Vesna Coric,[2,4] Ivan Milinkovic,[1] Marija Matic,[2,4] Tatjana Djukic,[2,4] Arsen Ristic,[1,2] Dijana Risimic,[2,6] Petar Seferovic,[1,2] Tatjana Simic,[2,4] Dragan Simic,[1,2] and Ana Savic-Radojevic[2,4]

[1]*Clinic of Cardiology, Clinical Center of Serbia, 8 Koste Todorovića, 11000 Belgrade, Serbia*
[2]*Faculty of Medicine, University of Belgrade, 8 Doktora Subotica, 11000 Belgrade, Serbia*
[3]*Section of Cardiovascular Medicine, Department of Internal Medicine, Yale School of Medicine, New Haven, Connecticut, USA*
[4]*Institute of Medical and Clinical Biochemistry, 2 Pasterova, 11000 Belgrade, Serbia*
[5]*University Clinical Hospital Center "Dr. Dragisa Misovic-Dedinje", Heroja Milana Tepica 1, 11000 Belgrade, Serbia*
[6]*Clinic of Ophthalmology, Clinical Center of Serbia, 2 Pasterova, 11000 Belgrade, Serbia*

Correspondence should be addressed to Dragan Simic; dvsimic@yahoo.com
and Ana Savic-Radojevic; ana.savic-radojevic@med.bg.ac.rs

Received 4 February 2019; Revised 18 April 2019; Accepted 7 May 2019; Published 2 June 2019

Guest Editor: Agata M. Bielecka-Dabrowa

Disturbed redox balance in heart failure (HF) might contribute to impairment of cardiac function, by oxidative damage, or by regulation of cell signaling. The role of polymorphism in glutathione transferases (*GSTs*), involved both in antioxidant defense and in regulation of apoptotic signaling pathways in HF, has been proposed. We aimed to determine whether GST genotypes exhibit differential risk effects between coronary artery disease (CAD) and idiopathic dilated cardiomyopathy (IDC) in HF patients. *GSTA1*, *GSTM1*, *GSTP1*, and *GSTT1* genotypes were determined in 194 HF patients (109 CAD, 85 IDC) and 274 age- and gender-matched controls. No significant association was found for *GSTA1*, *GSTM1*, and *GSTT1* genotypes with HF occurrence due to either CAD or IDC. However, carriers of at least one variant *GSTP1*∗Val (rs1695) allele were at 1.7-fold increased HF risk than *GSTP1*∗Ile/Ile carriers ($p = 0.031$), which was higher when combined with the variant *GSTA1*∗B allele (OR = 2.2, $p = 0.034$). In HF patients stratified based on the underlying cause of disease, an even stronger association was observed in HF patients due to CAD, who were carriers of a combined *GSTP1*(rs1695)/*GSTA1* "risk-associated" genotype (OR = 2.8, $p = 0.033$) or a combined *GSTP1*∗Ile/Val+Val/Val (rs1695)/*GSTP1*∗AlaVal+∗ValVal (rs1138272) genotype (OR = 2.1, $p = 0.056$). Moreover, these patients exhibited significantly decreased left ventricular end-systolic diameter compared to *GSTA1*∗AA/*GSTP1*∗IleIle carriers ($p = 0.021$). Higher values of ICAM-1 were found in carriers of the *GSTP1*∗IleVal+∗ValVal (rs1695) ($p = 0.041$) genotype, whereas higher TNFα was determined in carriers of the *GSTP1*∗AlaVal+∗ValVal genotype (rs1138272) ($p = 0.041$). In conclusion, *GSTP1* polymorphic variants may determine individual susceptibility to oxidative stress, inflammation, and endothelial dysfunction in HF.

1. Introduction

For more than a decade, it has been suggested that a complex interplay between oxidative stress and chronic inflammation represents one of the underlying mechanisms of gradual cardiac depression in heart failure (HF) [1–3]. Oxidative stress in HF is believed to be a consequence of increased circulating neurohormones and hemodynamic disorder, as well as inflammation and decreased oxygen delivery. On the other hand, disturbed redox balance in patients with HF might contribute to further impairment of cardiac function, either by oxidative damage to vital cellular molecules or by affecting

cell signaling involved in cell survival and death [4]. There is overwhelming evidence for the presence of oxidative stress in all phases of HF in animal models and humans [5, 6]. Regarding the mechanisms of oxidative stress in HF, both enhanced free radical production and diminished antioxidative defense are involved in the occurrence and progression of HF [5]. It is important to note that increased free radical production and inflammation are involved in cardiomyocyte apoptosis and progression of HF. Continuous release of free radicals in response to angiotensin II and catecholamines has also been found to take part in cardiac hypertrophy. Additionally, structural changes and activation of metalloproteinases are also dependent on free radicals produced in the course of fibroblast to myofibroblast transformation. Taken together, all these free radical-dependent processes contribute to the occurrence of end-stage HF [5]. Several biomarkers of oxidative distress, such as isoprostanes, malondialdehyde, uric acid, and protein carbonyl groups, have been shown to be elevated in different stages of HF [7, 8].

In addition to this well-established link, recent findings on the adverse effect of chemical and pollutant exposure to heart disease [9, 10] put special emphasis on the role of genetic polymorphisms of enzymes involved in detoxification of xenobiotics and antioxidant defense in the HF syndrome [11]. Members of the glutathione transferase (GST) enzyme superfamily belong to phase II detoxification enzymes but are also involved in regulation of the cellular redox state through different antioxidant catalytic and noncatalytic roles [12]. Moreover, almost all members of the GST family exhibit genetic polymorphisms, which can result in a complete lack or lowering of enzyme activity [13].

Considering the fact that HF represents a multifactorial, polygenic syndrome, the role of oxidative stress and consequently polymorphic expression of GSTs may have a different impact, especially regarding the specific cause of heart failure. In coronary artery disease (CAD) as the most common etiology of heart failure in industrialized countries, genetic epidemiologic studies mostly investigated the association of common *GSTA1*, *GSTM1*, *GSTT1*, and *GSTP1* polymorphisms with disease risk [14–16]. Among them, the most attention was focused on the investigation of *GSTM1* and *GSTT1* deletion polymorphisms [17], considering the fact that the homozygous deletions of these genes result in a complete lack of enzymatic activity and thus diminish detoxification capacity [18]. Based on the important role of the GSTM1 enzyme in detoxifying benzodiolepoxide, present in tobacco smoke and environmental pollution, it could be speculated that carriers of the *GSTM1*-null genotype could have increased risk of CAD, particularly in smokers. Until now, the results on the independent effect of the *GSTM1*-null genotype on increased susceptibility to CAD are still being debated [14, 17]. On the other hand, the recent meta-analysis involving 47596 subjects showed that the *GSTM1-null* genotype in association with smoking increases the risk for CAD [19]. Moreover, correlation between the *GSTM1-null* genotype and indices of inflammation and oxidative stress has been demonstrated in CAD. Thus, higher CRP and lower total antioxidant capacity have been observed in CAD patients lacking *GSTM1* than those with an active GSTM1 enzyme [20]. With regard to the *GSTT1-null* genotype, only few studies revealed that the *GSTT1-null* genotype carries higher risk for HF development [14, 17]. Two genetic variants in the *GSTP1* gene, the *GSTP1*∗G allele (rs1695) coding for protein in which amino acid isoleucine (Ile) is substituted with valine (Val) at position 105 and the *GSTP1*∗ allele (rs1138272) in which alanine (Ala) is substituted with (Val) at position 114, have been shown to confer altered catalytic and noncatalytic activity, whereas the *GSTA1*∗B allele (rs3957356) is associated with the lower expression of *GSTA1* than that of the common *GSTA1*∗A allele. It seems reasonable to assume that *GSTA1*- or *GSTP1-variant* genotypes also might contribute to the endogenous predisposition to oxidative damage in the setting of disrupted redox balance in HF patients due to CAD. However, the results of association of *GSTP1* and *GSTA1* polymorphisms with risk for CAD are still inconsistent [14, 21]. Interestingly, in idiopathic dilated cardiomyopathy (IDC), as a rare entity of HF syndrome, the effect of genetic polymorphisms of these enzymes has still not been investigated.

Having all that in mind, we conducted a pilot case-control study consisting of patients with HF due to coronary artery disease (CAD) or idiopathic dilated cardiomyopathy (IDC) in order to compare the distribution of common GST genotypes and the differential risk effect between these two entities.

2. Materials and Methods

2.1. Subjects. A total of 194 patients (51 women and 143 men, all Caucasian) with HF were enrolled in the study. We included two kinds of patients in the study: 109 of those with HF due to coronary artery disease (CAD) and 85 of those with heart failure due to idiopathic dilated cardiomyopathy (IDC). All patients were recruited between 2008 and 2012 from the Medical Center "Bezanijska Kosa" and from the Clinical Center of Serbia, during the dispensary checkups. Diagnosis of HF was based on the patient's history, physical examination, electrocardiography, chest X-ray, echocardiography, and coronary angiography. Distribution of the New York Heart Association (NYHA) stage was indicated for HF patients (Table 1). Major inclusion criteria were the left ventricular ejection fraction < 45% and stable HF over the two weeks prior to enrollment. For the CAD subpopulation, the inclusion criterion was evidence of CAD on angiography. For the IDC subpopulation, major inclusion criteria were the absence of CAD on coronary angiography and the evidence of chamber dilation. Patients with congenital, acquired valvular, or pericardial abnormalities were excluded from the study. Our case-control study also included a total of 274 individuals in the control group. The study was approved by the ethics committee of the Clinical Center of Serbia (470/XII-9 from 29/12/2008), and all study participants signed an informed consent.

2.2. GST Genotyping. Genomic DNA was isolated from whole blood using the QIAGEN QIAamp kit (QIAGEN Inc., Chatsworth, CA). *GSTA1* (-69C>T) and *GSTP1* (Ile105Val, rs1695) were examined by the polymerase chain reaction-

Table 1: Selected characteristics of patients with HF and controls.

	Controls	HF	IDC	CAD
Age (years) ± SD[a]	55.8 ± 10.9	54.3 ± 10.8	49.0 ± 13.6*	58.7 ± 4.3
Gender[b]				
Females (%)	90 (33)	51 (26)	15 (18)*	36 (33)
Males (%)	184 (67)	143 (74)	70 (82)*	73 (67)
Diabetes[b]				
Yes (*n* (%))	25 (9)	66 (35)*	25 (30)*	41 (38)*
No (*n* (%))	249 (91)	123 (65)*	57 (70)*	66 (62)*
Hypertension[b]				
Yes (*n* (%))	67 (26)	82 (52)*	16 (19)	68 (78)*
No (*n* (%))	191 (74)	77 (48)*	69 (81)	19 (22)*
Smoking status[b]				
Smokers (*n* (%))	138 (52)	99 (57)	42 (51)	57 (61)
Nonsmokers (*n* (%))	126 (48)	76 (43)	40 (49)	36 (39)
NYHA				
II		124 (64)	54 (64)	71 (65)
III		48 (25)	20 (24)	28 (26)
IV		18 (9)	8 (9)	10 (9)

HF: heart failure; IDC: idiopathic dilated cardiomyopathy; CAD: coronary artery disease; SD: standard deviation; NYHA: New York Heart Association functional classification of heart failure. [a]Student's *t*-test; [b]χ^2 test; *statistically significant in comparison to controls ($p < 0.05$).

restriction fragment length polymorphism (PCR-RFLP) method [22, 23], whereas the *GSTM1*/*GSTT1* were determined by the PCR method [24]. The *GSTP1* (Ala114Val, rs1138272) polymorphism was determined by qPCR (Applied Biosystems) only in CAD patients using an Applied Biosystems TaqMan Drug Metabolism Genotyping Assay (ID C_1049615_20). The primer sequences, PCR conditions, restriction enzymes used, and respective restriction conditions, as well as fragment lengths after electrophoresis on 2% agarose gel, can be found in Table 2.

2.3. Determination of Parameters of Inflammation, Oxidative Stress, and Endothelial Dysfunction in Plasma/Serum. Malondialdehyde (MDA) was determined spectrophotometrically (BIOXYTECH LPO-586 kit; OxIS Research, Portland, OR, USA). The results were expressed in μmol/L. Serum levels of hs-CRP were determined using a commercially available kit. Commercially available ELISA kits for TNFα, ICAM-1, VCAM-1 (Bender MedSystems, GmbH, Austria) were used for the measurement of those inflammatory markers in plasma/serum samples collected from each patient.

2.4. Noninvasive Assessment of Endothelium-Dependent and Endothelium-Independent Flow-Mediated Dilation (FMD) of the Brachial Artery. Endothelium-dependent and endothelium-independent FMD of the brachial artery was assessed by a 13.0 MHz linear array transducer (Vivid 7, GE Medical Systems, Little Chalfont, England, UK) as previously published.

2.5. Statistical Analysis. In descriptive statistics, we summarized all continuous variables by means ± standard deviations (SD). Differences in investigated parameters were assessed by using analysis of variance (ANOVA) and Student's t-test for continuous variables and χ^2 for categorical variables. The associations between the genotypes and HF risk were calculated by using logistic regression to compute odds ratios (ORs) and corresponding 95% confidence intervals (CIs), adjusted according to age, gender, smoking, hypertension, and diabetes as potential confounding factors. Haplotype analysis of *GSTP1* SNPs was examined using the SNPStats. In order to demonstrate the validity of our data, a positive control was introduced by assessing the well-established association between *GSTM1* deletion polymorphism in smokers and the risk of bladder cancer [25, 26]. For this purpose, an adjusted OR to age, gender, and BMI was calculated. For the data with a nonnormal distribution, we used the Mann-Whitney rank-sum test for between-two-group comparisons. Two-tailed p values of <0.05 were considered significant. Data were analyzed using the Statistical Package for the Social Sciences (SPSS) (version 17.0, Chicago, IL).

3. Results

3.1. General Characteristics of Patients. The characteristics of the whole group of HF patients, as well as patients stratified to underlying disease due to IDC and CAD, along with the characteristics of control participants are shown in Table 1. While the average age of both the control group and the HF patients is around 55 years, patients with IDC appear to be 6 years younger on average (mean age = 49.0) and thus statistically differ from the remaining two groups, which is consistent with findings in the literature [27, 28]. The occurrence of diabetes and hypertension was significantly higher in patients and patient subpopulations compared to controls.

Table 2: PCR-RFLP: primer sequences, PCR conditions, restriction enzymes, and fragment lengths.

Polymorphism	Primer sequences	PCR protocol	Gel electrophoresis results
GSTA1∗C-69T	F, 5′-GCATCAGCTTGCCCTTCA -3′ R, 5′-AAACGCTGTCACCGTCCTG-3′	Denature: 94°C for 3 min Followed by 94°C for 30 s Annealing: 56°C for 30 s Extension: 72°C for 30 s #cycles: 30 Final extension: 72°C for 10 min	Eam1104I incubation at 37°C overnight *GSTA1*∗CC: 400 bp *GSTA1*∗CT: 400 bp, 308 bp, and 92 bp *GSTA1*∗TT: 308 bp and 92 bp
GSTP1∗Ile105Val	F, 5′-ACCCCAGGGCTCTATGGGAA-3′ R, 5′-TGAGGGCACAAGAAGCCCCT-3′	Denature: 95°C for 10 min Followed by 94°C for 30 s Annealing: 59°C for 30 s Extension: 72°C for 30 s #cycles: 29 Final extension: 72°C for 10 min	Alw26I incubation at 37°C overnight *GSTP1*∗Ile/Ile: 176 bp *GSTP1*∗Ile/Val: 176 bp, 91 bp, and 85 bp *GSTP1*∗Val/Val: 91 bp and 85 bp
GSTM1	F, 5′-GAACTCCCTGAAAAGCTAAAGC-3′ R, 5′-GTTGGGCTCAAATATACGGTGG-3′	Multiplex PCR: Denature: 94°C for 3 min Followed by 94°C for 30 s Annealing: 59°C for 30 s Extension: 72°C for 45 s #cycles: 30 Final extension: 72°C for 4 min	*GSTM1*∗active: 215 bp band *GSTM1*∗null: absent band
GSTT1	F, 5′-TTCCTTACTGGTCCTCACATCTC-3′ R, 5′-TCACGGGATCATGGCCAGCA-3′		*GSTT1*∗active: 480 bp band *GSTT1*∗null: absent band
CYP1A1	F, 5′-GAACTGCCACTT CAGCTGTCT-3′ R, 5′-CAGCTGCATTTG GAAGTGCTC-3′		Successful PCR reaction: 312 bp band Unsuccessful PCR reaction: absent band

Table 3: Distribution of *GSTA1*, *GSTP1*, *GSTM1*, and *GSTT1* genotypes in HF patients and controls.

Genotype	Controls (*n* (%))	HF patients (*n* (%))	OR (95% CI)[a]	*p*
GSTA1				
∗A/A	112 (41)	68 (35)	1.0[b]	
∗A/B+B/B	162 (59)	125 (65)	1.5 (0.9-2.5)	0.097
GSTP1∗Ile105Val (rs1695)				
∗Ile/Ile	115 (42)	68 (35)	1.0[b]	
∗Ile/Val+∗Val/Val	159 (58)	124 (65)	1.7 (1.0-2.9)	0.031*
GSTM1				
Active	137 (50)	92 (47)	1.0[b]	
Null	137 (50)	102 (53)	1.1 (0.7-1.8)	0.671
GSTT1				
Active	203 (74)	146 (74)	1.0[b]	
Null	71 (26)	48 (26)	0.9 (0.5-1.7)	0.873
Combined *GSTA1*/ *GSTP1*(rs1695)				
∗AA/∗IleIle	54 (20)	29 (16)	1.0[b]	
∗AA/∗IleVal+∗ValVal	58 (21)	39 (20)	1.2 (0.5-2.6)	0.697
∗AB+∗BB/∗IleIle	61 (22)	39 (20)	1.0 (0.5-2.3)	0.913
∗AB+BB/∗IleVal+∗ValVal	101 (37)	84 (44)	2.2 (1.1-4.4)	0.034*
GST genotype/smoking status	Controls (*n* (%))	Bladder cancerpatients (*n* (%))	OR (95% CI)[c]	*p*
GSTM1-active/nonsmoker	50 (46)	16 (18)	1.00[b]	
GSTM1-null/smoker	58 (54)	75 (82)	4.4 (2.2-8.9)	<0.001

HF: heart failure; CI: confidence interval; OR: odds ratio. [a]Logistic regression to compute odds ratios (ORs)adjusted for gender, age, smoking, hypertension, and diabetes. [b]Reference group. [c]Logistic regression to compute odds ratios adjusted for gender, age, and body mass index. *Statistically significant in comparison with the reference genotype ($p < 0.05$).

Gender and smoking status did not differ significantly between HF patients and controls.

3.2. Distribution of GST Genotypes. The distribution of GST genotypes in all HF patients and controls is shown in Table 3. The frequencies of the GSTA1, GSTP1, GSTM1, and GSTT1 genotypes are in accordance with the reported values in the literature. In order to fully estimate the role of GST genotypes in HF development, respected ORs were adjusted to factors regarded as confounding variables: age, gender, smoking, hypertension, and diabetes. Significant association between the GST genotype and the risk of HF development was found only for the GSTP1 genotype (rs1695) (Table 3). Namely, the risk of HF was significantly higher in individuals with at least one variant, ∗Val allele, i.e., GSTP1∗Ile/Val or GSTP1∗Val/Val genotypes (OR = 1.7; 95%CI = 1.0 − 2.9; p = 0.031). The observed association to HF risk was even more potentiated when the risk-associated GSTP1 genotype was combined with at least one variant GSTA1 allele (OR = 2.2; 95%CI = 1.1 − 4.4; p = 0.034). On the other hand, data validity assessment demonstrated a 4.4-fold elevated risk of bladder cancer in smokers with the GSTM1-null genotype as opposed to GSTM1-active nonsmokers.

Patients with HF due to CAD and IDC demonstrated similar GST genotype distribution. No significant association was observed for GSTA1, GSTM1, and GSTT1 genotypes with the occurrence of HF due to either CAD or IDC. When we analyzed the effect of GSTP1 genotypes (rs1695 and rs1138272) according to the specific cause of HF, a 1.9-fold increased risk was observed for carriers of at least one GSTP1∗Val (rs1695) allele in the CAD group (95%CI = 1.0 − 3.6; p = 0.056) (Table 4(a)). Patients from the IDC group with the same genotype were at 1.4-fold risk of HF (95%CI = 0.7 − 2.7; p = 0.284) (Table 4(b)). Namely, although these results did not reach the level of statistical significance, the evident risk-associated trend was observed. However, combined GSTA1∗AB+BB/GSTP1∗IleVal+∗ValVal (rs1695) and GSTA1∗AB+BB/GSTP1∗AlaVal+∗ValVal (rs1138272) genotypes potentiated the risk in HF patients due to CAD (OR = 2.8, 95%CI = 1.1 − 7.3, p = 0.033, and OR = 2.1, 95%CI = 1.0 − 4.5, p = 0.056, respectively). Moreover, we performed haplotype analysis generating four GSTP1 haplotypes: wild-type GSTP1∗A (Ile105/Ala114), GSTP1∗B (Val105/Ala114), GSTP1∗C (Val105/Val114), and GSTP1∗D (Ile105/Val114). Haplotype analysis conferred small yet nonsignificant risk for CAD-related HF development in the case of the GSTP1∗B haplotype (OR = 1.4; 95%CI = 0.9 − 2.3; p = 0.170; Table 5). On the other hand, GSTP1∗C and GSTP1∗D haplotypes exhibited lower risk towards CAD-related HF development (OR = 0.5, 95%CI = 0.1 − 3.9, p = 0.490, and OR = 0.6, 95%CI = 0.1 − 3.1, p = 0.560, respectively; Table 5).

3.3. Risk-Associated GST Genotypes in relation to the Parameters of Oxidative Stress, Inflammation, and Endothelial Dysfunction in the CAD-Related HF Subgroup. Plasma levels of MDA, end product of lipid peroxidation,

Table 4

(a) Distribution of *GSTA1*, *GSTP1*, *GSTM1*, and *GSTT1* genotypes in HF patients due to CAD and controls

	Controls (*n* (%))	Patients (*n* (%))	OR (95% CI)[a]	*p*
GSTA1				
∗A/A	112 (41)	38 (35)	1.0[b]	
∗A/B+B/B	162 (59)	70 (65)	1.8 (0.9-3.5)	0.075
GSTM1				
Active	137 (50)	53 (49)	1.0[b]	
Null	137 (50)	56 (51)	1.1 (0.6-2.0)	0.749
GSTT1				
Active	203 (74)	82 (75)	1.0[b]	
Null	71 (26)	27 (25)	1.0 (0.5-2.0)	0.935
GSTP1∗Ile105Val (rs1695)				
∗Ile/Ile	115 (42)	39 (37)	1.0[b]	
∗Ile/Val+∗Val/Val	159 (58)	68 (63)	1.9 (1.0-3.6)	0.056
GSTP1∗Ala114Val (rs1138272)				
∗Ala/Ala	205 (85)	90 (86)	1.0[b]	
∗Ala/Val+∗Val/Val	38 (15)	15 (14)	0.5 (0.2-1.3)	0.157
Combined *GSTA1*/*GSTP1* (rs1695)				
∗AA/∗IleIle	54 (20)	16 (15)	1.0[b]	
∗AA/∗IleVal+∗ValVal	58 (21)	22 (21)	1.4 (0.5-4.1)	0.539
∗AB+∗BB/∗IleIle	61 (22)	23 (22)	1.4 (0.5-4.0)	0.560
∗AB+BB/∗IleVal+∗ValVal	101 (37)	45 (42)	2.8 (1.1-7.3)	0.033*
Combined *GSTA1*/*GSTP1* (rs1138272)				
∗AA/∗AlaAla	28 (11)	9 (9)	1.0[b]	
∗AA/∗AlaVal+∗ValVal	84 (33)	29 (28)	1.6 (0.4-5.4)	0.490
∗AB+∗BB/∗AlaAla	24 (9)	7 (7)	0.9 (0.2-3.4)	0.906
∗AB+BB/∗AlaVal+∗ValVal	121 (47)	60 (57)	2.1 (1.0-4.5)	0.056

CI: confidence interval; OR: odds ratio. [a]Logistic regression to compute odds ratios adjusted for gender, age, smoking, hypertension, and diabetes. [b]Reference group. *Statistically significant in comparison with the reference genotype ($p < 0.05$).

(b) Distribution of *GSTA1*, *GSTP1*, *GSTM1*, and *GSTT1* genotypes in IDC patients and controls

Genotype	Controls (*n* (%))	Patients (*n* (%))	OR (95% CI)[a]	*p*
GSTA1				
∗A/A	112 (41)	30 (35)	1.0[b]	
∗A/B+B/B	162 (59)	55 (65)	1.2 (0.6-2.2)	0.660
GSTP1∗Ile105Val (rs1695)				
∗Ile/Ile	115 (42)	29 (34)	1.0[b]	
∗Ile/Val+∗Val/Val	159 (58)	56 (66)	1.4 (0.7-2.7)	0.284
GSTM1				
Active	137 (50)	39 (46)	1.0[b]	
Null	137 (50)	46 (54)	1.2 (0.6-2.2)	0.620
GSTT1				
Active	203 (74)	64 (75)	1.0[b]	
Null	71 (26)	21 (25)	0.9 (0.4-1.9)	0.854
Combined *GSTA1*/*GSTP1*				
∗AA/∗IleIle	54 (20)	13 (15)	1.0[b]	
∗AA/∗IleVal+∗ValVal	58 (21)	17 (20)	1.3 (0.5-3.6)	0.618
∗AB+∗BB/∗IleIle	61 (22)	16 (19)	1.0 (0.4-2.9)	0.924
∗AB+BB/∗IleVal+∗ValVal	101 (37)	39 (46)	1.5 (0.6-3.8)	0.348

CI: confidence interval; OR: odds ratio. [a]Logistic regression to compute odds ratios adjusted for gender, age, smoking, hypertension, and diabetes. [b]Reference group.

Table 5: Haplotype analysis of *GSTP1* polymorphisms in CAD-related HF patients and controls.

Haplotype	*GSTP1* rs4925	*GSTP1* rs156697	Controls (%)	CAD patients (%)	OR (95% CI)[a]	*p*
GSTP1∗A	∗A	∗C	58	59	1.0[b]	
GSTP1∗B	∗G	∗C	33	34	1.4 (0.9-2.3)	0.170
GSTP1∗C	∗G	∗T	4	4	0.5 (0.1-3.9)	0.490
GSTP1∗D	∗A	∗T	4	3	0.6 (0.1-3.0)	0.560

CI: confidence interval; OR: odds ratio. SNPStats was used for haplotype analysis; [a]Logistic regression to compute odds ratios adjusted for gender, age, smoking, hypertension, and diabetes. [b]Reference group.

Table 6: Markers of oxidative stress, inflammation, and endothelial dysfunction in CAD-related HF patients stratified according to GST genotypes.

Genotype	MDA (μmol/L)[a]	hs-CRP (mg/L)[b]	TNFα (pg/mL)[b]	ICAM-1 (ng/L)[b]	VCAM-1 (ng/L)[b]
GSTA1					
∗A/A	7.53 ± 0.86	2.12 (0.49-43.51)	2.25 (0.15-47.63)	375.90 (206.43-696.91)	1113.12 (563.85-3697.45)
∗A/B+B/B	7.57 ± 0.73	2.14 (0.15-45.00)	2.25 (0.22-29.76)	380.98 (264.20-691.04)	1063.23 (144.45-7429.55)
	0.802	0.600	0.792	0.526	0.505
GSTP1 (rs1695)					
∗Ile/Ile	7.53 ± 0.87	1.91 (0.38-35.68)	2.15 (0.33-11.12)	363.38 (206.43-553.84)	1152.30 (563.85-1793.90)
∗Ile/Val+∗Val/Val	7.58 ± 0.72	2.29 (0.15-45.00)	2.34 (0.15-47.63)	390.10 (255.12-696.91)	1095.20 (144.45-7429.55)
p	0.745	0.382	0.557	0.041	0.882
GSTP1 (rs1138272)					
∗Ala/Ala	7.55 ± 0.79	2.14 (0.15-45.00)	2.21 (0.15-11.12)	381.25 (206.43-696.91)	1109.25 (144.45-7429.55)
∗Ala/Val+∗Val/Val	7.72 ± 0.76	2.08 (0.93-43.51)	4.69 (0.63-47.63)	351.35 (275.60-568.10)	1040.95 (759.25-1871.55)
p	0.436	0.777	0.045	0.152	0.899

MDA: malondialdehyde; hs-CRP: high-sensitivity C-reactive protein; TNFα: tumor necrosis factor-alpha; ICAM-1: intercellular adhesion molecule-1; VCAM-1: vascular cell adhesion molecule-1. [a]Student t-test was used. [b]Mann-Whitney test was used. *Statistically significant at $p < 0.05$.

and established marker of lipid oxidative damage were analyzed in CAD-related HF patients stratified according to polymorphism in GSTA1 and GSTP1 antioxidant enzymes (Table 6). No significant difference was observed in MDA levels between carriers of either GSTA1 or GSTP1 (rs1695 and rs1138272) genotypes in the CAD subgroup. Moreover, inflammatory markers TNFα and hs-CRP together with biochemical markers of endothelial dysfunction, ICAM-1 and VCAM-1, were also stratified according to GST risk genotypes. The results have shown that higher values of ICAM-1 were found in carriers of GSTP1∗IleVal+∗ValVal (rs1695) ($p = 0.041$), whereas higher TNFα was present in carriers of GSTP1∗AlaVal+∗ValVal (rs1138272) ($p = 0.041$) (Table 6).

3.4. The Association of GSTP1 Genotype with the Indices of HF Severity. The role of *GSTP1* polymorphism was further analyzed regarding parameters related to the severity of HF. The dimensions of the left ventricle after systole and diastole (LVESD and LVEDD), along with NO-dependent and NO-independent vasodilation of the brachial artery in CAD patients with different *GSTP1* genotypes, are shown in Table 7. The end-systolic (LVESD) and end-diastolic (LVEDD) diameters of the left ventricle did not differ significantly between patients with different *GSTP1* genotypes (rs1695 and rs1138272). Likewise, the degree of endothelium-dependent NO-mediated vasodilation and endothelium-independent nitroglycerin- (NTG-) mediated vasodilation of the brachial artery was similar between CAD-related HF patients with either the *GSTP1* wild-type genotype and carriers of at least one variant *GSTP1* allele. When we analyzed these parameters in CAD-related HF patients stratified according to combined *GSTA1*/*GSTP1* (rs1695) genotypes (Table 7), only carriers of variant *GSTA1*∗B/*GSTP1*∗Val (rs1695) alleles had significantly decreased LVESD compared to individuals with *GSTA1*∗AA/*GSTP1*∗IleIle ($p = 0.021$).

LVEDD: left ventricular end-diastolic diameter; LVESD: left ventricular end-systolic diameter; FMD-NO: endothelium-dependent NO-mediated vasodilation; FMD-NTG: endothelium-independent NTG-mediated vasodilation. [a]Student *t*-test was used for testing differences in LVEDD and LVESD, for each group compared to the reference group (*GSTP1*∗Ile/Ile or combined *GSTA1*/*GSTP1*∗AA/∗IleIle , *GSTA1*/*GSTP1*∗AA/∗AlaAla). [b]Mann-Whitney test was used for testing differences in FMD-NO and FMD-NTG, for each group compared to the reference group (*GSTP1*∗Ile/Ile or combined *GSTA1*/*GSTP1*∗AA/∗IleIle, *GSTA1*/*GSTP1*∗AA/∗AlaAla). *Statistically significant at $p < 0.05$.

Table 7: Echocardiographic and endothelial parameters stratified according to HF risk-associated GST genotypes in CAD subgroup.

Genotype	LVEDD[a]	LVESD[a]	FMD-NO[b]	FMD-NTG[b]
GSTP1∗Ile105Val (rs1695)				
∗Ile/Ile	6.0 ± 0.8	4.8 ± 1.0	3.8 ± 4.1	12.4 ± 7.1
∗Ile/Val+∗Val/Val	6.0 ± 0.7	4.6 ± 0.9	4.9 ± 5.1	11.3 ± 6.4
GSTP1∗Ala114Val (rs1138272)				
∗Ala/Ala	6.0 ± 0.8	4.7 ± 0.9	4.4 ± 4.7	11.83 ± 7.1
∗Ala/Val+∗Val/Val	6.0 ± 0.8	4.6 ± 1.1	5.51 ± 5.48	10.71 ± 5.1
Combined *GSTA1*/*GSTP1*(rs1695)				
∗AA/∗IleIle	6.3 ± 0.7	5.1 ± 0.8	3.8 ± 4.0	11.3 ± 7.4
∗AA/∗IleVal+∗ValVal	6.0 ± 0.7	4.6 ± 1.0	5.6 ± 4.8	11.4 ± 8.4
∗AB+∗BB/∗IleIle	5.8 ± 0.9	4.5 ± 1.1	3.8 ± 4.2	13.1 ± 7.0
∗AB+BB/∗IleVal+∗ValVal	5.9 ± 0.7	4.5 ± 0.9*	4.7 ± 5.3	11.2 ± 5.4
Combined *GSTA1*/*GSTP1*(rs1138272)				
∗AA/∗AlaAla	6.1 ± 0.6	4.8 ± 0.8	5.2 ± 4.9	11.6 ± 8.6
∗AA/∗AlaVal+∗ValVal	6.2 ± 0.9	4.9 ± 1.2	3.6 ± 2.5	10.7 ± 5.4
∗AB+∗BB/∗AlaAla	5.9 ± 0.8	4.5 ± 0.9	3.9 ± 4.6	11.9 ± 6.2
∗AB+BB/∗AlaVal+∗ValVal	5.9 ± 1.0	4.5 ± 1.0	7.4 ± 7.3	9.5 ± 5.4

4. Discussion

Based on different roles of GSTs and considering the fact that in the setting of heart failure the disturbances of redox regulation can contribute to disease progression, in this study, we investigated the effect of common *GST* polymorphisms regarding specific HF entities. Among tested *GST* polymorphisms, only the variant *GSTP1*∗Val allele has shown a significant association with HF, regardless of the specific cause. This HF risk conferred by *GSTP1* polymorphism was even higher when combined with the variant *GSTA1*∗B allele. In HF patients stratified according to the underlying cause of the disease, even more potentiated association was observed in HF patients due to CAD, while in those due to idiopathic cardiomyopathy, despite the evident trend, this association was not confirmed.

In our study, we found no significant association for individual GSTM1 and GSTT1 polymorphisms with the occurrence of HF due to either CAD or IDC. Our results are in concordance with the study of Norskov et al., who conducted a comprehensive analysis of the copy number variation for GSTM1 and GSTT1 in patients with ischemic heart disease and ischemic cerebrovascular disease, showing no significant association with disease risk, even among smokers.

It has been well established that GSTP1 exhibits both antioxidant and glutathionylation activity, having important role in the maintenance of the cellular redox state [29]. Namely, GSTP1 is necessary for the activation of peroxiredoxin VI (Prdx6), a member of the family of antioxidant enzymes, which catalyzes detoxification of lipid peroxides, particularly in biological membranes [30]. After the exposure of endothelial cells to laminar shear stress, as a result of increase in free radical production, the upregulation of these antioxidant enzymes has been observed, probably as adaptive phenomenon [31]. Even more, their important role in regulating endothelial cell activation during atherosclerosis has been proposed. The most recent data on MCF-7 cells showed that the polymorphic expression of GSTP1 differentially interposes the Prdx6 activity, implying that depending upon their *GSTP1* genotype, individuals will have significant differences in mounting an antioxidant response [30]. In carriers of the *GSTP1* variant genotype, changed GSTP1 catalytic activity could deepen the progression of the disease, which consequently results in multiple cellular responses, such as DNA synthesis, transcription factor activation, and alteration of protein expression. If these results are translated to the HF setting, it may be speculated that *GSTP1*∗Ile/Ile carriers might possibly have a higher antioxidant potential providing the favorable environment for better prognosis. Moreover, it is important to note that the highest HF risk was found for carriers of combined *GSTA1*∗B/*GSTP1*∗Val variant alleles. Namely, GSTA1-1 is one of the most promiscuous GST enzymes with wide substrate specificity, including powerful antioxidant activity [32]. Thus, the presence of the *GSTA1*∗B gene variant, which results in lower expression of the enzyme, in combination with the *GSTP1*∗Val allele, might significantly contribute to decreased antioxidant capacity of HF patients, carriers of the combined *GSTA1*∗B/*GSTP1*∗Val genotype. Regarding our previous data on the prognostic significance of oxidative stress and inflammatory parameters in HF [3, 7], we investigated whether *GSTA1* and *GSTP1* polymorphic variants could affect the plasma concentration of MDA, TNFα, and hs-CRP in our cohort of CAD-related HF patients. Indeed, we showed that carriers of the variant *GSTP1*∗Val (rs1138272) genotype demonstrated higher TNFα levels, revealing new functional relevance of this *GSTP1* polymorphism.

Aside from generation of reactive oxygen species (ROS) in the failing myocardium, endothelial activation also significantly contributes to myocyte apoptosis, necrosis, and

remodeling of the extracellular matrix in the heart [33]. GSTP1 participates in regulation of stress signaling and apoptosis via its noncatalytic activity. Specifically, through protein:protein interaction, GSTP1 acts as an endogenous inhibitor of several signaling molecules, including c-Jun N-terminal kinase (JNK) [34] and TNFα receptor-associated factor 2 (TRAF2) [35]. This interaction of GSTP1 with the MAPK and NF-κB axes of regulation is also responsible for its suggested anti-inflammatory role [36]. What is more, the degree of interaction between GSTP1 and JNK, a member of the mitogen-activated protein kinase (MAPK) signaling pathway, depends on the redox status of the cell. In that way, GSTP1 provides an important link between cellular redox potential and the regulation of kinase pathways involved in apoptosis and inflammation. The results of Andrukhova et al., showing elevated GSTP1 expression in the failing myocardium, were associated with reduced GSTP1:JNK interaction and consequent activation of the JNK-MAPK signaling cascade, essential for cardiomyocyte apoptosis [37], representing further confirmation of the contributing role of oxidative stress in the HF progression. Interestingly, the same authors indicated that a single dose of recombinant GSTP1 has cardioprotective effect in rats after myocardial infarction, affecting both inflammatory and apoptotic responses [37]. The substitutions of amino acid isoleucine (Ile) with valine (Val) at position 105 and alanine (Ala) with (Val) at position 114 as a consequence of *GSTP1* polymorphisms can also affect the aforementioned interaction with JNK, causing an alteration in the GSTP1-mediated inhibitory effect of JNK activity [38]. Indeed, it has been shown that the *GSTP*∗C (Val105/-Val114) haplotype is a more potent JNK inhibitor than the referent *GSTP1*∗A (Ile105/Ala114) [38]. Although we did not find significant association between different GSTP1 haplotypes and the CAD-related HF risk, the obvious trend for decreasing HF risk in carriers of the *GSTP1*∗C (Val105/Val114) haplotype might have a molecular explanation in its ability to prevent apoptosis more efficiently. A further indication of functional GST redundancy is provided by the fact that GSTA1 and GSTM1 were also capable of associating with JNK. Based on our results on increased disease risk for HF patient carriers of the combined *GSTA1*/*GSTP1* variant genotype, it might be speculated that the impaired GSTP1:JNK interaction in CAD [37] could be further modified in patient carriers of the combined *GSTA1*/*GSTP1* risk-associated genotype.

Finally, this seemingly "pleiotropic" modulatory role of GSTP1 was recently demonstrated for the key regulatory molecule of cell-cell communication in the heart, the signal transducer and activator of transcription 3 (STAT3) [39]. STAT3 is fundamental for physiological homeostasis and stress-induced remodeling of the heart, as reviewed in the article of Haghikia et al. [40]. Furthermore, Chen et al. demonstrated that GSTP1, due to its interaction with STAT3, can inhibit angiotensin II-induced STAT3 activation of vascular smooth muscle cells (VSMCs) *in vitro* [39], thus preventing VSMC proliferation. However, the potential effect of *GSTP1* polymorphism on this interaction still remains elusive.

Based on recent findings on increased GSTP1 catalytic activity in the metabolism of polycyclic aromatic hydrocarbons from tobacco smoke in carriers of the variant GSTP1∗Val allele, which is located in the substrate-binding site, it may be hypothesized that GSTP1 genotyping could provide additional information not exclusively regarding tobacco smoking but also to other recognized GSTP1 substrates present in air pollutants, dietary compounds, products of endogenous metabolism, and lipid peroxidation. It would be tempting to investigate whether metabolism of ubiquitous reactive aldehyde acrolein, as a typical example of such a GSTP1 substrate associated with increased cardiovascular disease risk, would be affected by GSTP1 polymorphism [41]. In conclusion, due to involvement of GSTs in detoxification of xenobiotics from tobacco smoke and also the metabolism of environmental and occupational pollutants, as well as various dietary constituents, different lifestyles might affect the role of GSTs within one population, while at the same time, the association observed in one may not be seen in other populations living in different environments.

To take further insight into molecular mechanisms and potential consequences of *GSTP1* and *GSTA1* polymorphisms with respect to CAD-related HF, we correlated the *GSTP1* and *GSTA1* variant genotypes with both the indices of heart remodeling and parameters of endothelial dysfunction. However, we found that only carriers of combined variant *GSTA1*∗B/*GSTP1*∗Val alleles had significantly decreased LVESD compared to individuals with *GSTA1*∗AA/*GSTP1*∗IleIle genotypes. Besides, the GSTP1 variant genotype was significantly associated with soluble ICAM-1 levels in these patients. As such, GSTP1 polymorphic variants may determine individual susceptibility to oxidative stress, inflammation, and endothelial dysfunction in HF, as well.

In our cohort of IDC patients, despite the evident trend, significant association of *GSTP1* polymorphism with disease risk was not confirmed. The most probable reason is the small number of patients with ICD, having in mind the findings of Inoue et al. and Cannon et al. on the presence of coronary microcirculatory dysfunction despite angiographically normal epicardial coronary arteries in these patients [42, 43]. Hence, altered coronary flow reserve (CFR), which reflects coronary microvascular function and integrity, has been reported as an independent predictor of subsequent cardiac events in patients with idiopathic LV dysfunction [44].

Certain limitations could be considered in our study. The study findings may be influenced by potential biases arising from relatively small number of participants and *GST* polymorphisms studied. The number of patients was further reduced by analyzing subgroups of HF due to CAD and IDC. Furthermore, the use of population controls may have been more appropriate. Additionally, we cannot entirely rule out the possibility that some of our results could be caused by confounding, although we adjusted all results by age, gender, smoking, hypertension, and diabetes as potential confounding factors. Moreover, despite a large number of smokers in our cohort of HF patients, the correction for continuous measure of smoking was not determined.

5. Conclusions

It may be concluded that the variant *GSTP1*∗Val allele is significantly associated with HF risk regardless of the specific cause. This association is even more potentiated in carriers of both *GSTP1*∗Val and *GSTA1*∗B alleles.

Data Availability

The database used to support the findings of this study is available from the corresponding author upon request.

Disclosure

The funding sponsors had no role in the design of the study; in the collection, analyses, or interpretation of the data; in the writing of the manuscript; and in the decision to publish the results.

Conflicts of Interest

The authors declare no conflict of interest.

Acknowledgments

This work was supported by Grant 175052 from the Serbian Ministry of Education, Science and Technological Development.

References

[1] E. Braunwald, "Biomarkers in heart failure," *New England Journal of Medicine*, vol. 358, no. 20, pp. 2148–2159, 2008.

[2] S. Radovanovic, A. Savic-Radojevic, M. Pljesa-Ercegovac et al., "Markers of oxidative damage and antioxidant enzyme activities as predictors of morbidity and mortality in patients with chronic heart failure," *Journal of Cardiac Failure*, vol. 18, no. 6, pp. 493–501, 2012.

[3] A. Savic-Radojevic, S. Radovanovic, T. Pekmezovic et al., "The role of serum VCAM-1 and TNF-α as predictors of mortality and morbidity in patients with chronic heart failure," *Journal of Clinical Laboratory Analysis*, vol. 27, no. 2, pp. 105–112, 2013.

[4] A. Savic-Radojevic, M. Pljesa-Ercegovac, M. Matic, D. Simic, S. Radovanovic, and T. Simic, "Novel Biomarkers of Heart Failure," *Advances in Clinical Chemistry*, vol. 79, pp. 93–152, 2017.

[5] K. F. Ayoub, N. V. K. Pothineni, J. Rutland, Z. Ding, and J. L. Mehta, "Immunity, inflammation, and oxidative stress in heart failure: emerging molecular targets," *Cardiovascular Drugs and Therapy*, vol. 31, no. 5-6, pp. 593–608, 2017.

[6] A. M. Rababa'h, A. N. Guillory, R. Mustafa, and T. Hijjawi, "Oxidative stress and cardiac remodeling: an updated edge," *Current Cardiology Reviews*, vol. 14, no. 1, pp. 53–59, 2018.

[7] S. Radovanovic, M. Krotin, D. V. Simic et al., "Markers of oxidative damage in chronic heart failure: role in disease progression," *Redox Report*, vol. 13, no. 3, pp. 109–116, 2008.

[8] S. Radovanovic, A. Savic-Radojevic, T. Pekmezovic et al., "Uric acid and gamma-glutamyl transferase activity are associated with left ventricular remodeling indices in patients with chronic heart failure," *Revista Española de Cardiología*, vol. 67, no. 8, pp. 632–642, 2014.

[9] A. Bhatnagar, "Environmental cardiology: studying mechanistic links between pollution and heart disease," *Circulation Research*, vol. 99, no. 7, pp. 692–705, 2006.

[10] D. J. Conklin and A. Bhatnagar, "Are *glutathione S* -transferase null genotypes "null and void" of risk for ischemic vascular disease?," *Circulation: Cardiovascular Genetics*, vol. 4, no. 4, pp. 339–341, 2011.

[11] F. M. F. Alameddine and A. M. Zafari, "Genetic polymorphisms and oxidative stress in heart failure," *Congestive Heart Failure*, vol. 8, no. 3, pp. 157–164, 172, 2007.

[12] C. J. Henderson and C. R. Wolf, "Disruption of the glutathione transferase pi class genes," *Methods in Enzymology*, vol. 401, pp. 116–135, 2005.

[13] T. Simic, A. Savic-Radojevic, M. Pljesa-Ercegovac, M. Matic, and J. Mimic-Oka, "Glutathione S-transferases in kidney and urinary bladder tumors," *Nature Reviews Urology*, vol. 6, no. 5, pp. 281–289, 2009.

[14] H.-L. Yeh, L.-T. Kuo, F.-C. Sung, C.-W. Chiang, and C.-C. Yeh, "GSTM1, GSTT1, GSTP1, and GSTA1 genetic variants are not associated with coronary artery disease in Taiwan," *Gene*, vol. 523, no. 1, pp. 64–69, 2013.

[15] V. Kovacs, B. Gasz, B. Balatonyi et al., "Polymorphisms in glutathione S-transferase are risk factors for perioperative acute myocardial infarction after cardiac surgery: a preliminary study," *Mol. Cell. Biochem.*, vol. 389, no. 1-2, pp. 79–84, 2014.

[16] R. Polimanti, S. Piacentini, N. Lazzarin, M. A. Re, D. Manfellotto, and M. Fuciarelli, "Glutathione S-transferase variants as risk factor for essential hypertension in Italian patients," *Molecular and Cellular Biochemistry*, vol. 357, no. 1-2, pp. 227–233, 2011.

[17] C. Marinho, I. Alho, D. Arduíno, L. M. Falcão, J. Brás-Nogueira, and M. Bicho, "GST M1/T1 and MTHFR polymorphisms as risk factors for hypertension," *Biochemical and Biophysical Research Communications*, vol. 353, no. 2, pp. 344–350, 2007.

[18] J. D. Hayes, J. U. Flanagan, and I. R. Jowsey, "Glutathione transferases," *Annual Review of Pharmacology and Toxicology*, vol. 45, no. 1, pp. 51–88, 2005.

[19] D. Zhou, W. Hu, Q. Wang, and Y. Jin, "Glutathione S-transferase M1 polymorphism and coronary heart disease susceptibility: a meta-analysis involving 47,596 subjects," *Heart, Lung and Circulation*, vol. 23, no. 6, pp. 578–585, 2014.

[20] J.-J. Tang, M.-W. Wang, E. Jia et al., "The common variant in the GSTM1 and GSTT1 genes is related to markers of oxidative stress and inflammation in patients with coronary artery disease: a case-only study," *Molecular Biology Reports*, vol. 37, no. 1, pp. 405–410, 2010.

[21] A. Phulukdaree, S. Khan, D. Moodley, and A. A. Chuturgoon, "GST polymorphisms and early-onset coronary artery disease in young South African Indians," *South African Medical Journal*, vol. 102, no. 7, pp. 627–630, 2012.

[22] J. Ping, H. Wang, M. Huang, and Z.-S. Liu, "Genetic analysis of glutathione S-transferase A1 polymorphism in the Chinese population and the influence of genotype on enzymatic properties," *Toxicological Sciences*, vol. 89, no. 2, pp. 438–443, 2006.

[23] L. W. Harries, M. J. Stubbins, D. Forman, G. C. Howard, and C. R. Wolf, "Identification of genetic polymorphisms at the glutathione S-transferase pi locus and association with

susceptibility to bladder, testicular and prostate cancer," *Carcinogenesis*, vol. 18, no. 4, pp. 641–644, 1997.

[24] S. Z. Abdel-Rahman, R. A. el-Zein, W. A. Anwar, and W. W. Au, "A multiplex PCR procedure for polymorphic analysis of GSTM1 and GSTT1 genes in population studies," *Cancer Letters*, vol. 107, no. 2, pp. 229–233, 1996.

[25] M. Matic, T. Pekmezovic, T. Djukic et al., "GSTA1, GSTM1, GSTP1, and GSTT1 polymorphisms and susceptibility to smoking-related bladder cancer: a case-control study," *Urologic Oncology: Seminars and Original Investigations*, vol. 31, no. 7, pp. 1184–1192, 2013.

[26] M. S. Norskov, R. Frikke-Schmidt, S. Loft et al., "Copy number variation in glutathione S-transferases M1 and T1 and ischemic vascular disease: four studies and meta-analyses," *Circulation: Cardiovascular Genetics*, vol. 4, no. 4, pp. 418–428, 2011.

[27] M. V. Raynolds, M. R. Bristow, E. W. Bush et al., "Angiotensin-converting enzyme DD genotype in patients with ischaemic or idiopathic dilated cardiomyopathy," *The Lancet*, vol. 342, no. 8879, pp. 1073–1075, 1993.

[28] J. E. Sanderson, R. P. Young, C. M. Yu, S. Chan, J. A. J. H. Critchley, and K. S. Woo, "Lack of association between insertion/deletion polymorphism of the angiotensin-converting enzyme gene and end-stage heart failure due to ischemic or idiopathic dilated cardiomyopathy in the chinese," *The American Journal of Cardiology*, vol. 77, no. 11, pp. 1008–1010, 1996.

[29] K. D. Tew, Y. Manevich, C. Grek, Y. Xiong, J. Uys, and D. M. Townsend, "The role of glutathione S-transferase P in signaling pathways and S-glutathionylation in cancer," *Free Radical Biology and Medicine*, vol. 51, no. 2, pp. 299–313, 2011.

[30] Y. Manevich, S. Hutchens, K. D. Tew, and D. M. Townsend, "Allelic variants of glutathione S-transferase P1-1 differentially mediate the peroxidase function of peroxiredoxin VI and alter membrane lipid peroxidation," *Free Radical Biology and Medicine*, vol. 54, pp. 62–70, 2013.

[31] A. L. Mowbray, D.-H. Kang, S. G. Rhee, S. W. Kang, and H. Jo, "Laminar shear stress up-regulates peroxiredoxins (PRX) in endothelial cells: PRX 1 as a mechanosensitive antioxidant," *Journal of Biological Chemistry*, vol. 283, no. 3, pp. 1622–1627, 2008.

[32] B. F. Coles and F. F. Kadlubar, "Human alpha class glutathione S-transferases: genetic polymorphism, expression, and susceptibility to disease," *Methods in Enzymology*, vol. 401, pp. 9–42, 2005.

[33] P. Carmeliet, "Mechanisms of angiogenesis and arteriogenesis," *Nature Medicine*, vol. 6, no. 4, pp. 389–395, 2000.

[34] V. Adler, Z. Yin, S. Y. Fuchs et al., "Regulation of JNK signaling by GSTp," *The EMBO Journal*, vol. 18, no. 5, pp. 1321–1334, 1999.

[35] Y. Wu, Y. Fan, B. Xue et al., "Human glutathione S-transferase P1-1 interacts with TRAF2 and regulates TRAF2-ASK1 signals," *Oncogene*, vol. 25, no. 42, pp. 5787–5800, 2006.

[36] B. Xue, Y. Wu, Z. Yin et al., "Regulation of lipopolysaccharide-induced inflammatory response by glutathione S-transferase P1 in RAW264.7 cells," *FEBS Letters*, vol. 579, no. 19, pp. 4081–4087, 2005.

[37] O. Andrukhova, M. Salama, M. Krssak et al., "Single-dose GSTP1 prevents infarction-induced heart failure," *Journal of Cardiac Failure*, vol. 20, no. 2, pp. 135–145, 2014.

[38] A. F. Thévenin, C. L. Zony, B. J. Bahnson, and R. F. Colman, "GST pi modulates JNK activity through a direct interaction with JNK substrate, ATF2," *Protein Science*, vol. 20, no. 5, pp. 834–848, 2011.

[39] D. Chen, J. Liu, B. Rui et al., "GSTpi protects against angiotensin II-induced proliferation and migration of vascular smooth muscle cells by preventing signal transducer and activator of transcription 3 activation," *Biochimica et Biophysica Acta (BBA) - Molecular Cell Research*, vol. 1843, no. 2, pp. 454–463, 2014.

[40] A. Haghikia, M. Ricke-Hoch, B. Stapel, I. Gorst, and D. Hilfiker-Kleiner, "STAT3, a key regulator of cell-to-cell communication in the heart," *Cardiovascular Research*, vol. 102, no. 2, pp. 281–289, 2014.

[41] N. DeJarnett, D. J. Conklin, D. W. Riggs et al., "Acrolein exposure is associated with increased cardiovascular disease risk," *Journal of the American Heart Association*, vol. 3, no. 4, p. 3, 2014.

[42] T. Inoue, Y. Sakai, S. Morooka et al., "Coronary flow reserve in patients with dilated cardiomyopathy," *American Heart Journal*, vol. 125, no. 1, pp. 93–98, 1993.

[43] R. O. Cannon III, R. E. Cunnion, J. E. Parrillo et al., "Dynamic limitation of coronary vasodilator reserve in patients with dilated cardiomyopathy and chest pain," *Journal of the American College of Cardiology*, vol. 10, no. 6, pp. 1190–1200, 1987.

[44] D. Erdogan, H. Gullu, M. Caliskan et al., "Nebivolol improves coronary flow reserve in patients with idiopathic dilated cardiomyopathy," *Heart*, vol. 93, no. 3, pp. 319–324, 2007.

Hindawi
Disease Markers
Volume 2019, Article ID 8632726, 10 pages
https://doi.org/10.1155/2019/8632726

Research Article

Amino Acid-Based Metabolic Profile Provides Functional Assessment and Prognostic Value for Heart Failure Outpatients

Chao-Hung Wang,[1,2] **Mei-Ling Cheng**,[3,4,5] **Min-Hui Liu**,[1,2,6] **and Tieh-Cheng Fu**[7,8]

[1]*Heart Failure Research Center, Division of Cardiology, Department of Internal Medicine, Chang Gung Memorial Hospital, Keelung, Taiwan*
[2]*Chang Gung University College of Medicine, Taoyuan, Taiwan*
[3]*Metabolomics Core Laboratory, Healthy Aging Research Center, Chang Gung University, Taoyuan, Taiwan*
[4]*Department and Graduate Institute of Biomedical Sciences, College of Medicine, Chang Gung University, Taoyuan, Taiwan*
[5]*Clinical Metabolomics Core Laboratory, Linkou Chang Gung Memorial Hospital, Taoyuan, Taiwan*
[6]*Department of Nursing, National Yang-Ming University, Taipei, Taiwan*
[7]*Department of Physical Medicine and Rehabilitation, Chang Gung Memorial Hospital, Keelung, Taiwan*
[8]*Graduate Institute of Clinical Medical Sciences, College of Medicine, Chang Gung University, Taoyuan, Taiwan*

Correspondence should be addressed to Chao-Hung Wang; bearty54@gmail.com

Received 2 February 2019; Accepted 21 April 2019; Published 19 May 2019

Guest Editor: Zhongjie Shi

Functional capacity is a crucial parameter correlated with outcomes. The currently used New York Heart Association functional classification (NYHA Fc) system has substantial limitations, leading to inaccurate classification. This study investigated whether amino acid-based assessment on metabolic status provides an objective way to assess functional capacity and prognosis in heart failure (HF) outpatients. Plasma concentrations of histidine, ornithine, and phenylalanine (HOP) were measured on 890 HF outpatients to assess metabolic status by calculating the HOP score. Cardiopulmonary exercise testing (CPET) was performed in 387 patients to measure metabolic equivalents (MET) in order to define the functional class based on MET (MET Fc). Patients were followed for composite events (death/HF-related rehospitalization) up to one year. We found only 47% concordance between the MET Fc and NYHA Fc. HOP scores worked better than NYHA Fc for discriminating patients with MET Fc II and III from those with MET Fc I, with the optimal cutoff value set at 8.8. HOP scores ≥ 8.8 were associated with risk factors for composite events in different kinds of HF populations and were a powerful predictor of composite events in univariate analysis. In multivariable analysis, HOP scores ≥ 8.8 remained a powerful event predictor, independent of other risk factors. Kaplan-Meier curves revealed that HOP scores of ≥8.8 stratified patients at higher risk of composite events in a variety of HF populations. In conclusion, amino acid-based assessment of metabolic status correlates with functional capacity in HF outpatients and provides prognostic value for a variety of HF populations.

1. Introduction

Heart failure (HF) is becoming a tremendous burden on healthcare systems worldwide. Functional capacity is a crucial parameter correlated with outcomes [1–4]. Currently, the gold standard for assessing the functional state is the cardiopulmonary gas exchange exercise test (CPET) [5, 6]. Because it requires instruments and is inconvenient to administer because it is time-consuming, the New York Heart Association functional classification (NYHA Fc) is widely used instead [7]. However, previous studies found that interobserver reproducibility of NYHA Fc when assessing class II and class III was only 56%, a result little better than chance [4]. A more precise assessment tool is needed.

Functional assessment estimates the severity of imbalance between cardiac supply and whole body demand, which can represent the entire body's metabolic status. Previously, we

and others demonstrated that patients' plasma-based metabolic profile provided valuable information about HF-related metabolic disturbance [8–10], diagnosis [11–13], and prognosis [11, 14, 15]. We subsequently simplified the metabolomics assessment into an amino acid-based profile that includes histidine, ornithine, and phenylalanine (HOP score) [16, 17]. We found that the HOP score was well-correlated with functional capacity, as estimated by a six-minute walking distance.

Although NYHA functional classes III and IV suggest poor outcomes, the largest group of outpatients is usually in the NYHA class II category, which is often overlooked by clinicians. However, results of recent clinical trials strongly recommend active intervention for all patients from classes II to IV [1, 2]. In this study, we would like to use CPET to investigate whether HOP scores could be an objective substitute for identifying HF outpatients in the functional class ≥ II. We also would like to see whether the HOP-defined worse functional classification represents higher risk of HF-related rehospitalization/death in 12 months among HF patients with reduced ejection fraction (HFrEF), mid-range EF (HFmrEF), and preserved EF (HFpEF) [18].

2. Methods

2.1. Patients and Study Design. From January 2014 to May 2017, patients were enrolled consecutively at an outpatient HF clinic based on these inclusion criteria: (1) had been hospitalized due to acute or decompensated chronic HF, (2) at least one month after discharge, (3) NYHA functional class ≤ III, and (4) ages 20 to 85 years old.

Exclusion criteria included (1) the presence of disorders other than HF that might compromise survival within 6 months; (2) patients being bed-ridden for >3 months; (3) the presence of systemic diseases such as hypothyroidism, decompensated liver cirrhosis, and systemic lupus erythematosus; (4) patients with severe coronary artery disease without complete revascularization therapy; and (5) patients with a serum creatinine of >3 mg/dl. Informed consent was obtained from all patients. The study was designed and carried out in accordance with the principles of the *Declaration of Helsinki* and with approval from the Ethics Review Board of Chang Gung Memorial Hospital.

2.2. Blood Sampling and Examination. Blood samples for the metabolic panel were collected in EDTA-containing tubes on the day of the HF outpatient clinic in the early morning, after fasting for eight hours. For patients undergoing CPET, blood samples were collected within seven days before or after the CPET. Plasma was analyzed by UPLC workflow. BNP was measured in triplicate with the Triage BNP Test (Biosite, San Diego, CA), which was a fluorescence immunoassay for quantitative determination of plasma BNP. Precision, analytical sensitivity, and stability characteristics of the assay were previously described [19]. The measurement of other parameters, including estimated glomerular filtration rate (eGFR), hemoglobin, and albumin, was conducted in the central core laboratory.

2.3. Ultraperformance Liquid Chromatography (UPLC). HOP scores were calculated as described in our previous study based on the values of histidine, ornithine, and phenylalanine, measured by UPLC [16]. EDTA plasma samples were collected and stored at −80°C until assayed. The plasma samples (100 μl) were precipitated by adding an equal volume (100 μl) of 10% sulfosalicylic acid containing an internal standard (norvaline, 200 μM). After protein precipitation, the samples were vortexed and centrifuged at 12,000g for 10 min at room temp. After the samples were centrifuged, 20 μl of the supernatant was mixed with 60 μl working buffer (borate buffer, pH 8.8). The derivatization was initiated by the addition of 20 μl of 10 mM AQC in acetonitrile. After 10 min incubation, the mixture was added with an equal volume of Eluent A (20 mM ammonium formate/0.6% formic acid/1% acetonitrile) and analyzed using the ACQUITY UPLC System [20, 21]. AQC derivatization reagent was obtained from Waters Corporation (Milford, MA, USA). An aqueous amino acid standard mixture was prepared at different concentrations (0, 25, 50, 100, 250, and 500 μM) for each amino acid and was done by the same procedure. The Waters ACQUITY UPLC System consisted of a Binary Solvent Manager (BSM), a sample manager fitted with a 10 μl loop, and a Tunable UV (TUV) detector. The system was controlled and data collected using Empower™ 2 Software. Separations were performed on a 2.1 × 100 mm ACQUITY UPLC BEH C18 column at a flow rate of 0.70 ml/min. The average intra-assay coefficient of variation was 4.3% for histidine, 4.6% for ornithine, and 4.6% for phenylalanine. A total coefficient of variation was 3.1% for histidine, 3.6% for ornithine, and 3.7% for phenylalanine. The detection limit was 0.5 μM for histidine, 2.0 μM for ornithine, and 3.3 μM for phenylalanine. The linear range was 25–500 μM for these three amino acids.

2.4. Cardiopulmonary Exercise Test. From January 2014 to May 2017, 387 patients performed graded exercise on a bicycle ergometer (150P; Ergoselect, Lindenstrasse, Germany) to evaluate their aerobic fitness and hemodynamic function. We correlated the peak metabolic equivalent (MET) ($\dot{V}_{O_{2peak}}$) on the test with the HOP scores. The exercise test was carried out in an air-conditioned laboratory with an atmospheric temperature of 22–25°C, a barometric pressure of 755 to 770 Torr, and a relative humidity of 55–65%. The exercise protocol comprised 2 min of unloaded pedaling followed by a continuous increase of work rate of 10 W every minute until exhaustion (progressive exercise to peak oxygen consumption, $\dot{V}_{O_{2peak}}$). Oxygen consumption ($\dot{V}_{O_2}$) was measured breath by breath using a computer-based system (MasterScreen CPX; Cardinal Health, Hoechberg, Germany). Heart rate was determined from the R-R interval on a 12-lead electrocardiogram, blood pressure was measured by an automatic blood pressure system (Tango; SunTech Medical, Eynsham, UK), and arterial O_2 saturation was monitored by finger pulse-oximetry (model 9500; Nonin Onyx, Plymouth, MN). The $\dot{V}_{O_{2peak}}$ was defined by the

following criteria: (1) the level of $\dot{V}_{O_2}$ increases less than 2 ml/kg per minute over at least 2 min, (2) heart rate exceeds 85% of its predicted maximal value, (3) the respiratory exchange ratio exceeds 1.15, or (4) some other symptom/sign limitations, according to the guidelines of the American College of Sports Medicine for exercise testing. Since the peak METs calculated for the bicycle exercise were 80% of the peak METs calculated for the treadmill exercise [22, 23], MET Fc I, II, and III were defined as peak MET ≥ 5.6, ≥ 4, and <4, respectively, as determined by bicycle exercise.

2.5. Follow-Up Program. Follow-up data were prospectively obtained every month from hospital records, personal communication with the patients' physicians, telephone interviews with patients, and patients' regular visits to staff physician outpatient clinics (followed for up to one year until they died, the study ended, or they were lost to follow-up). "Rehospitalization" was defined as HF-related rehospitalizations. A committee of three cardiologists adjudicated all hospitalizations without knowledge of patients' clinical variables to determine whether the events were related to worsening HF. "All-cause death" was chosen as an endpoint because of the interrelationship of HF with other comorbidities in the patient cohort. The composite event of HF-related rehospitalization and all-cause death (time to the first event) was analyzed for prognostic purposes.

2.6. Statistical Analyses. Results are expressed as the mean $\pm$ SD for variables with normal distribution and the median (interquartile range (IQR)) for variables with skewed distribution. Categorical variables are presented as numbers (percentages). Data were compared by two-sample t-tests, ANOVA (subgroup analysis was conducted by Bonferroni correction), and chi-square (multiple comparison with Bonferroni-adjusted p values) when appropriate. We estimated receiver operating characteristic (ROC) curves and used Youden's index to identify the cutoff values of variables. We used C-statistic to compare the diagnostic values between curves. Follow-up data were collected as scheduled or at the last available visit. We used Cox proportional hazard models to adjust the independent value of the HOP score in predicting the first defined events (death or HF-related rehospitalization). Variables with p value < 0.05 in the univariate analysis were selected for the multivariable analysis. Hazard ratios (HRs) and 95% confidence intervals (CIs) were calculated. To compare the time-dependent outcomes, we performed Kaplan-Meier analyses with a log-rank test. All statistical analyses were two-sided and performed using SPSS software (version 22.0, SPSS, Chicago, IL, USA) and R software (version 3.5.1). A p value of < 0.05 was considered significant.

3. Results

3.1. Baseline Characteristics and Laboratory Data among Patients with Differing MET Fc. CPET and HOP measurements were conducted on 387 patients. Based on the peak MET, patients were divided into three groups, including MET Fc I, II, and III. There was a significant trend associating higher MET Fc with older patients, less often male, who had higher LVEF, heart rate, and BNP levels. Higher MET Fc was also linked to higher incidence of diabetes mellitus, ischemic etiology, and use of diuretics, along with a wider QRS complex. Higher MET Fc was associated with lower body mass index, hemoglobin, albumin, and eGFR. We found only 47% concordance between MET Fc and NYHA Fc. Of 120 patients classified as NYHA Fc I, 43 (35.8%) and 15 (12.5%) were classified as MET Fc II and III, respectively.

3.2. HOP Scores in Patients with Different MET Fc. HOP scores significantly increased from MET Fc I to III, along with decreased histidine but increased ornithine and phenylalanine (Table 1). ROC curves were conducted to compare the value of HOP scores and NYHA Fc for discriminating patients with MET Fc II and III from those with MET Fc I (Figure 1(a)). The area under the ROC curve of the HOP scores was significantly larger than that of NYHA Fc (0.78 versus 0.63, $p < 0.001$). In addition, based on Youden's index, the optimal cutoff value for HOP scores was set at 8.8 (Figure 1(b)). Of the 58 MET Fc II-III patients diagnosed as NYHA Fc I, 25 (43.1%) had a HOP score of ≥ 8.8. What a HOP score of ≥ 8.8 represents was further investigated in patients with HFrEF, HFmrEF, and HFpEF, as follows.

3.3. Differences between Patients with HOP Scores ≥ 8.8 and <8.8 in HFrEF, HFmrEF, and HFpEF. Eligibility was assessed in 1041 patients. We excluded 151 patients due to systemic disease ($n = 16$), anticipated survival < 6 months ($n = 15$), being bed ridden ($n = 33$), and creatinine > 3 mg/dl ($n = 52$). The remaining 890 HF outpatients were enrolled and followed up for one year, including 404 HFrEF patients, 168 HFmrEF, and 318 HFpEF. The patients were enrolled in the study a median of 349 days (IQR 88-1128 days) after they were discharged from the hospital. Baseline characteristics of the patients are shown in Table 2. Compared to patients with HFrEF, patients with HFmrEF had higher systolic blood pressure and cholesterol levels and a higher incidence of hypertension, atrial fibrillation, and ischemic etiology but a lower incidence of diuretics use. Patients with HFpEF had higher systolic blood pressure, body mass index, and triglyceride levels, as well as a higher incidence of atrial fibrillation and use of ACEI/ARB but a lower incidence of ischemic etiology.

The prevalence of HOP scores ≥ 8.8 was highest in the HFrEF group (61.4%), followed by the LVmrEF group (42.3%) and the HFpEF group (30.5%). In the HFrEF group, patients with a HOP score ≥ 8.8 were older, more often male, and had higher BNP levels and a wider QRS complex compared to those with a HOP score < 8.8, but they also had lower LVEF and albumin. In the HFmrEF group, those with a HOP score of ≥ 8.8 were older and had higher BNP levels compared to patients with a HOP score < 8.8,

Table 1: Demographic and laboratory data in heart failure patients in different functional classes (Fc) as defined by cardiopulmonary exercise testing.

	MET Fc I $n = 135$	MET Fc II $n = 148$	MET Fc III $n = 104$	p for trend∗
Age (years)	52.0 ± 10.5	60.0 ± 13.3	65.1 ± 10.3	<0.001
Male (%)	126 (93.3)	105 (70.9)	55 (52.9)	<0.001
LVEF (%)	42.6 ± 17.9	42.7 ± 16.8	35.8 ± 12.9	0.002
NYHA functional classification				<0.001
I (%)	62 (45.9)	43 (29.1)	15 (14.4)	
II (%)	46 (34.1)	60 (40.5)	29 (27.9)	
III (%)	27 (20)	45 (30.4)	60 (57.7)	
Blood pressure (mmHg)				
Systolic	121 ± 17.6	122 ± 20.7	121 ± 21.4	0.888
Diastolic	73.5 ± 11.4	72.3 ± 12.5	70.6 ± 12.5	0.073
Heart rate (beats/min)	71.7 ± 16.2	81.5 ± 18.2	81.1 ± 16.8	<0.001
Comorbidity				
Diabetes mellitus (%)	41 (30.4)	43 (29.1)	61 (58.7)	<0.001
Hypertension (%)	77 (57)	95 (64.2)	61 (58.7)	0.724
Atrial fibrillation (%)	24 (17.8)	48 (32.4)	17 (16.3)	0.984
COPD (%)	10 (7.4)	16 (10.8)	10 (9.6)	0.519
Ischemia (%)	69 (51.1)	82 (55.4)	79 (76)	<0.001
Body mass index (kg/m^2)	25.8 ± 3.81	25.7 ± 4.54	24.0 ± 4.99	0.003
Medication				
ACEI or ARB (%)	135 (100)	146 (98.6)	103 (99)	0.358
β-Blocker (%)	130 (96.3)	144 (97.3)	98 (94.2)	0.459
Diuretic (%)	56 (41.5)	81 (54.7)	62 (59.6)	0.004
Laboratory data				
BNP (log)	1.98 ± 0.78	2.44 ± 0.62	2.64 ± 0.58	<0.001
Cholesterol (mg/dl)	192 ± 41.6	180 ± 41.5	182 ± 37.8	0.056
Triglyceride (mg/dl)	143 ± 87.3	152 ± 107.6	146 ± 94.0	0.845
Serum sodium (mEq/l)	140 ± 2.36	139 ± 10.7	140 ± 3.99	0.942
Hemoglobin (g/dl)	14.4 ± 1.31	13.4 ± 2.05	12.9 ± 2.27	<0.001
Albumin (g/dl)	4.3 ± 0.46	4.1 ± 0.44	4.0 ± 0.47	<0.001
eGFR (ml/min/1.73 m^2)	81.6 ± 19.2	73.1 ± 25.7	56.1 ± 27.1	<0.001
QRS complex (msec)	100 ± 16.6	102 ± 21.4	118 ± 32.9	<0.001
Metabolic equivalent (MET)	6.67 ± 0.86	4.71 ± 0.49	3.36 ± 0.51	<0.001
HOP score	6.43 ± 6.36	9.06 ± 6.56	11.6 ± 7.32	<0.001
Histidine (μM)	81.2 ± 13.9	75.8 ± 13.8	72.6 ± 12.8	<0.001
Ornithine (μM)	89.5 ± 26.6	92.8 ± 38.5	106 ± 36.7	<0.001
Phenylalanine (μM)	63.3 ± 11.0	63.6 ± 11.6	70.6 ± 17.8	<0.001

ACEI: angiotensin-converting enzyme inhibitor; ARB: angiotensin receptor blocker; COPD: chronic obstructive pulmonary disease; eGFR: estimated glomerular filtration rate; HF: heart failure; HOP: histidine, ornithine, and phenylalanine; LVEF: left ventricular ejection fraction; MET Fc: functional classification defined by metabolic equivalent (MET) measured by cardiopulmonary exercise testing; NYHA: New York Heart Association. ∗Comparison of patients from Fc I to Fc III.

but they also had a lower body mass index, hemoglobin, and incidence of using beta-blockers. In the HFpEF group, those with a HOP score ≥ 8.8, were older, had higher incidence of chronic obstructive pulmonary disease, higher use of diuretics, and higher BNP compared to patients with a HOP score < 8.8 but had lower hemoglobin and incidence of ischemic etiology.

3.4. Univariate and Multivariable Analysis. During one-year follow-up, there were 12 (3%) deaths in the HFrEF group, 4

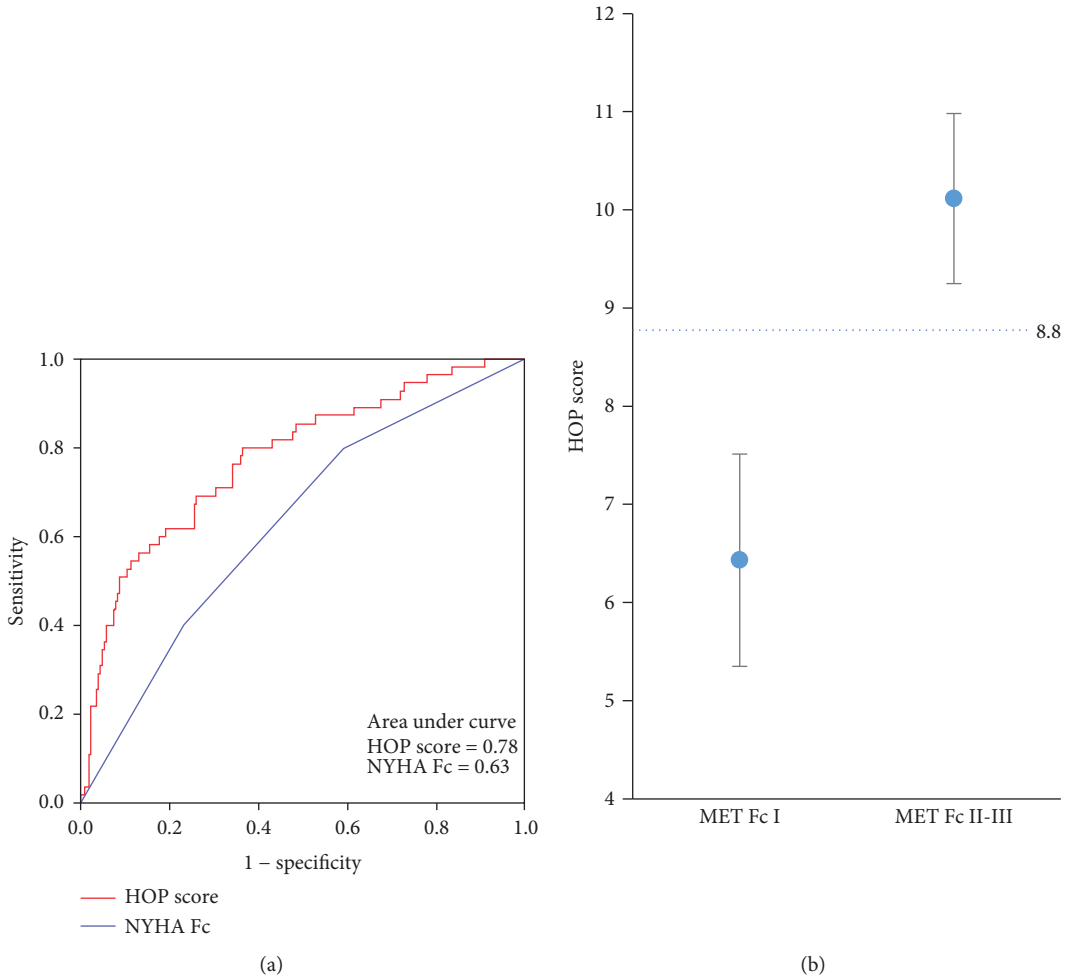

Figure 1: HOP scores in different functional classes as defined by cardiopulmonary exercise test (CPET). (a) The receiver operating characteristic (ROC) curves of the HOP score and the traditional New York Heart Association functional classification (NYHA Fc) in discriminating CPET-defined functional class ≥ II from class I. (b) The HOP score discriminates CPET-defined functional classes II and III from class I with the optimal cutoff value set at 8.8. MET Fc: functional classification defined by metabolic equivalent (MET) as measured by CPET.

(2.4%) in the HFmrEF group, and 3 (0.9%) in the HFpEF group. The numbers of patients with composite events were 89 (22%) in the HFrEF group, 20 (11.9%) in the HFmrEF group, and 28 (8.8%) in the HFpEF group. The one-year event-free survival for patients with a HOP score of ≥8.8 was 68.1% in the HFrEF group, 73.2% in the HFmrEF group, and 81.4% in the HFpEF group ($p < 0.001$). Univariate analysis shows that the predictors of one-year composite events were HOP score ≥ 8.8, age, albumin, and BNP in the HFrEF group. In the HFmrEF group, predictors were HOP score ≥ 8.8, age, body mass index, and BNP. In the HFmrEF group, predictors of one-year composite events were HOP score ≥ 8.8, age, albumin, and BNP in HFpEF (Table 3). In multivariable analysis, HOP scores ≥ 8.8 remained a one-year composite event predictor independent of other risk factors identified in the univariate analysis. Kaplan-Meier curves show that a HOP score of ≥8.8 significantly identified patients who were at higher risk of composite events in the HFrEF, HFmrEF, and HFpEF groups during the one-year follow-up period (Figure 2).

4. Discussion

This study focused on an outpatient population, ordinarily the largest group of patients we face in daily practice and the group that receives the majority of HF care. This population often does not receive optimal care due to inadequate functional assessment and lack of time. Our data show that the traditional NYHA Fc system over- or underestimates functional status. HOP scoring discriminated patients in different MET Fc categories better than NYHA Fc. A HOP score of ≥8.8 was associated with more risk factors for HF events. In addition to functional assessment, a HOP score ≥ 8.8 further identified patients at higher risk of composite events within one year in the HFrEF, HFmrEF, and HFpEF groups, independent of traditional risk factors.

4.1. Weakness of Traditional Functional Assessments. Although widely used, the NYHA Fc system has remarkable limitations. Our data showed that it underestimated MET Fc in 34.1% of patients and overestimated it in 44.2% of patients.

Table 2: Differences between patients with HOP scores ≥ 8.8 and HOP scores < 8.8 in HFrEF, HFmrEF, and HFpEF patients.

	HFrEF			HFmrEF			HFpEF			
	All $n = 404$	HOP < 8.8 $n = 156$	HOP ≥ 8.8 $n = 248$	All $n = 168$	HOP < 8.8 $n = 97$	HOP ≥ 8.8 $n = 71$	All $n = 318$	HOP < 8.8 $n = 221$	HOP ≥ 8.8 $n = 97$	p value[a]
Age (years)	61.4 ± 13.1	58.9 ± 12.4	63.0 ± 13.3 *	63.9 ± 11.5	60.4 ± 10.3	68.7 ± 11.4[#]	63.0 ± 14.4	60.6 ± 14.3	68.6 ± 13.2[#]	0.078
Male (%)	303 (75)	101 (64.7)	202 (81.5)[#]	120 (71.4)	66 (68)	54 (76.1)	223 (70.1)	149 (67.4)	74 (76.3)	0.322
LVEF (%)	27.6 ± 8.47	29.1 ± 8.19	26.7 ± 8.52[#]	44.2 ± 2.98	44.5 ± 3.12	43.9 ± 2.77	61.31 ± 7.34	60.9 ± 7.28	62.4 ± 7.40	<0.001
Blood pressure (mmHg)										
Systolic	117 ± 16.9	118 ± 17.1	116 ± 16.8	121 ± 18.2[†]	122 ± 19.1	120 ± 17.0	124 ± 15.8[‡]	124 ± 14.8	123 ± 18.0	<0.001
Diastolic	73.7 ± 11.3	74.7 ± 11.3	73.1 ± 11.3	74.5 ± 11.7	75.5 ± 12.2	73.1 ± 10.7	75.8 ± 12.2	76.5 ± 12.1	74.2 ± 12.3	0.060
Heart rate (beats/min)	76.6 ± 33.9	76.8 ± 35.6	76.5 ± 32.9	73.9 ± 33.3	74.5 ± 32.9	73.2 ± 34.1	74.4 ± 37.6	76.7 ± 36.2	69.3 ± 40.5	0.602
Comorbidities (%)										
Diabetes mellitus	177 (43.8)	61 (39.1)	116 (46.8)	84 (50)	46 (47.4)	38 (53.5)	133 (41.8)	89 (40.3)	44 (45.4)	0.219
Hypertension	250 (61.9)	98 (62.8)	152 (61.3)	122 (72.6)[†]	69 (71.1)	53 (74.6)	212 (66.7)	148 (67)	64 (66)	0.043
Atrial fibrillation	68 (16.8)	22 (14.1)	46 (18.5)	45 (26.8)[‡]	31 (32)	14 (19.7)	98 (30.8)[‡]	61 (27.6)	37 (38.1)	<0.001
COPD	30 (7.4)	13 (8.3)	17 (6.9)	16 (9.5)	6 (6.2)	10 (14.1)	24 (7.5)	9 (4.1)	15 (15.5)[#]	0.674
Ischemia	228 (56.4)	87 (55.8)	141 (56.9)	118 (70.2)[‡]	64 (66)	54 (76.1)	135 (42.5)[‡]	108 (48.9)	27 (27.8)[#]	<0.001
Body mass index (kg/m^2)	24.9 ± 4.26	25.4 ± 3.84	24.6 ± 4.48	25.5 ± 4.74	26.6 ± 4.87	24.0 ± 4.12[#]	25.8 ± 4.25[†]	25.5 ± 4.10	25.9 ± 5.58	0.023
Medication										
ACEI or ARB (%)	367 (90.8)	140 (89.7)	227 (91.5)	149 (88.7)	89 (91.8)	60 (84.5)	303 (95.3)[†]	214 (96.8)	89 (91.8)	0.019
β-Blocker (%)	350 (86.6)	134 (85.9)	216 (87.1)	152 (90.5)	92 (94.8)	60 (84.5)*	281 (88.4)	198 (89.6)	83 (85.6)	0.422
Diuretic (%)	250 (61.9)	92 (59)	158 (63.7)	80 (47.6)[‡]	49 (50.5)	31 (43.7)	175 (55)	107 (48.4)	68 (70.1)[#]	0.005
Laboratory data										
BNP (log)	2.7 ± 0.57	2.4 ± 0.58	2.9 ± 0.48[#]	2.3 ± 0.66[‡]	2.1 ± 0.59	2.6 ± 0.67[#]	1.9 ± 0.70[‡]	1.7 ± 0.61	2.4 ± 0.69[#]	<0.001
Cholesterol (mg/dl)	179 ± 45.6	182 ± 40.6	176 ± 48.5	192 ± 66.9[†]	195 ± 69.2	188 ± 63.9	189 ± 47.3[†]	193 ± 46.1	180 ± 48.8	0.003
Triglyceride (mg/dl)	118 ± 63.1	123 ± 66.2	116 ± 61.0	131 ± 95.2	137 ± 106.2	124 ± 77.9	140 ± 95.3[‡]	142 ± 92.7	135 ± 101.3	0.002
Serum sodium	139 ± 2.9	139 ± 2.9	139 ± 2.9	139 ± 3.3	138 ± 3.6	139 ± 2.7	139 ± 3.1	139 ± 3.1	139 ± 3.3	0.102
Hemoglobin (g/dl)	13.3 ± 1.9	13.0 ± 2.0	13.0 ± 1.8	13.4 ± 2.2	13.8 ± 2.2	12.9 ± 2.04[#]	13.7 ± 2.1	13.9 ± 2.12	13.2 ± 1.9[#]	0.071
Albumin (g/dl)	3.8 ± 0.53	3.9 ± 0.44	3.7 ± 0.58[#]	3.9 ± 0.52	3.9 ± 0.42	3.8 ± 0.63	3.8 ± 0.43	3.8 ± 0.45	3.8 ± 0.40	0.093
eGFR (ml/min/1.73 m^2)	71 ± 26.3	73 ± 25.4	69 ± 26.8	73 ± 33.6	76 ± 24.0	69 ± 43.2	73 ± 24.4	73.6 ± 24.1	71.9 ± 25.2	0.416
QRS complex (msec)	114 ± 28.7	110 ± 28.3	117 ± 28.7 *	106 ± 22.1[‡]	105 ± 20.6	108 ± 24.1	99 ± 24.2[‡]	98.6 ± 22.1	100.7 ± 28.4	<0.001
HOP score	10.5 ± 7.42	3.6 ± 4.37	14.8 ± 5.41[#]	8.1 ± 6.29[‡]	3.9 ± 3.50	13.9 ± 4.25[#]	6.5 ± 6.19[‡]	3.4 ± 4.10	13.6 ± 3.86[#]	<0.001
Histidine (μM)	74.2 ± 14.1	80.1 ± 12.3	70.5 ± 14.0[#]	75.0 ± 14.1	81.9 ± 10.6	67.9 ± 14.3[#]	79.9 ± 14.2[‡]	83.6 ± 12.6	71.5 ± 14.1[#]	<0.001
Ornithine (μM)	101 ± 40.9	85.8 ± 26.5	111 ± 45.24[#]	97.4 ± 30.8	87.6 ± 20.1	111 ± 37.4[#]	91.6 ± 30.9[‡]	83.8 ± 24.7	109 ± 36.0[#]	0.002
Phenylalanine (μM)	67.2 ± 15.9	59.4 ± 10.3	72.1 ± 16.8[#]	65.2 ± 13.6	61.7 ± 9.8	69.9 ± 16.5[#]	64.5 ± 12.5[†]	62.3 ± 9.94	69.6 ± 15.8[#]	0.034

ACEI: angiotensin-converting enzyme inhibitor; ARB: angiotensin receptor blocker; COPD: chronic obstructive pulmonary disease; HF: heart failure; HOP: histidine, ornithine, and phenylalanine; LVEF: left ventricular ejection fraction; LVrEF: LVEF < 40%, LVmrEF: LVEF = 40%–49%, LVpEF: LVEF ≥ 50%.*$p < 0.05$ and [#]$p < 0.01$, compared to patients with HOP score < 8.8. [†]$p < 0.05$ and [‡]$p < 0.01$, compared to patients with LVrEF. [a]ANOVA p value to compare LVrEF, LVmrEF, and LVpEF.

Table 3: COX univariate and multivariable analysis in HFrEF, HFmrEF, and HFpEF patients.

	HFrEF		HFmrEF		HFpEF	
	Univariate HR (95% CI)	Multivariable HR (95% CI)	Univariate HR (95% CI)	Multivariable HR (95% CI)	Univariate HR (95% CI)	Multivariable HR (95% CI)
HOP score ≥ 8.8	5.78 (2.99-11.16)†	3.80 (1.56-9.25)†	29.95 (4.01-103)†	9.60 (1.12-62.3)*	4.48 (2.07-9.70)†	3.05 (1.09-8.57)*
Age (years)	1.03 (1.01-1.45)†	1.02 (1.01-1.04)*	1.05 (1.01-1.09)*	0.97 (0.92-1.02)	1.04 (1.01-1.07)*	1.01 (0.97-1.05)
Sex	1.46 (0.86-2.48)		1.18 (0.43-3.25)		1.59 (0.65-3.93)	
LVEF (%)	0.99 (0.96-1.01)		0.85 (0.72-1.01)		0.99 (0.94-1.04)	
Hypertension	1.38 (0.88-2.15)		3.62 (0.84-15.58)		39.9 (1.56-102)	
Diabetes mellitus	1.02 (0.67-1.55)		2.40 (0.92-6.25)		1.90 (0.90-4.03)	
COPD	0.70 (0.28-1.73)		0.49 (0.067-3.67)		2.17 (0.75-6.26)	
Ischemic	1.35 (0.88-2.07)		0.76 (0.30-1.91)		0.64 (0.29-1.41)	
BMI (kg/m^2)	0.97 (0.92-1.02)		0.84 (0.75-0.93)†	0.93 (0.82-1.05)	0.98 (0.90-1.07)	
Cholesterol (mg/dl)	1.00 (0.99-1.01)		1.00 (0.99-1.01)		1.00 (0.99-1.01)	
Triglyceride (mg/dl)	1.00 (0.99-1.01)		1.00 (0.99-1.01)		1.00 (0.99-1.01)	
Serum sodium (mEq/l)	0.99 (0.99-1.00)		0.99 (0.99-1.00)		1.01 (0.99-1.03)	
Albumin (g/dl)	0.36 (0.25-0.52)†	0.41 (0.25-0.65)†	0.46 (0.20-1.06)		0.37 (0.16-0.83)*	0.40 (0.17-0.95)*
QRS (msec)	1.00 (0.99-1.01)		0.99 (0.98-1.01)		0.99 (0.98-1.00)	
BNP (log)	3.84 (2.26-6.53)†	2.02 (1.16-3.50)*	8.27 (2.30-29.66)†	3.36 (1.02-11.0)*	2.15 (1.04-4.46)*	1.47 (0.63-3.43)

*$p < 0.05$ and †$p < 0.01$ in the COX univariate and multivariable analysis. CI: confidence interval; COPD: chronic obstructive pulmonary disease; HF: heart failure; HOP: histidine, ornithine, and phenylalanine; HR: hazard ratio; LVEF: left ventricular ejection fraction; LVrEF: LVEF < 40%; LVmrEF: LVEF = 40% −49%; LVpEF: LVEF ≥ 50%.

It is noteworthy that 12.5% of patients classified as NYHA Fc I were actually MET Fc III. Cardiologists' subjective assessment or recognition of patients substantially interferes with NYHA Fc results. Importantly, the criteria committee of the NYHA described the NYHA Fc as "only approximate" and "representative of an expression of the physician's opinion" [7]. A previous interoperator variability study showed only 54% concordance between two cardiologists [4]. Most cardiologists asked patients about their walking ability; however, their self-reported walking status correlated poorly with their actual exercise capacity as measured by CPET. Although CPET is the gold standard, its use is greatly limited by its inconvenience. The reliability of the six min walking test has been shown to be high in patients with stable HF; however, results are affected by a variety of factors unrelated to HF status, including age, sex, height, weight, respiratory disease, peripheral arterial disease, musculoskeletal problems, depression, cognitive impairment, and fear of developing symptoms during the test [24]. By contrast, HOP can be used in patients with limited ability to perform an exercise test and can also avoid most sources of interference that affect NYHA functional classification.

4.2. The Value of HOP. Functional capacity actually represents the imbalance between the demand of the body and supply provided by the heart. Previous studies showed that metabolic status, as estimated by metabolomics in plasma, delineated HF metabolic disturbance and provided better prognostic value than BNP and gelactin-3 [8, 9, 16]. After simplifying the complex findings of plasma metabolomics into a HOP score, we noted that HOP retained diagnostic and prognostic value for HF, compensated the weakness of BNP, and was correlated with functional capacity as assessed by six min walk tests [16]. The current study further proves that HOP scores can discriminate functional classifications based on CPET.

The cutoff of 8.8 for HOP scoring not only identified patients with MET Fc ≥ II but also provided value for prognosis. A higher HOP score represented worse prognosis in HFrEF, HFmrEF, and HFpEF. Consistent with our previous studies on HFrEF, HOP scores ≥ 8.8 were related to older patients and higher BNP levels in all three HF populations [16]. In addition, in HFrEF, HOP scores ≥ 8.8 also identified those with a lower LVEF and malnutrition. Compared to HFrEF, in HFmrEF, more patients had atrial fibrillation and ischemic etiology. A HOP score of ≥8.8 in HFmrEF was associated with lower body mass index and hemoglobin, which are well known as factors in poor prognosis. Similar to HFmrEF, HFpEF also entailed a higher incidence of atrial fibrillation than HFrEF. Furthermore, HOP scores of ≥8.8 were associated with a higher incidence of lung disease and using diuretics but with lower hemoglobin, suggesting more comorbidities and more severe symptoms.

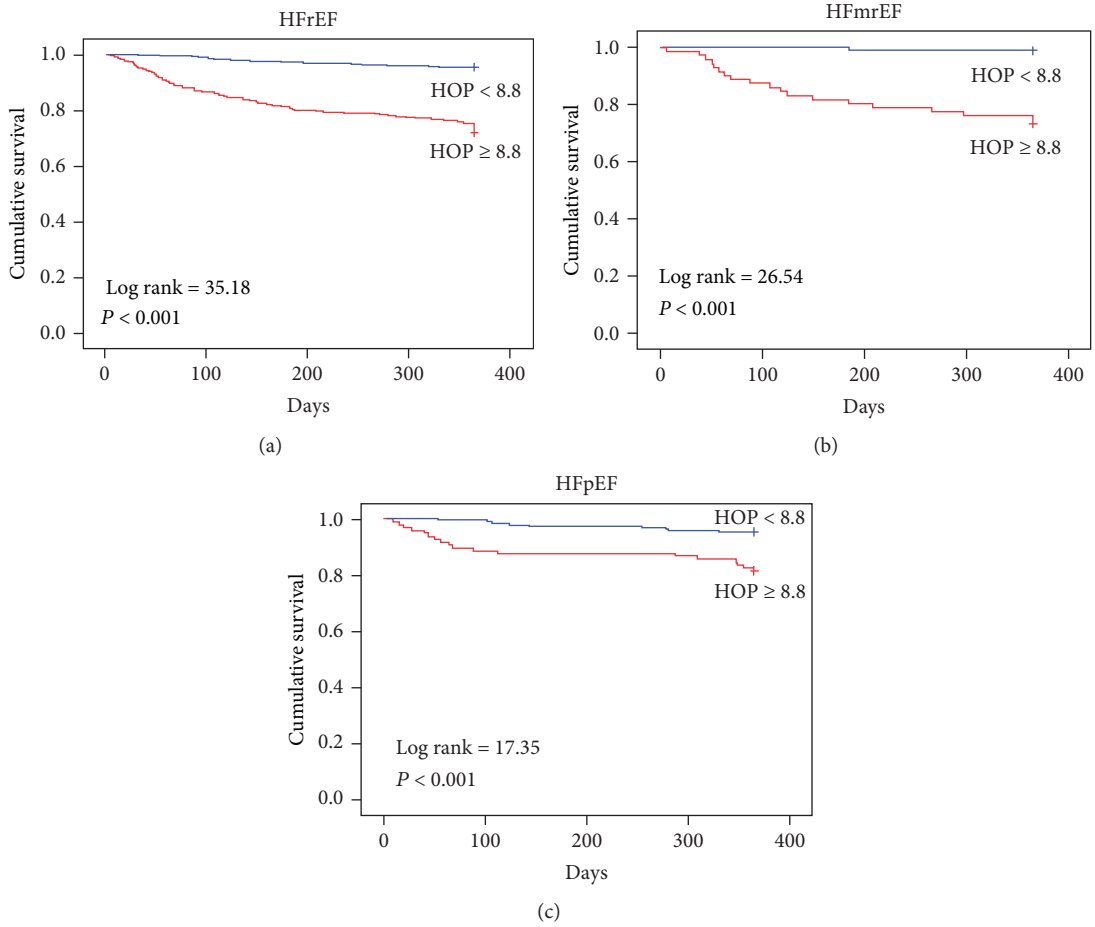

Figure 2: Prognostic value of the HOP score in different populations of heart failure (HF) patients. Kaplan Meier curves for HOP ≥ 8.8 versus <8.8 in HF with reduced ejection fraction (EF) (a), HF with midrange EF (b), and HF with preserved EF (c).

It is also interesting to consider the mechanisms that account for decreased histidine but increased phenylalanine and ornithine, which were correlated with functional classification. Previous studies have shown that increased phenylalanine levels are associated with increased muscular protein breakdown, nitric oxide synthesis dysregulation, and tetrahydrobiopterin depletion [16, 25–27]. To produce energy for cardiac tissues, histidine is converted to glutamate and enters the glutamate-ornithine-proline pathway or the Krebs cycle [8, 16]. Lower histidine levels can represent substantial histidine deficiency, since a large amount of histidine pools in hemoglobin and carnosine in the muscle [28]. Increased ornithine, an important component of the urea cycle, also indicates overload handling of the waste from using amino acids from muscular protein as an energy source. These mechanisms explain the tight link between HOP score and functional status.

4.3. Study Limitations. A few limitations are to be noted in this study. First, our data showed a significant trend revealing that a higher proportion of patients classed as MET Fc III was female. This could be caused by sex-related performance on CPET. However, metabolism-based assessment may be a substitute. Future studies may investigate how to apply HOP scores to different sexes. Second, our analyses are based on data from patients who are able to perform CPET. Whether the findings noted in this study can be applied to those unable to perform CPET requires further study. Finally, the correlation between the HOP score and METs was established based on a cohort of chronic HF patients. The value of HOP scores in patients with acute HF remains to be explored.

5. Conclusions

The traditional NYHA Fc assessment system under- and overestimates the MET Fc of a substantial number of HF outpatients. An amino acid-based metabolic profile (HOP score) provides a measure of the metabolic status that correlates with the functional status as estimated by CPET better than the NYHA Fc system. A HOP score of ≥8.8 identifies HF patients in the functional class ≥ II and at risk of HF-related events. Our data also proves that the HOP score ≥ 8.8 has prognostic value not only in HFrEF but also for patients with HFmrEF and HFpEF, providing evidence that patients with the functional class ≥ II warrant aggressive treatment. The value of utilizing the HOP score as a follow-up assessment tool merits further study.

Data Availability

The data that support the findings of this study are available from the corresponding author on reasonable request.

Conflicts of Interest

The authors declare that they have no conflict of interest.

Acknowledgments

This study was supported in part by the Ministry of Science and Technology of Taiwan (MOST107-2314-B-182-071-MY2), Chang Gung Memorial Hospital (CMRPG2G0601, 2G0611, 2G0641, and CORPG2J0021), and the Taiwan Ministry of Education (EMRPD1G0251, EMRPD1H0401). The authors thank the Cardiology Section, Department of Internal Medicine, Chang Gung Memorial Hospital, Keeling, Taiwan, for providing samples from patients. We also thank the Healthy Aging Research Center, Chang Gung University, from the Featured Areas Research Center Program within the Framework of the Higher Education Sprout Project by the Taiwan Ministry of Education.

References

[1] J. J. V. McMurray, M. Packer, A. S. Desai et al., "Angiotensin–neprilysin inhibition versus enalapril in heart failure," *New England Journal of Medicine*, vol. 371, no. 11, pp. 993–1004, 2014.

[2] F. Zannad, J. McMurray, H. Krum et al., "Eplerenone in patients with systolic heart failure and mild symptoms," *New England Journal of Medicine*, vol. 364, no. 1, pp. 11–21, 2011.

[3] C. Lucas, L. W. Stevenson, W. Johnson et al., "The 6-min walk and peak oxygen consumption in advanced heart failure: aerobic capacity and survival," *American Heart Journal*, vol. 138, no. 4, pp. 618–624, 1999.

[4] C. Raphael, C. Briscoe, J. Davies et al., "Limitations of the New York Heart Association functional classification system and self-reported walking distances in chronic heart failure," *Heart*, vol. 93, no. 4, pp. 476–482, 2007.

[5] J. Dunagan, J. Adams, D. Cheng et al., "Development and evaluation of a treadmill-based exercise tolerance test in cardiac rehabilitation," *Baylor University Medical Center Proceedings*, vol. 26, no. 3, pp. 247–251, 2013.

[6] M. Jetté, K. Sidney, and G. Blümchen, "Metabolic equivalents (METS) in exercise testing, exercise prescription, and evaluation of functional capacity," *Clinical Cardiology*, vol. 13, no. 8, pp. 555–565, 1990.

[7] Criteria Committee and New York Heart Association, Inc, *Diseases of the Heart and Blood Vessels. Nomenclature and Criteria for Diagnosis*, vol. 114, Brown and Co, Boston, Little, 6th edition, 1964.

[8] M. L. Cheng, C. H. Wang, M. S. Shiao et al., "Metabolic disturbances identified in plasma are associated with outcomes in patients with heart failure: diagnostic and prognostic value of metabolomics," *Journal of the American College of Cardiology*, vol. 65, no. 15, pp. 1509–1520, 2015.

[9] C. H. Wang, M. L. Cheng, M. H. Liu, L. T. Kuo, and M. S. Shiao, "Metabolic profile provides prognostic value better than galectin-3 in patients with heart failure," *Journal of Cardiology*, vol. 70, no. 1, pp. 92–98, 2017.

[10] H. Y. Tang, C. H. Wang, H. Y. Ho et al., "Lipidomics reveals accumulation of the oxidized cholesterol in erythrocytes of heart failure patients," *Redox Biology*, vol. 14, pp. 499–508, 2018.

[11] W. G. Hunter, J. P. Kelly, R. W. McGarrah, W. E. Kraus, and S. H. Shah, "Metabolic dysfunction in heart failure: diagnostic, prognostic, and pathophysiologic insights from metabolomic profiling," *Current Heart Failure Reports*, vol. 13, no. 3, pp. 119–131, 2016.

[12] D. Alexander, R. Lombardi, G. Rodriguez, M. M. Mitchell, and A. J. Marian, "Metabolomic distinction and insights into the pathogenesis of human primary dilated cardiomyopathy," *European Journal of Clinical Investigation*, vol. 41, no. 5, pp. 527–538, 2011.

[13] L. Tenori, X. Hu, P. Pantaleo et al., "Metabolomic fingerprint of heart failure in humans: a nuclear magnetic resonance spectroscopy analysis," *International Journal of Cardiology*, vol. 168, no. 4, pp. e113–e115, 2013.

[14] C. H. Wang, M. L. Cheng, M. H. Liu et al., "Increased p-cresyl sulfate level is independently associated with poor outcomes in patients with heart failure," *Heart Vessels*, vol. 31, no. 7, pp. 1100–1108, 2016.

[15] P. Würtz, A. S. Havulinna, P. Soininen et al., "Metabolite profiling and cardiovascular event risk: a prospective study of 3 population-based cohorts," *Circulation*, vol. 131, no. 9, pp. 774–785, 2015.

[16] C. H. Wang, M. L. Cheng, and M. H. Liu, "Amino acid-based metabolic panel provides robust prognostic value additive to B-natriuretic peptide and traditional risk factors in heart failure," *Disease Markers*, vol. 2018, Article ID 3784589, 11 pages, 2018.

[17] C. H. Wang, M. L. Cheng, and M. H. Liu, "Simplified plasma essential amino acid-based profiling provides metabolic information and prognostic value additive to traditional risk factors in heart failure," *Amino Acids*, vol. 50, no. 12, pp. 1739–1748, 2018.

[18] P. Ponikowski, A. A. Voors, S. D. Anker et al., "2016 ESC guidelines for the diagnosis and treatment of acute and chronic heart failure: the task force for the diagnosis and treatment of acute and chronic heart failure of the European Society of Cardiology (ESC)developed with the special contribution of the Heart Failure Association (HFA) of the ESC," *European Journal of Heart Failure*, vol. 37, no. 27, pp. 2129–2200, 2016.

[19] A. S. Maisel, P. Clopton, P. Krishnaswamy et al., "Impact of age, race, and sex on the ability of B-type natriuretic peptide to aid in the emergency diagnosis of heart failure: results from the Breathing Not Properly (BNP) multinational study," *American Heart Journal*, vol. 147, no. 6, pp. 1078–1084, 2004.

[20] A. Pappa-Louisi, P. Nikitas, P. Agrafiotou, and A. Papageorgiou, "Optimization of separation and detection of 6-aminoquinolyl derivatives of amino acids by using reversed-phase liquid chromatography with on line UV, fluorescence and electrochemical detection," *Analytica Chimica Acta*, vol. 593, no. 1, pp. 92–97, 2007.

[21] M. P. Frank and R. W. Powers, "Simple and rapid quantitative high-performance liquid chromatographic analysis of plasma amino acids," *Journal of Chromatography B*, vol. 852, no. 1-2, pp. 646–649, 2007.

[22] M. Miyamara and Y. Honda, "Oxygen intake and cardiac output during maximal treadmill and bicycle exercise," *Journal of Applied Physiology*, vol. 32, no. 2, pp. 185–188, 1972.

[23] H. N. Williford, K. Sport, N. Wang, M. S. Olson, and D. Blessing, "The prediction of fitness levels of United States Air Force officers: validation of cycle ergometry," *Military Medicine*, vol. 159, no. 3, pp. 175–178, 1994.

[24] C. Demers, R. McKelvie, A. Negassa, S. Yusuf, and RESOLVD Pilot Study Investigators, "Reliability, validity, and responsiveness of the six-minute walk test in patients with heart failure," *American Heart Journal*, vol. 142, no. 4, pp. 698–703, 2001.

[25] Y. Nishijima, A. Sridhar, I. Bonilla et al., "Tetrahydrobiopterin depletion and NOS2 uncoupling contribute to heart failure-induced alterations in atrial electrophysiology," *Cardiovascular Research*, vol. 91, no. 1, pp. 71–79, 2011.

[26] M. T. Ziolo, L. S. Maier, V. Piacentino III, J. Bossuyt, S. R. Houser, and D. M. Bers, "Myocyte nitric oxide synthase 2 contributes to blunted β-adrenergic response in failing human hearts by decreasing Ca^{2+} transients," *Circulation*, vol. 109, no. 15, pp. 1886–1891, 2004.

[27] R. Aquilani, M. T. la Rovere, O. Febo et al., "Preserved muscle protein metabolism in obese patients with chronic heart failure," *International Journal of Cardiology*, vol. 160, no. 2, pp. 102–108, 2012.

[28] W. Kriengsinyos, M. Rafii, L. J. Wykes, R. O. Ball, and P. B. Pencharz, "Long-term effects of histidine depletion on whole-body protein metabolism in healthy adults," *The Journal of Nutrition*, vol. 132, no. 11, pp. 3340–3348, 2002.

Hindawi
Disease Markers
Volume 2019, Article ID 6121696, 10 pages
https://doi.org/10.1155/2019/6121696

Research Article

Circulating MicroRNA-499 as a Diagnostic Biomarker for Acute Myocardial Infarction: A Meta-analysis

Jingyi Zhao,[1] Hairong Yu,[1] Peng Yan,[2] Xiaohui Zhou,[2] Ying Wang,[3] and Yinhui Yao[3]

[1]*Department of Functional Center, Chengde Medical College, Chengde 067000, China*
[2]*School of Basic Medicine, Chengde Medical College, Chengde 067000, China*
[3]*Department of Pharmacy, Affiliated Hospital of Chengde Medical College, Chengde 067000, China*

Correspondence should be addressed to Yinhui Yao; yaoyh_gc@163.com

Received 25 November 2018; Revised 11 March 2019; Accepted 2 April 2019; Published 2 May 2019

Guest Editor: Agata M. Bielecka-Dabrowa

Background. Recent studies have shown that circulating microRNA-499 could be a powerful biomarker of acute myocardial infarction (AMI). Interest in circulating microRNA-499 for detecting AMI is increasing rapidly. To evaluate the diagnosis of circulating microRNA-499 for AMI, this study was performed. *Methods*. We searched PubMed, Embase, and the Cochrane Library for studies published up to December 31, 2018, as well as the reference lists of relevant studies. Studies were included if they assessed the accuracy of blood circulating microRNA-499 or cardiac troponin T (cTnT) for AMI and provided sufficient data to construct a 2×2 contingency table. Extracted data were analysed for sensitivity, specificity, diagnostic odds ratio (DOR), and summary receiver operator curve (SROC) analyses. Prespecified subgroup analysis and metaregression were also performed. *Results*. Fourteen studies including 3816 participants were included in this meta-analysis. The overall pooled sensitivity and specificity were 0.84 (95% CI: 0.64-0.94) and 0.97 (95% CI: 0.90-0.99), respectively. The area under the SROC curve (AUC) was 0.98 (95% CI: 0.96-0.99). The studies had substantial heterogeneity ($I^2 = 98.74\%$). Seven studies also used cTnT as a marker for the diagnosis of AMI. The overall pooled sensitivity and specificity of cTnT were 0.95 (95% CI: 0.87-0.98) and 0.96 (95% CI: 0.85-0.99), respectively. The area under the SROC curve (AUC) was 0.99 (95% CI: 0.97-0.99). The DOR of circulating miR-499 and cTnT were 188 (95% CI: 19-1815) and 420 (95% CI: 86-2038), respectively. Metaregression analysis suggested that specimen and healthy controls were the main sources of heterogeneity. No publication bias was suggested by Deeks' regression test of asymmetrical funnel plot ($t = 0.85$; p value $= 0.41$). *Conclusion*. The results showed that circulating microRNA-499 is a reliable biomarker for diagnosing AMI patients.

1. Introduction

Acute myocardial infarction (AMI), which is the most common cause of death worldwide, is an acute necrosis caused by continued severe ischemia of the myocardial tissue. In 2020, an estimated 16 million people will suffer from AMI, and about 23 million people will suffer in 2030 [1]. Thus, rapid and accurate diagnosis of AMI plays a crucial role in therapy and prognosis, which would reduce morbidity and mortality of this disease. Currently, the usefulness of myocardial circulating biomarkers, such as cardiac troponin T (cTnT) and creatine kinase MB (CK-MB), maximizes the benefits of revascularization therapy, as the most effective biomarkers in clinical practice [2, 3]. However, there is still a relatively low diagnostic accuracy earlier than 4-8 h after the onset of AMI. The biomarkers of cTnT and CK-MB are likely to increase, whether AMI occurs or not [4, 5]. Previous studies also showed that the significant levels of cTnT were identified only around 6 hours, resulting in new biomarkers for extremely early diagnosis [6]. Thus, exploring novel biomarkers with both high sensitivity and specificity for AMI is urgently required.

MicroRNAs (miRNAs/miRs), a class of small (19-25 nucleotides) noncoding RNAs, are important posttranscriptional regulators of numerous biological processes including cell growth, proliferation, differentiation, and apoptosis [7]. The expression profile of miRNAs was found in tissue-specific or cell-specific distributions [8]. Recently, a number

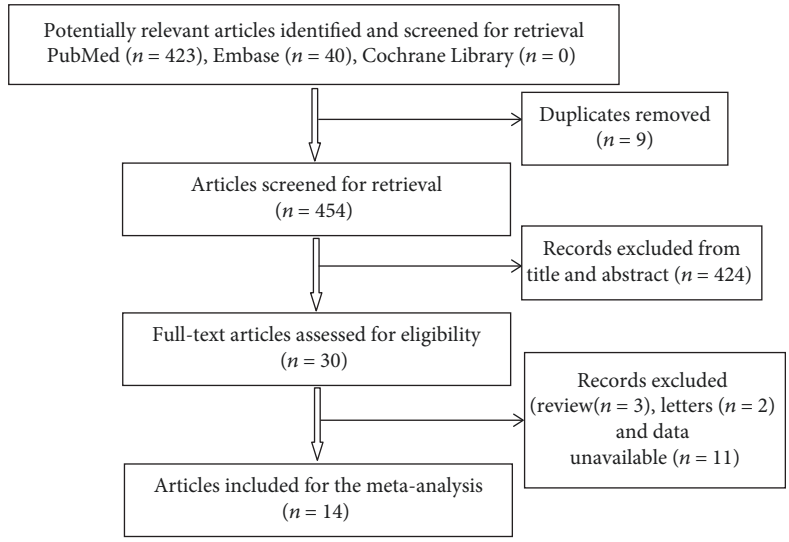

Figure 1: Flow chart of systematic literature search.

Table 1: Information of the included studies.

Author	Year	Country	Specimen	Case/control	Biomarkers	Sensitivity	Specificity
Corsten et al. [15]	2010	Luxembourg	Plasma	32/36	miR-499	84	95
Wang et al. [16]	2010	China	Plasma	33/33	miR-499	36.4	100
Devaux et al. [17]	2012	Luxembourg	Plasma	510/87	miR-499	100	100
Gidlöf et al. [18]	2013	Sweden	Plasma	319/88	miR-499	64	90
					cTnT	95	85
Li et al. [19]	2013	China	Plasma	67/32	miR-499	80	94
					cTnT	96	100
Devaux et al. [20]	2015	Luxembourg	Plasma	224/931	miR-499	35.7	90.3
					cTnT	70	96
Ji et al. [21]	2015	China	Serum	98/23	miR-499	53	100
					cTnT	94	82
Liu et al. [22]	2015	China	Plasma	70/72	miR-499	82.1	94
Zhao et al. [23]	2015	China	Plasma	59/60	miR-499	86.37	93.47
					cTnT	93.12	100
Zhang et al. [24]	2015	China	Plasma	142/85	miR-499	80	80.28
					cTnT	100	82
Shalaby et al. [25]	2016	Egypt	Serum	48/25	miR-499	93.4	100
Agiannitopoulos et al. [26]	2017	Egypt	Serum	110/121	miR-499	75	97.2
Fawzy et al. [27]	2018	Greece	Plasma	80/50	miR-499	98	100
					cTnT	94	100
Liu et al. [28]	2018	China	Plasma	145/30	miR-499	98	100

of studies reported that microRNAs are circulating in plasma/serum and can be considered as biomarkers in cardiovascular disease [9]. MicroRNA-499, a member of the microRNA family, has been shown to be expressed in myocardium and skeletal muscle in mammals [10]. Previous to this, some studies have showed that the sample of blood from AMI patients with the high expression level of microRNA-499 can be detected earlier [11]. So, its correlation suggests that the interplay of the specific circulating microRNA-499 and the development of cardiovascular disease might be useful diagnosis biomarkers and therapeutic targets for AMI [12]. Owing to studies with small sample sizes and controversial issues, we conducted the current evidence regarding the use of circulating microRNA-499 for the identification of AMI by performing a meta-analysis.

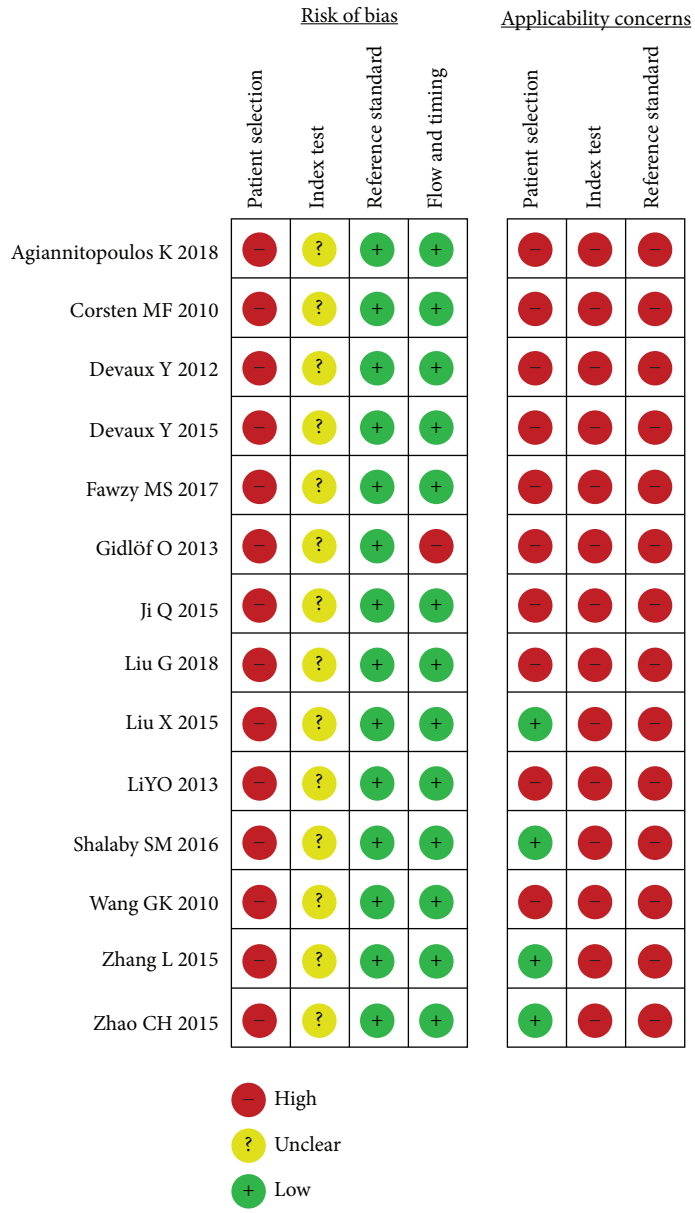

Figure 2: Risk of bias and applicability concern graph.

2. Methods

2.1. Search Strategy. Give attention to the three electronic databases (PubMed, Embase, and Cochrane Library) that clinical studies reported on the diagnostic accuracy of circulating microRNA-499 for AMI and published through December 31, 2018. The search keywords were "circulating microRNA-499" in combination with "acute myocardial infarction" or "AMI". There were no publication dates or language restrictions. The reference lists of all relevant review articles also were retrieved, and only raw data were used for further analysis. All relevant articles are based on previously published studies; thus, unpublished studies were not searched.

Studies were considered eligible if they were case-control studies that reported the diagnostic accuracy measures of the circulating microRNA-499 (or cTnT) in patients with AMI as the case group and non-AMI patients as the control group. Eligible studies contained sufficient information for the construction of 2×2 contingency tables to assess the diagnosis value of circulating microRNA-499 in AMI patients in the meta-analysis. The excluded studies are as follows: (a) review articles, (b) case reports, (c) editorials, (d) conference abstracts, and (e) clinical protocol.

2.2. Quality Assessment. We systematically assessed the quality of the studies included in the diagnostic meta-analysis with the Quality Assessment of Diagnostic Accuracy Studies-2 (QUADAS-2) tool [13].

2.3. Data Extraction. According to a standardized form, two reviewers independently extracted data from the eligible

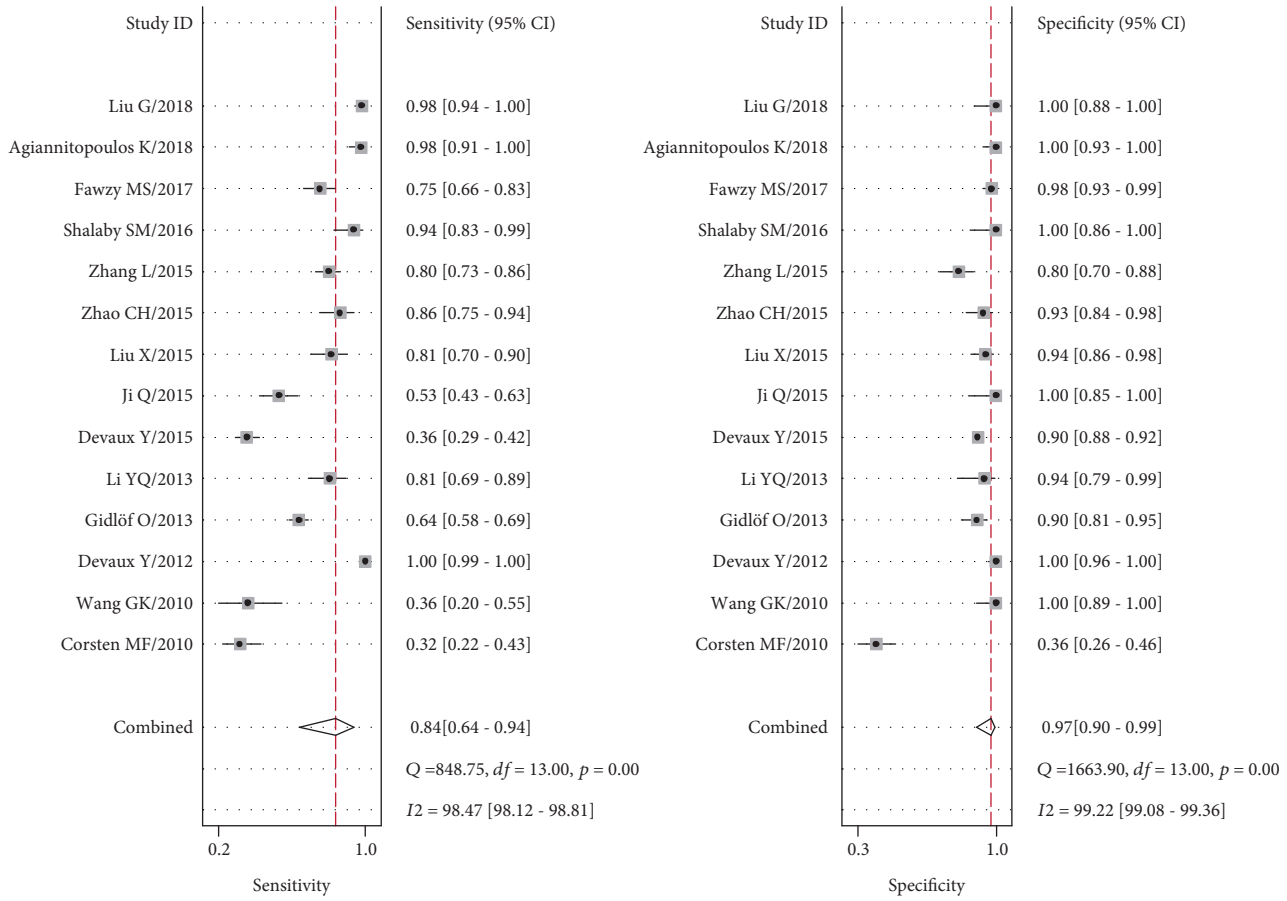

Figure 3: Forest plots for sensitivity and specificity for studies using circulating microRNA-499 to detect among patients with acute myocardial infarction.

studies and recorded information. If there was a disagreement regarding a particular article's eligibility for the analysis, it was better to be resolved by consensus. The elements of extracting data from the included studies are the author's name, the year of publication, the country of origin, the number of cases and controls, biomarkers, and the sensitivity and specificity of the indicated biomarker for the diagnosis of AMI.

2.4. Statistical Methods. The MIDAS module of STATA 14.0 (StataCorp, College Station, Texas, USA) and Meta-DiSc 1.4 (XI Cochrane Colloquium, Barcelona, Spain) were used for statistical analysis. In order to assess the overall diagnostic value of miR-499 in distinguishing AMI patients from controls, the pooled sensitivity, specificity, positive likelihood ratio (PLR), negative likelihood ratio (NLR), diagnostic odds ratio (DOR), the bivariate summary receiver operator characteristic (SROC) curve, and the area under the curve (AUC) were calculated. Statistical heterogeneity among the studies was assessed using I^2 statistics. Values of 25%, 50%, and 75% for the I^2 test were considered low, medium, and high statistical heterogeneities, respectively. Metaregression analysis was performed to find the effect of potential heterogeneity in sensitivity and specificity. To assess the publication bias of the included studies, we performed Deeks' regression test of funnel plot asymmetry [14]. A p value of <0.05 was considered statistically significant.

3. Results

3.1. Data Selection and Study Characteristics. Our initial search yielded 463 articles, of which 424 were eliminated after screening the title and abstract. We scrutinized 30 studies for full-text review and identified 14 studies that fulfilled our eligibility criteria (Figure 1). Overall, a total of 3816 patients were included from the 14 studies, 1989 of whom had AMI and 1732 of whom had non-AMI [15–28]. Among these 14 studies, 11 used plasma samples, whereas the rest used serum. The included studies were performed in China, Luxembourg, Sweden, Egypt, and Greece. Table 1 presents the detailed characteristics of each subject.

3.2. Quality of the Included Studies. QUADAS-2 quality assessment of the included studies and the results of critical appraisal are shown in Figure 2. The quality of all studies was considered mediocre. All the included studies did not describe fully the methods of patient selection, most notably with respect to whether a consecutive or random sample of patients was enrolled. We found no mention of a threshold of circulating miR-499 for AMI patient in terms of its

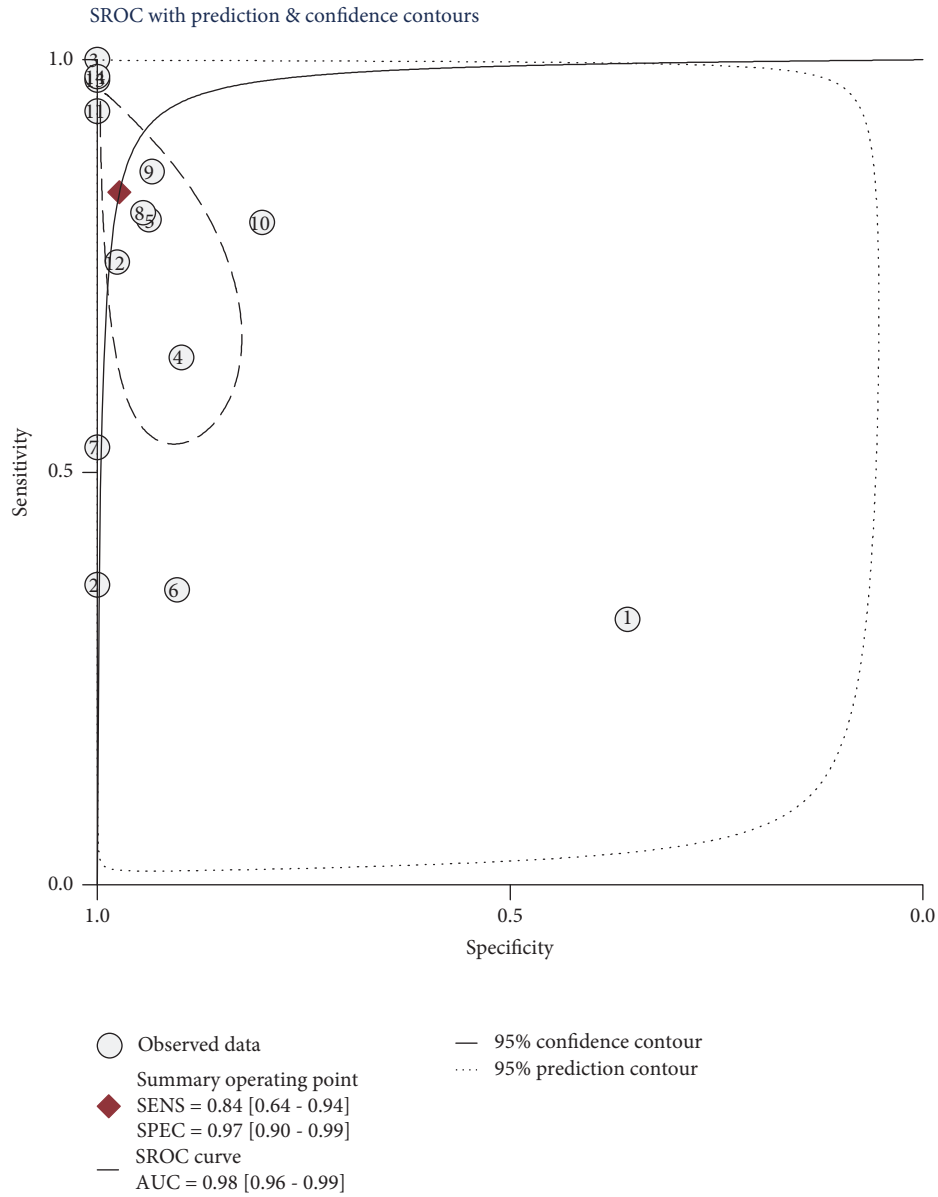

Figure 4: Symmetrical summary receiver operator curve (SROC) of circulating miR-499 for all 14 studies.

prespecificity in all the included studies. Many studies did explicitly state severity of the target condition, demographic features, and the presence of differential diagnosis [15–21, 26–28].

3.3. Diagnostic Accuracy. The pooled sensitivity and specificity estimates for the circulating miR-499 were 0.84 (95% CI: 0.64-0.94) and 0.97 (95% CI: 0.90-0.99), respectively (Figure 3). The pooled PLR was 31.1 (95% CI: 6.9-140.3), and the pooled NLR was 0.17 (95% CI: 0.07-0.41). The DOR was 188 (95% CI: 19-1815), indicating better discriminatory test performance. The area under the SROC curve for circulating miR-499 was 0.98 (95% CI: 0.96-0.99), indicating a high accuracy (Figure 4). The pooled sensitivity of cTnT for the diagnosis of AMI was 0.95 (95% CI: 0.87–0.98), and the pooled specificity of AMI for the diagnosis of AMI was 0.96 (95% CI: 0.85–0.99). The pooled PLR was 23.5 (95% CI: 5.8-94.8), and the pooled NLR was 0.06 (95% CI: 0.02-0.14). The area under the SROC curve was 0.99 (95% CI: 0.97-0.99), and the DOR was 420 (95% CI: 86-2038). Taking all of the findings into consideration, circulating miR-499 can be provided with highly diagnostic accuracy as well as cTnT to distinguish AMI from non-AMI.

3.4. Heterogeneity Analysis and Subgroup Analysis. The results of significant heterogeneity were observed among included studies. For all 14 studies, the heterogeneity (I^2) was 98.47% (sensitivity) and 99.22% (specificity).

The source of heterogeneity was completely examined by metaregression analysis using study covariates such as location, specimen, patient size, healthy controls, and cTnT. To examine the source of heterogeneity completely by making

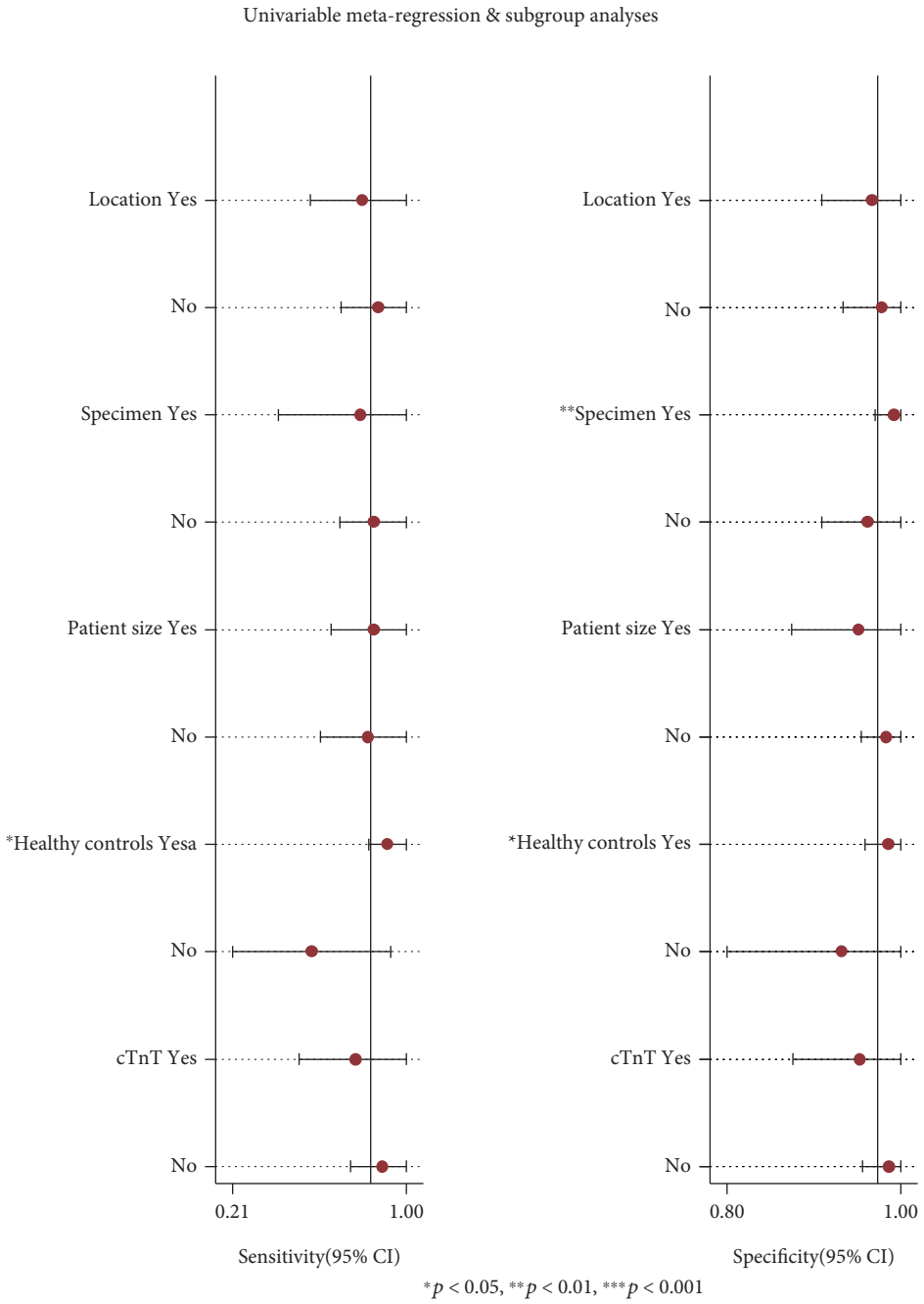

Figure 5: Univariable metaregression and subgroup analyses.

each covariate associate with logit (sensitivity) and logit (specificity), metaregression analysis showed that healthy controls were the most important of sources of heterogeneity (Figure 5). When exploring the source of heterogeneity by making study covariate associate with logit (specificity), metaregression analysis showed that the specimen significantly accounted for the heterogeneity for specificity. According to the specified groups, a subgroup analysis was performed to assess differences in diagnostic accuracy by healthy controls. The nine studies that reviewed healthy controls showed a high-pooled sensitivity (0.91, 95% CI: 0.83-1.00) and specificity (0.99, 95% CI: 0.96-1.00). In contrast, the rest of the five studies performed in nonhealthy controls showed a low-pooled sensitivity (0.57, 95% CI: 0.21-0.93), but the specificity was high (0.91, 95% CI: 0.80-1.00). Subgroup analysis by plasma showed a low-pooled sensitivity (0.85, 95% CI: 0.70-1.00) but a high-pooled specificity (0.96, 95% CI: 0.91-1.00). The remaining 3 studies of serum of the pool had sensitivity and specificity of 0.79 (95% CI: 0.42-1.00) and 0.99 (95% CI: 0.97-1.00), respectively.

3.5. Publication Bias. Deeks' funnel plot asymmetry test suggested no potential publication bias with asymmetry in our study data ($t = 0.85$; p value = 0.41) (Figure 6).

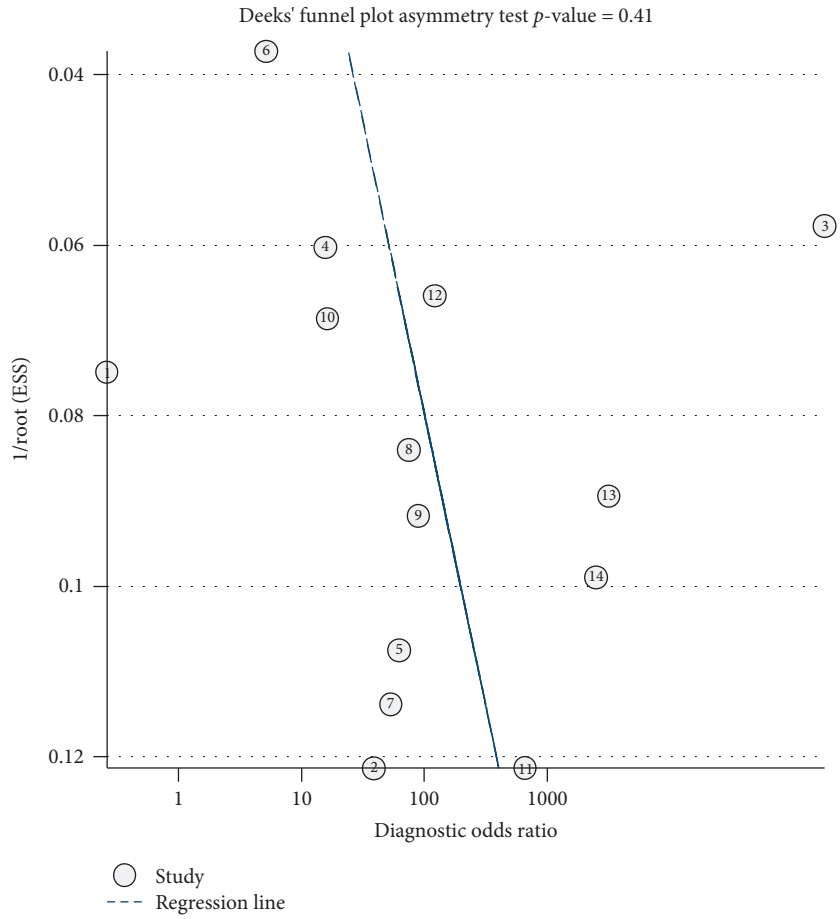

Figure 6: Deeks' funnel plot.

4. Discussion

Circulating miR-499 can differentiate effectively between AMI and non-AMI. Previously, two meta-analyses have revealed that the expression level of circulating miR-499 was a better biomarker for identifying patients with AMI [22, 29].

In a meta-analysis from 2015, including 8 studies published between April, 2010, and October, 2015, Liu et al. confirmed that the predictive values of plasma miR-499 for AMI were better than those of the miR-1 and miR-208 [22]. Owing to a relatively small study population being included in this meta-analysis, the heterogeneity of patients from the sample type had no evaluation. Furthermore, a previous meta-analysis indicated that miR-499 had better diagnostic accuracy over other miRNAs (miR-1 and miR-133) [29]. However, the investigators restricted the population to Asian. Therefore, no conclusion can be considered for AMI patients from the different regions.

The results of the current study prove that circulating miR-499 has good sensitivity and specificity for differentiating AMI from non-AMI (0.84 and 0.97, respectively). These results of sensitivity and specificity are similar or even better than those reported in two previous studies [22, 29]. In addition, our results of DOR and AUC for diagnosis of AMI were 188 and 0.98, respectively; these values are higher than the findings of Liu et al. [22] and Wang et al. [29]. In order to be more clinically informative in our results, the pooled LRs were used to estimate posttest probabilities. A PLR of 31.1 implies that a person with AMI has about 31 times more likely to be miR-499-positive than a non-AMI person. The NLR of 0.17 suggested that a person with AMI is 17% if the circulating miR-499 is negative. When the pretest probability of AMI was 53%, the pooled PLR [30] increased the posttest probability (positive predictive value) to 97%. Likewise, the pooled PLR (0.17) reduces the posttest probability (negative predictive value) to 16%. Therefore, only 29 out of 30 miR-499-positive patients had the chance to be diagnosed as AMI. In addition, only 1 out of 6 miR-499-negative patients may eventually have AMI (Figure 7).

DOR is a single index of diagnostic test performance, which has nothing to do with the disease prevalence rate. The pooled DOR of miR-499 included studies that were lower than cTnT (188 vs. 420). The differences found in those included studies may be caused by several reasons. First, because of the small number of studies, the results of cTnT tend to overestimate the effect size. Another possible reason was timing of measurement. Recent studies indicated that miRNAs were detected at an earlier stage of AMI and steadily present in circulation, but the cTnT level was very difficult to

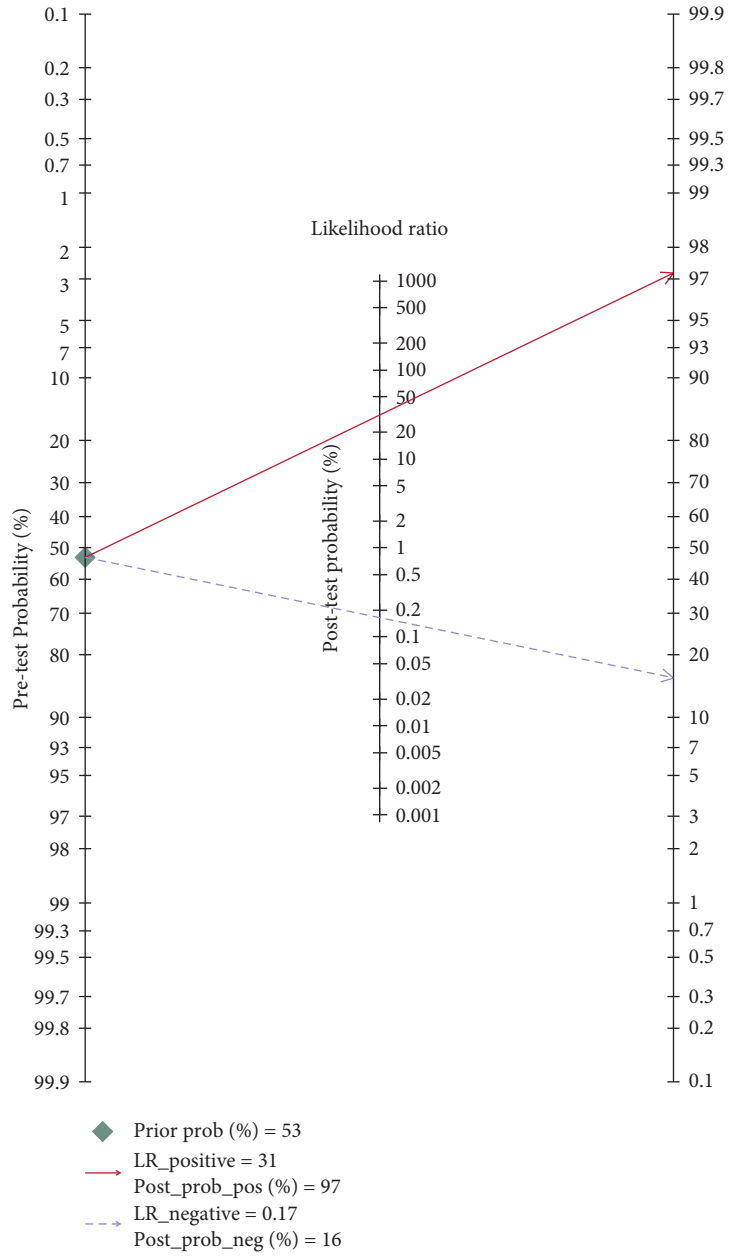

Figure 7: Fagan nomogram of circulating microRNA-499 for diagnosis of acute myocardial infarction.

observe and was below the cut-off value [18, 24]. Therefore, measurements of the cTnT levels were performed at 4-8 h later or as long as clinically indicated, which could increase the diagnostic efficiency of AMI.

There was substantial heterogeneity for miR-499 (I^2 = 97.95%, 95% CI: 95-99) in this meta-analysis. Thus, the source of heterogeneity could be found by several methods, such as threshold effect, publication bias, and metaregression. The result of Deeks' funnel plot asymmetry test showed that no publication bias exists in the analysis, which is not a source of heterogeneity. However, the Spearman correlation analysis (correlation coefficient =-0.6, $p = 0.023$) showed that there was a threshold effect. Although the proportion of heterogeneity was 65% due to a threshold effect, we were unable to discuss this threshold in metaregression because the thresholds of circulating miR-499 were not consistent between AMI and healthy controls. The results of metaregression have shown that the specimen and healthy controls demonstrate the source of heterogeneity from various covariates. Among 5 covariates, we investigated that the circulating miR-499 in plasma have higher sensitivity than that in serum. The reason may attribute it to a coagulation process that affected the expression level of circulating miR-499. Additionally, circulating miR-499 in nonhealthy controls showed that sensitivity and specificity were better than in patients who came from healthy controls. The reason for it may be that circulating miR-499 was nearly undetectable in healthy controls [17, 24], but

it increased in MI patients and geriatric non-ST elevation MI patients [18, 31].

In this meta-analysis, limitations should be noted. First, the study characteristics were the differences between research groups (e.g., age, sex, sample collection time, specimen, test method, and location), which may account for the majority of this heterogeneity. However, a relatively small study population limited our ability to detect potential sources of heterogeneity by metaregression. Second, there was s wide variation in sensitivity and specificity which a wide range of cut-offs in the reported circulating miR-499 tests separated patients who had AMI from those who did not. To obtain the most favourable results for diagnostic accuracy, some studies had different thresholds, even when the circulating miR-499 expression level was detected by using the same method. Third, although publication bias was not detected in our analysis, the number of included studies was small. Studies have good results that are more likely to be published, so the diagnostic accuracy of results is overestimated. Despite above limitations, this meta-analysis demonstrates a comprehensive assessment and robust evidence of the diagnostic accuracy of circulating miR-499 for assessing AMI.

In summary, this meta-analysis suggests that circulating miR-499 is of value to AMI. It may be considered for early diagnosis of AMI in emergency. Moreover, these findings indicate that incorporating circulating miR-499 into clinical decision-making has the potential to guide treatment more accurately. Therefore, further studies to formulate a standardized diagnostic criterion and to identify the optimal cut-off values are necessarily required.

Data Availability

The data of Table 1 used to support the findings of this study are included within the article (see References).

Conflicts of Interest

All the authors declare that they have no conflict of interest.

Authors' Contributions

Jingyi Zhao and Hairong Yu contributed equally to this work.

Acknowledgments

This project was sponsored by the Hebei Provincial Natural Science Foundation (Grant nos. C2011406009 and H2018406061) and the Key Project of Health Commission of Hebei Province (Grant no. 20181153).

References

[1] A. Moran, D. Gu, D. Zhao et al., "Future cardiovascular disease in China: Markov model and risk factor scenario projections from the coronary heart disease policy model–China," *Circulation: Cardiovascular Quality and Outcomes*, vol. 3, no. 3, pp. 243–252, 2010.

[2] R. J. de Winter, R. W. Koster, A. Sturk, and G. T. Sanders, "Value of myoglobin, troponin T, and CK-MBmass in ruling out an acute myocardial infarction in the emergency room," *Circulation*, vol. 92, no. 12, pp. 3401–3407, 1995.

[3] S. Celik, E. Giannitsis, K. C. Wollert et al., "Cardiac troponin T concentrations above the 99th percentile value as measured by a new high-sensitivity assay predict long-term prognosis in patients with acute coronary syndromes undergoing routine early invasive strategy," *Clinical Research in Cardiology*, vol. 100, no. 12, pp. 1077–1085, 2011.

[4] J. K. French and H. D. White, "Clinical implications of the new definition of myocardial infarction," *Heart*, vol. 90, no. 1, pp. 99–106, 2004.

[5] C. Li, Z. Fang, T. Jiang et al., "Serum microRNAs profile from genome-wide serves as a fingerprint for diagnosis of acute myocardial infarction and angina pectoris," *BMC Medical Genomics*, vol. 6, no. 1, p. 16, 2013.

[6] C. Chen, J. Xu, and F. Huang, "Recent players in the field of acute myocardial infarction biomarkers: circulating cell-free DNA or microRNAs?," *International Journal of Cardiology*, vol. 168, no. 3, pp. 2956-2957, 2013.

[7] D. P. Bartel, "MicroRNAs: genomics, biogenesis, mechanism, and function," *Cell*, vol. 116, no. 2, pp. 281–297, 2004.

[8] W. P. Kloosterman and R. H. A. Plasterk, "The diverse functions of microRNAs in animal development and disease," *Developmental Cell*, vol. 11, no. 4, pp. 441–450, 2006.

[9] C. Wang and Q. Jing, "Non-coding RNAs as biomarkers for acute myocardial infarction," *Acta Pharmacologica Sinica*, vol. 39, no. 7, pp. 1110–1119, 2018.

[10] T. Adachi, M. Nakanishi, Y. Otsuka et al., "Plasma microRNA 499 as a biomarker of acute myocardial infarction," *Clinical Chemistry*, vol. 56, no. 7, pp. 1183–1185, 2010.

[11] X. Chen, L. Zhang, T. Su et al., "Kinetics of plasma microRNA-499 expression in acute myocardial infarction," *Journal of Thoracic Disease*, vol. 7, no. 5, pp. 890–896, 2015.

[12] Y. Xin, C. Yang, and Z. Han, "Circulating miR-499 as a potential biomarker for acute myocardial infarction," *Annals of Translational Medicine*, vol. 4, no. 7, p. 135, 2016.

[13] P. F. Whiting, A. W. Rutjes, M. E. Westwood et al., "QUADAS-2: a revised tool for the quality assessment of diagnostic accuracy studies," *Annals of Internal Medicine*, vol. 155, no. 8, pp. 529–536, 2011.

[14] J. J. Deeks, P. Macaskill, and L. Irwig, "The performance of tests of publication bias and other sample size effects in systematic reviews of diagnostic test accuracy was assessed," *Journal of Clinical Epidemiology*, vol. 58, no. 9, pp. 882–893, 2005.

[15] M. F. Corsten, R. Dennert, S. Jochems et al., "Circulating microRNA-208b and microRNA-499 reflect myocardial damage in cardiovascular disease," *Circulation: Cardiovascular Genetics*, vol. 3, no. 6, pp. 499–506, 2010.

[16] G. K. Wang, J. Q. Zhu, J. T. Zhang et al., "Circulating microRNA: a novel potential biomarker for early diagnosis of acute myocardial infarction in humans," *European Heart Journal*, vol. 31, no. 6, pp. 659–666, 2010.

[17] Y. Devaux, M. Vausort, E. Goretti et al., "Use of circulating microRNAs to diagnose acute myocardial infarction," *Clinical Chemistry*, vol. 58, no. 3, pp. 559–567, 2012.

[18] O. Gidlöf, J. G. Smith, K. Miyazu et al., "Circulating cardio-enriched microRNAs are associated with long-term prognosis following myocardial infarction," *BMC Cardiovascular Disorders*, vol. 13, no. 1, p. 12, 2013.

[19] Y. Q. Li, M. F. Zhang, H. Y. Wen et al., "Comparing the diagnostic values of circulating microRNAs and cardiac troponin T in patients with acute myocardial infarction," *Clinics*, vol. 68, no. 1, pp. 75–80, 2013.

[20] Y. Devaux, M. Mueller, P. Haaf et al., "Diagnostic and prognostic value of circulating microRNAs in patients with acute chest pain," *Journal of Internal Medicine*, vol. 277, no. 2, pp. 260–271, 2015.

[21] Q. Ji, Q. Jiang, W. Yan et al., "Expression of circulating microRNAs in patients with ST segment elevation acute myocardial infarction," *Minerva Cardioangiologica*, vol. 63, no. 5, pp. 397–402, 2015.

[22] X. Liu, Z. Fan, T. Zhao et al., "Plasma miR-1, miR-208, miR-499 as potential predictive biomarkers for acute myocardial infarction: an independent study of Han population," *Experimental Gerontology*, vol. 72, pp. 230–238, 2015.

[23] C. H. Zhao, G. C. Cheng, R. L. He et al., "Analysis and clinical significance of microRNA-499 expression levels in serum of patients with acute myocardial infarction," *Genetics and Molecular Research*, vol. 14, no. 2, pp. 4027–4034, 2015.

[24] L. Zhang, X. Chen, T. Su et al., "Circulating miR-499 are novel and sensitive biomarker of acute myocardial infarction," *Journal of Thoracic Disease*, vol. 7, no. 3, pp. 303–308, 2015.

[25] S. M. Shalaby, A. S. El-Shal, A. Shoukry, M. H. Khedr, and N. Abdelraheim, "Serum miRNA-499 and miRNA-210: a potential role in early diagnosis of acute coronary syndrome," *IUBMB Life*, vol. 68, no. 8, pp. 673–682, 2016.

[26] K. Agiannitopoulos, P. Pavlopoulou, K. Tsamis et al., "Expression of miR-208b and miR-499 in Greek patients with acute myocardial infarction," *In Vivo*, vol. 32, no. 2, pp. 313–318, 2018.

[27] M. S. Fawzy, E. A. Toraih, E. O. Hamed, M. H. Hussein, and H. M. Ismail, "Association of MIR-499a expression and seed region variant (rs3746444) with cardiovascular disease in Egyptian patients," *Acta Cardiologica*, vol. 73, no. 2, pp. 131–140, 2018.

[28] G. Liu, X. Niu, X. Meng, and Z. Zhang, "Sensitive miRNA markers for the detection and management of NSTEMI acute myocardial infarction patients," *Journal of Thoracic Disease*, vol. 10, no. 6, pp. 3206–3215, 2018.

[29] Q. Wang, J. Ma, Z. Jiang, F. Wu, J. Ping, and L. Ming, "Identification of microRNAs as diagnostic biomarkers for acute myocardial infarction in Asian populations: a systematic review and meta-analysis," *Medicine*, vol. 96, no. 24, article e7173, 2017.

[30] F. Huang, J. P. Huang, R. X. Yin, and J. Z. Wu, "Circulating microRNAs as potential biomarkers for the early diagnosis of acute myocardial infarction: promises and challenges," *International Journal of Cardiology*, vol. 168, no. 4, pp. 4510-4511, 2013.

[31] F. Olivieri, R. Antonicelli, L. Spazzafumo et al., "Admission levels of circulating miR-499-5p and risk of death in elderly patients after acute non-ST elevation myocardial infarction," *International Journal of Cardiology*, vol. 172, no. 2, pp. e276–e278, 2014.

Hindawi
Disease Markers
Volume 2019, Article ID 2781234, 5 pages
https://doi.org/10.1155/2019/2781234

Research Article

The Predictive Value of Infant-Specific Preoperative Pulmonary Function Tests in Postoperative Pulmonary Complications in Infants with Congenital Heart Diseases

Xin Liu,[1] **Feng Qi**,[2] **Jichang Chen**,[1] **Songrong Yi**,[1] **Yanling Liao**,[1] **Zhuoxin Liang**,[1] **Jing Zhou**,[1] **and Yan Feng**[1]

[1]*Department of Pediatrics, Liuzhou Maternity and Child Health Hospital, Liuzhou 545001, China*
[2]*Department of Cardiac Surgery, the 2nd Affiliated Hospital of Harbin Medical University, Harbin 150086, China*

Correspondence should be addressed to Xin Liu; zhao2000xuan@gmail.com and Feng Qi; qifeng@hrbmu.edu.cn

Received 19 November 2018; Accepted 8 January 2019; Published 3 March 2019

Guest Editor: Zhongjie Shi

Background and Objective. To investigate the relationship between infant-specific preoperative pulmonary function tests (PFTs) and postoperative pulmonary complications (PPCs) in infants with congenital heart diseases (CHDs). *Methods*. Patients of 1-3 years of age who received surgical treatment for CHDs from January 1st, 2009, to December 31st, 2017, were retrieved. Records of preoperative PFTs, methods of operation, anesthesia procedures, intraoperative vital signs, respiratory support modalities, and PPCs was retrieved and analyzed. *Results*. 122 infants met the preset inclusion criteria, including 72 males and 50 females. There were 76 cases of thoracotomy and 46 cases of cardiac catheterization. The overall incidence of PPCs was 15.6%, including 19.7% after thoracotomy and 8.7% after cardiac catheterization, respectively ($p > 0.05$). The incidence of PPCs was 35.4% or 2.7% in infants with a rapid or a normal respiratory rate, respectively; 42.1% or 3.6% in infants with an abnormal or a normal time to reach peak tidal expiratory flow versus the total expiratory time (TPTEF/TE), respectively; 39.0% or 3.7% in infants with an abnormal or a normal volume to peak expiratory flow versus the total expiratory volume (VPEF/VE), respectively; and 46.9% or 4.4% in infants with a decreased or a normal lung compliance, respectively ($p < 0.01$ in all comparisons). *Conclusions*. The preoperative abnormal changes in respiratory rate, TPTEF/TE, VPEF/VE, and lung compliance are indicative of the risk of PPCs.

1. Introduction

Congenital heart diseases (CHDs) refer to a group of malformations due to abnormal cardiovascular development in fetal period and account for nearly 1/3 of all major congenital anomalies [1]. About 1.35 million newborns were born with CHDs worldwide every year, with the highest incidence rate being 9.3 per 1,000 live births reported in Asia. CHDs are the leading causes of birth defect-associated infant illness and death. About 25% of patients with CHDs need surgical or interventional therapies during neonatal period or infancy [2]. However, postoperative pulmonary complications (PPCs), such as respiratory infection or respiratory failure, remain common after surgical treatments [3], leading to prolonged hospital stay and even death.

At present, it is believed that adults with compromised lung functions are predisposed to PPCs [4]. Therefore, preoperative pulmonary function tests (PFTs) have been employed as important indices to evaluate the prognosis of PPCs in adults. However, the correlation between preoperative PFTs and PPCs in CHDs infants remains unclear. On the one hand, the PFTs performed in infants and adults are quite different, due to practical issues [5]. On the other hand, there are few studies analyzing preoperative PFTs in infants. In the present study, we analyzed infant-specific preoperative PFTs in CHDs infants treated with surgeries and their relationship to PPCs.

Table 1: Clinical characteristics of enrolled patients.

Cases	Catheterization	Thoracotomy	OR (95% CI)[#]	p value
Male[*]	25	47	0.73 (0.35, 1.54)	0.67
Duration of surgery (hr)[**]	0.48 ± 0.03	2.25 ± 0.21	—	<0.01
Height (cm) [**]	76.23 ± 4.15	77.51 ± 8.23	—	0.33
Weight (kg) [**]	9.93 ± 1.32	9.78 ± 1.73	—	0.61
Age (months) [**]	18.12 ± 4.65	18.22 ± 9.18	—	0.95
Total	46	76	—	—

[*] χ^2 test, number of patients. [**] t test, mean ± SD. [#]Odds ratio (95% confidence interval).

2. Methods

This retrospective cohort study was performed at Liuzhou Maternal and Child Health Hospital, a tertiary hospital and the regional specialized center for the treatment of CHDs in south China. Institutional review board approval was obtained before the start of the study. Included patients should meet all of the following criteria: (1) had complete admission records, postoperative course records, and pulmonary function tests and were admitted between January 1, 2009, and December 31, 2017, for surgical treatments of CHDs; (2) met the diagnostic criteria of CHDs [6] and indications of surgical treatment [7]; (3) be 1-3 years old when admitted; and (4) had no chromosomal abnormalities, or other chronic diseases, such as diabetes or endocrine disorders. Patient information about preoperative routine examination, preoperative PFTs, anesthesia procedures, intraoperative vital signs, respiratory support modalities, and PPCs was retrieved and analyzed.

The surgeries were performed by the same group of surgeons, with experience of similar surgeries for over 5 years before the start date of this study. The diagnosis of PPCs included respiratory infections (bronchiolitis and pneumonia), respiratory failure, atelectasis, pneumothorax, hypoxemia, bronchospasm, or postoperative respiratory support in ICU for more than 2 weeks after operation [8].

The preoperative PFTs were measured as described previously [9], with a few modifications. Briefly, all patients received oral choral hydrate (0.3-0.5 ml/kg) to be kept asleep during PFTs, which were performed at least 4 hours after feeding to avoid abdominal distension or vomiting. Temperature and humidity in the test room were maintained at 22°C and 40%, respectively. Infants lay flat on the test bed on their back, with their mouth and nose covered with an airtight mask. The PFTs were measured by a trained physician after smooth breath had been established, using a MasterScreen BabyBody plethysmograph (Jaeger, Germany), and 15-20 cycles of tidal breathing were recorded, with 5 repeats. The mean value of the 5 PFTs was calculated and used for analyses. An increased preoperative respiratory rate was defined as above 40 times/min [10]. The time to reach peak tidal expiratory flow versus the total expiratory time (TPTEF/TE) and the volume-to-peak expiratory flow versus the total expiratory volume (VPEF/VE) less than 30%, or above 50% were defined as abnormal, respectively [11, 12]. A lung compliance less than 10 ml/kPa/kg was defined as decreased [13]. Inspiratory to expiratory thoracoabdominal (TA) displacement ratio (TIF50/TEF50, where TIF50 is tidal inspiratory TA displacement rate at 50% of inspiratory displacement and TEF50 is tidal expiratory TA displacement rate at 50% of expiratory displacement), peak expiratory flow (PEF), and the time to peak tidal expiratory flow (TPTEF) were also measured.

2.1. Statistical Analysis. Discrete data were expressed as number of cases (percentages) and analyzed using the χ^2 test or Fisher's exact test, along with odds ratio (OR) and 95% confidence interval (95% CI), whichever was applicable. Continuous data were shown as mean ± standard deviation (SD) and were analyzed using the t test. The area under the receiver operating characteristic (ROC) curve was used to show the value of prediction. SPSS 24.0 (IBM Corp, Armonk, NY) was used for statistical analysis. A two-tailed $p < 0.05$ is considered significantly different.

3. Results

A total of 122 cases were retrieved according to the inclusion criteria, including 72 males and 50 females. There were 76 cases of thoracotomy and 46 cases of cardiac catheterization. There was no significant difference in age, gender, height, or weight between the two surgical groups ($p > 0.05$ in all comparisons), except in the duration of operation ($p < 0.01$, Table 1).

3.1. Incidence of PPCs in CHDs of Different Surgical Groups. There were 32 cases of patent ductus arteriosus (PDA, 3 PPC cases in 28 cases of the catheterization group and 1 PPC case in 4 cases of the thoracotomy group, $p > 0.05$), 4 cases of atrial septal defect (ASD, 0 PPC case in 1 case of the catheterization group and 0 PPC case in 3 cases of the thoracotomy group, $p > 0.05$), 55 cases of ventricular septal defect (VSD, 1 PPC cases in 14 cases of the catheterization group and 8 PPC cases in 41 cases of the thoracotomy group, $p > 0.05$), 6 cases of pulmonary stenosis (PS, no case of the catheterization group and 0 PPC case in 6 cases of the thoracotomy group, $p > 0.05$), 5 cases of tetralogy of Fallot (TOF, no case of the catheterization group and 1 PPC case in 5 cases of the thoracotomy group, $p > 0.05$), and 20 cases of ASD + VSD (0 PPC case in 3 cases of the catheterization group and 5 PPC cases in 17 cases of the thoracotomy group, $p > 0.05$). The overall incidence of PPCs was 15.6%, with

Table 2: Cases of congenital heart diseases in different surgical groups.

Cases	Catheterization	Thoracotomy	OR (95% CI)	p value
PDA	28 (3)	4 (1)	2.78 (0.21, 35.95)	0.43
ASD	1 (0)	3 (0)	—	1
VSD	14 (1)	41 (8)	3.15 (0.36, 27.76)	0.42
PS	0 (0)	6 (0)	—	1
TOF	0 (0)	5 (1)	—	1
ASD + VSD	3 (0)	17 (5)	—	0.54
Total	46 (4)	76 (15)	2.58 (0.8, 8.33)	0.13

Fisher's exact test for all comparisons. Numbers in brackets represent PPC cases. PDA: patent ductus arteriosus; ASD: atrial septal defect; VSD: ventricular septal defect; PS: pulmonary stenosis; TOF: tetralogy of Fallot.

Table 3: Relationship between preoperative pulmonary function tests (with normal range) and postoperative pulmonary complications.

Groups	PPC	Non-PPC	OR (95% CI)	p value	PPV	NPV
Respiratory rate	19 (17)	103 (41)	12.9 (2.8, 58.6)	<0.01	89.5%	60.2%
TPTEF/TE	19 (16)	103 (32)	11.8 (3.2, 43.5)	<0.01	84.2%	68.9%
VPEF/VE	19 (16)	103 (35)	10.4 (2.8, 38.0)	<0.01	84.2%	66.0%
Lung compliance	19 (15)	103 (27)	10.6 (3.2, 34.6)	<0.01	79.0%	73.8%

Fisher's exact test for all comparisons. Numbers in brackets represent abnormal cases. PPC: preoperative pulmonary function; PPV: positive predictive value; NPV: negative predictive value.

Table 4: Relationship between preoperative pulmonary function tests (without normal range) and postoperative pulmonary complications.

Groups	PPC (19)	Non-PPC (103)	p value
TIF50/TEF50	80.3 ± 15.6	86.5 ± 37.4	>0.05
PEF (ml/s)	99.1 ± 31.4	108.5 ± 14.9	>0.05
TPTEF (s)	0.27 ± 0.21	0.32 ± 0.21	>0.05

Numbers in brackets represent cases in PPC group or no-PPC group.

8.7% after cardiac catheterization and 19.7% after thoracotomy, respectively, without a significant difference ($p > 0.05$, Table 2).

3.2. Relationship between Preoperative PFTs and PPCs. The incidence of PPCs was 29.3% or 3.1% in infants with a rapid or a normal respiratory rate, respectively (positive predictive value, or PPV = 89.5%, and negative predictive value, or NPV = 60.2%, $p < 0.01$); 33.3% or 4.1% in infants with an abnormal or a normal TPTEF/TE, respectively (PPV = 84.2% and NPV = 68.9%, $p < 0.01$); 31.4% or 4.2% in infants with an abnormal or a normal VPEF/VE, respectively (PPV = 84.2% and NPV = 66.0%, $p < 0.01$); and 35.7% or 5% in infants with a decreased or a normal lung compliance, respectively (PPV = 79.0% and NPV = 73.8%, $p < 0.01$, Table 3). For PFTs without clear normal ranges, such as TIF50/TEF50, PEF, or TPTEF, there were no significant differences between the PPC group and the non-PPC group ($p > 0.05$, Table 4).

Using ROC curve analysis, we found that the area under the curve of respiratory rate, TPTEF/TE, VPEF/VE, and lung compliance were 0.748 ± 0.054 (95% CI: 0.643, 0.854, $p < 0.01$), 0.766 ± 0.056 (95% CI: 0.655, 0.876, $p < 0.001$), 0.751 ± 0.057 (95% CI: 0.639, 0.863, $p < 0.01$), and 0.764 ± 0.060 (95% CI: 0.646, 0.881, $p < 0.001$), respectively, whereas combination of the 4 positive PFTs (Combof4) improved the

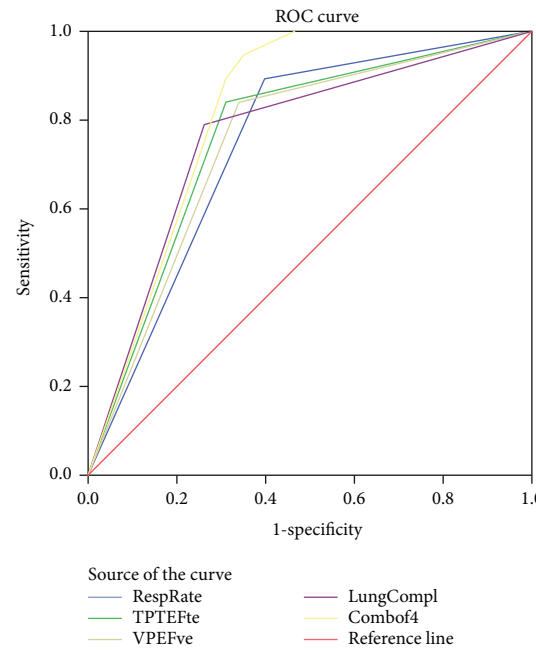

Figure 1: Receiver operating characteristic (ROC) curve of respiratory rate (blue), TPTEF/TE (green), VPEF/VE (pale), lung compliance (purple), and combination of respiratory rate, TPTEF/TE, VPEF/VE, and lung compliance patients (yellow).

Table 5: Details of area under the ROC curve in Figure 1.

Area under the curve					
Test result variable(s)	Area	Std. error[a]	Asymptotic sig.[b]	Asymptotic 95% confidence interval	
				Lower bound	Upper bound
RespRate	.748	.054	.001	.643	.854
TPTEFte	.766	.056	.000	.655	.876
VPEFve	.751	.057	.001	.639	.863
LungCompl	.764	.060	.000	.646	.881
Combof4	.821	.038	.000	.746	.896

predictive value to 0.821 ± 0.038 (95% CI: 0.746, 0.896, $p < 0.001$, Figure 1 and Table 5). Furthermore, we found that combination of the 4 positive PFTs can be included in a logistic regression equation for prediction of PPCs, i.e., $p = 1/[1 + e^{-(-4.763+0.887\text{Combof4})}]$,

4. Discussion

The pathogenesis of PPCs in infants has not been clearly characterized yet. Available studies in adults show that PPCs originate differently from respiratory infections without surgeries [14]. Atelectasis and respiratory infections seem to be related to disruption of the normal activity of the respiratory muscles during anesthesia procedures. Chest or abdomen surgeries in adults can cause diaphragmatic dysfunction as well as reduction of vital capacity, tidal volume, or forced expiratory volume in one second (FEV1), resulting in atelectasis. Furthermore, diaphragmatic dysfunction, postoperative pain, anesthetics, and postsurgical stress all suppress the clearance of secretions in the respiratory tract, leading to atelectasis or respiratory infections [15].

The preoperative PFTs of adult patients are among the key indices that influence the short-term prognosis after the surgery [16]. However, preoperative PFTs have not been well applied in the field of pediatrics. It has been shown that many of the lung function parameters, such as total lung capacity (TLC), residual volume (RV), functional residual capacity (FRC), forced vital capacity (FVC), and forced expiratory flows at 25, 50, 75, 85, and between 25% and 75% of expired FVC (FEF_{25}, FEF_{50}, FEF_{75}, FEF_{85}, and FEF_{25-75}, respectively) are all positively related to infant length, whereas RV/TLC, FRC/TLC, and FEF_{25-75}/FVC are all negatively related to infant length [17]. Therefore, we employed TPTEF/TE and VPEF/VE, which are more infant-specific [11]. In order to minimize the difficulty to carry out the measurements in infants of this age group, as well as to obtain results of good quality and reproducibility, oral choral hydrate (0.3-0.5 ml/kg) was given to all participants to keep them asleep during PFTs, according to previous studies [9].

Unexpectedly, in the present study, although the duration of operation is significantly longer in thoracotomy, we did not find a significant difference in the incidence of PPCs between the thoracotomy and the catheterization patients. This coincides with a previous report showing that the length of surgery is only a risk factor for PPCs when it is more than 3 hours [16]. Therefore, we pooled the patients from the two surgical groups and increased our stratified sample size. We found that the incidence of PPCs was significantly higher in infants with an abnormal respiratory rate, or with an abnormal VPEF/VE, or with an abnormal TPTEF/TE, or with a decreased lung compliance (all $p < 0.01$). The positive and negative predictive values are good for all of the 4 indices (Table 3), with an even better predictive value when these 4 PFTs are considered altogether, showing the reliability of infant-specific preoperative PFTs in the prediction of PPCs in infants. VPEF/VE and TPTEF/TE have been shown to be significantly lower in asthmatic children and significantly increased after salbutamol inhalation [12], thus their predictive value in the development of PPC might be rooted in the functional reserve of the respiratory tract.

Although it has been reported in elder children (>7 years old) that TIF50/TEF50 was significantly higher in asthma cases [18], and PEF variation was positively associated with asthma symptoms [19], due to the difference in ages and methods of measurement, we did not find any difference in TIF50/TEF50 or PEF between the PPC group and the non-PPC group. Also coinciding with previous reports analyzing TPTEF in airway obstruction in infants [20], we did not find a significant difference in TPTEF between the PPC group and the non-PPC group.

After the assessment of preoperative PFTs, special attention should be paid to infants at high risks during preoperative preparation to improve respiratory functions, including pulmonary ventilation reserves and compliance of lung to prepare for the incoming surgery. Surgeries are recommended only after the lung function indices have significantly improved. Lung function should also be protected during and after surgeries, such as reducing the time of surgery and facilitating the drainage of airway secretions [21]. Our retrospective study design and relatively small size of sample are limitations of our present study, and prospective studies involving more participants are needed in the future.

In summary, infant-specific preoperative PFTs are key prognostic predictive factors for CHD corrective surgeries. Patients with abnormal respiratory rate, VPEF/VE, TPTEF/TE, or lung compliance are at high risk for the development of PPCs. Those infant-specific PFTs have potential values in the decision of the mode and range of surgery, as well as the mode and depth of the anesthesia procedures, in order to reduce PPCs and postoperative mortality.

Data Availability

Original data could be obtained by contacting the corresponding author.

Conflicts of Interest

No conflict of interest exits in the submission of this manuscript, and the manuscript is approved by all authors for publication.

Authors' Contributions

Xin Liu and Feng Qi contributed equally to the study.

Acknowledgments

The study was supported by Liuzhou Science and Technology Bureau (2009021523).

References

[1] D. van der Linde, E. E. M. Konings, M. A. Slager et al., "Birth prevalence of congenital heart disease worldwide: a systematic review and meta-analysis," *Journal of the American College of Cardiology*, vol. 58, no. 21, pp. 2241–2247, 2011.

[2] Centers for Disease Control and Prevention, "Congenital Heart Defects (CHDs)," 2018, October 2018, https://www.cdc.gov/ncbddd/heartdefects/data.html.

[3] H. P. R. Bandla, R. L. Hopkins, R. C. Beckerman, and D. Gozal, "Pulmonary risk factors compromising postoperative recovery after surgical repair for congenital heart disease," *Chest*, vol. 116, no. 3, pp. 740–747, 1999.

[4] B. W. Fisher, S. R. Majumdar, and F. A. McAlister, "Predicting pulmonary complications after nonthoracic surgery: a systematic review of blinded studies," *The American Journal of Medicine*, vol. 112, no. 3, pp. 219–225, 2002.

[5] L. Seed, D. Wilson, and A. L. Coates, "Children should not be treated like little adults in the PFT lab," *Respiratory Care*, vol. 57, no. 1, pp. 61–74, 2012.

[6] C. Ferencz, J. D. Rubin, R. J. Mccarter et al., "Congenital heart disease: prevalence at livebirth. The Baltimore-Washington Infant Study," *American Journal of Epidemiology*, vol. 121, no. 1, pp. 31–36, 1985.

[7] A. J. Moss, F. H. Adams, J. V. Maloney Jr, W. P. Longmire Jr, and B. J. O'Loughlin, "Congenital cardiac defects-indications for surgical repair," *California Medicine*, vol. 89, no. 2, pp. 113–116, 1958.

[8] I. Jammer, N. Wickboldt, M. Sander et al., "Standards for definitions and use of outcome measures for clinical effectiveness research in perioperative medicine: European Perioperative Clinical Outcome (EPCO) definitions: a statement from the ESA-ESICM joint taskforce on perioperative outcome measures," *European Journal of Anaesthesiology*, vol. 32, no. 2, pp. 88–105, 2015.

[9] B. L. Lesnick and S. D. Davis, "Infant pulmonary function testing: overview of technology and practical considerations–new current procedural terminology codes effective 2010," *Chest*, vol. 139, no. 5, pp. 1197–1202, 2011.

[10] Normal Values in Children, 2018, October 2018, https://www.aclsmedicaltraining.com/normal-values-in-children/.

[11] J. Stocks, C. A. Dezateux, E. A. Jackson, A. F. Hoo, K. L. Costeloe, and A. M. Wade, "Analysis of tidal breathing parameters in infancy: how variable is TPTEF:TE?," *American Journal of Respiratory and Critical Care Medicine*, vol. 150, no. 5, pp. 1347–1354, 1994.

[12] K. H. Carlsen and K. C. Lødrup Carlsen, "Tidal breathing analysis and response to salbutamol in awake young children with and without asthma," *European Respiratory Journal*, vol. 7, no. 12, pp. 2154–2159, 1994.

[13] T. Gerhardt, D. Hehre, R. Feller, L. Reifenberg, and E. Bancalari, "Pulmonary mechanics in normal infants and young children during first 5 years of life," *Pediatric Pulmonology*, vol. 3, no. 5, pp. 309–316, 1987.

[14] D. O. Warner, "Preventing postoperative pulmonary complications: the role of the anesthesiologist," *Anesthesiology*, vol. 92, no. 5, pp. 1467–1472, 2000.

[15] S. Wilcox and H. Gaissert, "Diaphragmatic dysfunction after thoracic operations," *The Journal of Thoracic and Cardiovascular Surgery*, vol. 64, no. 8, pp. 621–630, 2016.

[16] G. W. Smetana, "Preoperative pulmonary evaluation," *The New England Journal of Medicine*, vol. 340, no. 12, pp. 937–944, 1999.

[17] R. Castile, D. Filbrun, R. Flucke, W. Franklin, and K. McCoy, "Adult-type pulmonary function tests in infants without respiratory disease," *Pediatric Pulmonology*, vol. 30, no. 3, pp. 215–227, 2000.

[18] H. Hmeidi, S. Motamedi-Fakhr, E. Chadwick et al., "Tidal breathing parameters measured using structured light plethysmography in healthy children and those with asthma before and after bronchodilator," *Physiological Reports*, vol. 5, no. 5, article e13168, 2017.

[19] P. L. P. Brand, E. J. Duiverman, H. J. Waalkens, E. E. M. van Essen-Zandvliet, K. F. Kerrebijn, and the Dutch CNSLD Study Group, "Peak flow variation in childhood asthma: correlation with symptoms, airways obstruction, and hyperresponsiveness during long-term treatment with inhaled corticosteroids. Dutch CNSLD Study Group," *Thorax*, vol. 54, no. 2, pp. 103–107, 1999.

[20] A. Hevroni, A. Goldman, M. Blank-Brachfeld, W. Abu Ahmad, L. Ben-Dov, and C. Springer, "Use of tidal breathing curves for evaluating expiratory airway obstruction in infants," *Journal of Asthma*, 2018.

[21] E. E. Apostolakis, E. N. Koletsis, N. G. Baikoussis, S. N. Siminelakis, and G. S. Papadopoulos, "Strategies to prevent intraoperative lung injury during cardiopulmonary bypass," *Journal of Cardiothoracic Surgery*, vol. 5, no. 1, 9 pages, 2010.

Hindawi
Disease Markers
Volume 2019, Article ID 6016931, 7 pages
https://doi.org/10.1155/2019/6016931

Research Article

Clinical Significance of Preoperative Serum CEA, CA125, and CA19-9 Levels in Predicting the Resectability of Cholangiocarcinoma

Tianyi Fang,[1,2] Hao Wang,[1] Yufu Wang,[1] Xuan Lin,[1] Yunfu Cui,[1] and Zhidong Wang[1]

[1]*Department of Hepatopancreatobiliary Surgery, Second Affiliated Hospital of Harbin Medical University, Harbin Medical University, Harbin, China*
[2]*Department of Gastrointestinal Surgery, Harbin Medical University Cancer Hospital, Harbin Medical University, Harbin, China*

Correspondence should be addressed to Yunfu Cui; yfcui777@hotmail.com and Zhidong Wang; wzd98y2@163.com

Tianyi Fang, Hao Wang, Yunfu Cui, and Zhidong Wang contributed equally to this work.

Received 9 October 2018; Revised 3 November 2018; Accepted 5 November 2018; Published 4 February 2019

Guest Editor: Zhongjie Shi

To explore the clinical significance of preoperative serum CEA, CA125, and CA19-9 levels in predicting the resectability of cholangiocarcinoma. Patients with cholangiocarcinoma diagnosed by radiologic examination and admitted to the Second Affiliated Hospital of Harbin Medical University from September 1, 2011, to November 30, 2017, were retrospectively included. The relationship between the preoperative serum CEA, CA125, and CA19-9 levels and the resectability of cholangiocarcinoma was analyzed by receiver operating characteristic (ROC) curve, as well as the best cut-off point. A total of 112 met the inclusion criteria. In 50 patients with radical surgeries, the levels of preoperative serums CEA, CA125, and CA19-9 were 5.0 ± 13.9 ng/mL, 15.3 ± 11.8 U/mL, and 257.5 ± 325.6 U/mL, respectively, which were lower than those in patients with unresectable tumor. Based on the ROC curve, the ideal CA19-9 cut-off value was determined to be 1064.1 U/mL in prediction of resectability, with a sensitivity of 53.2%, a specificity of 94.0%, and the area under the ROC curve of 0.73 ($P < 0.05$). The cut-off value of CA125 was 17.8 U/mL with a sensitivity of 72.6%, a specificity of 78.0%, and the area under the ROC curve of 0.81 ($P < 0.05$). The cut-off value of CEA was 2.6 ng/mL with a sensitivity of 79.0%, a specificity of 48.0%, and the area under the ROC curve of 0.66 ($P < 0.05$). In addition to this, we found that using the combination of three tumor markers could improve the value in predicting resectability of cholangiocarcinoma. In summary, this study suggested that the preoperative serum CEA, CA125, and CA19-9 levels can help predict the resectability of cholangiocarcinoma.

1. Introduction

Cholangiocarcinoma is the most common primary tumor of the biliary tract, with a poor prognosis at the advanced stages [1–3]. The morbidity and mortality of cholangiocarcinoma have increased over the past 40 years, especially in Asia [4]. Currently, radical resection is accepted widely as one of the preferred treatment options for cholangiocarcinoma [5, 6]. However, cholangiocarcinoma is closely associated with adjacent structures, such as the portal vein and hepatic artery [7], and it is characterized by an infiltrative growth [8, 9]. In addition, due to its insidious onset and high malignancy, it is often found in advanced stages at diagnosis [10]. Therefore, the surgical resection rate of cholangiocarcinoma is low [11, 12]. It is of increasing clinical importance to evaluate the resectability of the tumor before operation.

Currently, the assessment of resectability of cholangiocarcinoma is based on a combination of clinical, radiological, and biochemical approaches [13, 14]. Cholangiocarcinoma grows along the wall of the bile duct or the connective tissue around the bile duct, forming no nodule or mass in many cases, thus displaying no mass shadow in radiological examinations [15, 16], whereas surgical exploration is invasive and may result in a huge financial burden on patients.

There is no biomarker currently available for the resectability of cholangiocarcinoma that is sufficiently sensitive and specific. As key markers for the diagnosis of gastrointestinal malignancies and predicting their prognosis, carcinoembryonic antigen (CEA), carbohydrate antigen (CA)125, and CA19-9 have also been widely used to predict the resectability of tumors [17–19]. At present, they are also important markers in the diagnosis of cholangiocarcinoma. It was reported that preoperative serum CA19-9 level was positively associated with tumor stage. However, the increase in CA19-9 may be caused by cholangitis or obstructive jaundice. Thus, it may not be accurate to use CA19-9 alone in clinical practice. Mucins have been associated with human malignant tumors. CA125 is currently considered to be MUC16, and its amino acid sequence has some properties of mucin molecules, which may have better clinical application in adenocarcinoma [20]. CEA levels are not related to serum bilirubin levels and may be effective in predicting surgical resection rates. In general, it remains unclear whether their expression levels are valuable in determining the resectability of cholangiocarcinoma. In this study, we retrospectively analyzed the preoperative serum CEA, CA125, and CA19-9 levels in 112 patients with cholangiocarcinoma who were treated in our center from 2011 to 2017 and explored their clinical value in determining the resectability of cholangiocarcinoma.

2. Materials and Methods

We retrospectively analyzed clinically diagnosed or pathologically confirmed cholangiocarcinoma patients who had been admitted to the Second Affiliated Hospital of Harbin Medical University from September 1, 2011, to November 30, 2017. The clinical diagnosis was mainly based on clinical symptoms, imaging findings [computed tomography (CT), ultrasonography, magnetic resonance imaging, positron emission tomography–CT, and endoscopic ultrasonography], and tumor markers including CEA, CA125, and CA19-9 [21]. The patients were staged according to the American Joint Committee on Cancer (AJCC) Staging System. Tumor resectability was confirmed by intraoperative exploration; all patients were from more than two chief physicians to determine whether to perform radical surgery. In addition, a tumor was confirmed to be unresectable if radiological examination revealed the presence of hepatic metastasis or other distant metastasis. In order to make sure the decision is uniformed, most of the patients were selected from nearly three years and treated by three chief physicians. Patients with incomplete clinical data were excluded.

2.1. Determination of Serum CA19-9, CA125, and CEA Levels. Before treatment, 5 mL peripheral blood was extracted from the peripheral vein, and plasma and albumin were isolated by centrifugation at $2000 \times g$ for 15 min. The CA125 and CA19-9 levels were determined by radioimmunoassay [22, 23], with a normal upper limit of 35 U/mL and 37 U/mL, respectively. The CEA level was determined by ELISA [24], with a normal upper limit of 5 ng/mL.

2.2. Statistical Analysis. Statistical analysis was performed using SPSS 22.0. Numerical data were presented as the mean ± standard deviation. A two-tailed P value < 0.05 was considered statistically significant. The optimal cut-offs for CEA, CA125, and CA19-9 in determining the resectability were analyzed using the receiver operating characteristic (ROC) curves.

3. Results

In total, 112 cholangiocarcinoma patients (66 men and 46 women; male/female ratio 1.43; average age 62.5 years) were retrieved. The disease was pathologically confirmed in 72 cases and clinically diagnosed in 40 cases. Although pathological diagnosis was more reliable, clinical diagnosis was acceptable based on the patients' symptoms and accessory examinations.

3.1. General Clinical Features of Cholangiocarcinoma Patients. Cholangiocarcinoma was resectable in 50 cases (44.6%) and unresectable in 62 cases (55.4%). The lesions were located in hepatic segments in 16 cases, at the hepatic hilum in 35 cases, and in the distal bile duct in 61 cases. There were 50 cases of radical resection and 22 cases of palliative resection, which were also histologically classified as highly ($n = 24$), moderately ($n = 28$), or poorly ($n = 20$) differentiated. The rest of the patients were treated by endoscopic or ultrasound intervention, so there was no pathological diagnosis. The AJCC staging results were as follows: two stage I, resection rate 100%; 44 stage II, resection rate 93.2%; 24 stage III, resection rate 29.2%; and 42 stage IV, all of which were unresectable. The sizes of resectable tumor tissue were determined consistently by a trained pathologist, and those of the unresectable group were determined consistently by a trained radiologist. The average tumor diameter was 2.3 ± 0.9 cm in the resectable group, which was significantly smaller than that of the unresectable group (4.5 ± 1.6 cm, $P < 0.05$, Table 1).

3.2. Serum CEA, CA125, and CA19-9 Levels in Determining Cholangiocarcinoma Resectability. Table 2 shows the multivariate logistic regression models for predicting the resectability of cholangiocarcinoma. Multivariate logistic regression analysis for predicting the resectability of cholangiocarcinoma showed that the serum levels of CEA, CA125, and CA19-9 had a better predictive value in radical resection.

Serum CEA, CA125, and CA19-9 levels in the resectable group ($n = 50$) were 5.0 ± 13.9 ng/mL, 15.3 ± 11.8 U/mL, and 257.5 ± 325.6 U/mL, respectively, which were significantly lower than those in the unresectable group (19.1 ± 69.2 ng/mL, 48.8 ± 58.7 U/mL, and 730.1 ± 527.5 U/mL, respectively). According to the results of the ROC curve analysis, the optimal cut-offs for determining the resectability of cholangiocarcinoma were as follows (Figure 1). When CA19-9 was 1064.1 U/mL, it had a sensitivity of 53.2%, specificity of 94%, positive predictive value (PPV) of 80.8%, and negative predictive value (NPV) of 0.73, and the area under the ROC curve (AUC) was 0.73 [95% confidence interval (CI): 0.63–0.82]. When CA125 was 17.8 U/mL, it had a sensitivity

Table 1: Relationship between clinical features and resectability of cholangiocarcinoma patients.

Features	Resectable ($n = 50$)	Unresectable ($n = 62$)	Total ($n = 112$)	P value
Age (yr)	60.9 ± 7.7	63.7 ± 1 0.0	62.5 ± 9.1	
Sex (n)				0.172
Men	33	33	66	
Women	17	29	46	
Tumor location (n)				0.029
Intrahepatic	4	12	16	
Hilar	12	23	35	
Distal	34	27	61	
Differentiation (n)				0.003
High	20	4	24	
Moderate	22	6	28	
Poor	8	12	20	
Tumor diameter (cm)	2.3 ± 0.9	4.5 ± 1.6	3.5 ± 1.3	
AJCC stage (n)				0.000
I	2	0	2	
II	41	3	44	
III	7	17	24	
IV	0	42	42	
CEA (ng/mL)	5.0 ± 13.9	19.1 ± 69.2	12.8 ± 52.6	
CA125 (U/mL)	15.3 ± 11.8	48.8 ± 58.7	33.9 ± 47.3	
CA19-9 (U/mL)	257.5 ± 325.6	730.1 ± 527.5	519.1 ± 505.4	
Total bilirubin (μmol/L)	187.1 ± 121.7	219.3 ± 174.9	204.9 ± 153.5	

AJCC Cancer Staging Manual 7th edition. Patients were divided into the resectable and unresectable groups; some patients in the unresectable group were diagnosed according to imaging findings and therefore had no data on pathological stage or AJCC stage.

Table 2: Multivariate logistic regression models for predicting the resectability of cholangiocarcinoma.

Observation	Predicted value		Correct percentage
	Radical resection	Nonradical resection	
Radical resection	43	7	86.0%
Nonradical resection	25	37	59.7%
Overall percentage	60.7%	39.3%	71.4%

The accuracy of the model in predicting surgical resectability is higher, reaching 86.0% ($P < 0.05$).

of 72.6%, specificity of 78.0%, PPV of 76.7%, and NPV of 74.0%, and the AUC was 0.81 (95% CI: 0.72–0.89). When CEA was 17.8 U/mL, it had a sensitivity of 79.0%, specificity of 48.0%, PPV of 75.5%, and NPV of 53.0%, and the AUC was 0.66 (95% CI: 0.56–0.76).

By logistic regression analysis, we found that using the combination of three tumor markers could improve the value of predicting resectability of cholangiocarcinoma (Figure 2). The results of ROC curve analysis showed that when we used the combination of CEA and CA125, the AUC was 0.81 (95% CI: 0.89–0.73); when we used the combination of CEA and CA19-9, the AUC was 0.75 (95% CI: 0.84–0.66); when we used the combination of CA125 and CA19-9, the AUC was 0.74 (95% CI: 0.83–0.64); and when we used the combination of CEA, CA125, and CA19-9, the AUC was 0.87 (95% CI: 0.92–0.78). ($P < 0.05$).

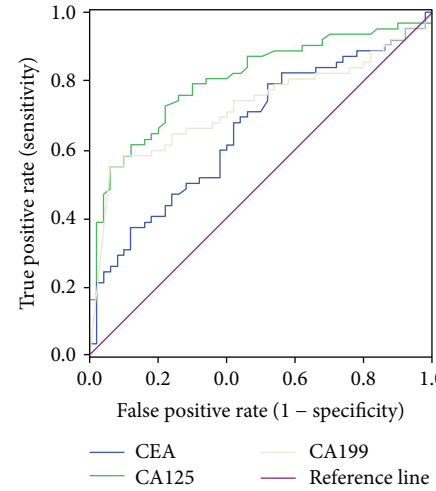

Figure 1: ROC curves for serum CEA, CA125, and CA19-9 levels in the determination of cholangiocarcinoma resectability. The AUC is 0.66 for CEA, 0.81 for CA125, and 0.73 for CA19-9.

3.3. Value of Serum Total Bilirubin in Determining Cholangiocarcinoma Resectability. ROC curve analysis showed that the AUC was 0.54 (95% CI: 0.43–0.65), suggesting that

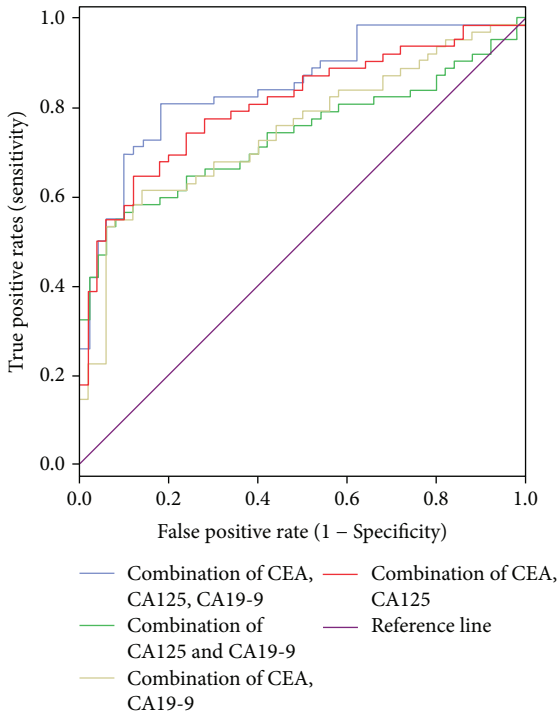

Figure 2: ROC curves for the combination of serum CEA, CA125, and CA19-9 levels in the determination of cholangiocarcinoma resectability. For the combination of CEA and CA125, the AUC is 0.81; for the combination of CEA and CA19-9, the AUC is 0.75; for the combination of CEA, CA125 and CA19-9, the AUC is 0.74; and for the combination of CEA, CA125, and CA19-9, the AUC is 0.87.

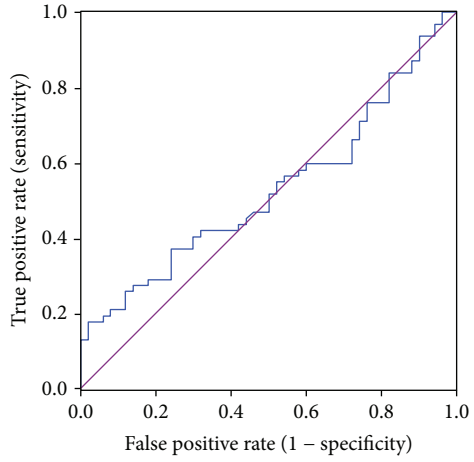

Figure 3: The ROC curve of serum total bilirubin level in the determination of cholangiocarcinoma resectability. The blue line is the total bilirubin, and the purple line is the reference line. The AUC of total bilirubin is 0.54.

serum total bilirubin had an extremely low accuracy in predicting the resectability of cholangiocarcinoma (Figure 3).

4. Discussion

Surgery remains the treatment of choice for cholangiocarcinoma [25, 26]. Radical resection can be achieved if the patient's general condition can tolerate the operation, and there is no distant metastasis [27–30]. Despite rapid advances in surgical techniques and postoperative management, the overall resection rate of cholangiocarcinoma remains low [1, 3, 31], and the incidence of postoperative fatal complications is still high [26, 32, 33]. Therefore, accurate and reliable determination of the resectability of cholangiocarcinoma before surgery is important. CT is the most common examination for determining the resectability of cholangiocarcinoma [34, 35]. However, it is often unable to detect occult metastatic lesions in the liver or abdominal cavity and may miss vascular invasion, resulting in unnecessary surgical trauma and waste of medical resources. Endoscopic ultrasonography and laparoscopy can also be used to determine the resectability before surgery, but they are time-consuming, invasive, and expensive. CEA, CA125, and CA19-9 are the most commonly used tumor markers for preoperative diagnosis and postoperative prognosis prediction of cholangiocarcinoma [36, 37]. According to Juntermanns et al. [38], serum CEA and CA19-9 levels are correlated with the stage of cholangiocarcinoma, and patients with higher preoperative CEA and CA19-9 levels tend to have poorer survival and prognosis. Hatzaras et al. [39] reported that a high preoperative serum CA19-9 level often suggests a low survival rate in patients with bile system cancer. However, little is known about the effects of these tumor markers on the resectability of cholangiocarcinoma.

In the present study, we analyzed the resectability of cholangiocarcinoma based on ROC curve analysis. We found that serum CA19-9 is one of the predictors of cholangiocarcinoma, with an AUC of 0.73 and an optimal cut-off of 1064.1 U/mL. Unlike many other previous studies, our results did not rule out the effect of high bilirubin level on CA19-9, mainly for the following two reasons: cholangiocarcinoma is characterized clinically by its insidious onset, and jaundice, as one of the early symptoms of cholangiocarcinoma, is highly suggestive for this disease in most patients [40–42]. Most of our patients presented with jaundice as the first symptom. Therefore, predicting the surgical resectability by analyzing the serum CA19-9 level in patients with jaundice is particularly significant. In contrast, it is believed that serum CA19-9 is mainly affected by tumor severity and serum bilirubin level [37, 43, 44]; however, it is not possible to completely rule out the effect of serum bilirubin and merely analyze the relationship between serum CA19-9 elevation and surgical resection rate in the statistical analysis. The results of our current analysis were more representative of resectability of cholangiocarcinoma. We also analyzed the relationship between bilirubin level and surgical resection rate of cholangiocarcinoma and found that its predictive value was extremely low, suggesting the feasibility of analyzing serum CA19-9 in patients with jaundice. Since CA19-9 is valuable in predicting the resectability of cholangiocarcinoma [45, 46], it can be used as a supplementary tool for preoperative imaging and for comprehensive evaluation of the success rate of an operation, so as to avoid unnecessary surgery.

Notably, serum CA 125 level had a higher correlation with the resectability of cholangiocarcinoma than CA19-9,

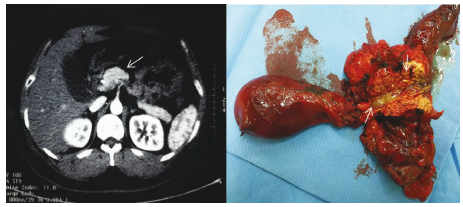

Figure 4: Findings of computed tomography: enhanced computed tomography (CT) revealed a marked high-density area at the distal bile duct (arrowhead). Macroscopic findings: opened bile duct of the resected specimen (arrowhead). Gross appearance of the cut surface of the resected ampulla shows a gray-white tumor measuring 16 mm × 5 mm × 8 mm (arrowhead).

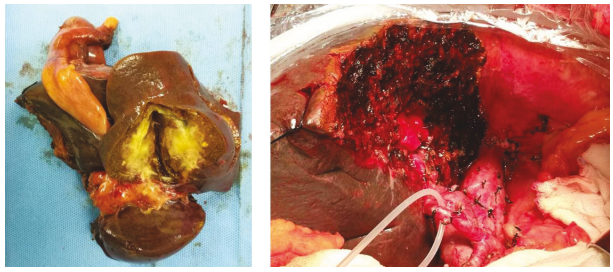

Figure 5: Macroscopic findings: gross appearance of the cut surface of the resected liver shows a gray-white tumor measuring 16 mm × 5 mm × 8 mm.

which may be explained by the fact that CA125 is less affected by bilirubin. In our study, the AUC of CA125 was 0.81 and the optimal cut-off was 17.8 U/mL. Therefore, it is necessary to measure serum CA125 before surgery, together with CA19-9 as an auxiliary marker, to compensate for the defect of preoperative imaging in predicting resectability and to better guide the treatment.

We also analyzed the relationship between serum CEA and the resectability of cholangiocarcinoma. For CEA, the AUC was 0.66, and the optimal cut-off was 2.6 g/mL; the sensitivity of CEA in predicting the resectability was 79.0%, along with a specificity of 48.0%, PPV of 75.5%, and NPV of 53.0%. However, CEA is a broad-spectrum tumor marker and cannot be used as a specific marker for the diagnosis of a malignancy [47, 48]. Therefore, the value of serum CEA in predicting the resectability of cholangiocarcinoma was lower than that of CA19-9 and CA125.

Generally it is not accurate to predict the resectability of cholangiocarcinoma using a single marker [6, 49]. The value of combining three tumor markers in evaluating resectability of cholangiocarcinoma is higher than that of two. Therefore, it is clinically significant for the preoperative detection of tumor markers in patients with cholangiocarcinoma.

On the other hand, tumor markers are supplement preoperative imaging [50]. Comprehensive analysis of clinical manifestations, preoperative imaging findings, and other prognostic factors (including tumor size) can better assess the resectability of cholangiocarcinoma and provide feasible, appropriate, and reasonable treatment for patients [51].

We also apply this combination to clinical practice. Figure 4 shows one case of distal cholangiocarcinoma. It

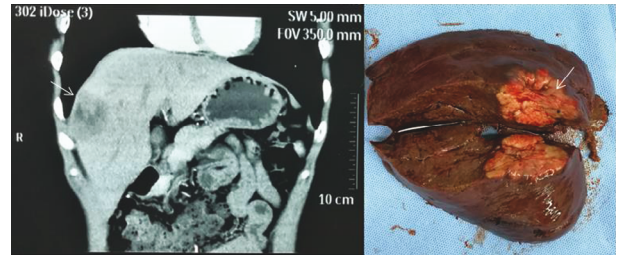

Figure 6: Findings of computed tomography: sagittal plane of computed tomography shows the low-density area (arrowhead) at the right anterior lobe of the liver. Macroscopic findings: gross appearance of the resected liver shows a gray-white tumor measuring 34 mm × 32 mm × 19 mm (arrowhead).

was difficult for us to know whether the cancer infiltrated the surrounding tissue by preoperative imaging. However, the CA19-9, CA125, and CEA of the patient were lower than the cut-off point in our study. Then radical resection was performed successfully with a negative postoperative pathological margin. Figures 5 and 6 show one case of hilar cholangiocarcinoma and one case of intrahepatic cholangiocarcinoma. It was judged resectable according to our prediction, and the radical resection was performed successfully.

In addition, our retrospective analysis also had limitations in the study design. First, most of the selected patients were diagnosed late and had accompanying hyperbilirubinemia, so it was not possible to accurately analyze the relationship between serum CA19-9 level and resectability of cholangiocarcinoma. Second, our study included patients with jaundice and the results need to be further validated in more comprehensive multicenter studies.

5. Conclusions

In conclusion, preoperative serum CEA, CA19-9, and CA125 levels are useful in predicting the resectability of cholangiocarcinoma and may become supplementary diagnostic indicators for evaluating the resectability of cholangiocarcinoma in the future.

Data Availability

The data used to support the findings of this study are available from the corresponding author upon request.

Disclosure

Zhidong Wang and Yunfu Cui can be considered co-corresponding authors.

Conflicts of Interest

The authors declare that they have no conflicts of interest.

Authors' Contributions

Tianyi Fang, Hao Wang, Zhidong Wang, and Yunfu Cui contributed equally to this paper. Tianyi Fang conceived,

designed, and performed the experiments, analyzed the data, and wrote the paper. Hao Wang conceived and designed the experiments. Yufu Wang and Xuan Lin collected the data. Zhidong Wang and Yunfu Cui supervised the study and gave administrative support for this article.

Acknowledgments

This study was supported by the National Nature Science Foundation of China (61572227 and 81170426).

References

[1] S. Rizvi, S. A. Khan, C. L. Hallemeier, R. K. Kelley, and G. J. Gores, "Cholangiocarcinoma - evolving concepts and therapeutic strategies," *Nature Reviews Clinical Oncology*, vol. 15, no. 2, pp. 95–111, 2017.

[2] S. P. O'Hara, T. H. Karlsen, and N. F. LaRusso, "Cholangiocytes and the environment in primary sclerosing cholangitis: where is the link?," *Gut*, vol. 66, no. 11, pp. 1873–1877, 2017.

[3] J. W. Valle, A. Lamarca, L. Goyal, J. Barriuso, and A. X. Zhu, "New horizons for precision medicine in biliary tract cancers," *Cancer Discovery*, vol. 7, no. 9, pp. 943–962, 2017.

[4] J. Bridgewater, P. R. Galle, S. A. Khan et al., "Guidelines for the diagnosis and management of intrahepatic cholangiocarcinoma," *Journal of Hepatology*, vol. 60, no. 6, pp. 1268–1289, 2014.

[5] F. Bagante, T. Tran, G. Spolverato et al., "Perihilar cholangiocarcinoma: number of nodes examined and optimal lymph node prognostic scheme," *Journal of the American College of Surgeons*, vol. 222, no. 5, pp. 750–759.e2, 2016.

[6] N. Bird, M. Elmasry, R. Jones et al., "Role of staging laparoscopy in the stratification of patients with perihilar cholangiocarcinoma," *The British Journal of Surgery*, vol. 104, no. 4, pp. 418–425, 2017.

[7] T. Maeta, T. Ebata, E. Hayashi et al., "Pancreatoduodenectomy with portal vein resection for distal cholangiocarcinoma," *The British Journal of Surgery*, vol. 104, no. 11, pp. 1549–1557, 2017.

[8] J. Chaisaingmongkol, A. Budhu, H. Dang et al., "Common molecular subtypes among asian hepatocellular carcinoma and cholangiocarcinoma," *Cancer Cell*, vol. 32, no. 1, pp. 57–70.e3, 2017.

[9] A. Jusakul, I. Cutcutache, C. H. Yong et al., "Whole-genome and epigenomic landscapes of etiologically distinct subtypes of cholangiocarcinoma," *Cancer Discovery*, vol. 7, no. 10, pp. 1116–1135, 2017.

[10] D. Alvaro, "The challenge of cholangiocarcinoma diagnosis: the turning point is in extracellular vesicles?," *Hepatology*, vol. 66, no. 4, pp. 1029–1031, 2017.

[11] H. L. Lewis, A. A. Rahnemai-Azar, M. Dillhoff, C. R. Schmidt, and T. M. Pawlik, "Current management of perihilar cholangiocarcinoma and future perspectives," *Chirurgia*, vol. 112, no. 3, pp. 193–207, 2017.

[12] M. Tsukamoto, Y. I. Yamashita, K. Imai et al., "Predictors of cure of intrahepatic cholangiocarcinoma after hepatic resection," *Anticancer Research*, vol. 37, no. 12, pp. 6971–6975, 2017.

[13] K. Wang, H. Zhang, Y. Xia, J. Liu, and F. Shen, "Surgical options for intrahepatic cholangiocarcinoma," *Hepatobiliary Surgery and cholangiocarcinoma*, vol. 6, no. 2, pp. 79–90, 2017.

[14] I. Hosokawa, H. Shimizu, H. Yoshidome et al., "Surgical strategy for hilar cholangiocarcinoma of the left-side predominance: current role of left trisectionectomy," *Annals of Surgery*, vol. 259, no. 6, pp. 1178–1185, 2014.

[15] E. Takahashi, M. Fukasawa, T. Sato et al., "Biliary drainage strategy of unresectable malignant hilar strictures by computed tomography volumetry," *World Journal of Gastroenterology*, vol. 21, no. 16, pp. 4946–4953, 2015.

[16] A. Singh, H. S. Mann, C. L. Thukral, and N. R. Singh, "Diagnostic accuracy of MRCP as compared to ultrasound/CT in patients with obstructive jaundice," *Journal of Clinical and Diagnostic Research*, vol. 8, no. 3, pp. 103–107, 2014.

[17] R. C. Dolscheid-Pommerich, S. Manekeller, G. Walgenbach-Brünagel et al., "Clinical performance of CEA, CA19-9, CA15-3, CA125 and AFP in gastrointestinal cancer using LOCI™-based assays," *Anticancer Research*, vol. 37, no. 1, pp. 353–360, 2017.

[18] S. Yamashita, G. Passot, T. A. Aloia et al., "Prognostic value of carbohydrate antigen 19-9 in patients undergoing resection of biliary tract cancer," *The British Journal of Surgery*, vol. 104, no. 3, pp. 267–277, 2017.

[19] C. J. Verberne, Z. Zhan, E. R. van den Heuvel et al., "Survival analysis of the CEAwatch multicentre clustered randomized trial," *The British Journal of Surgery*, vol. 104, no. 8, pp. 1069–1077, 2017.

[20] M. Felder, A. Kapur, J. Gonzalez-Bosquet et al., "MUC16 (CA125): tumor biomarker to cancer therapy, a work in progress," *Molecular Cancer*, vol. 13, no. 1, p. 129, 2014.

[21] I. Bartella and J. F. Dufour, "Clinical diagnosis and staging of intrahepatic cholangiocarcinoma," *Journal of Gastrointestinal and Liver Diseases*, vol. 24, no. 4, pp. 481–489, 2015.

[22] J. R. Bergquist, C. A. Puig, C. R. Shubert et al., "Carbohydrate antigen 19-9 elevation in anatomically resectable, early stage pancreatic cancer is independently associated with decreased overall survival and an indication for neoadjuvant therapy: a National Cancer Database Study," *Journal of the American College of Surgeons*, vol. 223, no. 1, pp. 52–65, 2016.

[23] K. Gidwani, K. Huhtinen, H. Kekki et al., "A nanoparticle-lectin immunoassay improves discrimination of serum CA125 from malignant and benign sources," *Clinical Chemistry*, vol. 62, no. 10, pp. 1390–1400, 2016.

[24] F. Feng, Y. Tian, G. Xu et al., "Diagnostic and prognostic value of CEA, CA19-9, AFP and CA125 for early gastric cancer," *BMC Cancer*, vol. 17, no. 1, p. 737, 2017.

[25] X.-F. Zhang, E. W. Beal, F. Bagante et al., "Early versus late recurrence of intrahepatic cholangiocarcinoma after resection with curative intent," *The British Journal of Surgery*, vol. 105, no. 7, pp. 848–856, 2018.

[26] A. Doussot, C. Lim, C. Gómez-Gavara et al., "Multicentre study of the impact of morbidity on long-term survival following hepatectomy for intrahepatic cholangiocarcinoma," *The British Journal of Surgery*, vol. 103, no. 13, pp. 1887–1894, 2016.

[27] T. Yoh, E. Hatano, S. Seo et al., "Long-term survival of recurrent intrahepatic cholangiocarcinoma: the impact and selection of repeat surgery," *World Journal of Surgery*, vol. 42, no. 6, pp. 1848–1856, 2018.

[28] K. Komaya, T. Ebata, K. Shirai et al., "Recurrence after resection with curative intent for distal cholangiocarcinoma,"

The British Journal of Surgery, vol. 104, no. 4, pp. 426–433, 2017.

[29] T. Ebata, T. Mizuno, Y. Yokoyama, T. Igami, G. Sugawara, and M. Nagino, "Surgical resection for Bismuth type IV perihilar cholangiocarcinoma," *The British Journal of Surgery*, vol. 105, no. 7, pp. 829–838, 2017.

[30] C. G. Ethun, A. G. Lopez-Aguiar, T. M. Pawlik et al., "Distal cholangiocarcinoma and pancreas adenocarcinoma: are they really the same disease? A 13-institution study from the US extrahepatic biliary malignancy consortium and the central pancreas consortium," *Journal of the American College of Surgeons*, vol. 224, no. 4, pp. 406–413, 2017.

[31] G. Atanasov, K. Schierle, H. M. Hau et al., "Prognostic significance of tumor necrosis in hilar cholangiocarcinoma," *Annals of Surgical Oncology*, vol. 24, no. 2, pp. 518–525, 2017.

[32] S. G. Farid, A. White, N. Khan, G. J. Toogood, K. R. Prasad, and J. P. A. Lodge, "Clinical outcomes of left hepatic trisectionectomy for hepatobiliary malignancy," *The British Journal of Surgery*, vol. 103, no. 3, pp. 249–256, 2016.

[33] T. Takagi, Y. Yokoyama, T. Kokuryo, J. Yamaguchi, and M. Nagino, "Liver regeneration following experimental major hepatectomy with choledochojejunostomy," *The British Journal of Surgery*, vol. 102, no. 11, pp. 1410–1417, 2015.

[34] J. H. Kim, H. K. Yoon, G. Y. Ko et al., "Nonresectable combined hepatocellular carcinoma and cholangiocarcinoma: analysis of the response and prognostic factors after transcatheter arterial chemoembolization," *Radiology*, vol. 255, no. 1, pp. 270–277, 2010.

[35] P. B. Olthof, J. K. Wiggers, B. Groot Koerkamp et al., "Postoperative liver failure risk score: identifying patients with resectable perihilar cholangiocarcinoma who can benefit from portal vein embolization," *Journal of the American College of Surgeons*, vol. 225, no. 3, pp. 387–394, 2017.

[36] Y. Li, D. J. Li, J. Chen et al., "Application of joint detection of AFP, CA19-9, CA125 and CEA in identification and diagnosis of cholangiocarcinoma," *Asian Pacific Journal of Cancer Prevention*, vol. 16, no. 8, pp. 3451–3455, 2015.

[37] H. J. Hu, H. Mao, Y. Q. Tan et al., "Clinical value of preoperative serum CA 19-9 and CA 125 levels in predicting the resectability of hilar cholangiocarcinoma," *Springerplus*, vol. 5, no. 1, p. 551, 2016.

[38] B. Juntermanns, S. Radunz, M. Heuer et al., "Tumor markers as a diagnostic key for hilar cholangiocarcinoma," *European Journal of Medical Research*, vol. 15, no. 8, pp. 357–361, 2010.

[39] I. Hatzaras, C. Schmidt, P. Muscarella, W. S. Melvin, E. C. Ellison, and M. Bloomston, "Elevated CA 19-9 portends poor prognosis in patients undergoing resection of biliary malignancies," *HPB: The Official Journal of the International Hepato Pancreato Biliary Association*, vol. 12, no. 2, pp. 134–138, 2010.

[40] J. M. Banales, V. Cardinale, G. Carpino et al., "Expert consensus document: cholangiocarcinoma: current knowledge and future perspectives consensus statement from the European Network for the Study of Cholangiocarcinoma (ENS-CCA)," *Nature Reviews. Gastroenterology & Hepatology*, vol. 13, no. 5, pp. 261–280, 2016.

[41] G. Sapisochin, M. Facciuto, L. Rubbia-Brandt et al., "Liver transplantation for "very early" intrahepatic cholangiocarcinoma: international retrospective study supporting a prospective assessment," *Hepatology*, vol. 64, no. 4, pp. 1178–1188, 2016.

[42] T. Tsukahara, T. Ebata, Y. Shimoyama et al., "Residual carcinoma in situ at the ductal stump has a negative survival effect: an analysis of early-stage cholangiocarcinomas," *Annals of Surgery*, vol. 266, no. 1, pp. 126–132, 2017.

[43] S. Y. Bangarulingam, E. Bjornsson, F. Enders et al., "Long-term outcomes of positive fluorescence in situ hybridization tests in primary sclerosing cholangitis," *Hepatology*, vol. 51, no. 1, pp. 174–180, 2010.

[44] P. L. Lian, Y. Chang, X. C. Xu, Z. Zhao, X. Q. Wang, and K. S. Xu, "Pancreaticoduodenectomy for duodenal papilla carcinoma: a single-centre 9-year retrospective study of 112 patients with long-term follow-up," *World Journal of Gastroenterology*, vol. 23, no. 30, pp. 5579–5588, 2017.

[45] S. Rizvi and G. J. Gores, "Pathogenesis, diagnosis, and management of cholangiocarcinoma," *Gastroenterology*, vol. 145, no. 6, pp. 1215–1229, 2013.

[46] X. W. Huang, Y. Huang, L. D. Chen et al., "Potential diagnostic performance of contrast-enhanced ultrasound and tumor markers in differentiating combined hepatocellular-cholangiocarcinoma from hepatocellular carcinoma and cholangiocarcinoma," *Journal of Medical Ultrasonics*, vol. 45, no. 2, pp. 231–241, 2018.

[47] R. A. Carr, M. T. Yip-Schneider, S. Dolejs et al., "Pancreatic cyst fluid vascular endothelial growth factor a and carcinoembryonic antigen: a highly accurate test for the diagnosis of serous cystic neoplasm," *Journal of the American College of Surgeons*, vol. 225, no. 1, pp. 93–100, 2017.

[48] M. Q. He, K. Wang, W. J. Wang, Y. L. Yu, and J. H. Wang, "Smart DNA machine for carcinoembryonic antigen detection by exonuclease III-assisted target recycling and DNA walker cascade amplification," *Analytical Chemistry*, vol. 89, no. 17, pp. 9292–9298, 2017.

[49] B. Le Roy, M. Gelli, G. Pittau et al., "Neoadjuvant chemotherapy for initially unresectable intrahepatic cholangiocarcinoma," *The British Journal of Surgery*, vol. 105, no. 7, pp. 839–847, 2017.

[50] A. Shafaghi, F. Mansour- Ghanaei, F. Joukar, F. Nabavi, A. Mansour- Ghanaei, and A. Esrafilian Soltani, "Stage association of preoperative serum carcinoembryonic antigen with gastric adenocarcinoma in Iranian patients," *Asian Pacific Journal of Cancer Prevention*, vol. 18, no. 10, pp. 2669–2672, 2017.

[51] M. Yamada, T. Ebata, Y. Yokoyama et al., "Pulmonary metastasis after resection of cholangiocarcinoma: incidence, resectability, and survival," *World Journal of Surgery*, vol. 41, no. 6, pp. 1550–1557, 2017.

Hindawi
Disease Markers
Volume 2019, Article ID 9056402, 9 pages
https://doi.org/10.1155/2019/9056402

Research Article

Predicting Long-Term Mortality after Acute Coronary Syndrome Using Machine Learning Techniques and Hematological Markers

Konrad Pieszko,[1,2] **Jarosław Hiczkiewicz**,[1,2] **Paweł Budzianowski**,[3] **Jan Budzianowski**,[1,2] **Janusz Rzeźniczak**,[4] **Karolina Pieszko**,[1] **and Paweł Burchardt**[4,5]

[1]*University of Zielona Góra, ul. Licealna 9, 65-417 Zielona Góra, Poland*
[2]*Clinical Department of Cardiology, Nowa Sól Multidisciplinary Hospital, ul. Chałubińskiego 7, 67-100, Poland*
[3]*Department of Engineering, University of Cambridge, Trumpington St, Cambridge CB2 1PZ, UK*
[4]*Department of Cardiology, J. Strus Hospital, ul. Szwajcarska 3, 61-285 Poznań, Poland*
[5]*Biology of Lipid Disorders Department, Poznan University of Medical Sciences, ul. Rokietnicka 8, 60-806 Poznań, Poland*

Correspondence should be addressed to Konrad Pieszko; pieszek@gmail.com

Received 27 September 2018; Accepted 11 December 2018; Published 30 January 2019

Guest Editor: Agata M. Bielecka-Dabrowa

Introduction. Hematological indices including red cell distribution width and neutrophil to lymphocyte ratio are proven to be associated with outcomes of acute coronary syndrome. The usefulness of machine learning techniques in predicting mortality after acute coronary syndrome based on such features has not been studied before. *Objective*. We aim to create an alternative risk assessment tool, which is based on easily obtainable features, including hematological indices and inflammation markers. *Patients and Methods*. We obtained the study data from the electronic medical records of 5053 patients hospitalized with acute coronary syndrome during a 5-year period. The time of follow-up ranged from 12 to 72 months. A machine learning classifier was trained to predict death during hospitalization and within 180 and 365 days from admission. Our method was compared with the Global Registry of Acute Coronary Events (GRACE) Score 2.0 on a test dataset. *Results*. For in-hospital mortality, our model achieved a *c*-statistic of 0.89 while the GRACE score 2.0 achieved 0.90. For six-month mortality, the results of our model and the GRACE score on the test set were 0.77 and 0.73, respectively. Red cell distribution width (HR 1.23; 95% CL 1.16-1.30; $P < 0.001$) and neutrophil to lymphocyte ratio (HR 1.08; 95% CL 1.05-1.10; $P < 0.001$) showed independent association with all-cause mortality in multivariable Cox regression. *Conclusions*. Hematological markers, such as neutrophil count and red cell distribution width have a strong association with all-cause mortality after acute coronary syndrome. A machine-learned model which uses the abovementioned parameters can provide long-term predictions of accuracy comparable or superior to well-validated risk scores.

1. Introduction

The term acute coronary syndrome (ACS) refers to many conditions which include non-ST-segment elevation acute coronary syndrome (NSTE-ACS) and ST-elevation myocardial infarction (STEMI). The common cause of these conditions is inadequate blood flow to the myocardium which can be related to acute cholesterol plaque rupture or erosion and thrombus formation. These conditions have a similar presentation, and the most frequent symptom reported by patients is chest pain, which is one of the most common causes of presentation to the emergency room accounting for up to 6% of emergency department attendances and 27% of medical admissions [1]. Current guidelines emphasize the usefulness of established quantitative risk scores for prognosis estimation [2], which is necessary for the adequate and cost-effective provision of evidence-based therapies.

An increased systemic and local inflammation plays a crucial role in the pathophysiology of ACS. Various hematological indices have been reported to be associated with poorer prognosis or the occurrence of major adverse cardiac events after ACS [3]. These indices include neutrophil to lymphocyte ratio (NLR) [4–6], platelet to lymphocyte

Table 1: Variables used in the Cox regression model, machine-learned model, and for the calculation of the GRACE score.

COX regression	Machine-learned model	GRACE score
$n = 4743$ (310 observations excluded due to missing values)	$n = 4969$ (84 observations excluded due to missing values that where required to calculate GRACE score)	
Troponin elevation ratio	Troponin elevation ratio	Age
Neutrophil to lymphocyte ratio Platelet to lymphocyte ratio	Red cell distribution width	Heart rate
Red cell distribution width	Platelet count	Systolic blood pressure
Platelet count	Creatinine level	Creatinine level
Creatinine level	Hemoglobin level	ST-segment deviation
Fibrinogen level	Mean cell volume	Troponin elevation (true or false)
Hemoglobin level	Sodium level	Killip class
Potassium level	Prothrombin time	
Mean cell volume	Fibrinogen level	
Monocyte count	Age	
Sodium level	Lymphocyte count	
Prothrombin level	Neutrophil count	
Age	LDL level	
Heart rate at admission	CRP level	
Systolic blood pressure	Sex	
ST-segment elevation	Heart rate	
Diabetes	Systolic blood pressure	
	Diastolic blood pressure	
	Body mass index	

LDL: low-density lipoprotein; CRP: C-reactive protein.

ratio (PLR) [7], red cell distribution width (RDW) [8], and mean platelet volume (MPV). These studies brought evidence that such nonspecific markers of the inflammatory response are associated with the GRACE score. [9] Moreover, they can improve its discriminative capabilities [10, 11].

Machine learning (ML) is a field of computer science that uses various computational algorithms to give computer systems the ability to progressively improve performance on a specific task with data, without being explicitly programmed. This term describes a vast spectrum of computational methods, many of which like logistic regression have been used extensively in medical sciences for many years [12]. The most state-of-the-art algorithms are currently subject of intense research and have been recently shown to perform on par with trained ophthalmologists in detecting diabetic retinopathy in eye fundus images [13], classify skin lesion images automatically with dermatologist-level accuracy [14], or detect hip fractures from frontal pelvic X-rays [15].

In our previous research, we successfully used ML techniques to predict in-hospital mortality [16]. In this study, we attempt to develop a new tool for long-term risk assessment following ACS and compare its performance with the GRACE 2.0 model. In contrast to existing risk scores, our tool relies on laboratory tests (including hematological indices) and simple measurements (including blood pressure and heart rate), rather than clinical features. The rationale for such approach is the proven association of inflammatory response with ACS outcomes.

2. Methods

We retrospectively examined electronic medical records of patients admitted to a cardiology department between January 2012 and December 2016 to select all patients hospitalized because of an ACS. The analyzed group comprised of patients who had their diagnosis confirmed by a cardiologist according to ESC guidelines [2].

5053 individual patients were qualified (1522 with STEMI, 857 with NSTEMI, and 2674 with unstable angina). We analyzed the descriptions of the electrocardiograms in the patient's medical records to identify patients who had an ST-segment elevation ($n = 1522$) or any ST-segment deviation-elevation or depression ($n = 4420$) according to current guidelines.

We obtained information on all-cause death or survival and on the exact date of death from the national death registry one year after the end of data collection. Patients who had incomplete records or had no blood sample taken during hospitalization were excluded from the study. If a patient was admitted with ACS more than one time in the analyzed period, only the last hospitalization was considered.

All patients were treated according to current guidelines and doctor's therapeutic decisions. Each patient had a venous blood sample taken within 30 minutes from admission. The complete blood count and hematological parameters were analyzed using an automated blood cell counter *CD-RUBY* (*Abbott*, *Lake Bluff*, *Illinois*, *USA*). Biochemical parameters were measured using *COBAS 6000*

Table 2: Baseline characteristics according to the survival or death status–numerical variables. Data is presented as median and interquartile range (IQR). *P* values refer to the results of the two-tailed Mann-Whitney *U* test.

	Survival ($n = 4287$)	Death ($n = 766$)	*P* value
Age (years)	65.5 (59.4-73.0)	72.1 (64.4-79.8)	<0.001
Troponin elevation (ratio)	0.9 (0.4-3.9)	3.1 (0.7-38.2)	<0.001
Systolic blood pressure (mmHg)	120.0 (110.0-130.0)	117.0 (110.0-130.0)	<0.001
Diastolic blood pressure (mmHg)	80.0 (75.0-90.0)	78.0 (70.0-85.0)	<0.001
Heart rate at admission	72.0 (64.0-83.0)	76.0 (66.0-89.0)	<0.001
C-reactive protein (mg/dl)	0.4 (0.2-1.8)	2.2 (0.6-6.4)	<0.001
Fibrinogen (mg/dl)	398.0 (344.0-467.0)	430.0 (363.8-517.2)	<0.001
Creatinine (mg/dl)	1.0 (0.8-1.1)	1.1 (0.9-1.4)	<0.001
Neutrophil ($10^3/mm^3$)	5.1 (3.9-6.6)	6.1 (4.5-8.6)	<0.001
Lymphocyte ($10^3/mm^3$)	1.9 (1.5-2.4)	1.6 (1.2-2.2)	<0.001
Monocyte ($10^3/mm^3$)	0.6 (0.5-0.7)	0.7 (0.5-0.9)	<0.001
Eosinophil ($10^3/mm^3$)	0.1 (0.1-0.2)	0.1 (0.0-0.2)	<0.001
Hematocrit (%)	42.7 (39.8-45.4)	40.3 (35.9-43.9)	<0.001
Hemoglobin (g/dl)	14.5 (13.5-15.5)	13.5 (11.9-14.8)	<0.001
Red cell distribution width	12.2 (11.6-12.9)	12.8 (12.0-14.0)	<0.001
Mean cell volume (fl)	91.1 (88.2-94.4)	91.6 (88.1-95.2)	0.1
Platelets ($10^3/mm^3$)	221.0 (186.0-261.0)	223.0 (174.2-269.0)	0.72
Mean platelet volume (fl)	8.6 (7.5-9.8)	8.3 (7.3-9.6)	0.001
Alanine aminotransferase (U/l)	24.0 (17.0-34.0)	23.0 (16.0-37.0)	0.01
Aspartate aminotransferase (U/s)	24.0 (19.0-32.0)	28.0 (20.0-52.0)	<0.001
Basophil count ($10^3/mm^3$)	0.1 (0.1-0.1)	0.1 (0.0-0.1)	0.02
Cholesterol level (mg/dl)	175.0 (144.0-216.0)	162.0 (135.0-198.0)	<0.001
Low-density lipoprotein (mg/dl)	106.0 (78.0-143.0)	97.0 (73.0-127.0)	<0.001
High-density lipoprotein (mg/dl)	50.0 (41.0-60.0)	46.0 (37.0-57.0)	<0.001
Triglycerides (mg/dl)	122.0 (88.0-172.0)	105.0 (79.8-149.2)	0.04
Sodium (mmol/l)	141.0 (139.0-143.0)	140.0 (138.0-142.0)	<0.001
Potassium (mmol/l)	4.4 (4.1-4.7)	4.4 (4.1-4.8)	0.01
Urea (mg/dl)	36.0 (30.0-45.0)	47.0 (36.0-65.2)	0.4
Neutrophil to lymphocyte ratio	2.6 (1.9-3.7)	3.6 (2.4-5.9)	<0.001
Platelet to lymphocyte ratio	114.4 (87.8-149.6)	131.6 (94.4-187.3)	<0.001
Days of hospitalization	4.0 (3.0-5.0)	4.0 (3.0-7.0)	<0.001

(*Roche*, *Basel*, *Switzerland*). The results of the laboratory tests as well as the clinical information were obtained retrospectively from the electronic medical record (EMR) system at the time of follow-up. During the period of data collection, both Troponin I and Troponin T were used. Therefore, we expressed troponin elevation as a ratio (actual value divided by the norm).

Statistical analyses were performed using the RStudio Software. The Shapiro-Wilk test was used to test the variables' distribution for normality. Most of the analyzed variables did not have a normal distribution. Median and interquartile ranges were selected as measures of central tendency. The univariable two-tailed Mann-Whitney *U* test was used to compare numerical features. We created a multivariable Cox regression model using variables with statistically significant differences (*P* value <0.05) in univariate analysis. 310 observations were excluded from the analysis because of missing values. We did not use automated stepwise backward elimination. Instead, all variables which were suspected to influence the outcome were entered into the model [17]. The list of variables used in the Cox regression model is presented in Table 1. The proportional hazard assumption was verified using Schoenfeld residuals. To assess the time-varying effects of the selected variables, Aalen's additive model was used. A *P* value <0.05 indicated statistical significance. The results were presented as hazard ratios with 95% confidence intervals (CI).

A probability of death during hospitalization and after 6 and 12 months from admission according to the GRACE 2.0 score was calculated using the model coefficients published on the GRACE project website (https://www.outcomes-umassmed.org/grace/). A Python package was developed to allow for the batch calculation of the GRACE 2.0 death probability based on relevant clinical and laboratory features. As the information about Killip class and creatinine level was available for almost all patients, the full version of the

algorithm was used. In 84 cases the missing data did not allow for the calculation of the GRACE probability. Table 1 presents and compares the variables analyzed in the COX regression model as well as the variables used by the ML model and for the calculation of the GRACE score.

2.1. Machine Learning Methods. Model selection, optimization, and fitting were performed using the Python 3.6 and scikit-learn software packages. We used 4969 observations for training and evaluating the ML model. We have excluded 84 observations where variables necessary to calculate the GRACE score were missing, as presented in Table 1. The remaining missing values which did not affect the calculation of the GRACE score were imputed using mean of all observations. The gradient-boosted tree algorithm was implemented using the xgboost [18] software package.

One-fifth of the available data ($n = 994$) was put aside as a test set and not used for training. Observations for the test set were chosen randomly, but in a way that preserved the ratio of positive to negative class (death and survival). The ML classifier was optimized using the training data only ($n = 3975$), using the 5-fold cross-validation. In this process, the training data was divided into 5 parts, and each of these parts was used to train the classifier and to measure its performance. We measured the performance of the GRACE score and our model by calculating the areas under Receiver Operating Characteristic (ROC) curves. The performance measurements during cross-validation were averaged and expressed by mean ± standard deviation. Finally, the performance of both classifiers was compared by calculating the areas under the ROC curves on the test set which was not used for training the ML model at all. This process was repeated in identical fashion for all analyzed endpoints: in-hospital death, 6-month death, and 12-month death.

3. Results

The in-hospital mortality rate was 1.64% ($n = 83$) within 6 months from admission 5.87% ($n = 297$) and within a year from admission 7.85% ($n = 397$). 766 patients (15%) died during the period of the study (from January 2012 until acquisition of the survival data in December 2017). The baseline clinical characteristics and laboratory test results according to survival status are presented in Tables 2 and 3. Some variables including the presence of ST-segment elevation, troponin elevation, sodium levels, and systolic blood pressure did not meet the proportional hazard assumption. However, examining Aalen's additive model indicated that these parameters have a high prognostic value shortly after admission that decreases over time. The results of the multivariable Cox regression analysis are visualized in the form of a forest plot on Figure 1. High RDW, NLR, monocyte count, creatinine level, prothrombin time, age, and heart rate as well as low sodium and hemoglobin were significantly associated with all-cause mortality in the multivariable model. Due to a large number of missing values for CRP and LDL levels, they were not considered for survival analysis, but we kept them in the machine-learned model because of their known association with ACS pathophysiology and outcomes [19].

Table 3: Baseline characteristics according to the survival or death status–categorical variables.

	Survival ($n = 4287$)	Death ($n = 766$)
Sex		
Male	2908	493
Female	1379	273
Diabetes		
No diabetes	3106	503
Type 1 diabetes	20	2
Type 2 diabetes	1161	261
PCI during hospitalization		
True	2565	468
False	1722	298
Killip Class		
I	4196	708
II	74	24
III	9	9
IV	8	25
ST-segment elevation		
False	3047	484
True	1240	282
ST-segment deviation		
False	3521	699
True	766	67

3.1. Machine Learning Results. The model based on the gradient-boosted trees was trained using the following variables as input: troponin elevation ratio, NLR, PLR, RDW, CRP, platelet count, creatinine, hemoglobin, mean cell volume, sodium, prothrombin time, fibrinogen, age, neutrophil count, body mass index, systolic and diastolic blood pressure, heart rate, and sex. The variables were selected to maximize the model's performance, but clinical parameters including the data from the patient's medical history and physical examination were not included in the model. The point was to create a model that could use data that is routinely collected in the EMR system for all patients. The model's performance metrics are summarized in Table 4. Figure 2 presents the Receiver Operating Characteristic curves for our classifier and the GRACE score 2.0 for the detection of in-hospital, 6-month, and one-year mortality. Eyeballing the Receiver Operating Characteristic (ROC) curves and analysis of areas under these curves (AUROC) reveal that the results of our model and the GRACE score 2.0 are similar. GRACE performed slightly better for short-term results (AUROC 0.9 vs. 0.89) while our model scored better in long-term results (AUROC 0.77 vs. 0.73 and 0.72 vs. 0.71 for 6-month and one-year mortality, respectively).

4. Discussion

The results of the survival analysis using Cox regression confirm findings from numerous studies regarding the association of hematological indices including RDW, NLR, and

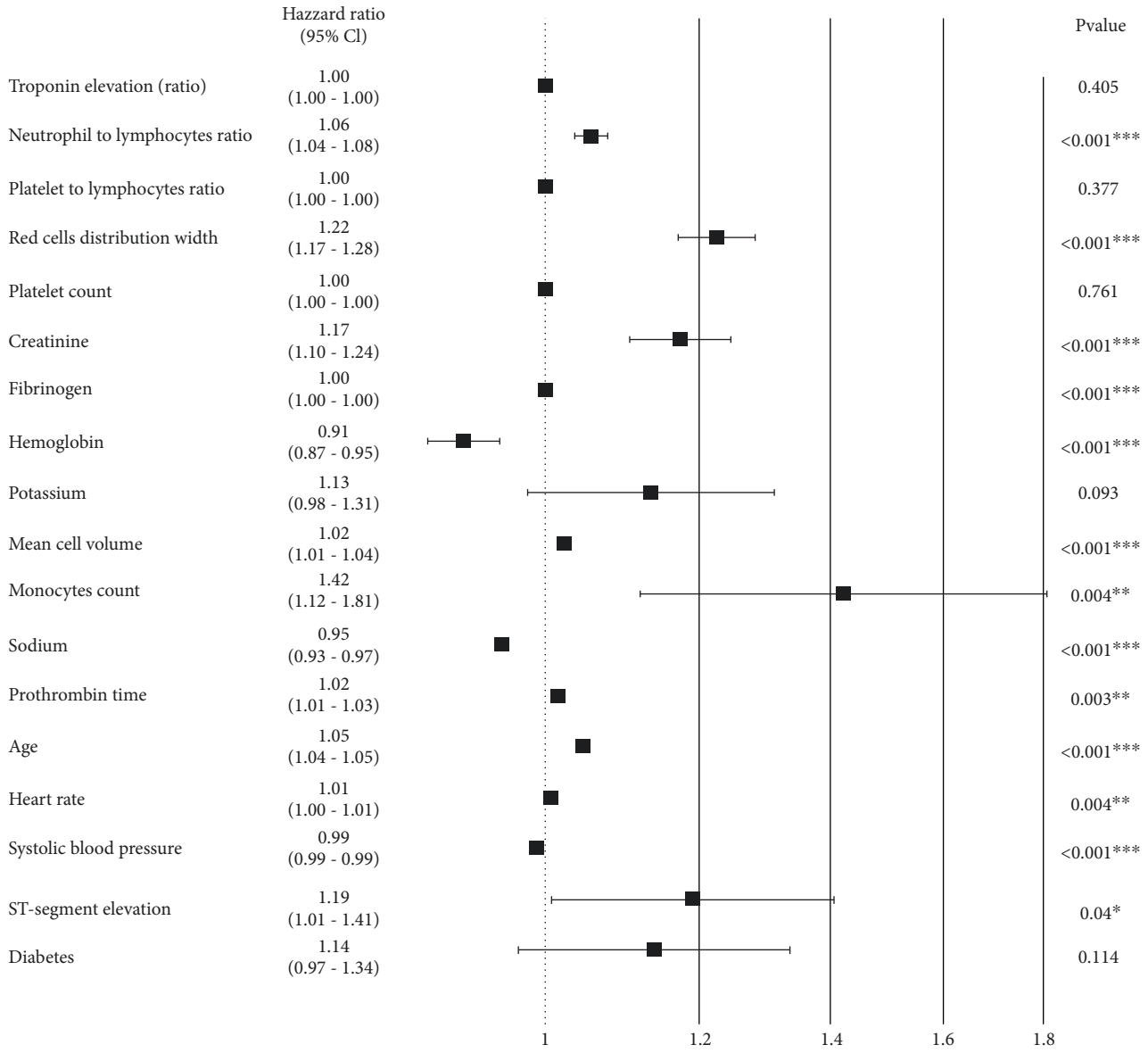

Figure 1: Results of Cox regression. Hazard ratios are presented as black rectangles, and confidence level bands are presented as whiskers. The central vertical line indicates a hazard ratio of 1.

Table 4: Performance of classifiers in predicting death during hospitalization, within 6 months, and one year after admission.

	In-hospital mortality	6-month mortality	One-year mortality
Our algorithm on validation set	0.85 ± 0.04	0.78 ± 0.03	0.78 ± 0.03
GRACE 2.0 on validation set	0.89 ± 0.04	0.77 ± 0.03	0.76 ± 0.03
Our algorithm on test set	0.89	0.77	0.72
GRACE 2.0 on test set	0.90	0.73	0.71

neutrophil count with short- and long-term prognosis after acute coronary syndrome [3]. The low-grade inflammatory process plays an important role in the formation and subsequent destabilization and rupture of the atherosclerotic plaque [20]. In the multivariable Cox regression model, RDW had a strong association with all-cause mortality (HR 1.22, 95% Cl 1.17-1.28). These results are consistent with the findings from other studies that identified RDW as a prognostic marker in cardiovascular diseases and heart failure [21] and also as a predictor of all-cause mortality [22]. It was suggested that patients with increased RDW have lower oxygen supply at tissue level due to decreased red blood cell deformability and impaired blood flow through microcirculation [23]. Our results also seem to confirm the findings

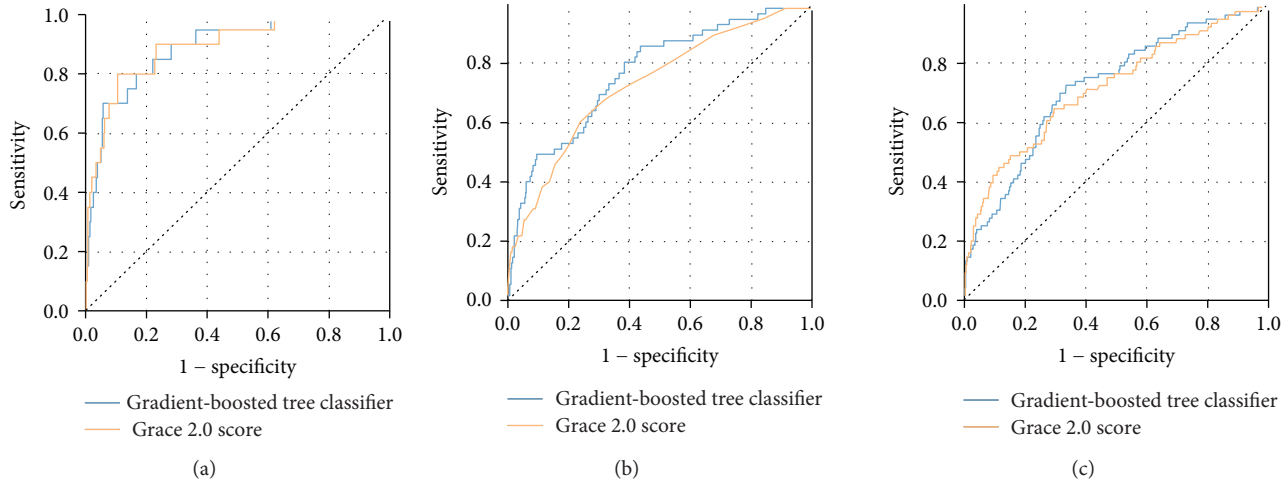

Figure 2: (a), (b), and (c) represent Receiver Operating Characteristic (ROC) curves for in-hospital mortality, 6-month mortality, and one-year mortality, respectively. ROC curves for our classifier are drawn using a blue line, while ROC curves for the Global Registry of Acute Coronary Events (GRACE) 2.0 score are drawn using an orange line.

from other studies [24] on the impact of admission anemia on long-term prognosis in ACS.

Our model performed better than GRACE score for medium- and long-term prognosis. However, the difference in performance was small, and the calculations of the GRACE scores in our study were made based on retrospective data and could be inaccurate in some cases. This result needs to be confirmed in prospective validation. Better long-term performance of our model might be related to the fact that it uses inflammation biomarkers. The underlying inflammation process is known to be related to atherosclerosis, but the currently used risk scores do not take advantage of this fact.

GRACE score 2.0 has been extensively validated in various populations and proved to have superior discriminatory accuracy for predicting major adverse cardiac events when compared to other risk assessment tools [25, 26]. However, the adoption of its use in a clinical setting was reported to be unsatisfactory. One of the reasons for such situation is the necessity of use of an external application which requires manual data input and consumes extra time [27]. Studies have shown that the integration of risk assessment scores into IT solutions resulted in higher compliance [28]. With all the necessary data available in the electronic medical record system, after integration into existing software, our solution can provide risk assessment without any additional input from the physician. The result could then trigger relevant alerts, helping to select the highest risk patients.

Several studies investigated the application of machine learning techniques to risk stratification in ACS. Most of these studies used data collected retrospectively from a large number of electronic medical reports, similarly as we did in our study [29, 30]. The models they created, however, were based on numerous clinical features, and it is difficult to reproduce the results and apply their solution in a different setting. For instance, VanHouten et al. reported that their machine-learned model could outperform the GRACE score. They used numerous sparse features including the full blood count in most patients and their classifier achieved area under receiver operating curve of 0.85. Our model yields comparable performance, but thanks to using the smaller number of free-of-interpretation features, it is easier to apply and validate externally.

5. Study Limitations

In our study, we retrospectively analyzed the electronic medical records of patients hospitalized over several years. This allowed for rapid development on an ML algorithm but is also a significant limitation.

Data stored in medical records are often incomplete, complex, messy, and can be biased [31]. The naive use of raw medical records as input for either inferential statistics or machine learning models can lead to false conclusions. A good example of such situation is the study of Fine et al., in which patients who were admitted with severe community-acquired pneumonia and died in the emergency department had very little information stored in medical records. As a result, some deceased patients appeared healthier than those who survived [32].

The most concerning limitation of our study is related to variables that were stored in medical records as unstructured data in the form of physicians' notes (e.g., descriptions of electrocardiograms). When designing our classifier, we only intended to use features that are available in the medical records as single measurements. Clinical features, including the results of physical examination, patient's symptoms, and medical history, were not considered. This approach is different than those proposed by many other studies exploring the application of machine learning methods in predicting ACS outcomes [29, 30], where all the features that were available in EMR were used. Nevertheless, determining the presence of ST-segment deviation was necessary for calculating the GRACE score. We did not analyze the

electrocardiograms directly, and the classification of some ECG descriptions was not obvious. Therefore, the calculations of the GRACE score were especially prone to bias. To make a justified statement on the performance of our classifier vs. any other existing score, it is necessary to evaluate it prospectively, and the scores should be calculated on the day of admission to the hospital.

The follow-up in our study was limited to death or survival status. This is also an important limitation because it was not possible to assess the occurrence of major adverse cardiac events other than all-cause death. Many patients suffered from recurrent ACS, which we did not analyze in this study. Instead, we only took into account the last available hospitalization.

Another important limitation is related to using the Cox regression model. Some of the variables which we used in this model did not meet the proportional hazard assumption. Nevertheless, after analyzing different regression models, we concluded that the predictive value of ST-segment elevation, troponin elevation, sodium levels, and systolic blood pressure may decrease over time and that it is worth presenting the results in this form.

Finally, although the study included patients hospitalized over many years, this dataset is still modest in terms of machine learning model development. The performance of our classifier varied slightly, depending on which observations were chosen randomly for the test set. In contrast, GRACE score was validated on over 100000 patients worldwide, thus the evidence that supports its usefulness is strong. We do not aim to prove that our method is better than any existing well-validated risk score, but to present a new approach to long-term risk prediction in ACS based on different analytic methods and different variables than existing scores.

6. Conclusions

Hematological markers of inflammation show strong correlation with the outcomes of ACS, and they can be successfully incorporated into numerical models designed to support clinical decisions. Our model predicted long-term mortality better than GRACE score, but the difference might not be significant, and it requires prospective validation. The potential of such solution lies in taking advantage of the easily available hematological biomarkers and in eliminating the necessity to enter the results of clinical examination or the past medical history into the model.

Abbreviations

ACS: Acute coronary syndrome
AUROC: Area under the receiver operating characteristic curve
BMI: Body mass index
CABG: Coronary artery bypass grafting
CRP: C-reactive protein
EMR: Electronic medical records
GFR: Glomerular filtration rate
GRACE: Global registry of acute coronary events
HDL: High-density lipoprotein
HR: Hazard ratio
IQR: Interquartile range
LDL: Low-density lipoprotein
MCV: Mean cell volume
ML: Machine learning
MPV: Mean platelet volume
NLR: Neutrophil to lymphocyte ratio
NSTE-ACS: Non-ST-segment elevation acute coronary syndrome
NSTEMI: Non-ST-segment elevation myocardial infarction
PLR: Platelet to lymphocyte ratio
RDW: Red cell distribution width
ROC: Receiver operating characteristic
STEMI: ST-segment myocardial infarction.

Data Availability

The datasets used and analyzed during the study contain at least four indirect identifiers of patients which were used as input variables for machine learning algorithms (sex, age, weight, height, and place of treatment). For this reason, the data cannot be made publicly available in this form. However, authors are willing to share their data on reasonable request and after case-by-case assessment of such request by a local ethics committee.

Conflicts of Interest

The authors have no conflicts of interest to declare.

Authors' Contributions

All the authors have had access to the data and all drafts of the manuscript. KP, JH, PB, PB, and JR designed the study. KP, KP, JH, and JB managed and analyzed the data. KP, KP, PB, and JH developed the machine-learning models. KP, PB, and JH wrote the draft of the manuscript. KP, JH, PB, and JB reviewed the manuscript. All the authors read and approved the final manuscript.

Acknowledgments

The Python implementation of the GRACE 2.0 death probability calculation, as well as the Python implementation of our classifier, will be published on GitHub repository https://github.com/konradpieszko upon publication of this manuscript. The Center for Outcomes Research did not evaluate nor formally approve our implementation of the GRACE 2.0 algorithm. However, they were informed about it and had no objections to us sharing the source code of our implementation.

References

[1] S. Goodacre, E. Cross, J. Arnold, K. Angelini, S. Capewell, and J. Nicholl, "The health care burden of acute chest pain," *Heart*, vol. 91, no. 2, pp. 229-230, 2005.

[2] M. Roffi, C. Patrono, J.-P. Collet et al., "2015 ESC guidelines for the management of acute coronary syndromes in patients presenting without persistent ST-segment elevation," *European Heart Journal*, vol. 37, no. 3, pp. 267–315, 2016.

[3] J. Budzianowski, K. Pieszko, P. Burchardt, J. Rzeźniczak, and J. Hiczkiewicz, "The role of hematological indices in patients with acute coronary syndrome," *Disease Markers*, vol. 2017, Article ID 3041565, 9 pages, 2017.

[4] U. U. Tamhane, S. Aneja, D. Montgomery, E. K. Rogers, K. A. Eagle, and H. S. Gurm, "Association between admission neutrophil to lymphocyte ratio and outcomes in patients with acute coronary syndrome," *The American Journal of Cardiology*, vol. 102, no. 6, pp. 653–657, 2008.

[5] B. Azab, M. Zaher, K. F. Weiserbs et al., "Usefulness of neutrophil to lymphocyte ratio in predicting short- and long-term mortality after non–ST-elevation myocardial infarction," *The American Journal of Cardiology*, vol. 106, no. 4, pp. 470–476, 2010.

[6] S. Chatterjee, P. Chandra, G. Guha et al., "Pre-procedural elevated white blood cell count and neutrophil-lymphocyte (N/L) ratio are predictors of ventricular arrhythmias during percutaneous coronary intervention," *Cardiovascular & Hematological Disorders Drug Targets*, vol. 11, no. 2, pp. 58–60, 2011.

[7] H. Vakili, M. Shirazi, M. Charkhkar, I. Khaheshi, M. Memaryan, and M. Naderian, "Correlation of platelet-to-lymphocyte ratio and neutrophil-to-lymphocyte ratio with thrombolysis in myocardial infarction frame count in ST-segment elevation myocardial infarction," *European Journal of Clinical Investigation*, vol. 47, no. 4, pp. 322–327, 2017.

[8] W. Li, Q. Liu, and Y. Tang, "Platelet to lymphocyte ratio in the prediction of adverse outcomes after acute coronary syndrome: a meta-analysis," *Scientific Reports*, vol. 7, no. 1, article 40426, 2017.

[9] H. Acet, F. Ertaş, M. A. Akıl et al., "Relationship between hematologic indices and global registry of acute coronary events risk score in patients with ST-segment elevation myocardial infarction," *Clinical and Applied Thrombosis/Hemostasis*, vol. 22, no. 1, pp. 60–68, 2016.

[10] X. Niu, C. Yang, Y. Zhang, H. Zhang, and Y. Yao, "Mean platelet volume on admission improves risk prediction in patients with acute coronary syndromes," *Angiology*, vol. 66, no. 5, pp. 456–463, 2015.

[11] A. T. Timóteo, A. L. Papoila, A. Lousinha et al., "Predictive impact on mediumterm mortality of hematological parameters in acute coronary syndromes: added value on top of GRACE risk score," *European Heart Journal: Acute Cardiovascular*, vol. 4, no. 2, pp. 172–179, 2015.

[12] A. L. Beam and I. S. Kohane, "Big data and machine learning in health care," *JAMA*, vol. 319, no. 13, pp. 1317-1318, 2018.

[13] V. Gulshan, L. Peng, M. Coram et al., "Development and validation of a deep learning algorithm for detection of diabetic retinopathy in retinal fundus photographs," *JAMA*, vol. 316, no. 22, pp. 2402–2410, 2016.

[14] A. Esteva, B. Kuprel, R. A. Novoa et al., "Dermatologist-level classification of skin cancer with deep neural networks," *Nature*, vol. 542, no. 7639, pp. 115–118, 2017.

[15] W. Gale, L. Oakden-Rayner, G. Carneiro, A. P. Bradley, and L. J. Palmer, *Detecting Hip Fractures with Radiologist-Level Performance Using Deep Neural Networks*, 2017, https://arxiv.org/abs/1711.06504.

[16] K. Pieszko, J. Hiczkiewicz, P. Budzianowski et al., "Machine--learned models using hematological inflammation markers in the prediction of short-term acute coronary syndrome outcomes," *Journal of Translational Medicine*, vol. 16, no. 1, p. 334, 2018.

[17] P. L. Flom and D. L. Casell, "Stopping stepwise: why stepwise and similar selection methods are bad, and what you should use," in *NESUG 2007 Proceedings; NorthEast SAS Users Group 22th Annual Conference*, pp. 13–16, Baltimore, MD, USA, November 2007.

[18] T. Chen and C. Guestrin, "XGBoost: a scalable tree boosting system," in *Proceedings of the 22nd ACM SIGKDD Conference on Knowledge Discovery and Data Mining*, pp. 785–794, San Francisco, CA, USA, 2016.

[19] J. Munkhaugen, J. E. Otterstad, T. Dammen et al., "The prevalence and predictors of elevated C-reactive protein after a coronary heart disease event," *European Journal of Preventive Cardiology*, vol. 25, no. 9, pp. 923–931, 2018.

[20] S. Balta, T. Celik, D. P. Mikhailidis et al., "The relation between atherosclerosis and the neutrophil–lymphocyte ratio," *Clinical and Applied Thrombosis/Hemostasis*, vol. 22, no. 5, pp. 405–411, 2016.

[21] B. Szyguła-Jurkiewicz, Ł. Siedlecki, Ł. Pyka, E. Romuk, P. Przybyłowski, and M. Gąsior, "Red blood cell distribution width, relative lymphocyte count, and type 2 diabetes predict all-cause mortality in patients with advanced heart failure," *Polish Archives of Internal Medicine*, vol. 128, no. 2, pp. 1–6, 2018.

[22] Y. Arbel, D. Weitzman, R. Raz et al., "Red blood cell distribution width and the risk of cardiovascular morbidity and all-cause mortality," *Thrombosis and Haemostasis*, vol. 111, no. 2, pp. 300–307, 2014.

[23] K. V. Patel, J. G. Mohanty, B. Kanapuru, C. Hesdorffer, W. B. Ershler, and J. M. Rifkind, "Association of the red cell distribution width with red blood cell deformability," *Advances in Experimental Medicine and Biology*, vol. 765, pp. 211–216, 2013.

[24] A. Tomaszuk-Kazberuk, S. Bolińska, E. Młodawska, P. Łopatowska, B. Sobkowicz, and W. Musiał, "Does admission anaemia still predict mortality six years after myocardial infarction?," *Kardiologia Polska*, vol. 72, no. 6, pp. 488–493, 2014.

[25] G. P. De Araújo, J. Ferreira, C. Aguiar, and R. Seabra-Gomes, "TIMI, PURSUIT, and GRACE risk scores: sustained prognostic value and interaction with revascularization in NSTE-ACS," *European Heart Journal*, vol. 26, no. 9, pp. 865–872, 2005.

[26] K. G. Aragam, U. U. Tamhane, E. Kline-Rogers et al., "Does simplicity compromise accuracy in ACS risk prediction? A retrospective analysis of the TIMI and GRACE risk scores," *PLoS One*, vol. 4, no. 11, article e7947, 2009.

[27] D. Corcoran, P. Grant, and C. Berry, "Risk stratification in non-ST elevation acute coronary syndromes: risk scores, biomarkers and clinical judgment," *IJC Heart & Vasculature*, vol. 8, pp. 131–137, 2015.

[28] D. P. Chew, C. Juergens, J. French et al., "An examination of clinical intuition in risk assessment among acute coronary syndromes patients: observations from a prospective multi-center international observational registry," *International Journal of Cardiology*, vol. 171, no. 2, pp. 209–216, 2014.

[29] J. P. VanHouten, J. M. Starmer, N. M. Lorenzi, D. J. Maron, and T. A. Lasko, "Machine learning for risk prediction of acute coronary syndrome," *AMIA Annual Symposium proceedings Archive*, vol. 2014, pp. 1940–1949, 2014.

[30] J. Wallert, M. Tomasoni, G. Madison, and C. Held, "Predicting two-year survival versus non-survival after first myocardial infarction using machine learning and Swedish national register data," *BMC Medical Informatics and Decision Making*, vol. 17, no. 1, p. 99, 2017.

[31] G. Hripcsak and D. J. Albers, "Next-generation phenotyping of electronic health records," *Journal of the American Medical Informatics Association*, vol. 20, no. 1, pp. 117–121, 2013.

[32] G. Hripcsak, C. Knirsch, L. Zhou, A. Wilcox, and G. Melton, "Bias associated with mining electronic health records," *Journal of Biomedical Discovery and Collaboration*, vol. 6, pp. 48–52, 2011.